

Modelling responses of perennial ryegrass pastures to future  
climate scenarios in Tasmania

by

David Charles Phelan  
B.App.Sc. (Agr) (Hons.)  
University of Tasmania

Submitted in fulfillment of the requirements for the degree of  
Master of Agriculture Science  
University of Tasmania, Hobart  
May 2012

## **Declaration of Originality**

This thesis contains no material which has been excepted for a degree or diploma by the University or any other institution, except by the way of background information and duly acknowledged in the thesis, and to the best of my knowledge and belief no material previously published or written by another person except where due acknowledgement is made in the text of this thesis, nor does this thesis contain any material that infringes copyright.

David Phelan  
May 2012

## **Authority of Access**

This thesis may be made available for loan and limited copying in accordance with the *Copyright Act 1968*.

## **Statement of ethical conduct**

The research associated with this thesis abides by the International and Australian codes on human and animal experimentation, the guidelines by the Australian Government's Office of the Gene Technology Regulator and the rulings of the Safety, Ethics and Institutional Biosafety Committees of the University.

## **Acknowledgments**

There are so many people to sincerely thank who have provided support and assistance throughout the journey that has been this Masters thesis.

Principally though, my supervisors. Dr. Richard Rawnsley and Dr Greg Holz for continual guidance, patience, wisdom and dedication throughout this project. I am extremely appreciative of their time, effort and support and I sincerely believe I was gifted an opportunity to work with both.

I am greatly thankful to the School of Agricultural Science for the opportunity to undertake this work along with the funding bodies of, Dairy Australia, the University of Tasmania and the Tasmanian Institute of Agricultural Research (TIAR) for providing the funding to undertake this thesis.

Special thanks to Dr. Michael Grose for critical last minute input and Ian Johnson for additional help, guidance and functionality with the model DairyMod. Thank you to Lydia Turner who unearthed a raft of errors in proof reading the thesis, and a very special thanks to a dear friend, Katrina Harwood who volunteered to offer help and encouragement at every turn, not only with this project, but in life as well.

*“I’ve worked too hard for my illusions just to throw them all away”*

This thesis is for Ruby Elizabeth Phelan. “For her” it’s what I would write on my left hand on a basis daily, from late March 2011. At times when there was little desire or inspiration to continue this work, I would read these two words written on my left hand and press on, for her.

Of my dear immediate family, Mum, Dad and Paul and my extended family of Sue, Lyn, Mei Mei and Charlie. Its difficult to put in words what your love, support and encouragement has meant through this period, not only from December 14, but of what seems now another life ago, way back when I first begun this project. I am very fortunate to belong to such a wonderful and strong family, I love each of you very dearly.

To my dear sister Anne-Maree, I wonder of where you are, I hope you are ok, I hope you feel at peace. I struggle immensely with your absence from my life today, I am forever changed. I want to tell you that I will come to terms with your choice, it just takes time. You now have a beautiful niece, of which I’m sure you would be very proud, she was born three months to the day after you passed away. In time Ruby will come to know you very well, because I will forever tell her of her wonderful Aunty Annie, your life will not fade, it will grow.

I love you, may tranquility be yours xx.

*“I once found a rainbow lying flat on the ground, but I just kept on walking thinking more were around”*

## **Abstract**

Evidence for the warming of the climate system is considered unequivocal. Observations from all continents and most oceans show many natural systems are being disturbed by regional climate change (IPCC 2007). Agricultural production is strongly influenced by climate and so climate change will have profound effects on food production and the natural resources on which agriculture depends. In Tasmania, dairy is the largest agriculture industry contributing nearly 30% of the gross value of agricultural production. Production and consumption of high quality temperate pastures and the availability of irrigation underpin the competitiveness of the Tasmanian dairy industry. As a result, the Tasmanian dairy industry will need to adapt to any changes in climate that affect the productivity of temperate pastures or the availability of irrigation water. Therefore, there is an urgent need to evaluate climate change impacts on agricultural production in Tasmania.

Although relatively small in area, Tasmania has a diverse range of regional climates that are the result of different synoptic influences. Consequently, climate change might be expected to vary in different regions of the state. The aim of this thesis is to quantify the regional impacts of projected climate change on the productivity of pasture based dairy systems for six regions within Tasmania. Six sites were selected to represent the dairying regions of the north west (Woolnorth and Flowerdale), central north (Merseylea), the northern Midlands (Cressy), the north east (Ringarooma) and the south (Ouse).

Observed and interpolated historical climate data from four different climate data sources are available. A meteorological and biophysical comparison between the four sources of observed and interpolated gridded daily climate data for the period 1971 to 2007 was undertaken at each site. The data obtained were SILO Patched Point data (observed), SILO Data Drill (0.05°), Australian Water Availability Project (AWAP 0.05°) and Australian Water Availability Project (AWAP 0.1°). Differences were observed between the four daily climate data sources for each region for the climate variables mean daily minimum temperature, rainfall and potential evaporation. In addition, outputs from a biophysical model DairyMod (version 4.9.2) compared simulated monthly and annual pasture production. There were few significant differences in annual pasture production but there were significant differences for the months of October and November.

Climate Futures for Tasmania (CFT) used CSIROs Conformal Cubic Atmospheric Model (CCAM) to dynamically downscale five General Circulation Models (GCMs) (ECHAM5/MPI-OM, GFDL-CM2.0, GFDL-CM2.1, MIROC3.2 (medres) and UKMO-

HADCM3) reported in the IPCC fourth assessment report and a sixth GCM, CSIRO-Mk3.5. The CFT project provided projections under the A2 emissions scenario at a scale of 0.1° (≈10km) grid across Tasmania for the period 1961 to 2100. Climate models have variable skill and inherent biases. To manage these biases, a bias-adjustment method was undertaken to scale the climate modelling outputs to the historical interpolated data of AWAP 0.1. The aim was to preserve the change in the frequency distributions from the six GCMs projections. The suitability of the downscaled bias-adjusted GCM data for use in a biophysical model was evaluated by comparing simulated pasture yields from DairyMod from the downscaled GCMs with that from the AWAP 0.1° data source for the period 1990 to 2007. The mean annual simulated pasture yields from the downscaled bias-adjusted GCMs and from the AWAP 0.1° data source were generally comparable, giving confidence that the bias-adjusted GCM simulations were suitable for projections of pasture production.

The projected climate for the A2 emissions scenario at each site was described over the period of 1971 to 2100. The mean of daily maximum and daily minimum temperatures at each site are projected to increase from a baseline period (1971 to 2000) to 2085 (2071 to 2100) ranging from 2.4°C at Woolnorth to 2.7°C at Ringarooma. Mean annual rainfall is projected to slightly increase at each site except Flowerdale, from the baseline period to 2085. Seasonal rainfall is projected to increase slightly at each site except Woolnorth (summer) and Flowerdale (summer and spring). Inter-annual rainfall variability is projected to increase for each region. Mean annual potential evapotranspiration rates as calculated by Morton's wet method (Bennett *et al.* 2010) are projected to increase by 3% to 4% for each region from the baseline period to 2085. No changes in solar radiation are projected for any of the regions.

The Tasmanian dairy industry is a vital component of the state's agricultural sector. The industry is comprised of approximately 450 farms and produces approximately 7% of the national milk production. Regional variation in the projected climate is likely to result in regional variation in pasture production across Tasmania. The biophysical model DairyMod was used to simulate the growth of perennial ryegrass (*Lolium perenne* L.) under rainfed and irrigated conditions at each site. The simulations were nutrient non-limited, pasture was harvested monthly to a residual of 1400 kg /DM/ha, and identical soil physical and chemical parameters were used for each site. Throughout the 21<sup>st</sup> century mean annual pasture yields under rainfed conditions at each site are projected to increase above the baseline varying from a 29% increase at Woolnorth to 150% increase at Cressy by 2085. Mean annual irrigated pasture yields are projected to increase until mid-century, then decrease to 2085. The reduction of irrigated pasture yields in the latter half of this century is the result of an increase in the number of warm days with maximum temperatures exceeding 28°C. The impact of

higher daily maximum temperatures are more evident under the irrigated simulations, because the irrigated simulations were not limited by soil moisture. In contrast, the major limitation to growth under the rainfed simulations during the summer months is inadequate soil moisture. Yield increases under both rainfed and irrigated simulations are projected to occur during late winter and spring. The increase in yield is a result of increases in both daily maximum and minimum temperatures and the progressive increase of atmospheric CO<sub>2</sub> concentrations under the A2 scenario.

Inter-annual yield variability for each region is projected to decrease throughout the 21<sup>st</sup> century under both the rainfed and irrigated simulations, except at Cressy under irrigation. The decrease in inter-annual yield variability is being driven by a marked reduction in yield variability during autumn and spring.

Irrigation demand progressively increases throughout the 21<sup>st</sup> century for each region, except at Cressy and Ouse. Although irrigation requirements are projected to increase, there is a corresponding increase in the water use efficiency (WUE) of the pastures. This increase in WUE is driven by increasing atmospheric CO<sub>2</sub> concentrations resulting in an increase in the net influx of CO<sub>2</sub>, increased stomatal resistance and a decline in transpiration per unit of CO<sub>2</sub> fixed (Clark *et al.* 1995).

Surface runoff was quantified at each site, using the downscaled bias-adjusted GCMs simulations within the hydrological model SIMHYD (Chiew *et al.* 2002) for the period 1971 to 2100 (Bennett *et al.* 2010). At each site, except Flowerdale, mean annual surface runoff at 2085 was projected to increase as a result of increased runoff during the winter months. A case study farm at Ringarooma was selected to quantify the projected surface runoff and river flow impacts on an irrigated perennial ryegrass based dairy system. Currently the farm is 166 ha in size with 75 ha of the farm supported by irrigation infrastructure. Irrigation water is accessed from both an on-farm catchment (dam) and access to River flows (Ringarooma River). Under the projected climate, hydrological modelling indicates that irrigation demand by 2085 will be met by the on-farm storage dam 50% of the time in comparison to the current baseline of 23%. In contrast, water accessed from the Ringarooma River during summer is projected to continually fail to meet irrigation demand from the baseline to 2085.

Modelling the climate change impacts indicate a progressive increase in pasture growth within Tasmania throughout the 21<sup>st</sup> century (particularly under rainfed conditions). The low cost of milk production associated with pasture based dairy systems underpins the national and international competitive advantage of the Tasmania dairy industry. This study has found

the current forage base of Tasmanian dairy regions is resilient to future climate scenarios and that adaptations are likely to be within system adaptations, with the industry continuing to focus on milk production per hectare and pasture consumption per hectare as key determinants of business success. This will allow the Tasmanian dairy industry to retain its comparative advantage.

## Table of Contents

<b>Acknowledgements</b>	ii
<b>Abstract</b>	iii
<b>Table of contents</b>	vii
<b>CHAPTER 1: Introduction</b>	1
<b>CHAPTER 2: Review of literature</b>	
2.1 Dairying in Australia	4
2.2 Pasture production and climate	12
2.3 Climate and climate change	15
2.4 Evaluating climate change on dairying	27
<b>CHAPTER 3: Historical comparison between an observed and three interpolated climate data sources</b>	
3.1 Introduction	29
3.2 Materials and methods	31
3.3 Results and discussion	35
3.3.1 Temperature	35
3.3.2 Rainfall	37
3.3.3 Potential evaporation	39
3.3.4 DairyMod simulations	41
3.4 Conclusion	47
<b>CHAPTER 4: A comparison of the AWAP 0.1 data source against the six downscaled General Circulation Model climate data sources</b>	
4.1 Introduction	48
4.2 Materials and methods	50
4.3 Results and discussion	51
4.3.1 Annual climate metrics	51
4.3.2 DairyMod simulations	57
4.4 Conclusion	64
<b>CHAPTER 5: Projected climate using the six bias-adjusted dynamically downscaled General Circulation Models for six dairy regions</b>	
5.1 Introduction	65
5.2 Materials and methods	67
5.3 Results and discussion	67
5.3.1 Woolnorth	68
5.3.2 Flowerdale	69
5.3.3 Merseylea	70

5.3.4	Cressy	71
5.3.5	Ringarooma	72
5.3.6	Ouse	73
5.3.7	Climate variability	77
5.3.8	Rainfall intensity	79
5.4	Conclusion	81
<b>CHAPTER 6: Modelled responses of perennial ryegrass to the projected climate</b>		
6.1	Introduction	82
6.2	Materials and methods	83
6.3	Results and discussion	85
6.3.1	Rainfed and irrigated pasture cut yields	85
6.3.2	Annual and monthly irrigation requirements	96
6.3.3	Gross production water-use index	99
6.3.4	Annual and seasonal cut yield variability	100
6.3.5	Perennial ryegrass growth comparisons under two CO <sub>2</sub> comparisons	104
6.4	Conclusion	109
<b>CHAPTER 7: Modelled surface runoff in response to the projected climate change at each site and projected River flow at Ringarooma</b>		
7.1	Introduction	110
7.2	Materials and methods	112
7.3	Results and discussion	115
7.3.1	Surface runoff at each of the six dairy regions	115
7.3.2	Ringarooma on-farm catchment and irrigation supply	120
7.3.3	Ringarooma River flows and irrigation supply	123
7.4	Conclusion	125
<b>CHAPTER 8: Conclusions and recommendations</b>		126
<b>REFERENCES</b>		131
<b>Appendices</b>		
A.1	Mean monthly maximum temperature from the data sources of AWAP 0.1, AWAP 0.5, PP and DD.	147
A.2	Mean monthly minimum temperature from the data sources of AWAP 0.1, AWAP 0.5, PP and DD.	148
A.3	Mean monthly rainfall from the data sources of AWAP 0.1, AWAP 0.05, PP and DD.	150
A.4	Mean monthly potential evaporation from the data sources of AWAP 0.1, AWAP 0.5, PP and DD.	151
A.5	Mean simulated monthly cut yield (kg DM/ha) from the data sources of AWAP 0.1,	

	AWAP 0.5, PP and DD.	153
<b>A.6</b>	Mean monthly rainfall (mm) from the data sources of AWAP 0.1, CSIRO-Mk3.5, ECHAM5/MPI-OM, GFDL-CM2.0, GFDL-CM2.1, MIROC3.2 (medres) and UKMO-HADCM3.	154
<b>A.7</b>	Mean simulated monthly rainfed pasture cut yield (kg DM/ha) from the data sources of AWAP 0.1, CSIRO-Mk3.5, ECHAM5/MPI-OM, GFDL-CM2.0, GFDL-CM2.1, MIROC3.2 (medres) and UKMO-HADCM3.	156
<b>A.8</b>	Multi-model mean seasonal rainfall intensity (mm) from the data sources of CSIRO-Mk3.5, ECHAM5/MPI-OM, GFDL-CM2.0, GFDL-CM2.1, MIROC3.2 (medres) and UKMO-HADCM3.	159
<b>A.9</b>	Multi-model mean seasonal GPWUI (kg DM/mm) from the data sources of CSIRO-Mk3.5, ECHAM5/MPI-OM, GFDL-CM2.0, GFDL-CM2.1, MIROC3.2 (medres) and UKMO-HADCM3.	160
<b>A.10</b>	Mean simulated monthly runoff (mm) from the data sets of AWAP 0.1, CSIRO-Mk3.5, ECHAM5/MPI-OM, GFDL-CM2.0, GFDL-CM2.1, MIROC3.2 (medres) and UKMO-HADCM3.	161
<b>A.11</b>	Mean simulated monthly river flow (GL) from the data sets of AWAP 0.1, CSIRO-Mk3.5, ECHAM5/MPI-OM, GFDL-CM2.0, GFDL-CM2.1, MIROC3.2 (medres) and UKMO-HADCM3.	162

## CHAPTER 1: INTRODUCTION

Warming of the climate system is considered unequivocal (IPCC 2007). This is evident from observed increases in global average air and ocean temperatures, widespread melting of snow and ice, and rising global average sea levels. In addition, observations from all continents and most oceans show many natural systems are being disturbed by regional climate change, in particular from increasing temperatures (IPCC 2007).

Australia, the driest of all inhabited continents, is characterised by an arid to semi-arid climate with highly variable rainfall both temporally and spatially (Taschetto & England 2009). Climate trends in Australia are consistent with those evident from around the world. Gradual increases in mean annual daily temperatures in nearly all locations have been observed particularly in overnight minimums (Pittock 2003; Karoly & Braganza 2005). Changes have also been observed in mean annual rainfall although these are not consistent. Since 1950, north Western Australia has become wetter while much of eastern and southern Australia has become drier (Gallant *et al.* 2007; Nicholls 2007).

Tasmania is the most southerly permanently inhabited island of Australia, lying some 240 km off the south-east coast of mainland Australia and located between 40° to 43° south in latitude. It has a mostly temperate maritime climate. A prevailing westerly airstream leads to a marked variation of cloudiness, rainfall and temperature. Consequently, the west coast and highlands are generally cool, wet and cloudy, while the east coast and lowlands are milder, drier and sunnier. Rainfall is commonly less (in both amount and frequency) in summer, most notably in the west and north west. Winters are not excessively cold, especially compared to places at similar latitudes in the northern hemisphere that do not have the surrounding oceans moderating influence. The mean daily temperature for Tasmania is 10.4°C (Bureau of Meteorology 2011). Since the 1950's this has risen by 0.1°C per decade, significantly less than for Australia or the globe (Grose *et al.* 2010). Daily minimum temperatures have increased at a greater rate than daily maximum temperatures. The lower rate of warming of daily maximum temperatures is consistent with greenhouse warming and analyses of observations globally (McInnes *et al.* 2004; Grose *et al.* 2010). Since the 1950's mean annual rainfall in Tasmania has declined by 22 mm per decade. Trends since 1970 show an even greater decrease of 45 mm per decade (Bureau of Meteorology 2011). While these changes in Tasmania's climate are apparent it remains unclear how much of the change is part of natural background variability or how much represents a fundamental change in climate due to anthropogenic influences.

The observed climatic changes are beginning to, and have the potential to, strongly influence agricultural production. These changes are likely to increase both the biophysical and economic stress within the sector (Harle *et al.* 2006). Specifically, the impacts of a changing climate may include changes to crop yields, product quality and changes in the timing of farm operations such as planting and harvesting. Furthermore, changes may occur in suitable crop species and cultivars at one level and the suitability of whole farming systems at another.

In 2007, agricultural production in Tasmania contributed approximately \$950 million (16%) to the state's economy. Dairy is Tasmania's largest agricultural industry, contributing approximately 30% of the state's gross agricultural production (Australian Bureau of Statistics 2010a). The Tasmanian dairy industry is located along the higher rainfall northern coastal areas of the state from Ringarooma in the north east to Smithton in the north west, with a smaller number of farms in the Deloraine region, King Island and Derwent Valley. The industry is pasture based with the dominant pasture grass species being perennial ryegrass (*Lolium perenne* L.) commonly sown in a mixed sward with white clover (*Trifolium repens* L.). The reliable production of high quality pasture reduces the demand for supplementary feed and provides a competitive advantage for Tasmanian dairy farmers against mainland and international producers. However, a heavy reliance on pasture results in the industry being vulnerable to climate change either directly through the influences on the production and persistence of pasture, or indirectly through a reduction in the availability of irrigation water.

Although the impact of the projected climate change on pasture production remains uncertain, it is likely to vary regionally according to the existing regional climate and amount of change likely at any one site (Cullen *et al.* 2009). Currently there is a paucity of climate projection data at a regional scale. General Circulation Models (GCMs) are used for creating future climate scenarios. These models are based on established physical principles and are capable of reproducing the most significant features of the observed climate (Perkins & Pitman 2009; Brankovic *et al.* 2010). However, projections of climate change are not evenly distributed over the globe. This necessitates that local or regional climate projections are required to quantify local or regional climate impacts (Corney *et al.* 2010).

The Climate Futures for Tasmania (CFT) project generated climate projections specific to Tasmania through fine scale climate modelling using dynamical downscaling (Corney *et al.* 2010). The CFT project used CSIRO's Conformal Cubic Atmospheric Model (CCAM) to dynamically downscale five of the twenty three GCMs reported in the IPCC fourth assessment report (AR4) and a sixth GCM, CSIRO-Mk3.5, under two Special Report on Emission Scenarios (SRES); a higher emissions scenario (A2) and a low emission scenario

(B1) (Nakicenovic & Swart 2000). The downscaling increases the spatial resolution from 2° to 3° grid cells in the GCMs down to a 0.1° grid ( $\approx 10\text{km}$ ) for Tasmania (Corney *et al.* 2010). The dynamically downscaled climate projections produced by CFT captures regional and sub-regional differences allowing the projected climate change impacts to be quantified on a regional level (Corney *et al.* 2010).

Using the bias-adjusted dynamically downscaled GCMs data from the CFT project, this study will quantify daily climate outputs for the period 1971 to 2100 for six dairy regions of Tasmania. The six sites selected in the study are representative of the Tasmanian dairying regions of the north west (Woolnorth and Flowerdale) central north (Merseylea), the northern Midlands (Cressy), the north east (Ringarooma) and the south (Ouse). Regional impacts of the projected climate change on pasture production, irrigation demand and runoff will be quantified using simulation modelling. This study aims to provide assessments of local climate change at a regional level across the dairy industry where information has previously been scarce. The research will be undertaken to quantify and provide an information base for the Tasmanian dairy industry to prepare for the uncertainty and develop adaptation strategies to the projected future climate regimes most likely, given current knowledge.

The specific objectives were;

1. To compare meteorological and biophysical modelling of four observed and interpolated daily climate data sources at six sites in Tasmania for the period 1971 to 2007.
2. To compare meteorological and biophysical modelling between AWAP 0.1° daily climate data and six bias-adjusted dynamically downscaled GCMs daily climate data sources at six sites in Tasmania for the period 1990 to 2007.
3. Evaluate the projected daily climate data from six bias-adjusted dynamically downscaled GCMs data sources at six sites in Tasmania for the period 1971 to 2100.
4. Evaluate the impacts of projected climate change on perennial ryegrass yields at six sites within Tasmania for the period 1971 to 2100 using a biophysical modelling approach.
5. Quantify projected surface runoff at six sites in Tasmania from a hydrological model using the six bias-adjusted dynamically downscaled GCMs daily climate data for the period 1971 to 2100. And undertake an on-farm case study to quantify the projected surface runoff and River flow impacts on an irrigated pasture based dairy system.

## CHAPTER 2: REVIEW OF LITERATURE

### 2.1 Dairying in Australia

Since European settlement in 1788, the production of cow's milk has been an important feature of Australian agriculture. When the first fleet established itself at Farm Cove, Port Jackson, they had brought with them 7 cows and 2 bulls to supply milk for the colony and also to serve as the foundation stock for future herds. This was the beginning of an extraordinary industry in Australian agriculture (Dairy Australia 2011).

Today, primary production in Australia contributes approximately \$31.9 billion (5.3%) to the national economy. The dairy industry is the third largest agriculture industry within Australia (behind wheat and meat production), accounting for 9% of the total gross value of primary production (Dairy Australia 2011). In 2009/10 the industry produced approximately 9 billion litres of milk at a farmgate value of \$3.4 billion, of which \$2.4 billion was the result of export markets (Dairy Australia 2011). There are eight main dairy regions in Australia where dairying is well established (Figure 2.1). The dairy industry is concentrated in the south eastern corner of Australia, with Victoria (66%), Tasmania (7%) and South Australia (7%) accounting for around 80% of the national output (Table 2.1) (Dairy Australia 2011).

**Table 2.1** Annual milk production (L) for each state and percentage of national production (source Dairy Australia 2011).

State	Production litres	% National production
Victoria	6,296,934	65.7
NSW	1,104,942	11.5
SA	654,702	6.8
Tasmania	642,239	6.7
Queensland	534,409	5.6
WA	349,423	3.6
<b>Total</b>	<b>9,582,649</b>	<b>99.9</b>

Over the last two decades the phasing out of government support and the deregulation of the milk industry in 2000 has led to a substantial restructuring of the Australian dairy industry. Throughout this period the number of dairy farms in Australia has more than halved. Restructuring has led to more efficient production at farm scale and an expansion of dairy production nationally. The average farm and herd size, volumetric milk production, milk yield per cow and supplementary feed inputs have all increased (Dairy Australia 2011).

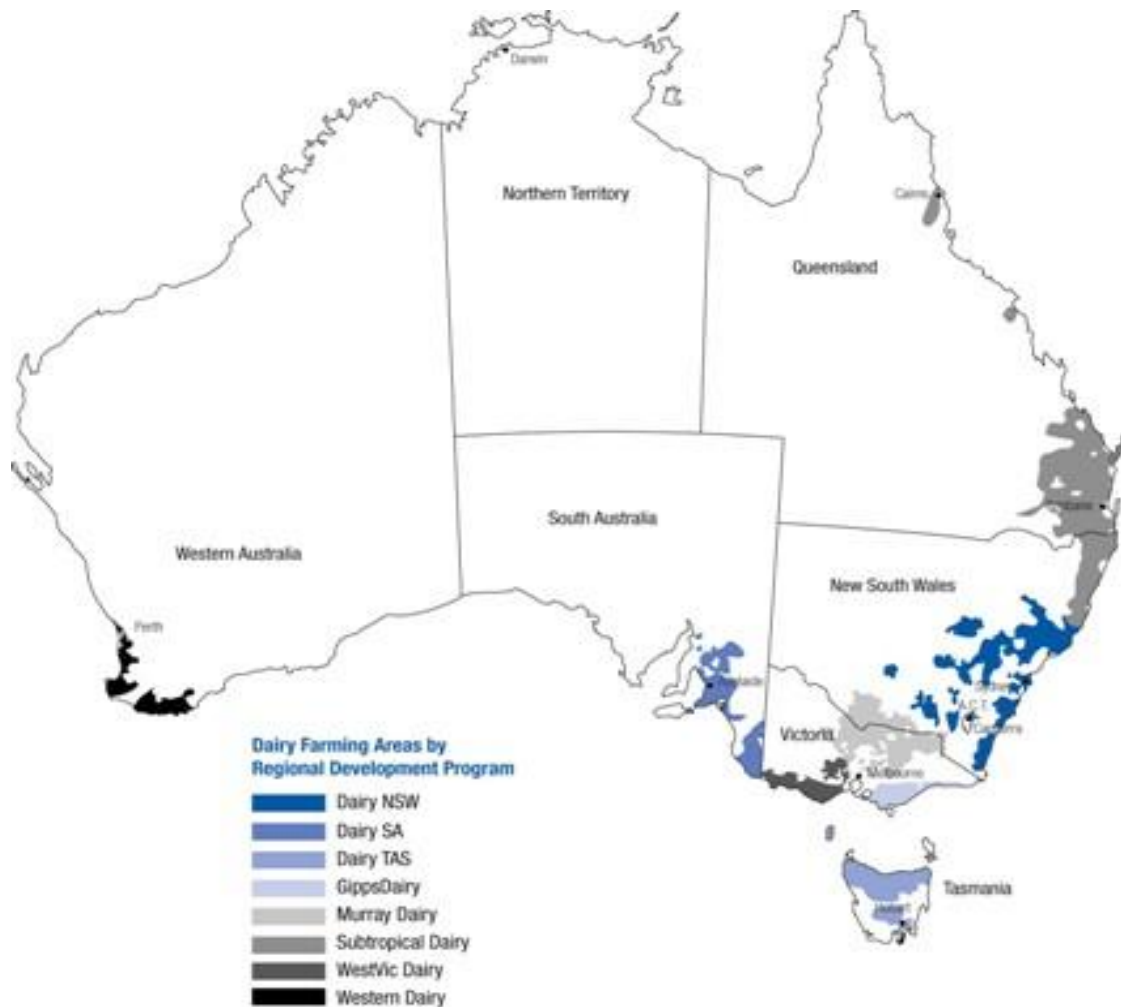


**Figure 2.1** Main dairy regions of Australia (source Dairy Australia 2011).

Pasture based dairy systems are found in temperate regions throughout the world, such as those operated in the Atlantic Arc of Europe, New Zealand and southern Australia. Pasture is generally the cheapest source of feed for dairy cows and there is a strong positive relationship between on-farm profit and total pasture dry matter (DM) consumed per hectare (Chapman *et al.* 2009). In Australia and New Zealand pasture comprises between 50% to 80% and 85% to 95% of the dairy cows' diet respectively (McDonald *et al.* 2010). In southern Australia, perennial ryegrass is the most widely sown dairy pasture species supplying 60% to 70 % of the diet of lactating cows due to its high nutritional value and digestibility (Armstrong *et al.* 2000; Chapman *et al.* 2008a). Perennial ryegrass based pastures can provide high quality forage for most of the year under appropriate environmental and management conditions. However, pasture based systems regularly fail to meet the feed requirements for lactating dairy cows during late winter and summer. During winter low temperatures restrict perennial ryegrass growth, while during summer high maximum temperatures and soil moisture deficits restrict growth (Doyle *et al.* 2000; Chapman *et al.* 2008a) and can result in poor persistence due to low tiller survival (Waller & Sale 2001; Garcia & Fulkerson 2005).

The low cost of milk production associated with pasture based dairy systems underpins the national and international competitive advantage of the Tasmanian dairy industry. Supplementary feeding within the national dairy industry is becoming increasingly common, however, increased milk production reliant on increased supplementary feed is less profitable than those dairy systems based exclusively on increasing pasture production in order to meet the energy requirements of the herd (Chapman *et al.* 2008b). In Tasmania approximately 80% of dairy farmers utilise some form of supplementary feed, with only 20% being totally reliant on pasture to meet the herd's energy requirements. This figure is considerably higher than for mainland Australia, where the total reliance on a pasture ranges from 2% to 9% (Dairy Australia 2011).

The heavy reliance of the Tasmanian dairy industry on pasture production is not without risk, as neither the quantity nor quality of pastures remains constant (Christie 2006). Maintaining high milk production levels via effective pasture management, optimising DM intake and maximising pasture production per hectare are important elements for the success of a pasture based dairy system (MacDonald *et al.* 2008; Chapman *et al.* 2009). More than 80% of dairy farms within Tasmania calve their cows in late winter/early spring, such that the peak feed requirements of the dairy herd coincide with increased pasture growth during spring. Autumn calving occurs on a smaller number of farms, while approximately 16% of farms calve cows in both autumn and spring (split) in order to supply milk year round.

The dairy industry is a significant proportion of both the agricultural and manufacturing sectors of the state, along with being an important export industry. Approximately 91% of the state's milk production is manufactured into products such as cheese, milk powders and butter (Australian Bureau of Statistics 2010a). Dairy milk manufacturers in Tasmania are export orientated. Approximately 65% of milk produced in the state is exported to international markets and 26% is consumed within Australia as manufactured product with the remaining 9% supplying the local fresh milk market. Despite the state's geographic isolation and high transport costs, the industry competes profitably against both interstate and international competitors (Bailey *et al.* 2004; Dairy Australia 2011).

Over the last two decades, the Tasmanian dairy industry has mirrored trends on mainland Australia with reduced dairy farm numbers (approximately 460 farms), increased herd sizes and increased milk production per cow. While farm numbers have declined over the last two decades, milk production has increased steadily from an annual figure of 450 million litres in 1990 to approximately 700 million litres in 2008 (Figure 2.2) (Dairy Australia 2011).

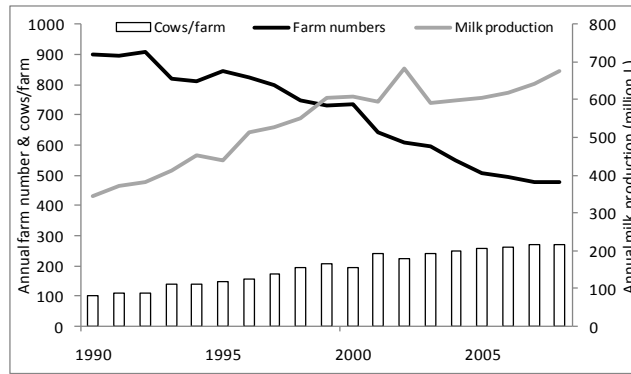


**Figure 2.2** Annual number of Tasmanian dairy farms, cows per farm and annual milk production (million L) for the period 1990 to 2008 (Anon. 2009).

The dairy industry in Tasmania is statewide, and can be summarised geographically into three main dairying regions; the north west, north and south. The industry is predominately located along the higher rainfall northern coastal areas of the state from Ringarooma in the north east to Smithton in the far north west. A smaller number of farms are located in the Cressy/Deloraine region (central north), King Island (north west) and the Derwent Valley (south) (Figure 2.3).

The north west region includes greater than 60% of the state’s dairy farms and comprises the sub regions King Island, the far north west and the central north west. King Island has an ideal climate for dairy production, with an annual rainfall of 900 mm to 1000 mm and very few frosts, although irrigation on King Island is limited owing to a lack of large streams and irrigation storages (Anon. 2009).

The far north west, along the coastal regions from Woolnorth to Wynyard is considered the best dairying region in Tasmania and among the best in Australia. As a result a large proportion of the state’s dairy production is based within this area. Mean annual rainfall varies from 1000 mm to 1400 mm, and there are comparatively few frosts. The central north west includes farms from Wynyard to Devonport and inland regions. Mean annual rainfall varies from 800 mm close to the coast to 1000 mm further inland and is winter dominant. This results in summer moisture deficits and as such irrigation is required to maintain reliable milk production throughout the year. The number of dairy farms in this region has decreased over time due to competition from alternative land uses. In particular, land has been converted to high value intensive horticulture and land marginal for dairy production has been converted to forestry plantations (Anon. 2009).

The northern region extends from the central north (Deloraine/Cressy) and to the north east (Gladstone/Ringarooma) and incorporates greater than 30% of the state's dairy farms. Mean annual rainfall across the region varies from less than 800 mm in areas of the north east and south of Launceston, to a 1000 mm to 1200 mm closer to the central plateau and north east highlands. Inland areas may experience up to 100 frosts per annum (Anon. 2009).

The majority of the dairy production in the southern region of Tasmania is concentrated in the Derwent Valley to the north west of Hobart. Mean annual rainfall is comparatively low in contrast to the other dairying regions (Table 2.2), ranging from 500 mm to 700 mm, although there is potential for further development of large scale irrigated dairy production in the area.

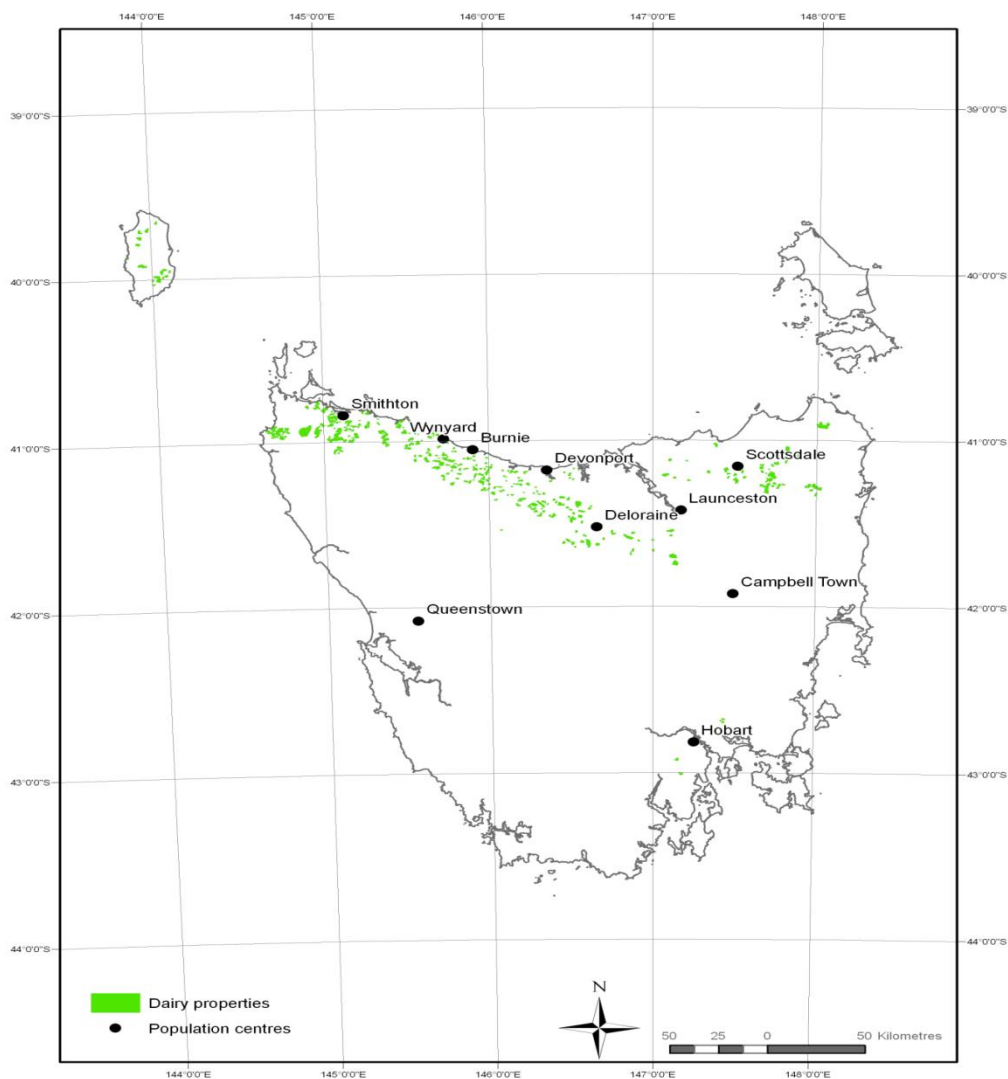


**Figure 2.3** Location of dairy properties in Tasmania.

The regional variation in climatic conditions that exist between the dairying regions are highlighted in Table 2.2. These sites are representative of the dairying regions of the north west (Woolnorth and Flowerdale) central north (Merseylea), the northern Midlands (Cressy), the north east (Ringarooma) and the south (Ouse). Mean annual daily maximum temperatures at all sites are similar with little regional variation, whilst regional variation is observed in mean annual daily minimum temperatures, particularly between the coastal regions of Woolnorth and Flowerdale and the inland regions of Cressy and Ouse (Table 2.2). The spatial distribution of Tasmania's mean annual rainfall is reflected between the sites, varying from 1204 mm at Ringarooma to 534 mm at Ouse. Each site is characterised as being climatically temperate maritime with a winter dominant rainfall, although at Ouse the highest seasonal rainfall occurs during spring ([www.longpaddock.qld.gov.au/silo/](http://www.longpaddock.qld.gov.au/silo/); Jeffrey *et al.* 2001).

**Table 2.2** Location, elevation (AMSL) (m), mean annual daily maximum and minimum temperature (°C), and mean annual rainfall (mm) for the sites of Woolnorth, Flowerdale, Merseylea, Cressy, Ringarooma and Ouse for the period 1961 to 1990 ([www.longpaddock.qld.gov.au/silo/](http://www.longpaddock.qld.gov.au/silo/); Jeffrey *et al.* 2001).

Site	Lat. Long.	Elevation	Daily maxT	Daily minT	Annual rainfall
Woolnorth	-40.68, 144.72	10	16.2	9.3	955
Flowerdale	-40.99, 145.61	18	16.4	8.1	1187
Merseylea	-41.33, 146.41	41	16.8	7.2	1037
Cressy	-41.72, 147.08	166	17.2	5.7	621
Ringarooma	-41.25, 147.73	282	16.5	6.9	1204
Ouse	-42.48, 146.71	95	17	5.9	534

In contrast to the Tasmanian dairying regions, the main dairying regions on the mainland are much more climatically diverse. The Goulburn Valley, Southern New South Wales (Jerry's Plains), South Australia and Western Australia, experience a Mediterranean climate (Table 2.3). These regions are characterised by cool wet winters and hot dry summers. The distribution and amount of rainfall and high evaporation rates during summer result in soil moisture being the major limitation for pasture growth (Turner & Asseng 2005). Northern New South Wales and Southern Queensland experience a sub tropical climate characterised by hot humid summers and mild to cool winters with a summer dominant rainfall. North Queensland is a tropical environment characterised by a high summer rainfall and warm dry winters. The Western district and Gippsland in Victoria are both classified as temperate regions (Table 2.3). Both the Tasmanian dairy regions and the southern dairy regions in Victoria are characterised by milder summer temperatures and a winter dominant rainfall. Whilst these regions are considered temperate, high evaporation levels and low rainfall during summer create a Mediterranean like climate for pasture production (Waller & Sale 2001).

**Table 2.3** Mean annual daily maximum and minimum temperature (°C), mean annual rainfall (mm) for the main dairying regions in Victoria, NSW, SA, WA and Queensland for the period 1961 to 1990 ([www.longpaddock.qld.gov.au/silo/](http://www.longpaddock.qld.gov.au/silo/); Jeffrey *et al.* 2001).

State	Region	Daily maxT	Daily minT	Annual rainfall
Victoria	Goulburn Valley	21.2	8.3	482
	Gippsland	18.6	9.4	921
	Western district	19.2	7.6	782
NSW	Casino	26.7	13.2	1097
	Jerry's plains	24.5	10.8	665
SA	Murray Bridge	22.5	9.9	353
WA	Donnybrook	23.3	10.1	970
Queensland	Gympie	27.1	14.1	1134
	Cairns	28.9	20.7	2064

The Australian dairy industry uses more water than any other industry (Garcia & Fulkerson 2005). Irrigation provides the opportunity for more intensive pasture production resulting in higher and more reliable yields. In Tasmania, approximately 67% of dairy farms utilise some form of irrigation, with approximately 30% of dairy land irrigated (Table 2.4) (Australian Bureau of Statistics 2010b). The Tasmanian dairy industry is the major consumer of irrigation water using approximately 38% of the total water, on approximately 23% of the total area of irrigated land. The average rate of irrigation water applied per ha across the industry is 4.8 ML (Table 2.4), which is a similar amount to the mainland dairy regions (NSW 3.4 ML/ha, Victoria 4.3 ML/ha, Queensland 4.4 ML/ha and SA 6.5 ML/ha) (Australian Bureau of Statistics 2010b). Irrigation water for the dairy industry in Tasmania is primarily sourced from surface water, which includes rivers and streams and on-farm storage dams. A small percentage of irrigation water in the southern region of the state is sourced from government irrigation schemes (e.g. Coal River Valley irrigation scheme) as well as limited access to groundwater supplies (Anon. 2009).

**Table 2.4** Number of dairy farms in each region, number of farms irrigating with percentage and application rate (ML/ha) for the period 2008/09 (Australian Bureau of Statistics 2010b).

Dairy region	Total farms	Farms irrigating	% Farms irrigating	ML/ha
North West	290	198	68	4.1
North	155	103	66	6.2
South	16	9	56	4.2
<b>Total</b>	<b>461</b>	<b>310</b>	<b>Average 67%</b>	<b>Average 4.8</b>

The diversity of climatic regions across Australia and the availability of irrigation water results in diverse feed bases for each dairying region. In the sub-tropical/tropical dairy regions of northern New South Wales and south east Queensland in the higher rainfall areas (coastal and tablelands) sub-tropical pasture species ( $C_4$  plant spp. which have a competitive advantage over plants possessing the more common  $C_3$  carbon fixation pathway under conditions of high temperatures and drought) provide the major feed base throughout

summer. During winter and spring both annual ryegrass and perennial ryegrass provide the major feed base although the pastures lack persistence (Donaghy *et al.* 1997). In the sub-tropical/tropical dairy regions just 25% of the feed base is met by pasture production, creating a heavy reliance on supplementary feed (Barlow 2008). In south eastern Australia swards of perennial ryegrass growth with white clover are the dominant forage source providing 50% to 80% of the feed base (Barlow 2008), although this is reliant on regional climate and the presence or absence of available irrigation water. The management requirements of perennial ryegrass are well understood. Perennial ryegrass is suited to regions with a mean annual rainfall of > 650 mm with mild summers and its survival during drought years is poor (Waller & Sale 2001; Cullen *et al.* 2006). Perennial ryegrass is characterised by strong spring growth, low summer productivity and poor persistence, creating management challenges for the effective feeding of high producing dairy cows year round from a perennial ryegrass pasture based diet (Waller & Sale 2001; Nie *et al.* 2004).

Within Tasmania mean annual pasture consumption currently varies from 2.7 to 12.7 t DM/ha under rainfed conditions, to 5.1 to 14.7 t DM/ha under irrigation. These figures are significantly below the potential pasture consumption which has been achieved under farmlet and experimental studies and biophysical modelling within Tasmania (Rawnsley *et al.* 2008). The modelled production potential of perennial ryegrass within the Tasmanian dairy regions is estimated at between 9 and 15 t DM/ha under rainfed conditions and between 15 and 21 t DM/ha under irrigation. The inter-annual variability and the variations in production potential between regions are strongly determined by climate. The two climatic factors that have the greatest influence on pasture production and persistence in Tasmanian dairy regions are temperature and rainfall (Rawnsley *et al.* 2008). Even under irrigation, the growth of perennial ryegrass is reduced by higher temperatures (Waller & Sale 2001).

Perennial ryegrass pastures are most productive and achieve higher water use efficiency (WUE) when irrigated frequently (Dunbabin *et al.* 1997). Perennial ryegrass is a shallow rooting plant with 40% of plant roots in the top 10 cm of soil and 80% of plant roots in the top 30 cm of soil (Crush *et al.* 2005). The quantity of readily available water held within the soil profile is commonly low during the summer months, subsequently soil moisture needs to be maintained at close to field capacity to maximise pasture growth (Rawnsley *et al.* 2008). Soil moisture deficits, caused by extended periods of low or intermittent rainfall and high daily evapotranspiration rates are major constraints to pasture production in south eastern Australia (Guobin & Kemp 1992; Rawnsley *et al.* 2008).

## 2.2 Pasture production and climate

The climate is the driver of pasture development and growth and fundamentally determines the amount of seasonal feed available (Zhang *et al.* 2007). The climate is modified by ocean currents and topography. The influence of season, latitude, longitude, altitude, aspect and coastal proximity on pasture production can be related to their regulating effect on temperature and moisture availability for radiation driven plant growth (White & Hodgson 1999). The dominant climatic factors that influence plant growth are temperature, rainfall, evaporation and solar radiation.

Temperature affects the rate at which biochemical reactions occur and is an important factor in the rate of plant development. Photosynthesis, respiration and nutrient uptake are all temperature dependant (White & Hodgson 1999). The optimum temperature range for the growth of temperate pasture species ranges from 20°C to 25°C and growth can cease between 5°C and 10°C (White & Hodgson 1999). The length of the growing season of perennial ryegrass is determined by temperature which influences both the frequency at which leaves appear and the rate at which they expand (Peacock 1974). Perennial ryegrass growth during winter and early spring in temperate regions is severely restricted by low temperatures (Kemp *et al.* 1989; Harrison *et al.* 1997). Numerous studies have examined growth responses of perennial ryegrass to temperature. Mitchell (1956) and Forde (1966) established the optimum temperature for the growth of perennial ryegrass to be 17°C to 21°C. Hunt & Halligan (1981) reported the effect of temperature increased linearly with temperature from 7°C to 20°C with a new leaf appearing in less than 6 days at a daily maximum temperature of 25°C compared with 10 days at 10°C. Temperature affects the duration of leaf expansion, at optimal temperature leaf expansion is more rapid for a shorter period producing a longer leaf (Waller & Sale 2001). Leaf appearance rates (days per leaf) vary from as low as 18 to 21 days during winter to 10 days during late spring (Peacock 1974; Clark *et al.* 1995) and leaves produced in warmer conditions tend to be longer and slightly narrower than those produced under cooler conditions (Langer 1973).

Perennial ryegrass is a temperate grass that does not tolerate high temperatures (>28°C) that can occur from late spring through to autumn in south east Australia (Waller & Sale 2001). Mitchell (1956) states that ryegrass growth ceases above a temperature of 30°C to 35°C, while Blaikie & Martin (1987) found the productivity of ryegrass decreased as temperatures were increased from 20°C to 40°C and at a temperature range of 33°C to 38°C, the rate of net photosynthesis at a given level of irradiance, was less than half that of 21°C to 24°C. High temperatures result in low water soluble carbohydrate reserves, threatening the survival of the

plant primarily because the loss of carbohydrates through respiration exceeds assimilate production. In order to avoid damage by high temperatures during summer, perennial ryegrass enters conditional dormancy (Waller & Sale 2001). If the plant remains alive during summer its carbohydrate reserves are generally low and plant growth declines, although many plants fail to survive. Perennial ryegrass enters conditional dormancy in order to avoid damage by high temperatures, however, it is unknown whether perennial ryegrass is able to switch quickly to dormancy when sudden hot conditions occur or whether sudden temperature stress compounded by low carbohydrate reserves results in the death of the plants (Waller & Sale 2001).

Rainfall and evaporation are the primary drivers of available soil moisture. Soil moisture is essential for pasture production processes including photosynthesis, translocation, leaf extension and evaporative cooling (Lazenby & Swain 1972). Excess soil moisture can cause a lack of oxygen in the soil for root growth and metabolism reducing pasture production (White & Hodgson 1999). Soil moisture deficits, caused by extended periods of low or intermittent rainfall and high daily evapotranspiration rates are major constraints on pasture production that can reduce pasture growth and persistence through the summer and early autumn months (Guobin & Kemp 1992; Rawnsley *et al.* 2008). Field experiments where moisture stress was imposed for several months on perennial ryegrass reduced DM production and tiller density markedly (Waller & Sale 2001). Perennial ryegrass has a variety of mechanisms that enable it to withstand soil moisture deficits that occur in dry summers including responding to short-term water stress by partially or completely closing the stomata to maintain cell turgor (White & Hodgson 1999). Cell growth is more sensitive to water stress than photosynthesis, with reduced cell expansion restricting the size of new leaves (Jones 1988). Leaf rolling and leaf death resulting from decreased transpiration is also a short-term water stress response of perennial ryegrass, and grazing can further reduce plant survival by defoliating tillers already experiencing severe moisture stress (Boschma *et al.* 1996).

Solar radiation is the primary source of energy on the planet and provides the energy for photosynthesis (Lovett & Scott 1997). Perennial ryegrass growth is influenced by seasonal changes of temperature and solar radiation. Potential production of perennial ryegrass under optimal nutrient and water supply is set by the seasonal input of solar radiation and the efficiency which it is utilised by the plant (Peacock 1974). The efficiency is determined primarily by the duration and photosynthetic rate of the canopy, reliant on the size and structure of the canopy and the photosynthetic capacity of individual leaves (Peacock 1974), although the effective use of this energy can be restricted by the climatic factors of temperature and water stress (Cooper 1964). Seasonal changes in the rate of solar radiation

affect the components of leaf expansion in different ways. In many temperate grasses an increase in solar radiation increases the rate of leaf appearance, but has different effects on leaf length and width (Cooper 1964).

Pastures of the future are likely to be grown under higher levels of atmospheric CO<sub>2</sub> levels. Increasing atmospheric levels of CO<sub>2</sub> have a strong influence on plant physiological processes such as water and nutrient efficiency, growth and development and plant productivity (Rogers *et al.* 1998; Ludwig & Asseng 2006). The influence of elevated atmospheric CO<sub>2</sub> and air temperature on plants has been studied extensively over the past three decades. Crop development and production are sensitive to and directly affected by atmospheric CO<sub>2</sub> concentrations (Thomson *et al.* 2005). Much knowledge has been acquired concerning elevated levels of atmospheric CO<sub>2</sub> impacts on photosynthesis, water use, biomass allocation and general plant growth for many agricultural plants under a range of both environmental and nutritional conditions (Romanova 2005; Smith *et al.* 2005). In field studies using free-air CO<sub>2</sub> enrichment (FACE) facilities and in experiments in controlled environments, a CO<sub>2</sub> fertilization effect has been observed. Agricultural crops grown under increased CO<sub>2</sub> levels show increased growth rates, improved water use efficiency and higher yields (Smith *et al.* 2005; Ludwig & Asseng 2006). For example, major C<sub>3</sub> agricultural crops (wheat, barley, rice and soybean) grown under elevated atmospheric CO<sub>2</sub> levels of 660 ppm showed an increase in yields ranging from 24 to 43% (Ainsworth & Long 2004; Long *et al.* 2005; Ziska & Bunce 2007). Further, many studies have shown that an approximate doubling of atmospheric CO<sub>2</sub> concentrations (750 ppm) enhances growth and yield of C<sub>3</sub> plant species by an average of 30 to 40% (Schenk *et al.* 1997), although there is considerable variation between species (Long *et al.* 2005; Soussana *et al.* 1996).

Perennial ryegrass responds to elevated levels of CO<sub>2</sub> concentrations by increased photosynthetic responses and higher DM production resultant of an increase in the net influx of CO<sub>2</sub>, increased stomatal resistance and a decline in transpiration per unit of CO<sub>2</sub> fixed (Clark *et al.* 1995; Long *et al.* 2004). Suter *et al.* (2001) reported that photosynthetic rates at elevated CO<sub>2</sub> levels of 600 ppm increased the highest in young fully expanded leaves. The plants developed a greater number of new tillers, in contrast to plants grown at ambient CO<sub>2</sub> levels of 360 ppm, resulting in higher yields, increased leaf area index (LAI) and higher total DM. Under optimum environmental conditions the additional DM production of perennial ryegrass due to elevated levels of CO<sub>2</sub> has shown to range between 7% and 30% (Daepf *et al.* 2000; Daepf *et al.* 2001; Suter *et al.* 2001).

Perennial ryegrass leaf emergence and leaf extension rates are temperature dependant and the potential for increased shoot growth under elevated CO<sub>2</sub> levels is also temperature dependant (Soussana *et al.* 1996). Projected increases in mean daily temperatures for the 21<sup>st</sup> century correlated with an increase of atmospheric CO<sub>2</sub> levels (fertilisation effect) are likely to enhance perennial ryegrass production via a shift toward increased optimum conditions for growth, particularly in regions that are currently temperature limited (Ryle *et al.* 1992). Despite the difficulties associated with reproducing the interactions between elevated CO<sub>2</sub> and other climatic variables under experimental conditions a number of studies have examined such interactions. Greer *et al.* (2000) found that photosynthetic activity is stimulated more by elevated CO<sub>2</sub> at higher temperatures (>25°C) than at lower temperatures. Experimental evidence from numerous studies on C<sub>3</sub> crop species under increased temperatures (>25°C), and elevated CO<sub>2</sub> levels (>600 ppm) showed an increase in biomass production of 30% to 40% (Laing *et al.* 2002). Although Laing *et al.* (2002) reported that five temperate C<sub>3</sub> pasture species (including perennial ryegrass) grown at 12°C (constant) under elevated CO<sub>2</sub> (700 ppm) still showed a strong growth response to elevated CO<sub>2</sub> levels.

### **2.3 Climate and climate change**

Climate change refers to a change in the state of the climate that can be measured by changes in the mean and/or variability of its properties and that persist for an extended period, commonly decades or longer (IPCC 2007).

The 100-year global linear trend (1906 to 2005) shows an increase of 0.74°C in mean temperature (IPCC 2007). The linear mean warming trend over 50 years from 1956 to 2005 of 0.65°C is nearly twice that for the 100 years from 1906 to 2005 (IPCC 2007). Increases in observed temperatures have been widely reported around the globe but have been greater at higher northern latitudes. Average Arctic temperatures have increased at almost twice the global average rate in the past 100 years (IPCC 2007). Observations since 1961 show that the average temperature of the global ocean has increased at depths of at least 3000 m and that the ocean has been taking up over 80% of the heat being added to the climate system (IPCC 2007).

Climate trends in Australia are consistent with global trends (Pittock 2003; Karoly & Braganza 2005). Gradual increases in mean annual daily temperatures in nearly all locations around the continent have been observed with daily minimum temperatures warming faster than daily maximum temperatures (Hughes 2003). Australian mean annual temperatures have

increased by 0.9°C since 1910, with greater increases observed since 1950 (Hughes 2003; CSIRO and Bureau of Meteorology 2007). Since 1950, mean annual temperatures have increased by 0.1°C to 0.2°C per decade, with a comparable increase in the frequency of very warm days (>35°C) and a decrease in the frequency of frosts and very cold nights (<5°C) (CSIRO and Bureau of Meteorology 2007; Murphy & Timbal 2008). Daily minimum temperatures have risen at a faster rate (0.11°C/decade) than daily maximum temperatures (0.06°C/decade) (Deuter 2006; Murphy & Timbal 2008).

Tasmania lies between 144.5°E and 148.0°E and stretches from 40.0°S and 43.5°S and is an island with no place more than 115 km from the ocean (Bureau of Meteorology 1993). Tasmania has a distinct gradient in topography, with high mountains in the west extending into the central regions while the east of the state remains relatively flat (Hill *et al.* 2009). The mountainous regions in the west of the state affect the flow of air over land and therefore rainfall distribution and the principle characteristic of the Tasmania climate is the interaction between the westerly wind and mountain ranges near the west coast and central plateau (Hill *et al.* 2009; Grose *et al.* 2010). This interaction strongly influences the spatial variation of cloudiness and rainfall across Tasmania (Langford 1965). The Tasmanian climate is classified as temperate maritime and the diurnal range in daily temperature from the coastal regions to the inland areas ranges from 7° to 14°C, indicating a slight continental effect. Seasonal temperature differences are moderate, with mean daily maximum temperatures in summer of 18°C to 23°C and in winter 9°C to 14°C (Bureau of Meteorology 1993).

Tasmania has experienced a 0.1°C per decade warming since the 1950's, significantly less than for Australia or the globe (Grose *et al.* 2010). Minimum temperatures have increased at a greater rate than maximum temperatures, consistent with greenhouse warming and analyses of observations globally (McInnes *et al.* 2004; Grose *et al.* 2010). Seasonally, summer temperatures across Tasmania have increased at a slightly greater rate compared to other seasons for the period 1950 to 2010.

Regional variation in the rate of warming across Tasmania is evident from temperature records at the six sites which are representative of the dairying regions. All sites recorded a rise in mean annual daily temperature since 1950 ranging from 0.07° per decade at Ouse to 0.19°C per decade at Woolnorth (Table 2.5). However, at all sites since 1950, mean annual daily maximum temperatures have risen at a greater rate than mean annual daily minimum temperatures while at Ouse the mean annual daily minimum temperature has decreased.

**Table 2.5** Mean decadal temperature trend (°C) for the period 1950 to 2010 for the sites of Woolnorth, Flowerdale, Merseylea, Cressy, Ringarooma and Ouse ([www.longpaddock.qld.gov.au/silo/](http://www.longpaddock.qld.gov.au/silo/); Jeffrey *et al.* 2001).

	Woolnorth	Flowerdale	Merseylea	Cressy	Ringarooma	Ouse
Annual mean	0.19	0.10	0.17	0.10	0.10	0.07
Annual maximum	0.20	0.20	0.17	0.19	0.14	0.20
Annual minimum	0.17	0.00	0.16	0.00	0.08	-0.07

Australia is characterised by an arid to semi-arid climate, being the driest of all inhabited continents, with highly variable rainfall both temporally and spatially (Karoly *et al.* 2005; Taschetto & England 2009). Since 1900, mean annual rainfall has increased slightly by 7.0 mm per decade (Deuter 2006), although this trend is not significant because of high inter-annual variability (Bureau of Meteorology 2011; Hughes 2003). Since 1950, north Western Australia has become wetter while much of eastern and southern Australia has become drier (Gallant *et al.* 2007) (Figure 2.4) due to a weakening or southward shift of the frontal systems that bring most of the rain to these regions (Deuter 2006). Pittock (2003) states that the largest and most statistically significant change in observed rainfall has been a decline in the winter rainfall dominated region of the far south west of Western Australia, where in the period 1975 to 2000 winter rainfall has declined by 25%. The observed rainfall decline since the mid 1990's over south eastern Australia has been driven by a reduction in autumn rainfall. This trend exhibits similar characteristics to the rainfall decline in the south west of Western Australia (Cai & Cowan 2008). The observed decrease in autumn rainfall over south eastern Australia has been linked to changes in sea surface temperature of the Indian Ocean (Cai & Cowan 2008).

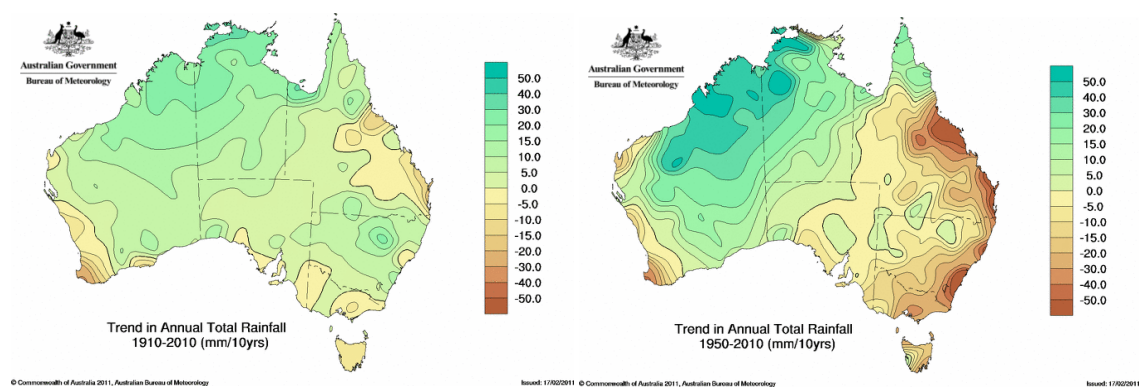


**Figure 2.4** Mean annual Australian rainfall decadal trends (mm) for the period 1910 to 2010 and 1950 to 2010 (source Bureau of Meteorology 2011).

The inter-annual and inter-seasonal variability of Australian rainfall is due to various factors including the influences of the surrounding Pacific and Indian oceans (England *et al.* 2005;

Ummenhofer *et al.* 2009). The El Niño/Southern Oscillation (ENSO) has been linked to rainfall anomalies over eastern Australia. The ENSO is responsible for global scale sea surface temperature (SST), sea level pressure (SLP) and rainfall anomalies, with a strong influence in the equatorial Pacific Ocean and over the adjoining land masses (Suppiah 2004; Hill *et al.* 2008; Taschetto & England 2009). The Southern Oscillation Index (SOI) is the standardised anomaly between the mean sea level pressure over Darwin and Tahiti. The SOI fluctuates between a positive phase (La-Niña) and a negative phase (El-Niño) and has an irregular period of 3 to 7 years (Hill *et al.* 2008). The relationship is an increase of rainfall over eastern and south eastern Australia during La Niña events, and a decrease of rainfall during El Niño events (Hunt 2008). Hughes (2003) and Suppiah (2004) report that since the 1970's a reduction has occurred in La Niña events while El Niño events have increased, with a negative trend observed in the SOI. Trenberth & Hoar (1997) have suggested that this trend and the prolonged 1990 to 1995 ENSO event have a probability of natural occurrence of roughly once in 2000 years.

Exceptions to the strong link with ENSO inter-annual variability are extended periods of above or below average rainfall (Cai *et al.* 2007). Recent observed rainfall decline in south eastern Australia is only now being studied and is yet to be attributed to external causes (Ummenhofer *et al.* 2009). Suppiah (2004) summarises that linking the recent increasing trend of El Niño events (1970 onwards) to climate change is too simplistic, stating that there are other factors to be considered such as an increase in aerosols, land cover changes and natural variability.

Tasmania has a large gradient in mean annual rainfall from the west coast (> 3000 mm) to the central midlands (500 mm to 600 mm) (Figure 2.5) (Hill *et al.* 2008; Grose *et al.* 2010). Tasmania lies in the 'Roaring 40s' belt of westerly airflow and the primary characteristic of the Tasmanian climate is the interaction between prevailing westerly wind and the mountain ranges near the west coast and the central plateau (Hill *et al.* 2009; Grose *et al.* 2010). These interactions strongly influence the spatial variation of rainfall across Tasmania.

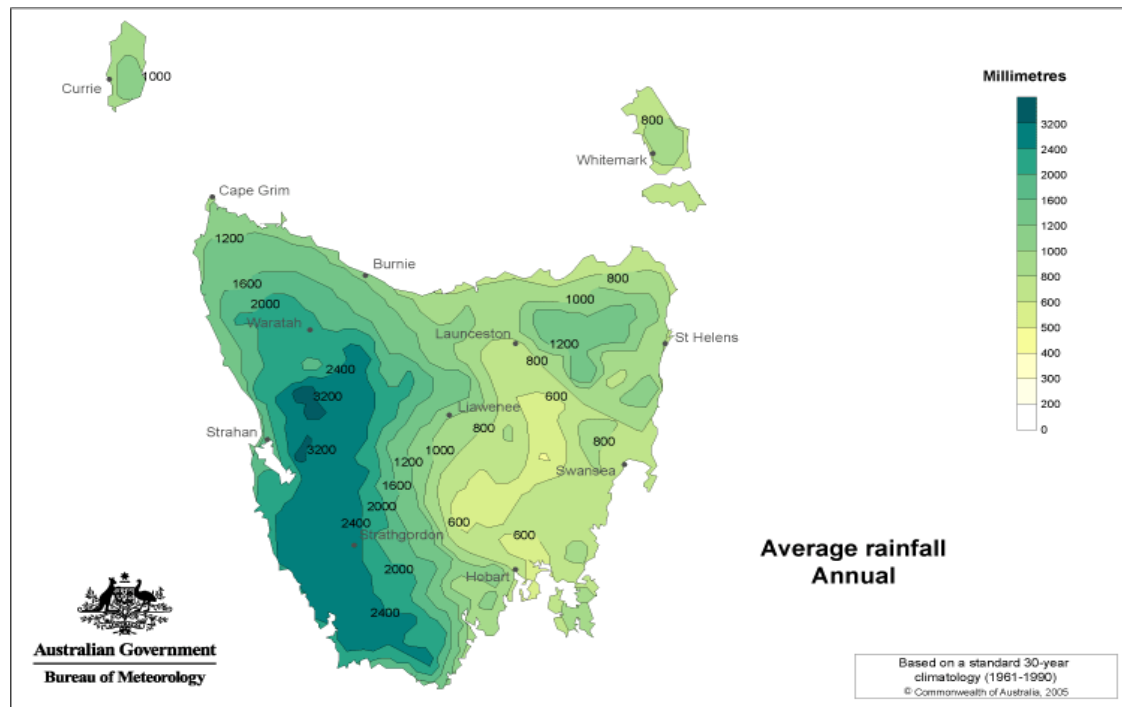


**Figure 2.5** Tasmanian mean annual rainfall for the period 1961 to 1990 (source Bureau of Meteorology 2011).

Since 1910, long term mean annual rainfall in Tasmania has remained relatively stable with no significant trend in rainfall, although a slight decrease in inter-annual variability has been observed. However since 1950, mean annual rainfall in Tasmania has declined by 22 mm per decade (Bureau of Meteorology 2011). In the south east and north west of the state rainfall has declined by 20 mm to 30 mm per decade and in the south west of the state rainfall appears to have increased by up to 30 mm per decade (McInnes *et al.* 2004). Mean annual rainfall trends since 1970 show an even greater decrease across the state (45 mm/decade) (Figure 2.6) (Bureau of Meteorology 2011) although, care must be taken in interpreting these trends since the 1970's were particularly wet in many regions, while conversely in many regions the 1990's were drier (McInnes *et al.* 2004). A characteristic of this trend has been a reduction in inter-annual variability, along with a decrease in the number of exceptionally wet years since the mid 1970's (Grose *et al.* 2010). Observed changes of rainfall have not been seasonally uniform, with the largest observed seasonal decrease occurring in autumn. The decrease in autumn rainfall has been largest in the west of the state, although total autumn rainfall for this region is also higher (Grose *et al.* 2010).

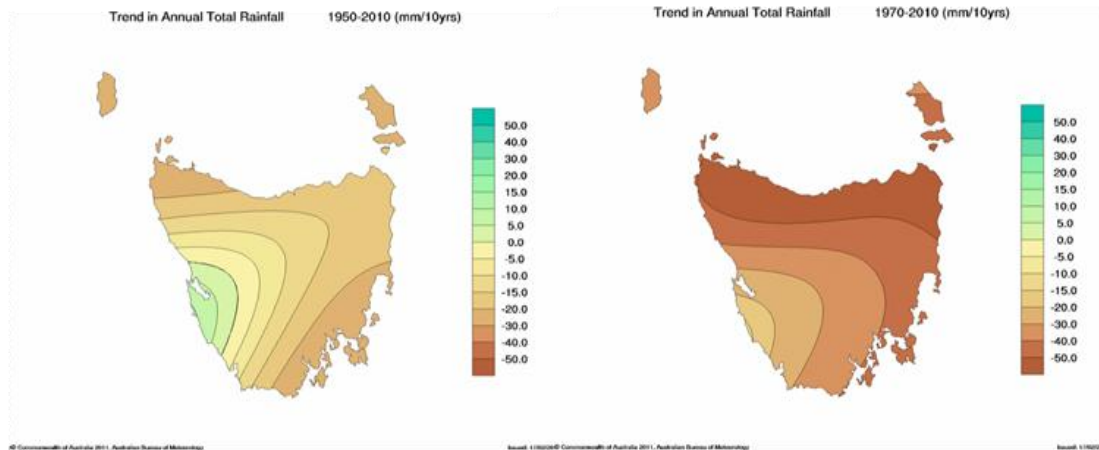


**Figure 2.6** Mean annual Tasmanian rainfall decadal trends (mm) for the period 1950 to 2010 and 1970 to 2010 (source Bureau of Meteorology 2011).

Regional rainfall trends across Tasmania’s dairying regions are evident from the rainfall records at Woolnorth, Flowerdale, Merseylea, Cressy, Ringarooma and Ouse. Since 1950, a decline has been observed in mean annual rainfall at all sites. The largest decrease of 37 mm per decade has been observed at Ringarooma, in contrast a minimal decrease of 2 mm per decade has been observed at Ouse (Table 2.6). The patterns of change in rainfall have been relatively uniform at each site across seasons (except spring at Ouse), with the largest decadal decreases in rainfall at each site having been observed in autumn (Table 2.6). However since 1910, long term mean annual rainfall at each of the six sites is consistent with statewide rainfall observations, where no significant rainfall trends are evident.

**Table 2.6** Mean decadal rainfall trends (mm) for the period 1950 to 2010 for the sites of Woolnorth, Flowerdale, Merseylea, Cressy, Ringarooma and Ouse. ([www.longpaddock.qld.gov.au/silo/](http://www.longpaddock.qld.gov.au/silo/); Jeffrey *et al.* 2001).

	Woolnorth	Flowerdale	Merseylea	Cressy	Ringarooma	Ouse
Annual mean	-21	-26	-19	-13	-37	-2
Summer mean	-3	-6	-7	-2	-6	-1
Autumn mean	-13	-13	-12	-9	-16	-10
Winter mean	0	-5	-2	-2	-10	2
Spring mean	-5	-3	1	-1	-6	6

The climate variables evaporation, potential evaporation and potential evapotranspiration are difficult to measure accurately and therefore difficult to assess trends (Gifford *et al.* 2005; Jovanovic *et al.* 2008). Evaporation is an important component of soil water balance and crop water availability (Kirono *et al.* 2009) and potential evaporation is the amount of evaporation that would occur if a non limiting water source were available (Jovanovic *et al.* 2008; Shuttleworth *et al.* 2009). Potential evapotranspiration is a function of temperature, vapour pressure, radiation, wind and available soil water moisture and is a collective term for the

transfer of water vapour to the atmosphere from both vegetated and un-vegetated land surfaces (Murphy & Timbal 2008). A number of methods are used to calculate potential evaporation. The most commonly used methods are the Penman-Monteith (Monteith 1965) and Priestly-Taylor (Priestly & Taylor 1972). The Penman-Monteith equation is the calculated evaporation rate from stretches of open water and incorporates the variables of temperature, solar radiation, wind speed and humidity. The Priestly-Taylor equation was developed as a substitute to the Penman-Monteith equation to remove the dependence on multiple observations and can be calculated using solar radiation observations alone.

There has long been an expectation that potential evaporation will increase as the average surface air temperature increases (Roderick & Farquhar 2004; Jovanovic *et al.* 2008). However, Roderick & Farquhar (2004) reported for the period 1970 to 2002 (30 sites, across the continent) a reduction in Class A pan evaporation across Australia was observed despite an increase in daily maximum temperatures and no evidence of a decline in solar radiation (Nicholls 2007). Pan evaporation declined on average 4 mm per year (Roderick & Farquhar 2004). In addition, pan evaporation data sourced from the Bureau of Meteorology (2011) shows a negative trend of 30 mm per decade for the period 1975 to 2010. The observed decreases in pan evaporation rates in Australia are similar to averaged trends in the Northern Hemisphere over the last 30 to 50 years (Roderick & Farquhar 2004).

Roderick & Farquhar (2004) suggest there are three possibilities to explain a reduction in pan evaporation across Australia, decreases in one or more of vapour pressure deficit, net radiation and wind speed. However, Jovanovic *et al.* (2008) questioned the reliability of the pan evaporation data for the period 1970 to 2005. The reliability of the observed historical data can be affected by non-climatic factors such as station relocations, changes in exposure, or changes in observational practices. These factors can lead to inhomogeneities in the observed historical data which can lead to misleading trend estimates. For the period 1970 to 2005, homogenised data from 60 sites across the continent exhibited a slight negative trend of  $-2.5 \pm 5.1$  mm per year in annual pan evaporation (Jovanovic *et al.* 2008). Despite regional changes on a continental scale, there has been no marked change in Class A pan evaporation over the prior four decades (Jovanovic *et al.* 2008). Across Tasmania a slight decrease of 0.6 mm per decade in annual pan evaporation has been observed for the period of 1975 to 2010 (Bureau of Meteorology 2011). Trends since 1970 vary spatially and between seasons, a decrease in pan evaporation has been observed in summer while an increase has been observed in winter pan evaporation rates (Grose *et al.* 2010).

The climate of the earth changes over a range of timescales, although evidence of an anthropogenic influence on recent climate has steadily increased during the past two decades (CSIRO and Bureau of Meteorology 2007). The IPCC (2007) concluded that most of the observed increase in globally averaged temperatures since the mid 20<sup>th</sup> century is very likely due to the observed increase in anthropogenic greenhouse gas concentrations. Increases in atmospheric greenhouse gases change the radiative heat balance of the earth, influencing the entire climate system (CSIRO and Bureau of Meteorology 2007). Global atmospheric concentrations of carbon dioxide (CO<sub>2</sub>), methane (CH<sub>4</sub>) and nitrous oxide (N<sub>2</sub>O) have increased significantly as a result of human activities since 1750 and now far exceed pre-industrial values determined from ice cores spanning many thousands of years (IPCC 2007; Petit *et al.* 1999). Furthermore, the IPCC (2007) state that the atmospheric concentrations of CO<sub>2</sub> and CH<sub>4</sub> in 2005 far exceed the natural range over the past 10,000 years (Figure 2.7). The global increases in CO<sub>2</sub> concentrations are primarily due to fossil fuel use, with land use change providing another significant but smaller contribution. The increase in observed CH<sub>4</sub> concentrations is primarily due to agriculture and fossil fuel use, while the increase in N<sub>2</sub>O concentrations is primarily due to agriculture (IPCC 2007). Mean annual atmospheric CO<sub>2</sub> concentrations have increased at a rate of 1.7 ppm per year over the period 1999 to 2008 (Le Quere *et al.* 2009). Further, Petit *et al.* (1999) state that the current atmospheric CO<sub>2</sub> concentrations exceed those of the past 420,000 years and the current rate of increasing CO<sub>2</sub> levels is unprecedented during the past 20,000 years.

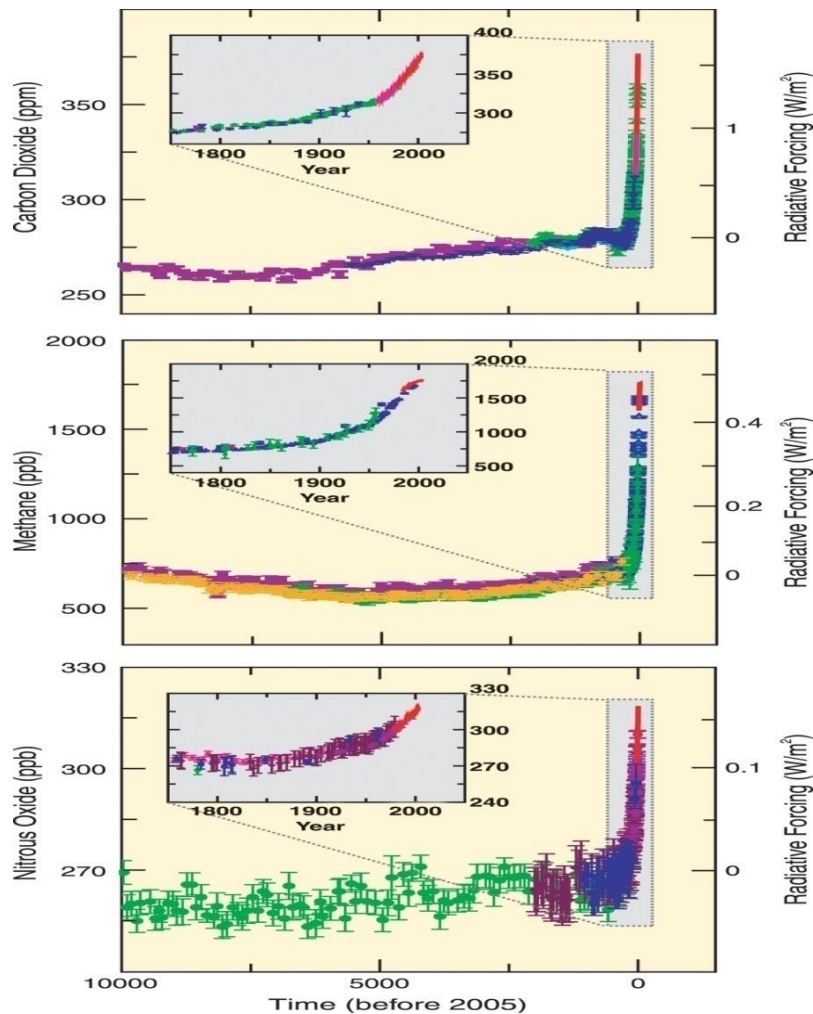


**Figure 2.7** Increases in greenhouse gases (CO<sub>2</sub> ppm, CH<sub>4</sub> ppb, N<sub>2</sub>O ppb) over the last 10,000 years (large panels) and since 1750 (insert panels) from ice cores and modern data (source IPCC 2007).

Global atmospheric CO<sub>2</sub> concentrations have increased from a pre-industrial level of approximately 280 ppm to 390 ppm in 2010. To estimate future climate change the IPCC Special Report on Emissions Scenarios (SRES), Nakicenovic & Swart (2000) calculated 40 greenhouse gas and sulfate aerosol emission scenarios for the 21<sup>st</sup> century. The SRES scenarios were the result of combining a variety of assumptions about demographic, economic and technological driving forces most likely to influence emissions in the future (Anwar *et al.* 2007). The SRES scenarios are divided into four primary groups: A1, A2, B1 and B2 (Nakicenovic & Swart 2000). The A2 scenario features less rapid technological changes and a more heterogeneous world, and by the end of the 21<sup>st</sup> century, the A2 scenario has a lower emission rate than the A1FI scenario. The A1FI scenario is characterised by a future of rapid economic growth and is fossil energy intensive. However, since 2001 the observed global greenhouse gas emissions have been tracking above the A1FI scenario (Le

Quere *et al.* 2009), indicating that a higher emission scenario is probable, at least in the foreseeable future. Under the A2 emissions scenario, atmospheric CO<sub>2</sub> levels are projected to be greater than 800 ppm by the end of the 21<sup>st</sup> century (IPCC 2007; Leakey *et al.* 2009). Romanova (2005) states that the maximum level of the projected atmospheric levels of CO<sub>2</sub> based on known fossil fuel resources and rate of use, could feasibly attain a level of 1500 to 2000 ppm.

Projecting the impact of increasing greenhouse gases on the global, continental and regional scale is considered a major scientific challenge. General Circulation Models (GCMs) provide the best available estimates for assessing potential climate change on a global scale and are at the centre of climate projections (Mitchell 2004; Brankovic *et al.* 2010). General circulation models are based on established physical principles and are capable of reproducing the most significant features of the observed climate (Perkins & Pitman 2009). The models are designed to simulate the main components (atmosphere, oceans, sea ice and land surface) of the earth's climate system in a simplified although robust manner (Grose *et al.* 2010). There is now confidence that GCMs are able to provide credible quantitative estimates of future climate predictions (Randall *et al.* 2007), particularly at a continental scale. Confidence levels are higher for some climate variables such as maximum and minimum temperatures than other variables such as precipitation (Corney *et al.* 2010).

Estimates of future greenhouse concentrations are an important element of modelling climate change. Approximately half the uncertainty in the extent of climate change is due to differences in the emissions scenarios (Nicholls 2007). The SRES scenarios of the IPCC (Nakicenovic & Swart 2000) incorporate six primary CO<sub>2</sub> emissions scenarios based on various assumptions regarding economic growth, technological development, social change and demographics for the 21<sup>st</sup> century (Figure 2.8).

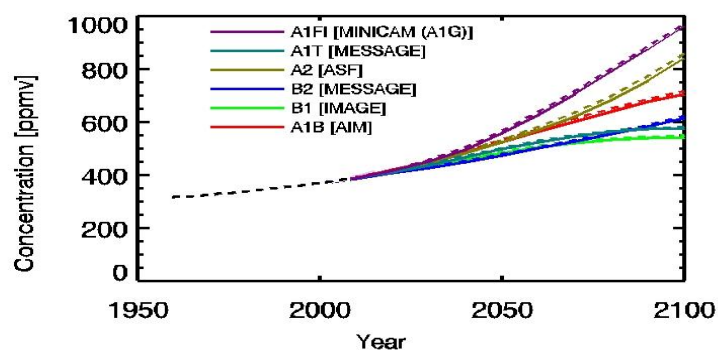


**Figure 2.8** Projected atmospheric CO<sub>2</sub> concentrations (ppmv), from six primary SRES scenarios (Nakicenovic & Swart 2000).

Climate models have been improving in accuracy as the physical parameters improve and as the spatial resolution increases due to increasing computer speed (McIntosh *et al.* 2005). In addition, the observed warming trends in the 20<sup>th</sup> century are now reproduced by many GCMs. The Coupled Model Intercomparison Project (CMIP) stated ‘that the disparity between a typical model simulation and a baseline set of observations is not much greater than the difference between sets of observations’ (Covey 2003). Although GCMs adequately simulate climate changes due to increasing greenhouse gases, it remains difficult to simulate natural climate variability (McIntosh *et al.* 2005).

Climate change is a global occurrence, of which the specific impacts will be felt in changes to dominant local weather conditions. Smith *et al.* (2005) report that global mean temperature change, while useful as a measure of the overall strength of greenhouse warming, is not the most relevant measure for regional impact analysis. The spatial resolutions of GCMs are typically 200 km to 400 km, a scale that does not represent regional climates especially where complex topography plays an important role in weather patterns (Thomson *et al.* 2002). This necessitates that local or regional studies are required to understand the likely effects of climate change to specific areas (Corney *et al.* 2010). High quality climate projections at a local scale in Tasmania were previously unavailable. The Climate Futures for Tasmania (CFT) project addressed this issue.

The CFT project generated climate projections specific to Tasmania through fine scale climate modelling using a dynamical downscaling approach (Corney *et al.* 2010). The CFT project used CSIROs Conformal Cubic Atmospheric Model (CCAM) to dynamically downscale five of the twenty three GCMs reported in the IPCC fourth assessment report (AR4) and a sixth GCM, CSIRO-Mk3.5 (Corney *et al.* 2010). Dynamical downscaling allows synoptic weather systems to be expressed at finer scales than those in GCMs while taking into account the interaction between the weather systems and Tasmania’s topography and vegetation (Bennett *et al.* 2010; Holz *et al.* 2010).

The downscaling undertaken by CFT increased the spatial resolution from 2° to 3° grid cells in the GCMs down to a 0.1° grid (approximately 10 x 10 km) for Tasmania (Corney *et al.* 2010). Two SRES emission scenarios were used; A2, a higher greenhouse gas emission scenario, and B1, a lower emission scenario (Nakicenovic & Swart 2000). The models used were CSIRO-Mk3.5, ECHAM5/MPI-OM, GFDL-CM2.0, GFDL-CM2.1, MIROC3.2 (medres) and UKMO-HADCM3 and the GCMs were primarily selected on objective metrics of the models skill in simulating the climate over south east Australia (Corney *et al.* 2010).

Grose *et al.* (2010) reported that the CFT modelling outputs displayed a high level of skill in reproducing the recent climate of Tasmania across a range of climate variables. The multi-model mean of the Tasmanian mean daily maximum temperature for the period 1961 to 1990 was within 0.1°C of the Bureau of Meteorology (2010) observed value of 10.4°C. The modelled total annual Tasmanian rainfall of 1385 mm was very close to the observed value of 1390 mm. In addition, the mean monthly temperature had a spatial correlation of 0.99 with gridded observations over the state, while for rainfall the spatial correlation was 0.69.

The CFT modelling projections under the A2 scenario show an increase in mean daily temperature of 2.9°C over the 21<sup>st</sup> century. The temperature increase for Tasmania under the A2 scenario is less than mainland Australia and the global projections of 3.4°C. The relatively lower projected changes for Tasmania are due in part to the temperate Southern Ocean storing excess heat and moderating the temperature of the maritime climate in Tasmania (Grose *et al.* 2010). The six GCMs show a range of temperature rise from 2.6°C to 3.3°C. In addition the projections indicate that temperature increases are lower in the early part of the century, although the rate of change increases towards the end of the century. The daily maximum temperature rise is projected to be slightly lower (2.85°C) than the daily minimum temperature rise (2.89°C) (Grose *et al.* 2010).

The CFT multi model mean projections of mean annual rainfall shows changes of less than 100 mm throughout the modelling period under the A2 emissions scenario and decadal variability is projected to remain constant. However, there are projected seasonal and regional changes to occur throughout the 21<sup>st</sup> century (Grose *et al.* 2010). The multi-model mean of the projected changes indicate an increase of 20% to 30% of summer and autumn rainfall along the east coast. On the west coast a 15% decrease is projected in winter rainfall and an 18% decrease in summer rainfall. In the central plateau region seasonal rainfall is projected to decrease through all seasons (Grose *et al.* 2010; Holz *et al.* 2010). Grose *et al.* (2010) report that the projected changes to the general climate in the CFT simulations also impact on a range of other climate variables. The increasing temperature over the 21<sup>st</sup> century is the dominant driver of a significant increase in pan evaporation (up to 19%). Spatially complex changes to the average wind speed are projected, average cloud cover is projected to decrease slightly and solar radiation is projected to remain relatively constant.

## 2.4 Evaluating climate change on dairying

Changes in climate across the dairy regions of Tasmania are likely to alter pasture growth rates, which has the potential to modify current dairy farming practices. Even subtle changes in the projected amount or seasonal distribution of rainfall, or changes projected to occur in temperature and evaporation rates, will influence regional seasonal pasture growth patterns, irrigation requirements and water availability. Currently within the Tasmanian dairy industry, there is limited information regarding the impact of regional climate change on pasture based dairy systems. Necessitating the need for biophysical modelling to quantify the impacts climate change will have on regional pasture based dairy systems in Tasmania.

Projections of climate change impacts on agriculture are largely based on biophysical and hydrological modelling (Soussana *et al.* 2010). Biophysical models incorporate climate indices that simulate crop or pasture growth while hydrological models are used to estimate water yields from catchments and river flows. Long term meteorological records are often only available for a few climate variables and these models are generally developed to use the climate data available. Numerous models require only daily minimum and maximum temperature and rainfall, while other models can utilise potential evaporation, solar radiation and relative humidity (Holz *et al.* 2010).

Climate change projections and scenarios provide the input into simulation models, and the models are considered essential tools in order to quantify the impacts of a changing climate on agriculture and to further evaluate adaptation strategies (Holz *et al.* 2010). Simulation models have a role in projecting and understanding the impacts of climate on biophysical systems (White *et al.* 2008) and are also a valuable support for biophysical research, enabling the effects of regional environments and weather patterns to be quantified (Johnson *et al.* 2008).

Pasture systems are complex, involving interactions between soils, plants, water, animals, weather and management (Bryant & Snow 2008; White *et al.* 2008). Experimental observations alone provide limited, although essential information given the temporal and spatial scale of the processes in a pasture system. The use of biophysical models are able to provide greater insights and understanding (Johnson *et al.* 2003; White *et al.* 2008), particularly for long term analyses such as the impact of variability in weather or climate change projections (Johnson *et al.* 2008). Modelling allows a means of extrapolating research site outcomes to other sites and seasons and explore the relative impact of a range of

management interventions along with regional climate variation at a whole farm system level (Johnson *et al.* 2008).

Experimental observations of plant responses to climate variables has resulted in the development of a wide range of biophysical models (Gobin 2010) and include models such as the EcoMod suite (EcoMod, DairyMod, SGS Pasture Model) (Johnson *et al.* 2008), APSIM (Keating *et al.* 2003), GRAZZPLAN (GrazFeed, GrossGro, AusFarm) (Moore *et al.* 1997) and the DairyNZ Whole farm Model (Wastney *et al.* 2002; Beukes *et al.* 2005). The biophysical simulation model DairyMod simulates biophysical processes in greater detail than a typical computer based decision support system, and generates a greater amount of output for analysis (Johnson *et al.* 2008). Evaluating models such as DairyMod is a complex and ongoing process. DairyMod uses daily climate and comprises soil water, soil nutrient, pasture growth and animal production modules and allows the ability to explore the inter-relationships between these modules, either in a whole systems context, or as individual components over many years (Cullen *et al.* 2008). For DairyMod to be used in this context the degree of confidence in the simulation of the components of a system need to be quantified particularly for grazing systems. The model must be capable of simulating the temporal dynamics of pasture growth and removal, since these are the drivers of many other key system properties such as nutrient cycling, organic matter accumulation or loss and animal intake (Cullen *et al.* 2008). Therefore, it is important to test and quantify the performance of a simulation model. Comparing model outputs with experimental data is considered a fundamental test of a model (White *et al.* 2008).

Cullen *et al.* (2008) collated a range of pasture growth rates (perennial ryegrass, annual ryegrass and white clover) for a range of environments and management systems across Australia and New Zealand. The environments ranged from cool temperate climates in Tasmania and New Zealand to the subtropical regions of south eastern Queensland. The aim of the study was to quantify whether DairyMod could satisfactorily simulate pasture growth rates by comparing measured and modelled net herbage accumulation rates. The modelled herbage accumulation rates were similar to that in the measured range of the pasture growth herbage accumulation data across all the sites. In general the modelled predictions were better in the temperate than in the subtropical environments. The results of Cullen *et al.* (2008) study showed that DairyMod can realistically simulate monthly herbage accumulation rates and seasonal yields of ryegrass based pastures in both temperate and subtropical environments, across a range of soil types and pasture management options.

## CHAPTER 3: HISTORICAL COMPARISON BETWEEN AN OBSERVED AND THREE INTERPOLATED CLIMATE DATA SOURCES

### 3.1 Introduction

Historical surface observed climate data is an important component of climate knowledge. Within Australia the Bureau of Meteorology is the custodian of a vast quantity of surface observed climate data collected from a variety of instruments and locations (Rayner *et al.* 2004). Spatial modelling applications require gridded climate datasets, which are estimates of climate variables over large areas rather than observed climate records. Gridded climate data sets are constructed by spatial interpolation of climate observations. Time series from such gridded data sources can be utilised at locations where there are no observed climate records, or to fill in gaps of incomplete records. In some instances synthetic time series are preferable over observed climate records as the spatial interpolation algorithm smoothes out local site specific environmental effects. A complete and accurate climate data source is a prerequisite for the efficient modelling of a wide variety of environmental processes (Jeffrey *et al.* 2001; Rayner *et al.* 2004).

The use of biophysical and hydrological models is driving an increasing demand for spatially interpolated climate data. However Daly (2006) concludes that many users do not have a substantial background in geospatial climatology and as a result are not in a position to critically assess the suitability of spatial climate data sets. Errors associated with and between spatial climate data sets are commonly assumed to be negligible. This assumption may effect the interpretation of results, conclusions and decisions made from these results. There is a growing awareness that spatially interpolated climate data sets contain a degree of error (Willmott & Johnson 2005).

The complexity of interpolating observed climate variables onto gridded cells is highlighted by irregular topography and under representation of high elevation areas (Beesley *et al.* 2009). The complexity is reflected in rainfall and potential evaporation, where these metrics can be highly variable over area and time, making them difficult to reliably interpolate from surrounding station observations (Jeffrey *et al.* 2001). There are currently three sources of historical, continuous, daily climate data within Australia;

- SILO Patched Point data
- SILO Data Drill – 0.05°
- Australian Water Availability Project (AWAP) – 0.05°.

Climate Futures for Tasmania (CFT) created a fourth daily climate data source, AWAP – 0.1°. This data source was created to compare directly to regional climate model outputs at 0.1°C resolution in validation exercises, and is not available commercially as a formal gridded climate data product. This data source is included in this analysis to illustrate effects of interpolating to larger grid scales.

The SILO data sources ([www.longpaddock.qld.gov.au/silo/](http://www.longpaddock.qld.gov.au/silo/); Jeffrey *et al.* 2001) are presently the most easily accessible and are frequently used in agricultural models, although the AWAP data source is increasingly being used. The historical daily climate data sources are not however, fully consistent with one another due to the scale and interpolation methods (Beesley *et al.* 2009).

Jeffrey *et al.* (2001) undertook a comprehensive archiving of Australian rainfall and climate data constructed from ground based observational data. Continual daily time step records were constructed using spatial interpolation algorithms to estimate missing data. The product of this was the SILO Patched Point Data set which was constructed for daily rainfall, maximum and minimum temperature, evaporation, solar radiation and vapour pressure for approximately 4600 locations across Australia. Locations without observational data, (e.g. maximum temperature) contain interpolated estimates that are computed for those locations, or in some instances are taken directly from gridded surfaces.

Jeffrey *et al.* (2001) also produced SILO Data Drill – 0.05° which is a high resolution gridded surface generated by spatial interpolation calculated by splining and kriging techniques of observed daily data. All climate variables (except mean sea level pressure) were generated by spatial interpolation using a trivariate thin plate smoothing spline with latitude, longitude and elevation as independent variables. Elevation was expressed in kilometers to minimise the validated root mean square interpolation error, latitude and longitude were in units of degrees. All surfaces were fitted by minimising the generalised cross validation error with constraint of first order smoothness imposed. The daily climate data in the SILO data drill sets are all synthetic with no original meteorological station data left in the calculated grid fields. SILO Data drill data has been produced on a regular grid 0.05° extending from latitude 10°S to 44°S and longitude 112°E to 154°E.

The Bureau of Meteorology and CSIRO also generated a meteorological analysis and remotely sensed datasets for Australia as a contribution to AWAP ([www.bom.gov.au/jsp/awap](http://www.bom.gov.au/jsp/awap)). The AWAP product provides interpolated data sets from 1900 onwards. Jones *et al.* (2007) state that robust topography resolving analysis methods have

been developed and applied to meteorological observations of rainfall, maximum and minimum temperature, potential and total evaporation, solar radiation and vapour pressure to produce analyses at a resolution of  $0.05^\circ$  by  $0.05^\circ$ . The analyses (grids) are computer generated using a sophisticated technique which incorporates an optimised Barnes successive correction technique that applies a weighted averaging process to the station data (Jones *et al.* 2007). Topographical information is included by the use of temperature ratio (actual temperature divided by monthly average) in the analysis process. The AWAP climate data is interpolated from observations catalogued by the Bureau of Meteorology's climate databank (Australian Data Archive for Meteorology).

The objectives of this Chapter were to:

1. Compare the monthly and annual means between the climate variables maximum and minimum temperature, rainfall and potential evaporation of the four currently available data sources at six sites, for the period 1971 to 2007.
2. Compare monthly and annual means of simulated perennial ryegrass growth from the biophysical model DairyMod between the four currently available data sources at six sites, for the period 1971 to 2007.

### **3.2 Materials and methods**

Four climate data sources were compared. These were;

- 1 SILO Patched Point Data – observations at climate stations with missing data interpolated (Jeffrey *et al.* 2001).
- 2 SILO Data Drill –  $0.05^\circ$  gridded data set with all values interpolated (Jeffrey *et al.* 2001).
- 3 Australian Water Availability Project (AWAP) –  $0.05^\circ$  gridded data set of interpolated values (Jones *et al.* 2009).
- 4 Australian Water Availability Project (AWAP) –  $0.01^\circ$  gridded data set of interpolated values (Corney *et al.* 2010).

The SILO Patched Point Data and SILO Data Drill continuous daily climate were obtained from the SILO database (<http://www.longpaddock.qld.gov.au/silo/>, Jeffrey *et al.* 2001). The Australian Water Availability Project (AWAP) –  $0.05^\circ$  gridded data set of interpolated values of continuous daily climate data was obtained from (<http://www.bom.gov.au/jsp/awap/>). The Australian Water Availability Project (AWAP) –  $0.01^\circ$  gridded data set of interpolated values of continuous daily climate data was obtained from the Tasmanian Partnership for Advanced Computing (TPAC) portal (<https://dl.tpac.org.au/>). The daily climate data sets for each site for

the period 1<sup>st</sup> January 1961 to 31<sup>st</sup> December 2007 were accessed, the climate metrics of maximum and minimum temperature (°C), rainfall (mm) and potential evaporation (mm) were accessed. The latitude and longitude coordinates shown in Table 3.1 are the location of the SILO Patched Point Data observation stations at each site. The six sites selected are representative of the dairying regions of the north west (Woolnorth and Flowerdale) central north (Merseylea), the northern Midlands (Cressy), the north east (Ringarooma) and the south (Ouse).

**Table 3.1** Latitude, Longitude and Elevation (AMSL) (m) at the sites of Woolnorth, Flowerdale, Merseylea, Cressy, Ringarooma and Ouse.

Location	Latitude	Longitude	Elevation (m)
Woolnorth	40°.68' S	144°.72' E	10
Flowerdale	40°.99' S	145°.61' E	18
Merseylea	41°.33' S	146°.41' E	41
Cressy	41°.72' S	147°.08' E	166
Ringarooma	41°.25' S	147°.73' E	282
Ouse	42°.48' S	146°.71' E	95

Hereafter the climate data sources will be referred to as PP (SILO Patched Point Data), DD (SILO Data Drill – 0.05°), AWAP 0.1 (AWAP 0.1°) and AWAP 0.05 (AWAP 0.05°).

DairyMod version 4.9.2 (Johnson *et al.* 2008) was used to simulate rainfed perennial ryegrass production. A cutting treatment was applied where the pasture was harvested on the last day of each month to a residual dry matter of 1400 kg DM/ha. All simulations were conducted without nutrient limitation and the soil was a generic clay loam (Table 3.2). The same soil physical and chemical parameters were used across each site as the principle aim was to determine climatic differences and trends.

The Growth Limiting Factor of Temperature ( $GLF_{\text{temperature}}$ ) is on a scale of 0 to 1, and is defined as the ratio between leaf gross photosynthesis temperature response at the current temperature ( $f_p(T)$ ) to that of leaf gross photosynthesis temperature response function at optimal temperature ( $f_p(T_{\text{opt}})$ ) such that  $GLF_{\text{temperature}}$  is;

$$GLF_T = \frac{f_p(T)}{f_p(T_{\text{opt}})} \quad (1)$$

With DairyMod, perennial ryegrass responses to temperature are described by a generic empirical curve. This curve defines the minimum, optimum and maximum temperature for photosynthesis based on a representative diurnal temperature that simulate growth restrictions in response to high temperature stress 28°C and frost 2°C (Cullen *et al.* 2009). Both the frost

(2°C) and high temperature stress (28°C) temperature parameters were activated within the model for the simulations.

High temperatures during the day can affect growth on that day, and subsequent growth. The reduction in pasture growth of perennial ryegrass due to high daily temperature extremes lies linearly between 28°C (onset temperature – when plant function begins to decrease) and 35°C (full temperature – when plant function ceases). The recovery period following exposure to heat stress required by the perennial ryegrass plant before photosynthetic function resumes, is represented in DairyMod by the critical T-sum. The default critical T-sum setting of 50 in DairyMod relates to accumulative temperature difference during the recovery period (calculated as 25°C minus the mean daily temperature reaches 50 or more, photosynthesis and plant growth in the model resumes) (Equation 2) (Johnson 2005).

$$T_{sum} = \sum \max(0, 25 - T_{mean}) \quad (2)$$

**Table 3.2** Key variables and associated parameter values used in DairyMod (Version 4.9.2) to simulate growth of perennial ryegrass pastures on a generic clay loam soil.

<i>Plant variables</i>				
Maximum photosynthesis rate at reference temperature (mg CO <sub>2</sub> /m <sup>2</sup> /s)				1.0
Light extinction coefficient m <sup>2</sup> ground/m <sup>2</sup> leaf				0.5
C partitioned to total shoot (% of total net C assimilated)				80.0
C partitioned to leaf (% of C partitioned to total shoot)				20.0
C partitioned to leaf (% of C partitioned to total shoot)				70.0
Optimum N content of leaf tissue (%DM)				4.0
Leaf appearance interval at 5 MJ/m <sup>2</sup> / irradiance (d)				22.0
Leaf appearance interval at 25 MJ/m <sup>2</sup> / irradiance (d)				9.0
Number of live leaves per tiller				3.0
Transfer of dead material to litter at reference irradiance (%/day)				12.5
Maximum root depth (cm)				40.0
Depth to 50% of root mass (cm)				15.0
Root senescence rate at reference irradiance (% total live weight/day)				2.0
Initial shoot dry weight (t DM/ha)				1.0
Fraction of green material in initial shoot weight (%)				50.0
Initial root dry weight (t DM/ha)				1.0
Atmospheric CO <sub>2</sub> concentration (ppm) - constant				380
<i>Soil profile description</i>				
	Soil profile layer			
	Surface	A	B1	B2
Depth to bottom of horizon (cm)	2	50	100	200
Texture	C-L	C-L	C-L	C-L
Saturated water content (% volume)	48	48	48	48
Saturated hydraulic conductivity (cm/day)	6.7	6.7	6.7	6.7
Field capacity (% volume)	40	40	40	40
Wilting point (% volume)	19	19	19	19
Air dry water content (% volume)	13	13	13	13
<i>Soil variables</i>				
Initial water content to wilting point (mm)				274
Organic C content of the surface soil (% mass)				3.0
Organic content to 10cm depth (% mass)				2.1
C:N ratio of organic matter				8.0
Rate of decay of fast turnover pool or organic matter (%/day)				1.5
Rate of decay of slow turnover pool of organic matter (%/day)				0.012
Half life of fast turnover of organic matter (d)				46
Half life of slow turnover pool of organic matter (year)				15.8

Daily climate data from the four climate data sources at each site for the period 1<sup>st</sup> January 1961 to 31<sup>st</sup> December 2007 were used to drive the DairyMod simulations, and the annual and monthly pasture growth rates were exported to a spreadsheet for further computation. The daily weather data used were maximum and minimum temperature (°C), rainfall (mm) and potential evaporation (mm). Results for the first 10 years were discarded to allow the model to equilibrate, and the simulated monthly and annual cut yields for the remaining 36 years were averaged to compare the four climate data sources.

A test of normality was carried out on each climate variable within each climate data set using the statistical analysis package SPSS (Version 11.5, SPSS Corporation, IL, USA). Climate metrics and the simulated annual and monthly pasture production for each region were analysed as one-way ANOVA with replication (year) using SPSS. Least significant difference

(LSD), as defined by Steel and Torrie (1960) were used to compare difference between means for the four climate data sources. Inter-annual rainfall variability was quantified using the coefficient of variation (CV) (standard deviation/average) over the 36-year time period.

### 3.3 Results and Discussion

#### 3.3.1 Temperature

At all sites except Cressy, there were significant ( $P < 0.05$ ) differences in the mean annual daily maximum temperature between the four sources of climate data. At Woolnorth, the PP data had a significantly ( $P < 0.05$ ) lower mean annual daily maximum temperature than the other climate data sources. For the region of Flowerdale, AWAP 0.1 data had a significantly ( $P < 0.05$ ) lower mean daily maximum temperature than the other climate data sources. At the site of Merseylea the DD had a significantly ( $P < 0.05$ ) lower mean annual daily maximum temperature than the other three climate data sources. For the region of Ringarooma the DD data had a significantly ( $P < 0.05$ ) lower mean annual daily maximum temperature than the other climate data sources, while the PP data was significantly ( $P < 0.05$ ) higher than AWAP 0.1 but not AWAP 0.05 data. At Ouse the AWAP 0.1 data had a significantly ( $P < 0.05$ ) lower mean annual daily maximum temperature than the other climate data sources (Table 3.3). Across all sites, none of the four climate data sources were consistently lowest or highest. The differences between the mean annual daily maximum temperature ranged from 0.20°C (Cressy) to 0.57°C (Ouse).

**Table 3.3** Mean annual daily maximum temperature (°C) for the sites Woolnorth, Flowerdale, Merseylea, Cressy, Ringarooma and Ouse from the data sources of AWAP 0.1, AWAP 0.05, PP and DD for the period 1971 to 2007.

Data set	Woolnorth	Flowerdale	Merseylea	Cressy	Ringarooma	Ouse
AWAP 0.1	16.53 <sup>a</sup>	16.30 <sup>b</sup>	16.97 <sup>a</sup>	17.45	16.53 <sup>b</sup>	16.73 <sup>b</sup>
AWAP 0.05	16.63 <sup>a</sup>	16.58 <sup>a</sup>	16.86 <sup>a</sup>	17.46	16.74 <sup>ab</sup>	17.18 <sup>a</sup>
PP	16.24 <sup>b</sup>	16.55 <sup>a</sup>	16.90 <sup>a</sup>	17.48	16.76 <sup>a</sup>	17.30 <sup>a</sup>
DD	16.70 <sup>a</sup>	16.55 <sup>a</sup>	16.57 <sup>b</sup>	17.28	16.22 <sup>c</sup>	17.30 <sup>a</sup>
LSD ( $P = 0.05$ )	0.2	0.18	0.17	ns	0.21	0.26

Means with differing subscripts next to values indicate a significant difference at  $P < 0.05$ .

For all regions except Woolnorth, significant differences ( $P < 0.05$ ) in mean monthly maximum temperatures between the four climate data sources occurred during the months of April to October (Appendix 1.2-6). At Woolnorth the PP mean monthly maximum temperature was significantly lower year round than the other three data sources (Appendix 1.1). This is most probably the result of the coastal effect on temperature at Woolnorth, where

the water temperature can be significantly different from the adjacent land temperature. Daly *et al.* (2002), report that the thermodynamic properties of water are very different than those of land, creating complex temperature gradients along coastlines and at adjacent land areas. A temperature gradient is evident at Woolnorth, where each of the gridded climate data sources, incorporates Bass Strait.

At all sites except Woolnorth, there were significant ( $P < 0.05$ ) differences in the mean annual daily minimum temperature between the four sources of climate data. For the region of Flowerdale the AWAP 0.05 data had a significantly ( $P < 0.05$ ) higher mean annual daily minimum temperature than the PP and DD data. At Merseylea, AWAP 0.05 data had a significantly ( $P < 0.05$ ) lower mean annual daily minimum temperature than the PP data. For the region of Cressy, AWAP 0.05 data had a significantly ( $P < 0.05$ ) lower mean annual daily minimum temperature than the PP and DD data. At Ringarooma, the DD data had a significantly ( $P < 0.05$ ) lower mean annual daily minimum temperature than the AWAP 0.05 and PP data. For the region of Ouse the PP data had a significantly ( $P < 0.05$ ) higher mean annual daily minimum temperature than the other climate data sources, while the AWAP 0.1 data had a significantly ( $P < 0.05$ ) lower mean annual daily minimum temperature than the other climate data sources (Table 3.4). At all sites except Flowerdale, the PP data had the highest mean annual daily minimum temperature and the DD data at all sites except Merseylea and Cressy had the lowest mean annual daily minimum temperature. The differences between the mean annual daily minimum temperature ranged from 0.18°C (Woolnorth) to 0.70°C (Ouse).

**Table 3.4** Mean annual daily minimum temperature (°C) for the sites Woolnorth, Flowerdale, Merseylea, Cressy, Ringarooma and Ouse from the data sources of AWAP 0.1, AWAP 0.05, PP and DD for the period 1971 to 2007.

Data set	Woolnorth	Flowerdale	Merseylea	Cressy	Ringarooma	Ouse
AWAP 0.1	9.55	8.18 <sup>ab</sup>	7.37 <sup>ab</sup>	5.91 <sup>bc</sup>	6.86 <sup>ab</sup>	5.24 <sup>c</sup>
AWAP 0.05	9.56	8.28 <sup>a</sup>	7.25 <sup>b</sup>	5.87 <sup>c</sup>	6.97 <sup>a</sup>	5.49 <sup>b</sup>
PP	9.68	8.02 <sup>b</sup>	7.47 <sup>a</sup>	6.22 <sup>a</sup>	7.04 <sup>a</sup>	5.94 <sup>a</sup>
DD	9.50	8.00 <sup>b</sup>	7.29 <sup>ab</sup>	6.08 <sup>ab</sup>	6.71 <sup>b</sup>	5.65 <sup>b</sup>
LSD ( $P = 0.05$ )	ns	0.21	0.20	0.18	0.19	0.16

Means with differing subscripts next to values indicate a significant difference at  $P < 0.05$ .

For the regions of Merseylea, Cressy, Ringarooma and Ouse the PP data had a significantly ( $P < 0.05$ ) higher mean monthly minimum temperature during the winter months and also during spring at Ouse than the other climate data sources. Additionally at Ouse, the PP and DD data had a significantly ( $P < 0.05$ ) higher mean monthly minimum temperature during January, February and March than the AWAP 0.1 data. At Ringarooma the DD data had a

significantly ( $P < 0.05$ ) lower mean monthly minimum temperature than the AWAP 0.05 data during January and February and AWAP 0.1 and AWAP 0.05 during December (Appendix 2.1-6).

Dodson & Marks (1997), state that both maximum and minimum temperatures, exhibit a strong predictable decrease with an increase in elevation where the atmosphere is well mixed, particularly during the warmer months. Winter temperatures, and daily minimum temperatures across all seasons, have a more complex relationship with elevation. Mountains acting as physical barriers, force air to move vertically (orographic uplift). The rising air will then expand and cool provided no heat is exchanged with the outside system. For the region of Ouse the statistically significant differences between the PP data and AWAP 0.1 data between both mean monthly maximum and minimum temperatures is a reflection of the steep gradient that exists. The observation station of the PP data is at an elevation of 95 m, in contrast, the elevation of the AWAP 0.1 data is 234 m. The lower daily maximum and minimum temperature within the AWAP 0.1 data source is the result of the interpolation of the adjacent cells at a higher elevation where a steep gradient is prevalent (average lapse rate of  $-6.5^{\circ}\text{C}/1,000\text{ m}$ ).

### **3.3.2 Rainfall**

At all sites except Flowerdale, there were significant ( $P < 0.05$ ) differences in the mean annual rainfall between the four sources of climate data. At the site of Woolnorth, the PP data had a significantly ( $P < 0.05$ ) lower mean annual rainfall than the other climate data sources. For the region of Merseylea, the AWAP 0.1 data had a significantly ( $P < 0.05$ ) lower mean annual rainfall than the other climate data sources. At Cressy, the PP data had a significantly ( $P < 0.05$ ) lower mean annual rainfall than the other climate data sources. For the region of Ringarooma, the AWAP 0.1 data had a significantly ( $P < 0.05$ ) lower mean annual rainfall than the AWAP 0.05 data. At Ouse, the PP and DD data had a significantly ( $P < 0.05$ ) lower mean annual rainfall than the AWAP 0.1 and AWAP 0.05 data (Table 3.5). Across all sites none of the four climate data sources were consistently highest. The PP data at the sites of Woolnorth, Cressy, Ringarooma and Ouse had the lowest mean annual rainfall. The differences in mean annual rainfall between the four climate data sources ranged from 30 mm (Flowerdale) to 190 mm (Ouse).

**Table 3.5** Mean annual rainfall (mm) for the sites Woolnorth, Flowerdale, Merseylea, Cressy, Ringarooma and Ouse from the data sources of AWAP 0.1, AWAP 0.05, PP and DD for the period 1971 to 2007.

Data set	Woolnorth	Flowerdale	Merseylea	Cressy	Ringarooma	Ouse
AWAP 0.1	1023 <sup>a</sup>	1159	901 <sup>b</sup>	751 <sup>a</sup>	1120 <sup>b</sup>	737 <sup>a</sup>
AWAP 0.05	999 <sup>a</sup>	1189	965 <sup>ab</sup>	759 <sup>a</sup>	1230 <sup>a</sup>	738 <sup>a</sup>
PP	934 <sup>b</sup>	1184	1038 <sup>a</sup>	619 <sup>b</sup>	1189 <sup>ab</sup>	548 <sup>b</sup>
DD	1040 <sup>a</sup>	1169	949 <sup>ab</sup>	724 <sup>a</sup>	1193 <sup>ab</sup>	565 <sup>b</sup>
LSD ( $P = 0.05$ )	65	ns	102	67	101	51

Means with differing subscripts next to values indicate a significant difference at  $P < 0.05$ .

For the regions of Woolnorth, Flowerdale, Merseylea and Ringarooma there were no significant ( $P > 0.05$ ) differences in mean monthly rainfall between the four sources of climate data (Figure 3.1a-c,e). At Cressy, the PP data had a significantly ( $P < 0.05$ ) lower mean monthly rainfall during July and August than the other climate data sources. Additionally, the PP data had a significantly ( $P < 0.05$ ) lower mean monthly rainfall during June than the data of AWAP 0.1 and AWAP 0.05 (Figure 3.1d). At Ouse, the AWAP 0.1 and AWAP 0.05 data had a significantly ( $P < 0.05$ ) higher mean monthly rainfall than the PP and DD data for all months except February (Figure 3.1f) (Appendix 3.1-6).

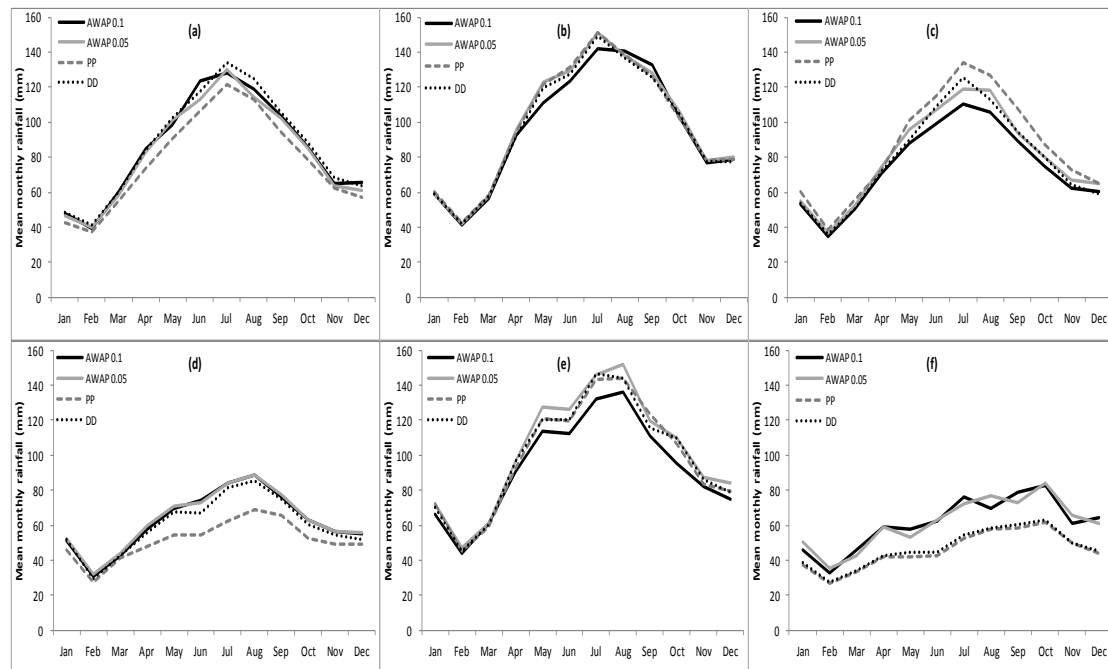


**Figure 3.1** Mean monthly rainfall (mm) at Woolnorth (a), Flowerdale (b), Merseylea (c), Cressy (d), Ringarooma (e) and Ouse (f) from the data sources of AWAP 0.1, AWAP 0.05, PP and DD for the period 1971 to 2007.

The variation between the four climate data sources from the highest to the lowest mean annual rainfall ranged from 3% at Flowerdale to 35% at Ouse. Terrain and water bodies commonly have major effects on spatial climate patterns. Regions that have significant terrain features (Ouse) along with cold air drainage and temperature inversions are difficult to interpolate accurately. Slope and aspect, riparian zones, vegetation and land use are commonly not accounted for in spatial climate interpolation. Daly (2006) states that slope and aspect even at a relatively small scale contribute in determining the local orographic enhancement of rainfall and has the potential to modulate near surface temperatures on the basis of exposure to solar radiation and wind.

For the regions of Woolnorth, Cressy and Ouse the PP data had the lowest mean annual rainfall. Beesley *et al.* (2009) state that rainfall is highly variable over area and time and hence is difficult to reliably interpolate from surrounding station observations. Numerous factors influence the reliability of interpolation and these include observation error, irregular geographical distributions of rainfall observations and under representation of steep gradient areas which commonly tend to have higher rainfall (Oke *et al.* 2009). The relationship between elevation and rainfall is complex and is highly variable in space. Rainfall generally increases with elevation due to forced uplift and cooling of moisture bearing winds by terrain barriers (Daly 2006). Hijmans *et al.* (2005) also concluded that the highest uncertainty with interpolated climate data sources is in regions with high variation in elevation. This is consistent with the finding from this analysis.

### **3.3.3 Potential evaporation**

At all sites except Ouse, there were significant ( $P < 0.05$ ) differences in the mean annual potential evaporation between the four sources of climate data. For the regions of Woolnorth, Merseylea and Cressy the AWAP 0.1 and AWAP 0.05 data had a significantly ( $P < 0.05$ ) lower mean annual potential evaporation than the PP and DD data. At Flowerdale, the AWAP 0.1 data had a significantly lower mean annual potential evaporation than the other climate data sources, the AWAP 0.05 data had a significantly ( $P < 0.05$ ) higher mean annual potential evaporation than the AWAP 0.1 data and a significantly ( $P < 0.05$ ) lower mean annual potential evaporation than the PP and DD data. For the region of Ringarooma, the AWAP 0.1 and AWAP 0.05 data had a significantly ( $P < 0.05$ ) lower mean annual potential evaporation than the PP and DD data, and the PP data had a significantly ( $P < 0.05$ ) higher mean annual potential evaporation than the other climate data sources (Table 3.6).

**Table 3.6** Mean annual potential evaporation (mm) for the sites Woolnorth, Flowerdale, Merseylea, Cressy, Ringarooma and Ouse from the data sources of AWAP 0.1, AWAP 0.05, PP and DD for the period 1971 to 2007.

Data set	Woolnorth	Flowerdale	Merseylea	Cressy	Ringarooma	Ouse
AWAP 0.1	945 <sup>b</sup>	968 <sup>c</sup>	1021 <sup>b</sup>	1004 <sup>b</sup>	932 <sup>c</sup>	979
AWAP 0.05	948 <sup>b</sup>	985 <sup>b</sup>	1012 <sup>b</sup>	1005 <sup>b</sup>	930 <sup>c</sup>	1000
PP	1076 <sup>a</sup>	1074 <sup>a</sup>	1108 <sup>a</sup>	1151 <sup>a</sup>	1055 <sup>a</sup>	997
DD	1090 <sup>a</sup>	1074 <sup>a</sup>	1097 <sup>a</sup>	1141 <sup>a</sup>	1025 <sup>b</sup>	997
LSD ( $P = 0.05$ )	20	16	20	27	28	ns

Means with differing subscripts next to values indicate a significant difference at  $P < 0.05$ .

At all sites except Ouse, mean monthly potential evaporation from the AWAP 0.1 and AWAP 0.05 data was significantly ( $P < 0.05$ ) lower from the months of February through to September than the PP and DD data (at Cressy, from January to September) (Figure 3.2). For the region of Ouse, mean monthly potential evaporation from the AWAP 0.1 and AWAP 0.05 data was significantly ( $P < 0.05$ ) lower than from the PP and DD data from April to August (Figure 3.2f). At the sites of Woolnorth, Flowerdale, Merseylea and Ouse mean monthly potential evaporation from the AWAP 0.1 and AWAP 0.05 data was significantly ( $P < 0.05$ ) higher than the PP and DD data during the months of October, November and December. In addition, at Ouse, the AWAP 0.1 and AWAP 0.05 data was significantly ( $P < 0.05$ ) higher than PP and DD data during January (Figure 3.2f) (Appendix 4.1-6)

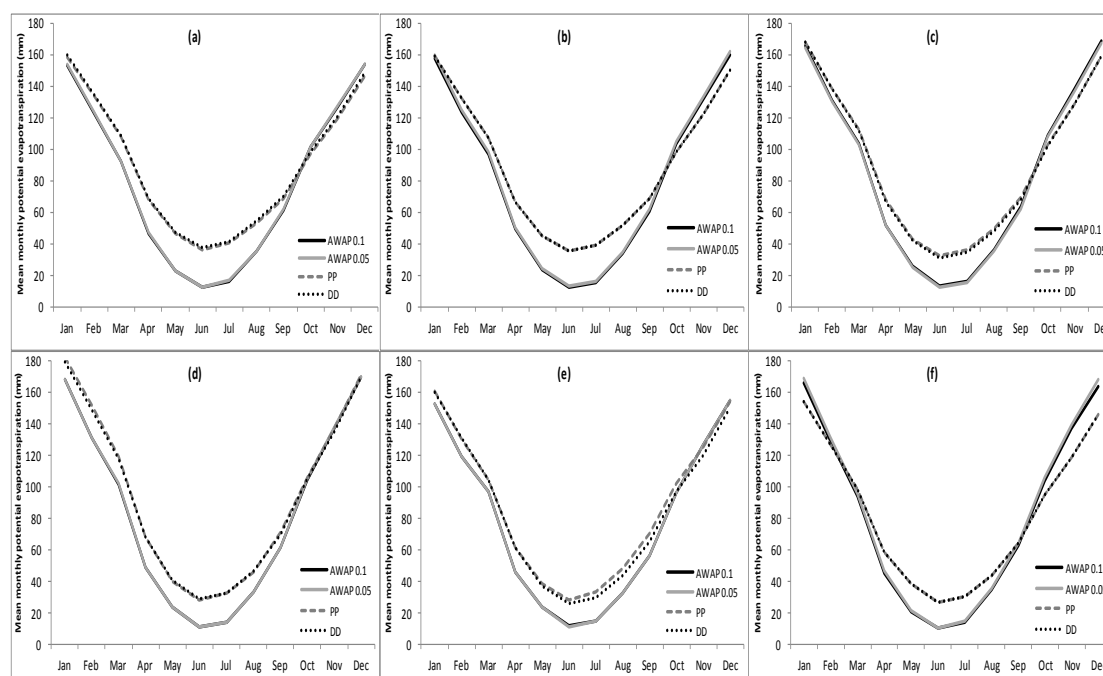


**Figure 3.2** Mean monthly potential evaporation (mm) at Woolnorth (a), Flowerdale (b), Merseylea (c), Cressy (d), Ringarooma (e) and Ouse (f) from the data sources of AWAP 0.1, AWAP 0.05, PP and DD for the period 1971 to 2007.

Across all sites except Ouse, the potential evaporation values from PP and DD were consistently higher than the AWAP 0.1 and AWAP 0.05 data, with differences between climate data sources ranging from 15% at Woolnorth to 2% at Ouse. The significant differences between the AWAP data and DD and PP data can be explained by the different interpolation methods and the different potential evaporation calculation methods. Both AWAP data sources had potential evaporation calculated using the Priestly-Taylor method while the data sources of DD and PP had potential evaporation calculated from a linear combination of gridded solar radiation and vapour pressure deficit from within the climate data sets (Rayner *et al.* 2004).

### 3.3.4 DairyMod simulations

For the region of Woolnorth, the simulated mean annual pasture yield from each climate data source ranged from 11,291 kg DM/ha (PP) to 12,325 kg DM/ha (DD) (Figure 3.3a). The mean annual simulated pasture yield from the PP data was significantly ( $P < 0.05$ ) lower than the DD data (Table 3.7). The mean monthly simulated pasture yield from the PP data was significantly ( $P < 0.05$ ) lower during April (AWAP 0.1), May (AWAP 0.1, AWAP 0.05) and October (AWAP 0.1, AWAP 0.05 and DD). Conversely, the mean monthly simulated pasture yield from the PP data was significantly ( $P < 0.05$ ) higher during July than AWAP 0.1 data (Figure 3.3b), (Appendix 5.1).

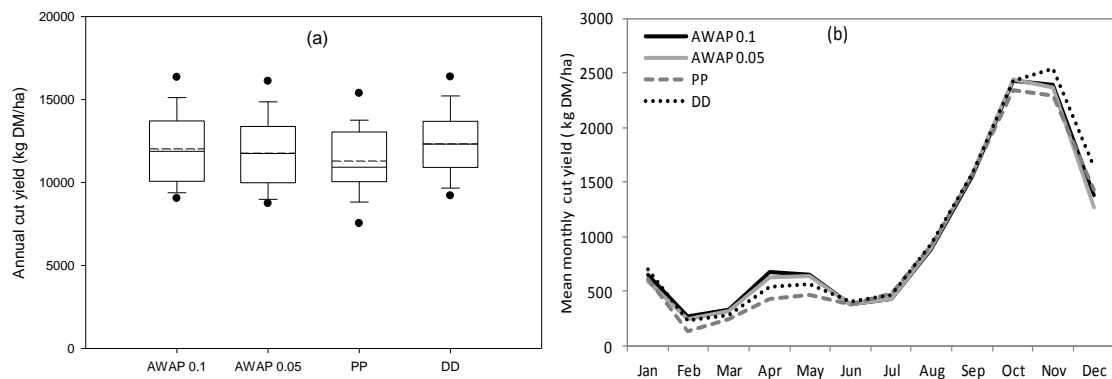


**Figure 3.3** Annual simulated pasture cut yield (kg DM/ha) for Woolnorth shown as box plots (5<sup>th</sup>, 10<sup>th</sup>, 25<sup>th</sup>, 50<sup>th</sup>, 75<sup>th</sup>, 90<sup>th</sup> and 95<sup>th</sup> percentile, with dashed mean line) (a) and mean simulated monthly cut yield (kg DM/ha) (b) from the climate data sources of AWAP 0.1, AWAP 0.05, PP and DD for the period 1971 to 2007.

At Flowerdale, the simulated mean annual pasture yield from each climate data source varied from 11,083 kg DM/ha (DD) to 11,628 kg DM/ha (AWAP 0.05) and there was no significant ( $P > 0.05$ ) difference between the climate data sources (Figure 3.4a). The mean monthly

simulated pasture yield from the AWAP 0.05 data was significantly ( $P < 0.05$ ) lower than the PP and DD data during the months of August, September and October (Figure 3.4b), (Appendix 5.2).

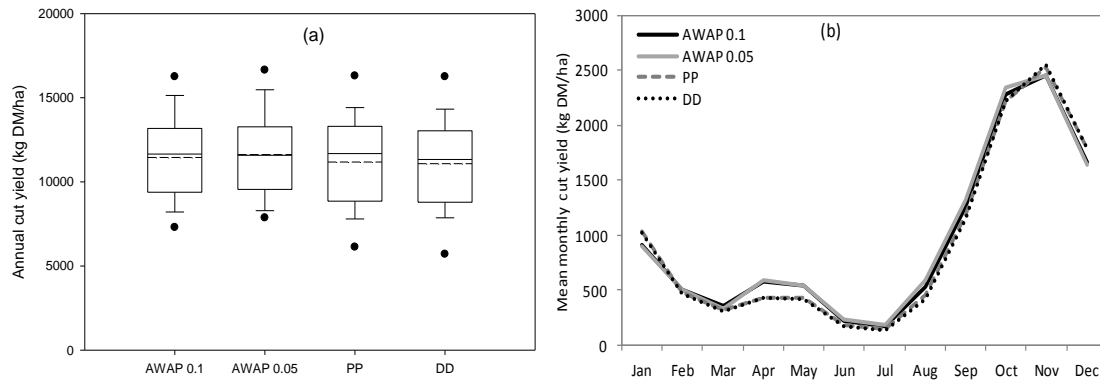


**Figure 3.4** Annual simulated pasture cut yield (kg DM/ha) for Flowerdale shown as box plots (5<sup>th</sup>, 10<sup>th</sup>, 25<sup>th</sup>, 50<sup>th</sup>, 75<sup>th</sup>, 90<sup>th</sup> and 95<sup>th</sup> percentile, with dashed mean line) (a) and mean simulated monthly cut yield (kg DM/ha) (b) from the climate data sources of AWAP 0.1, AWAP 0.05, PP and DD for the period 1971 to 2007.

For the region of Merseylea, the simulated mean annual pasture yield from each climate data source ranged from 8,003 kg DM/ha (AWAP 0.1) to 9,271 kg DM/ha (PP) (Figure 3.5a). The mean annual simulated pasture yield from the AWAP 0.1 data was significantly ( $P < 0.05$ ) lower than the PP data source (Table 3.7). The mean monthly simulated pasture yield from the PP data was significantly ( $P < 0.05$ ) higher than the AWAP 0.05 data (August) and DD (August, September). The mean monthly pasture yield from the DD data was significantly ( $P < 0.05$ ) lower than the AWAP 0.1 and AWAP 0.05 data during October (Figure 3.5b), (Appendix 5.3).

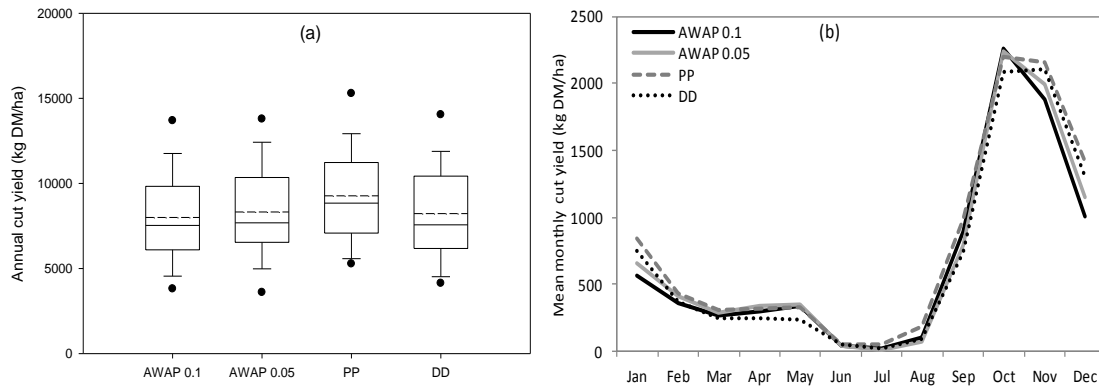


**Figure 3.5** Annual simulated pasture cut yield (kg DM/ha) for Merseylea shown as box plots (5<sup>th</sup>, 10<sup>th</sup>, 25<sup>th</sup>, 50<sup>th</sup>, 75<sup>th</sup>, 90<sup>th</sup> and 95<sup>th</sup> percentile, with dashed mean line) (a) and mean simulated monthly cut yield (kg DM/ha) (b) from the climate data sources of AWAP 0.1, AWAP 0.05, PP and DD for the period 1971 to 2007.

At Cressy, the simulated mean annual pasture yield from each climate data source ranged from 4,144 kg DM/ha (PP) to 4,882 kg DM/ha (AWAP 0.1) and there was no significant ( $P > 0.05$ ) difference between climate data sources (Figure 3.6a). The mean monthly simulated pasture yield from the PP data was significantly ( $P < 0.05$ ) higher than the other data sources during September. In contrast the mean monthly simulated pasture yield from the PP data was significantly ( $P < 0.05$ ) lower than the AWAP 0.1 and AWAP 0.05 data during November (Figure 3.6b), (Appendix 5.4).

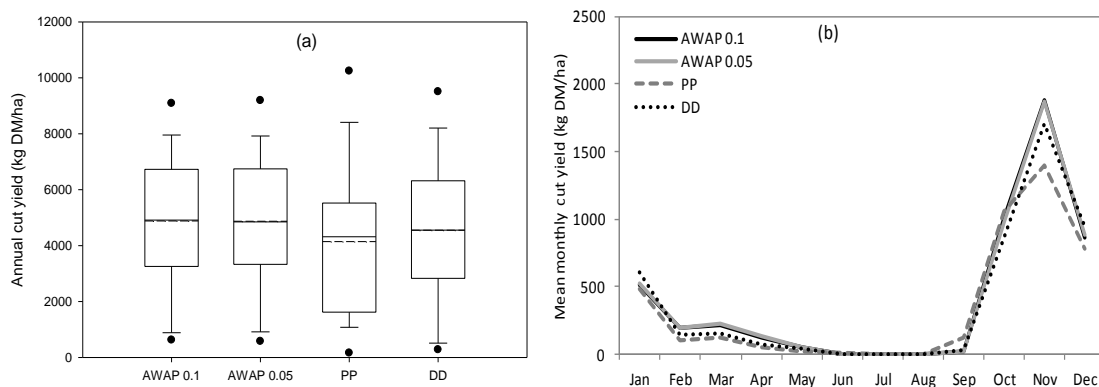


**Figure 3.6** Annual simulated pasture cut yield (kg DM/ha) for Cressy shown as box plots (5<sup>th</sup>, 10<sup>th</sup>, 25<sup>th</sup>, 50<sup>th</sup>, 75<sup>th</sup>, 90<sup>th</sup> and 95<sup>th</sup> percentile, with dashed mean line) (a) and mean simulated monthly cut yield (kg DM/ha) (b) from the climate data sources of AWAP 0.1, AWAP 0.05, PP and DD for the period 1971 to 2007.

For the region of Ringarooma, the simulated mean annual pasture yield from each climate data source ranged from 9,628 kg DM/ha (DD) to 10,369 kg DM/ha (AWAP 0.05) and there was no significant ( $P > 0.05$ ) differences between the climate data sources (Figure 3.7a). The

mean monthly simulated pasture yield from the PP data was significantly ( $P < 0.05$ ) higher than AWAP 0.1 data (August, September) and DD data (September, October). The mean monthly simulated pasture yield from the AWAP 0.05 data was significantly ( $P < 0.05$ ) higher than the DD data during October (Figure 3.7b), (Appendix 5.5).

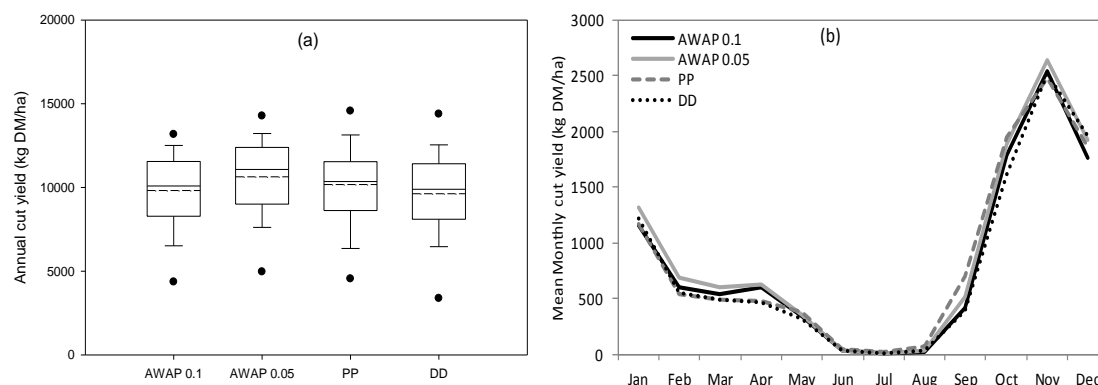


**Figure 3.7** Annual simulated pasture cut yield (kg DM/ha) for Ringarooma shown as box plots (5<sup>th</sup>, 10<sup>th</sup>, 25<sup>th</sup>, 50<sup>th</sup>, 75<sup>th</sup>, 90<sup>th</sup> and 95<sup>th</sup> percentile, with dashed mean line) (a) and mean simulated monthly cut yield (kg DM/ha) (b) from the climate data sources of AWAP 0.1, AWAP 0.05, PP and DD for the period 1971 to 2007.

For the region of Ouse, the simulated mean annual pasture yield from each climate data source ranged from 4,275 kg DM/ha (DD) to 4,918 kg DM/ha (AWAP 0.05) and there was no significant ( $P > 0.05$ ) differences between the climate data sources (Figure 3.8a). The mean monthly simulated pasture yield from the PP data was significantly ( $P < 0.05$ ) lower than the AWAP 0.1 and AWAP 0.05 data during April. During September the mean monthly simulated pasture yield from the PP data was significantly ( $P < 0.05$ ) higher than the AWAP 0.1 and AWAP 0.05 data and during October the mean monthly simulated pasture yield from the PP data was significantly ( $P < 0.05$ ) higher than the AWAP 0.1 and DD data (Figure 3.8b), (Appendix 5.6).

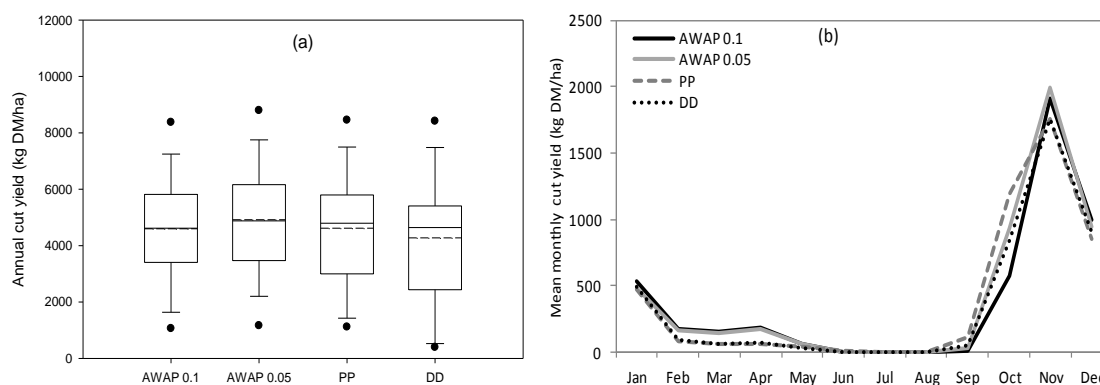


**Figure 3.8** Annual simulated pasture cut yield (kg DM/ha) for Ouse shown as box plots (5<sup>th</sup>, 10<sup>th</sup>, 25<sup>th</sup>, 50<sup>th</sup>, 75<sup>th</sup>, 90<sup>th</sup> and 95<sup>th</sup> percentile, with dashed mean line) (a) and mean simulated monthly cut yield (kg DM/ha) (b) from the climate data sources of AWAP 0.1, AWAP 0.05, PP and DD for the period 1971 to 2007.

The variation between the four climate data sources for simulated pasture yields ranged from 5% at Flowerdale to 18% at Cressy. For the regions of Flowerdale, Ringarooma and Ouse the AWAP 0.05 data had the highest mean annual simulated pasture yield, and the DD data had the lowest mean annual pasture yield (Table 3.7). At all sites except Cressy, the data source that had the highest mean annual rainfall (Table 3.5) also had the highest mean annual simulated pasture yield. This was reflected in the mean monthly simulated pasture yields during the summer and autumn months, where the data source that had the highest mean monthly rainfall also had the highest mean monthly simulated pasture yields. In addition, the data source that had the lowest mean monthly rainfall also had the lowest mean monthly simulated pasture yield during the summer and autumn months (Appendix 3.0, 5.0).

**Table 3.7** Mean annual simulated pasture cut yields (kg DM/ha) at Woolnorth, Flowerdale, Merseylea, Cressy, Ringarooma and Ouse from the climate data sources of AWAP 0.1, AWAP 0.05, PP and DD for the period 1971 to 2007.

	Woolnorth	Flowerdale	Merseylea	Cressy	Ringarooma	Ouse
AWAP 0.1	12026 <sup>ab</sup>	11450	8003 <sup>b</sup>	4882	9820	4596
AWAP 0.05	11767 <sup>ab</sup>	11628	8321 <sup>ab</sup>	4871	10639	4918
PP	11291 <sup>b</sup>	11181	9271 <sup>a</sup>	4144	10173	4617
DD	12325 <sup>a</sup>	11083	8226 <sup>ab</sup>	4549	9628	4275
LSD ( $P = 0.05$ )	929	ns	1263	ns	ns	ns

Means with differing subscripts next to values indicate a significant difference at  $P < 0.05$ .

During winter and spring at all sites except Woolnorth, the differences between mean monthly simulated pasture yields were closely correlated with mean monthly minimum temperatures from the four climate data sources. The data source that had the highest mean monthly minimum temperature also had the highest mean monthly simulated pasture yield,

and the data source that had the lowest mean monthly temperature also had the lowest mean monthly simulated pasture yield (Appendix 2.0, 5.0).

The coefficient of variation (CV) of the simulated pasture yields was notably higher at Cressy and Ouse (Figure 3.9b), in comparison to the other four sites. This was a result of the lower mean annual rainfall at both Cressy and Ouse (Table 3.5) creating greater inter-annual yield variability. Perennial ryegrass is suited to regions with a mean annual rainfall of > 650 mm (Waller & Sale 2001). At Cressy and Ouse mean annual rainfall is only marginally above this value.

The CV of annual rainfall across all sites, averaged from all four climate data sources, ranged from 14% at Woolnorth to 23% at Merseylea (Figure 3.9a). The CV of annual rainfall at Cressy and Ouse was 21% and 17% respectively. While inter-annual rainfall variability at Cressy and Ouse is not discernibly high in comparison to the other sites, the inter-annual rainfall variability has had a greater impact on simulated pasture yields due to a greater number of years where the annual rainfall would be below the optimum for pasture growth. This is most evident during spring, where the inter-seasonal variability of simulated cut yields was higher at Cressy and Ouse in contrast to the other sites. Each site has a winter dominant rainfall, with lower mean spring rainfall at Cressy and Ouse creating greater variability in the pasture yields in comparison to the other sites where spring rainfall is higher.

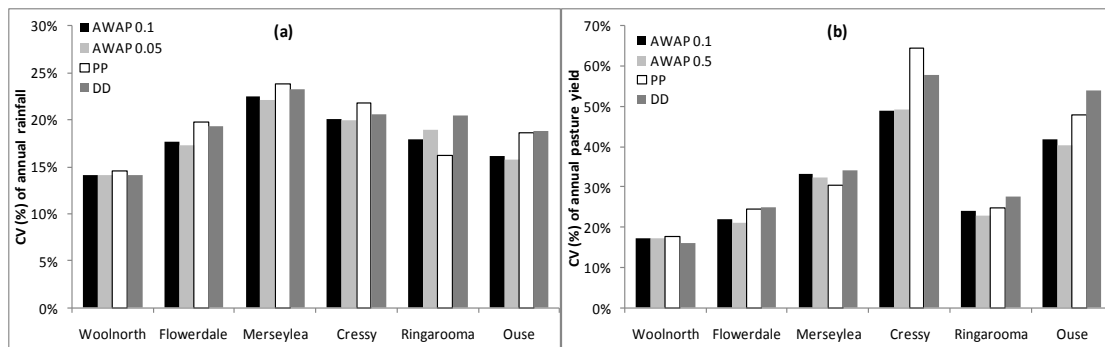


**Figure 3.9** CV (%) of annual rainfall (a) and CV (%) of annual pasture cut yields (b) at Woolnorth, Flowerdale, Merseylea, Cressy, Ringarooma and Ouse from the climate data sources of AWAP 0.1, AWAP 0.05, PP and DD for the period 1971 to 2007.

### 3.4 Conclusion

The meteorological and simulated biophysical comparison between the four climate data sources of AWAP 0.1, AWAP 0.05, PP and DD is an important step in understanding the variation that can exist between observed and spatially interpolated climate data sets. Evaluation and comparisons between the four climate data sources has provided an insight into the geographic distribution of uncertainty between the four climate data sources at each of the six sites.

The significant differences observed between the four climate data sources, can be partly attributed to different interpolation methods that have been applied to the observed station data. Daly (2006) concludes that spatial data sets represent a source of error in any analysis that uses them as an input. There is no one satisfactory method for quantitatively estimating error in spatial climate data sets, primarily because the field that is being estimated is unknown between data points.

While there were significant differences observed between the simulated biological comparisons of the four climate data sources, ultimately the significant differences that occurred were the exception. Differences were observed between the four climate data sources at each site, primarily between the climate metrics as opposed to the simulated mean pasture yields. The variation between the four climate data sources of simulated mean pasture yields for each of the six sites were similar, demonstrating that the variation between the climate data sources at each site is less important than the variation in pasture yields between the six sites. However, observed and spatially interpolated climate data sets contain a certain degree of error and this error is sometimes measurable as has been shown here. Ultimately no observed or spatially interpolated data set is perfect, but they are nevertheless useful for a variety of regions and applications providing their limitations and assumptions are understood.

The AWAP 0.1 data source was created to compare directly to the regional CFT GCM outputs, the AWAP 0.1 data is interpolated onto a larger grid resolution than both the AWAP 0.05 and DD. The differences that were observed between the four climate data sources is not so much a reflection of the each data sources accuracy, but rather the grid resolution of each climate data source.

## **CHAPTER 4: A COMPARISON OF THE AWAP 0.1 DATA SOURCE AGAINST THE SIX DOWNSCALED GENERAL CIRCULATION MODEL CLIMATE DATA SOURCES**

### **4.1 Introduction**

General Circulation Models are the best available tools for simulating future climates under anthropogenic forcing and projected emissions of greenhouse gases and their use in impact assessment studies of climate change is widespread (Suppiah *et al.* 2007; Perkins & Pittman 2009; Soussana *et al.* 2010). The development of GCMs for future climate projections has placed increasing demands that the models simulate present day climate well (Perkins *et al.* 2007). However, the spatial resolution of most GCMs is low, which reduces the realism of local projections of climate change, especially in areas with complex terrain (Soussana *et al.* 2010) such as Tasmania. Corney *et al.* (2010) reported that Tasmania, due to its diverse geography and climate over a small area, is a particularly difficult region for modelling climate change when relying solely on GCMs.

In order to address this issue, the CFT project provided credible projections of major climatic features specific to Tasmania, by dynamically downscaling six GCMs down to a 0.1° grid (Grose *et al.* 2010). The CFT project dynamically downscaled the GCM climatic outputs using the CCAM (Corney *et al.* 2010). Dynamical downscaling allows synoptic weather systems to be expressed at finer scales than those in GCMs, while taking into account the interaction between the weather systems and Tasmania's topography and vegetation (Bennett *et al.* 2010; Holz *et al.* 2010). Corney *et al.* (2010) report that modelling the atmosphere at a much finer scale than is possible using a coupled GCM, allows the drivers of Tasmania's climate to be captured with greater accuracy.

A greater level of confidence in a GCMs ability to simulate a future climate scenario is provided if the GCM is able to simulate the historical climate with some degree of accuracy. Poor agreement between simulated and observed climate data can indicate that certain physical or dynamical processes have been misrepresented (IPCC 2007). The CFT downscaled GCM simulations when compared to a historical gridded climate data source such as AWAP 0.1, will have systematic differences (Corney *et al.* 2010). In reporting trends in climate data, and for most applications that require climate data as input, a bias in the CFT GCM simulations will not adversely affect the output (Corney *et al.* 2010). However, most dynamically downscaled climate simulations need to be bias-adjusted, particularly if the

climate simulations are intended to be used in biophysical or hydrological models (Holz *et al.* 2010).

The CFT used a bias-adjustment process to correct for systematic errors for five climate variables (Corney *et al.* 2010). These five climate variables were daily maximum and minimum temperature, daily rainfall, daily total pan evaporation and daily solar radiation. The bias-adjusted variables were modified on a cell by cell basis for each of the land grid cells and applied on a seasonal basis using the AWAP 0.1 gridded data source. All five climate metrics were bias-adjusted using a percentile binning method (1% bin size) based on the work of Panofsky and Brier (1968). Several different techniques for implementing bias-adjustment exist. The percentile binning method has an advantage over other bias-adjustment methods as it does not assume that the offset is constant for all values of the variable being adjusted or even that the distribution of the variable being adjusted is normally distributed about a mean (Corney *et al.* 2010). The bias-adjusted dynamically downscaled GCM data are designed to be used within biophysical, hydrological or similar models. In many previous studies where climate simulations have been used as input into simulation models, anomalous or perturbed historical datasets have been used (Corney *et al.* 2010).

To have an acceptable degree of confidence in the projections produced by the CFT modelling it is necessary to compare and contrast the bias-adjusted downscaled GCMs with observational data. In addition to a meteorological comparison, a biophysical comparison between the GCMs and observational climate data is considered an important step in further building confidence in the timing and magnitude of simulated weather events.

The objectives of this chapter were to:

1. Compare the monthly and annual means between the climate variables maximum, minimum and diurnal temperature, rainfall and solar radiation from the observed gridded climate dataset AWAP 0.1 and the six bias-adjusted dynamically downscaled GCMs at six sites for the period 1990 to 2007.
2. Quantify simulated perennial ryegrass yields from the biophysical model DairyMod, using the AWAP 0.1 gridded data and the six bias-adjusted dynamically downscaled GCMs as inputs into DairyMod at six sites, for the period 1990 to 2007.

## 4.2 Materials and methods

The Australian Water Availability Project (AWAP 0.1°) gridded data source of interpolated values of continuous daily climate data and the 0.1° gridded bias-adjusted dynamically downscaled CSIRO-Mk3.5, ECHAM5/MPI-OM, GFDL-CM2.0, GFDL-CM2.1, MIROC3.2 (medres) and UKMO-HADCM3 data for each of the six sites (Section 3.2) was obtained from the TPAC portal (<https://dl.tpac.org.au/>). Daily climate data for the period 1<sup>st</sup> January 1981 to 31<sup>st</sup> December 2007, for the climate variables of maximum and minimum temperature (°C), rainfall (mm) and solar radiation (MJ/m<sup>2</sup>) were accessed.

In the previous chapter, daily potential evaporation values from the four climate data sources PP, DD, AWAP 0.5 and AWAP 0.1 were quantified. In this chapter and in future chapters, daily potential evapotranspiration values as calculated by Bennett *et al.* (2010) (using the Morton's Wet method) is used from both the bias-adjusted downscaled GCMs and AWAP 0.1 data, as opposed to the daily potential evaporation values.

Daily solar radiation values within the AWAP 0.1 data prior to 1990 are constant monthly means, and as such there is no inter-annual variability. Estimates of solar radiation at the earth's surface with complete spatial coverage have only been possible since 1990 with the advent of satellite records of cloud cover and albedo (Corney *et al.* 2010). As a result the differences in daily solar radiation values prior to 1990 between the AWAP 0.1 data source and the bias-adjusted downscaled GCMs prevented the solar radiation values being used from the AWAP 0.1 data source prior to 1990.

The suitability of the bias-adjusted downscaled GCMs for use in biophysical models was tested by comparing simulated pasture yields from the bias-adjusted downscaled GCMs against AWAP 0.1 and is considered an important step in further building confidence in the bias-adjusted downscaled GCMs. DairyMod version 4.9.2 (Johnson *et al.* 2008) was used to simulate rainfed perennial ryegrass for the period 1<sup>st</sup> January 1981 to 31<sup>st</sup> December 2007, results for the first 10 years were discarded to allow the model to equilibrate. The methods and parameters of the model used here were identical to those described in Section 3.2. Daily climate data from the seven climate data sources at each site for the period 1<sup>st</sup> January 1991 to 31<sup>st</sup> December 2007 were used and monthly and annual pasture yield data were exported to a spreadsheet for further computation.

A test of normality was carried out on each climate variable within each climate data set using the statistical analysis package SPSS (Version 11.5, SPSS Corporation, IL, USA). Climate

metrics and the simulated annual and monthly pasture yield for each region were analysed as one-way ANOVA with replication (year) using SPSS. Least significant difference (LSD), as defined by Steel and Torrie (1960) were used to compare differences between means for the seven climate data sources.

### 4.3 Results and Discussion

#### 4.3.1 Annual climate metrics

At all sites except Merseylea, there were no significant ( $P > 0.05$ ) differences in the mean annual daily maximum temperature between the seven sources of climate data (Table 4.1). At Merseylea, the AWAP 0.1 and MIROC3.2 (medres) data had a significantly ( $P < 0.05$ ) lower mean annual daily maximum temperature than the ECHAM5/MPI-OM data. Across all sites the ECHAM5/MPI-OM data consistently had the highest mean annual daily maximum temperature and the MIROC3.2 (medres) was consistently the lowest at all sites except Woolnorth. Differences between climate data sources of the mean annual daily maximum temperature ranged from  $0.22^{\circ}$  at Flowerdale and Merseylea to  $0.30^{\circ}\text{C}$  at Ouse.

**Table 4.1** Mean annual daily maximum temperature ( $^{\circ}\text{C}$ ) at the sites of Woolnorth, Flowerdale, Merseylea, Cressy, Ringarooma and Ouse from the data sources of AWAP 0.1, CSIRO-Mk3.5, ECHAM5/MPI-OM, GFDL-CM2.0, GFDL-CM2.1, MIROC3.2 (medres) and UKMO-HADCM3 for the period 1990 to 2007. Standard deviation is shown in parentheses.

Data source	Woolnorth	Flowerdale	Merseylea	Cressy	Ringarooma	Ouse
AWAP 0.1	16.53 (0.43)	16.34 (0.42)	16.97 <sup>b</sup> (0.38)	17.51 (0.47)	16.61 (0.44)	16.85 (0.56)
CSIRO-Mk3.5	16.58 (0.31)	16.37 (0.27)	17.02 <sup>ab</sup> (0.23)	17.49 (0.23)	16.57 (0.21)	16.75 (0.28)
ECHAM5/MPI-OM	16.76 (0.37)	16.52 (0.23)	17.18 <sup>a</sup> (0.24)	17.67 (0.21)	16.75 (0.25)	17.00 (0.22)
GFDL-CM2.0	16.60 (0.27)	16.38 (0.25)	17.01 <sup>ab</sup> (0.26)	17.50 (0.31)	16.57 (0.26)	16.86 (0.33)
GFDL-CM2.1	16.57 (0.36)	16.38 (0.33)	17.04 <sup>ab</sup> (0.33)	17.54 (0.36)	16.59 (0.33)	16.79 (0.39)
MIROC3.2 (medres)	16.56 (0.41)	16.30 (0.36)	16.96 <sup>b</sup> (0.35)	17.44 (0.37)	16.51 (0.32)	16.70 (0.39)
UKMO-HADCM3	16.73 (0.31)	16.43 (0.26)	17.05 <sup>ab</sup> (0.24)	17.51 (0.26)	16.61 (0.23)	16.83 (0.28)
LSD ( $P = 0.05$ )	ns	ns	0.19	ns	ns	ns

Means with differing subscripts next to values indicate a significant difference at  $P < 0.05$ .

At all sites except Merseylea, there were significant ( $P < 0.05$ ) differences in mean annual daily minimum temperature between the seven sources of climate data (Table 4.2). At Woolnorth, the UKMO-HADCM3 data had a significantly ( $P < 0.05$ ) higher mean annual daily minimum temperature than all the other data sources except ECHAM5/MPI-OM. For the regions of Flowerdale and Cressy, the ECHAM5/MPI-OM and UKMO-HADCM3 data had a significantly ( $P < 0.05$ ) higher mean annual daily minimum temperature than AWAP 0.1, CSIRO-Mk3.5 and MIROC3.2 (medres) data. At Ringarooma, the ECHAM5/MPI-OM data had a significantly ( $P < 0.05$ ) higher mean annual daily minimum temperature than the

AWAP 0.1, CSIRO-Mk3.5 and MIROC3.2 (medres) data. For the region of Ouse, the ECHAM5/MPI-OM and UKMO-HADCM3 data had a significantly ( $P < 0.05$ ) higher mean annual daily minimum temperature than the other climate data sources except the GFDL-CM2.0 data. At the sites of Woolnorth, Flowerdale, Merseylea and Cressy the UKMO-HADCM3 data had the highest mean annual daily maximum temperature and at the sites of Flowerdale, Cressy and Ouse the AWAP 0.1 data had the lowest mean annual daily minimum temperature. The differences between climate data sources of the mean annual daily maximum temperature ranged from 0.23° at Flowerdale and Merseylea to 0.34°C at Ouse.

At all sites, there were significant ( $P < 0.05$ ) differences in the mean monthly maximum and minimum temperature between the AWAP 0.1 data and the bias-adjusted downscaled GCMs.

**Table 4.2** Mean annual daily minimum temperature (°C) at the sites of Woolnorth, Flowerdale, Merseylea, Cressy, Ringarooma and Ouse from the data sources of AWAP 0.1, CSIRO-Mk3.5, ECHAM5/MPI-OM, GFDL-CM2.0, GFDL-CM2.1, MIROC3.2 (medres) and UKMO-HADCM3 for the period 1990 to 2007. Standard deviation is shown in parentheses.

Data source	Woolnorth	Flowerdale	Merseylea	Cressy	Ringarooma	Ouse
AWAP 0.1	9.53 <sup>b</sup> (0.40)	8.11 <sup>b</sup> (0.40)	7.40 (0.43)	5.91 <sup>b</sup> (0.39)	6.93 <sup>b</sup> (0.41)	5.16 <sup>b</sup> (0.39)
CSIRO-Mk3.5	9.49 <sup>b</sup> (0.30)	8.12 <sup>b</sup> (0.24)	7.34 (0.23)	5.94 <sup>b</sup> (0.26)	6.91 <sup>b</sup> (0.25)	5.30 <sup>b</sup> (0.24)
ECHAM5/MPI-OM	9.69 <sup>ab</sup> (0.34)	8.33 <sup>a</sup> (0.28)	7.55 (0.28)	6.16 <sup>a</sup> (0.25)	7.15 <sup>a</sup> (0.30)	5.50 <sup>a</sup> (0.23)
GFDL-CM2.0	9.51 <sup>b</sup> (0.19)	8.19 <sup>ab</sup> (0.16)	7.41 (0.19)	6.06 <sup>ab</sup> (0.16)	6.95 <sup>ab</sup> (0.18)	5.35 <sup>ab</sup> (0.15)
GFDL-CM2.1	9.52 <sup>b</sup> (0.29)	8.16 <sup>ab</sup> (0.28)	7.39 (0.30)	6.02 <sup>ab</sup> (0.31)	6.95 <sup>ab</sup> (0.32)	5.31 <sup>b</sup> (0.27)
MIROC3.2 (medres)	9.51 <sup>b</sup> (0.38)	8.13 <sup>b</sup> (0.33)	7.33 (0.32)	5.95 <sup>b</sup> (0.31)	6.89 <sup>b</sup> (0.32)	5.27 <sup>b</sup> (0.26)
UKMO-HADCM3	9.75 <sup>a</sup> (0.29)	8.34 <sup>a</sup> (0.29)	7.56 (0.27)	6.17 <sup>a</sup> (0.26)	7.09 <sup>ab</sup> (0.27)	5.45 <sup>a</sup> (0.23)
LSD ( $P = 0.05$ )	0.21	0.19	ns	0.19	0.19	0.17

Means with differing subscripts next to values indicate a significant difference at  $P < 0.05$ .

The standard deviation values of mean annual daily maximum and minimum temperatures across all sites from the AWAP 0.1 data were consistently higher than the bias-adjusted downscaled GCMs. Corney *et al.* (2010) state that the AWAP 0.1 data is interpolated using a statistical model from the observing station data and that all gridded data sets based on station records are influenced by the location and number of stations. As such, the spatial pattern of AWAP 0.1 data is fixed, given a particular set of observations. This statistical scaling from limited observations may lead to underestimates in the variability of temperature across Tasmania. In Tasmania there are a limited number of long term observational stations (six for temperature, dating from 1910) that make up the observational network forming the basis of the AWAP 0.1 gridded data (Grose *et al.* 2010).

At all sites except Cressy and Ouse, there were no significant ( $P < 0.05$ ) differences in the mean annual daily diurnal temperature range between the seven sources of climate data (Table 4.3). For the region of Cressy, the UKMO-HADCM3 data had a significantly ( $P <$

0.05) lower mean annual daily diurnal temperature range than the AWAP 0.1 and CSIRO-Mk3.5 data. At Ouse, the AWAP 0.1 data had a significantly ( $P < 0.05$ ) higher mean annual daily diurnal temperature range than the other climate data sources. Across all the sites, none of the seven climate data sources had consistently the highest mean annual daily diurnal temperature. The UKMO-HADCM3 data had the lowest mean annual daily diurnal temperature range at each site. The differences between climate data sources of the mean annual daily diurnal temperature range ranged from 0.11° at Woolnorth to 0.31°C at Ouse.

**Table 4.3** Mean annual daily diurnal temperature range (°C) at the sites of Woolnorth, Flowerdale, Merseylea, Cressy, Ringarooma and Ouse from the data sources of AWAP 0.1, CSIRO-Mk3.5, ECHAM5/MPI-OM, GFDL-CM2.0, GFDL-CM2.1, MIROC3.2 (medres) and UKMO-HADCM3 for the period 1990 to 2007. Standard deviation is shown in parentheses.

Data source	Woolnorth	Flowerdale	Merseylea	Cressy	Ringarooma	Ouse
AWAP 0.1	7.00 (0.20)	8.23 (0.25)	9.58 (0.28)	11.60 <sup>a</sup> (0.38)	9.67 (0.33)	11.69 <sup>a</sup> (0.36)
CSIRO-Mk3.5	7.09 (0.20)	8.24 (0.22)	9.68 (0.17)	11.55 <sup>a</sup> (0.21)	9.66 (0.16)	11.46 <sup>b</sup> (0.20)
ECHAM5/MPI-OM	7.07 (0.15)	8.19 (0.24)	9.63 (0.31)	11.50 <sup>ab</sup> (0.32)	9.61 (0.31)	11.50 <sup>b</sup> (0.19)
GFDL-CM2.0	7.09 (0.18)	8.19 (0.23)	9.60 (0.28)	11.44 <sup>ab</sup> (0.31)	9.62 (0.25)	11.51 <sup>b</sup> (0.26)
GFDL-CM2.1	7.05 (0.17)	8.23 (0.21)	9.66 (0.25)	11.51 <sup>ab</sup> (0.30)	9.64 (0.22)	11.48 <sup>b</sup> (0.27)
MIROC3.2 (medres)	7.05 (0.17)	8.17 (0.25)	9.63 (0.26)	11.49 <sup>ab</sup> (0.30)	9.62 (0.24)	11.43 <sup>b</sup> (0.25)
UKMO-HADCM3	6.98 (0.17)	8.09 (0.20)	9.50 (0.22)	11.34 <sup>b</sup> (0.26)	9.52 (0.22)	11.38 <sup>b</sup> (0.20)
LSD ( $P = 0.05$ )	ns	ns	ns	0.20	ns	0.17

Means with differing subscripts next to values indicate a significant difference at  $P < 0.05$ .

Corney *et al.* (2010) state that the ability of GCMs to reproduce the diurnal temperature range is more difficult than maximum and minimum temperature alone and hence gives a second order assessment of the GCMs performance. In order to simulate the observed diurnal temperature range, the seasonality of the daily minimums and maximums of temperature in the GCM must be correctly aligned. For example, a hot summer day is likely to have a warmer overnight minimum temperature. The bias-adjusted downscaled GCMs, in comparison to the AWAP 0.1 data source, have achieved an acceptable standard of capturing the broad features of the diurnal temperature range that is exhibited in the AWAP 0.1 data source.

At all sites, there were no significant ( $P > 0.05$ ) differences in the mean annual rainfall between the seven sources of climate data (Table 4.4). The differences between the data sources of the mean annual rainfall across all sites ranged from 25 mm at Ouse to 90 mm at Flowerdale. At all sites, the UKMO-HADCM3 data consistently had the highest mean annual rainfall and the CSIRO-Mk3.5 data at Woolnorth, Flowerdale and Merseylea had the lowest mean annual rainfall.

**Table 4.4** Mean annual rainfall (mm) at the sites of Woolnorth, Flowerdale, Merseylea, Cressy, Ringarooma and Ouse from the data sources of AWAP 0.1, CSIRO-Mk3.5, ECHAM5/MPI-OM, GFDL-CM2.0, GFDL-CM2.1, MIROC3.2 (medres) and UKMO-HADCM3 for the period 1990 to 2007. Standard deviation is shown in parentheses.

Data source	Woolnorth	Flowerdale	Merseylea	Cressy	Ringarooma	Ouse
AWAP 0.1	998 (122)	1131 (197)	874 (186)	724 (135)	1076 (184)	727 (111)
CSIRO-Mk3.5	995 (118)	1098 (137)	867 (119)	730 (99)	1092 (143)	738 (120)
ECHAM5/MPI-OM	1025 (141)	1132 (178)	898 (159)	753 (118)	1122 (167)	723 (137)
GFDL-CM2.0	1003 (91)	1142 (112)	905 (90)	750 (93)	1125 (121)	728 (94)
GFDL-CM2.1	1036 (123)	1166 (139)	907 (111)	741 (89)	1138 (137)	734 (98)
MIROC3.2 (medres)	1036 (108)	1148 (141)	900 (110)	738 (92)	1142 (101)	730 (90)
UKMO-HADCM3	1053 (104)	1188 (154)	915 (138)	761 (142)	1151 (152)	758 (144)
LSD ( $P = 0.05$ )	ns	ns	ns	ns	ns	ns

The standard deviation values of mean annual rainfall from the AWAP 0.1 data at the sites of Flowerdale, Merseylea and Ringarooma were higher than the bias-adjusted downscaled GCMs (Figure 4.1). Rainfall is considered one of the most important climate metrics for agriculture and is also recognised as being a challenging physical process for GCMs to accurately simulate (Randall *et al.* 2007). Annual and seasonal rainfall trends are complex both spatially and seasonally (Grose *et al.* 2010). Tasmania exhibits a complex spatial pattern of rainfall encompassing both positive and negative trends that vary considerably for each calendar season. Shepherd (1995) summarises that it is difficult to isolate the cause of rainfall patterns for Tasmania. Possible drivers and mechanisms behind the state's rainfall patterns and the magnitude of the rainfall trends, are driven by an alteration of pressure, atmospheric circulation and wind over the Australian region, along with an increase in sea surface temperatures off the east coast (Grose *et al.* 2010).

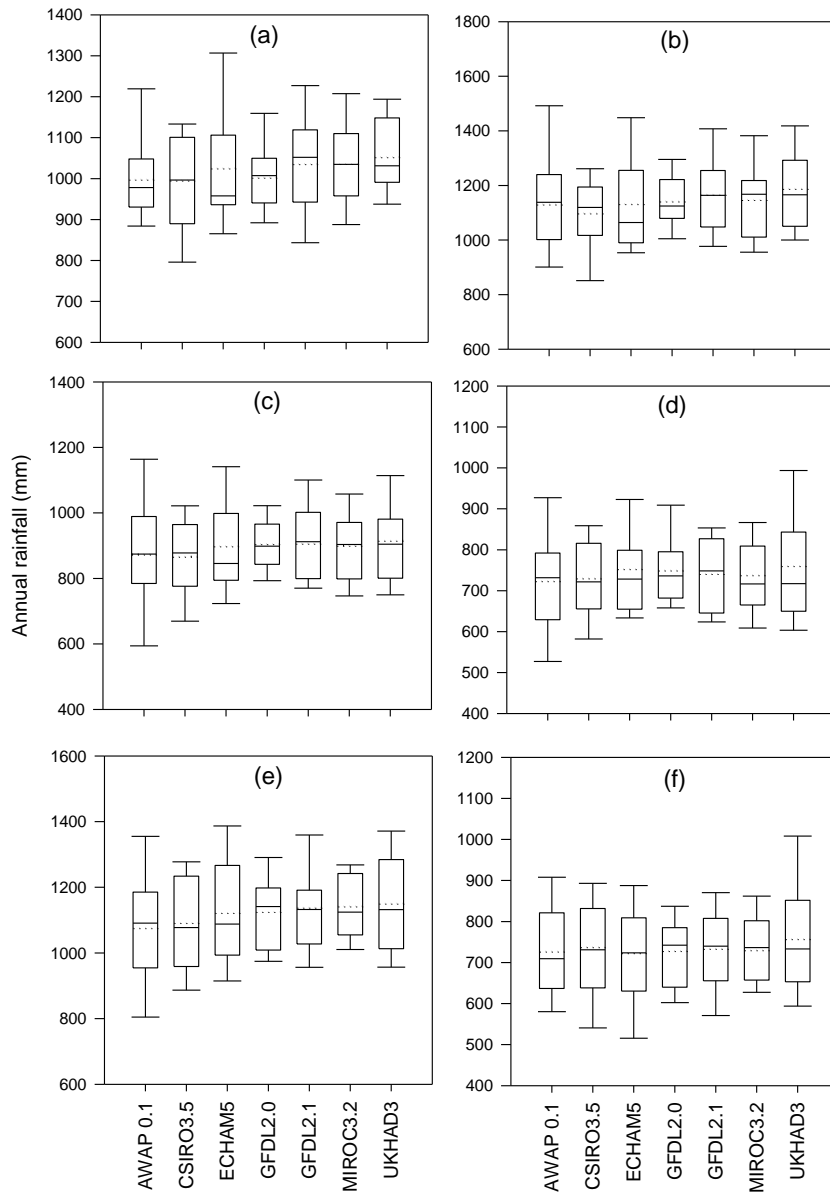


**Figure 4.1** Annual rainfall (mm) shown as box plots (10<sup>th</sup>, 25<sup>th</sup>, 50<sup>th</sup>, 75<sup>th</sup>, and 90<sup>th</sup> percentile, with dotted mean line) at Woolnorth (a), Flowerdale (b), Merseylea (c), Cressy (d), Ringarooma (e) and Ouse (f) from the climate data sources of AWAP 0.1, CSIRO-Mk3.5, ECHAM5/MPI-OM, GFDL-CM2.0, GFDL-CM2.1, MIROC3.2 (medres) and UKMO-HADCM3 for the period 1990 to 2007.

At all sites, there were significant ( $P < 0.05$ ) differences in the mean monthly rainfall between the AWAP 0.1 data and the bias-adjusted downscaled GCMs. At Woolnorth, the AWAP 0.1 data had a significantly ( $P < 0.05$ ) lower mean monthly rainfall during May than the GFDL-CM2.0 and GFDL-CM2.1 data (Appendix 6.1). For the region of Flowerdale the AWAP 0.1 data had a significantly ( $P < 0.05$ ) lower mean monthly rainfall during March than the CSIRO-Mk3.5, GFDL-CM2.0 and GFDL-CM2.1 data (Appendix 6.2). At Merseylea, the

AWAP 0.1 data had a significantly ( $P < 0.05$ ) lower mean monthly rainfall during March than the CSIRO-Mk3.5 and GFDL-CM2.0 data, and a significantly ( $P < 0.05$ ) higher mean monthly rainfall during January than the CSIRO-Mk3.5 data (Appendix 6.3). For the region of Cressy, the AWAP 0.1 data had a significantly ( $P < 0.05$ ) lower mean monthly rainfall during March than all the bias-adjusted downscaled GCMs except UKMO-HADCM3, and a significantly ( $P < 0.05$ ) higher mean monthly rainfall during January than the CSIRO-Mk3.5 and MIROC3.2 (medres) data (Appendix 6.4). At Ringarooma, the AWAP 0.1 data had a significantly ( $P < 0.05$ ) lower mean monthly rainfall during March than the CSIRO-Mk3.5 data, during May than the GFDL-CM2.1 data and during September than the ECHAM5/MPI-OM and UKMO-HADCM3 data. The AWAP 0.1 data also had a significantly ( $P < 0.05$ ) higher mean monthly rainfall during January than the CSIRO-Mk3.5 data (Appendix 6.5). For the region of Ouse, the AWAP 0.1 data had a significantly ( $P < 0.05$ ) lower mean monthly rainfall during March than the CSIRO-Mk3.5 data, during May than the GFDL-CM2.1 data and during November than the MIROC3.2 (medres) and UKMO-HADCM3 data, and a significantly ( $P < 0.05$ ) higher mean monthly rainfall during October than the MIROC3.2 (medres) data (Appendix 6.6).

The AWAP 0.1 monthly rainfall data was often found to be significantly lower than the GCM data during autumn. Grose *et al.* (2010) state that autumn rainfall has shown the largest decline of any season on a Tasmanian wide basis over the last 30 years. This analyses has indicated that the bias-adjusted downscaled GCMs have not been able to capture the observed decline in autumn rainfall. There is much conjecture, whether it is a result of changes in synoptic patterns as a result of climate change, or whether the observed reduction in mean autumn rainfall is the result of background climate variability (Corney *et al.* 2010; Grose *et al.* 2010). In addition, the 1% bias-adjustment binning method, which effectively smooth's the data may have contributed to why the bias-adjusted downscaled GCMs failed to capture the observed decline in autumn rainfall (Corney *et al.* 2010).

At all sites, there were no significant ( $P > 0.05$ ) differences in the mean annual daily solar radiation range between the seven sources of climate data (Table 4.5). The differences between the data sources of the mean annual daily solar radiation across all sites ranged from 0.11 MJ/m<sup>2</sup> at Woolnorth to 0.21 MJ/m<sup>2</sup> at Ouse. In addition, at all sites, there were no significant ( $P > 0.05$ ) differences in the mean monthly solar radiation between the seven sources of climate data.

**Table 4.5** Mean annual daily solar radiation (MJ/m<sup>2</sup>) at the sites of Woolnorth, Flowerdale, Merseylea, Cressy, Ringarooma and Ouse from the data sources of AWAP 0.1, CSIRO-Mk3.5, ECHAM5/MPI-OM, GFDL-CM2.0, GFDL-CM2.1, MIROC3.2 (medres) and UKMO-HADCM3 for the period 1990 to 2007. Standard deviation is shown in parentheses.

Data source	Woolnorth	Flowerdale	Merseylea	Cressy	Ringarooma	Ouse
AWAP 0.1	14.49 (0.45)	14.57 (0.38)	15.14 (0.47)	15.29 (0.41)	14.21 (0.47)	14.42 (0.44)
CSIRO-Mk3.5	14.53 (0.41)	14.64 (0.33)	15.18 (0.25)	15.36 (0.21)	14.25 (0.35)	14.57 (0.25)
ECHAM5/MPI-OM	14.53 (0.34)	14.66 (0.38)	15.22 (0.44)	15.42 (0.35)	14.33 (0.56)	14.63 (0.26)
GFDL-CM2.0	14.50 (0.44)	14.48 (0.47)	15.05 (0.42)	15.23 (0.40)	14.16 (0.44)	14.44 (0.44)
GFDL-CM2.1	14.51 (0.37)	14.65 (0.39)	15.18 (0.36)	15.34 (0.37)	14.27 (0.39)	14.53 (0.40)
MIROC3.2 (medres)	14.51 (0.42)	14.62 (0.49)	15.20 (0.51)	15.38 (0.51)	14.25 (0.55)	14.48 (0.39)
UKMO-HADCM3	14.42 (0.48)	14.49 (0.48)	15.09 (0.44)	15.31 (0.42)	14.24 (0.41)	14.46 (0.36)
LSD ( $P = <0.05$ )	ns	ns	ns	ns	ns	ns

A considerable issue when assessing the bias-adjusted downscaled GCMs is that the simulations provide an independent time series of the climate that does not correspond to the observational record (Holz *et al.* 2010). That is, there is nothing within a GCM run to assure that the weather on a particular day, week or month should be the same as the observed weather for the same period (Grose *et al.* 2010).

### 4.3.2 DairyMod simulations

For the region of Woolnorth, the simulated mean annual pasture yield from each climate data source ranged from 7,408 kg DM/ha (ECHAM5/MPI-OM) to 8,332 kg DM/ha (UKMO-HADCM3) (Figure 4.2a), and there was no significant ( $P > 0.05$ ) differences between the climate data sources (Table 4.6). The difference in simulated mean annual pasture yields between the bias-adjusted downscaled GCMs and the AWAP 0.1 data ranged from -9% to 2%. The mean monthly simulated cut yield from the AWAP 0.1 data was significantly ( $P < 0.05$ ) higher than the GFDL-CM2.0 data during August and significantly ( $P < 0.05$ ) higher than all downscaled GCMs, except MIROC3.2 medres, during September. During December the mean simulated pasture yield from the AWAP 0.1 data was significantly ( $P < 0.05$ ) lower than the MIROC3.2 (medres) and UKMO-HADCM3 data (Figure 4.2b; Appendix 7.1).

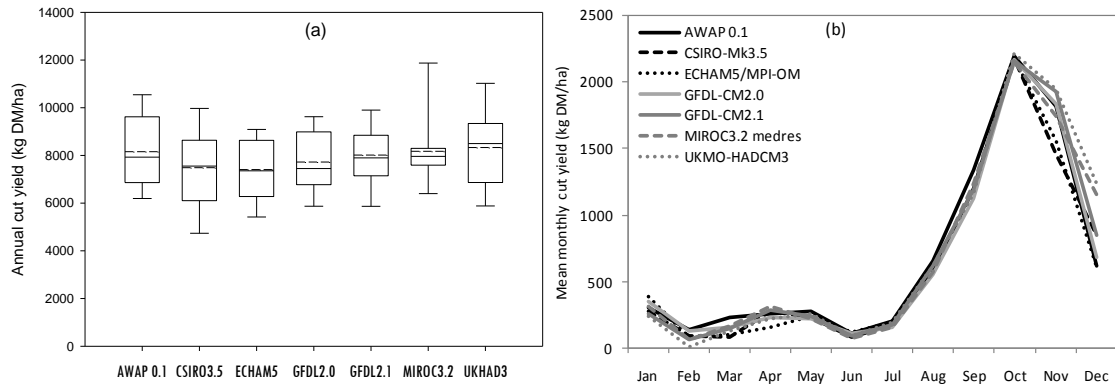


**Figure 4.2** Annual simulated pasture yields (kg DM/ha) for Woolnorth shown as box plots (10<sup>th</sup>, 25<sup>th</sup>, 50<sup>th</sup>, 75<sup>th</sup>, and 90<sup>th</sup> percentile, with dashed mean line) (a) and mean simulated monthly yield (kg DM/ha) (b) from the climate data sources of AWAP 0.1, CSIRO-Mk3.5, ECHAM5/MPI-OM, GFDL-CM2.0, GFDL-CM2.1, MIROC3.2 (medres) and UKMO-HADCM3 for the period 1990 to 2007.

At Flowerdale, the simulated mean annual pasture yield from each climate data source varied between 7,760 kg DM/ha (CSIRO-Mk3.5) and 8,892 kg DM/ha (UKMO-HADCM3) (Figure 4.3a) and there was no significant ( $P > 0.05$ ) differences between the climate data sources (Table 4.6). The difference in simulated mean annual pasture yields between the bias-adjusted downscaled GCMs and the AWAP 0.1 data ranged from -1% to 14%. The mean monthly simulated pasture yield from the AWAP 0.1 data was significantly ( $P < 0.05$ ) lower than GFDL-CM2.1 data during April, ECHAM5/MPI-OM data during June, and UKMO-HADCM3 data during December. In contrast, during December the mean monthly simulated pasture yield from the AWAP 0.1 data was significantly ( $P < 0.05$ ) higher than the GFDL-CM2.0 data (Figure 4.3b; Appendix 7.2).

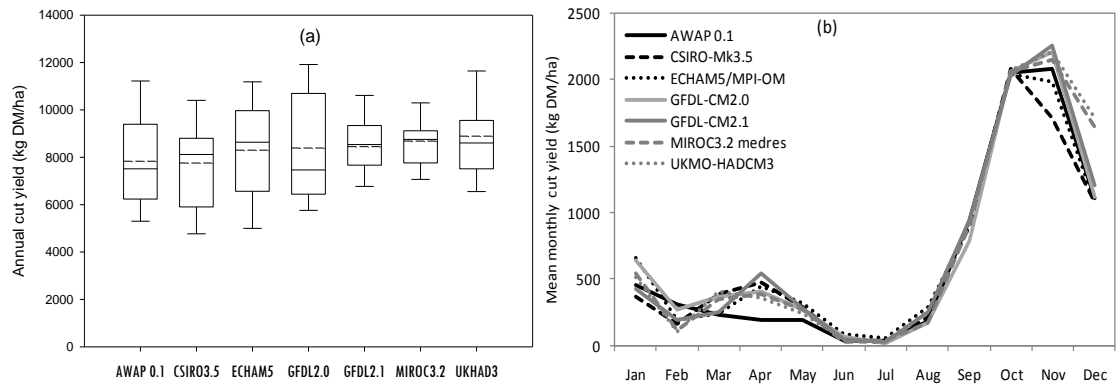


**Figure 4.3** Annual simulated pasture yields (kg DM/ha) for Flowerdale shown as box plots (10<sup>th</sup>, 25<sup>th</sup>, 50<sup>th</sup>, 75<sup>th</sup>, and 90<sup>th</sup> percentile, with dashed mean line) (a) and mean simulated monthly yield (kg DM/ha) (b) from the climate data sources of AWAP 0.1, CSIRO-Mk3.5, ECHAM5/MPI-OM, GFDL-CM2.0, GFDL-CM2.1, MIROC3.2 (medres) and UKMO-HADCM3 for the period 1990 to 2007.

For the region of Merseylea, the simulated mean annual pasture yield from each climate data source ranged from 4,607 kg DM/ha (CSIRO-Mk3.5) to 5,891 kg DM/ha (UKMO-HADCM3) (Figure 4.4a) and there was no significant ( $P > 0.05$ ) difference between the climate data sources (Table 4.6). The difference in simulated mean annual pasture yields between the bias-adjusted downscaled GCMs and the AWAP 0.1 data ranged from -11% to 13%. The mean monthly simulated cut yield from the AWAP 0.1 data was significantly ( $P < 0.05$ ) lower than the CSIRO-Mk3.5, GFDL-CM2.1 and MIROC3.2 (medres) data sources during May. During November the mean monthly simulated pasture yield from the AWAP 0.1 data was significantly ( $P < 0.05$ ) higher than the CSIRO-Mk3.5 data (Figure 4.4b; Appendix 7.3).

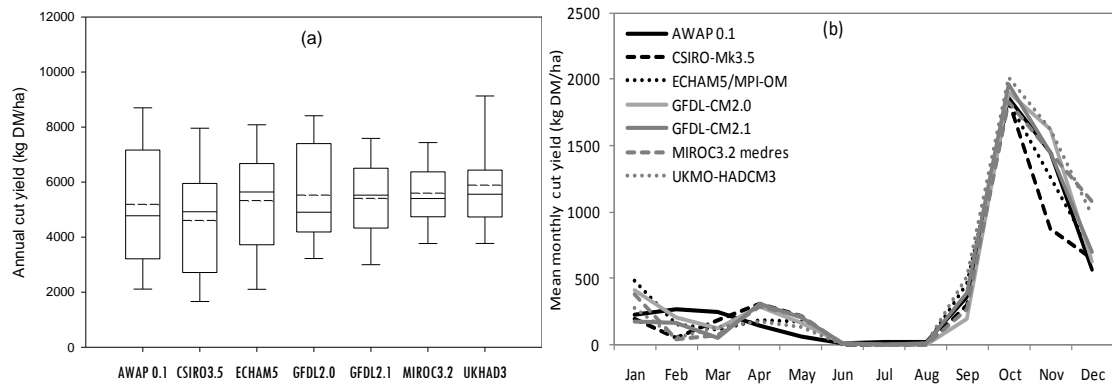


**Figure 4.4** Annual simulated pasture yields (kg DM/ha) for Merseylea shown as box plots (10<sup>th</sup>, 25<sup>th</sup>, 50<sup>th</sup>, 75<sup>th</sup>, and 90<sup>th</sup> percentile, with dashed mean line) (a) and mean simulated monthly yield (kg DM/ha) (b) from the climate data sources of AWAP 0.1, CSIRO-Mk3.5, ECHAM5/MPI-OM, GFDL-CM2.0, GFDL-CM2.1, MIROC3.2 (medres) and UKMO-HADCM3 for the period 1990 to 2007.

At Cressy, the simulated mean annual pasture yield from each climate data sources ranged from 1,350 kg DM/ha (CSIRO-Mk3.5) to 2,665 kg DM/ha (UKMO-HADCM3) (Figure 4.5a) and there was no significant ( $P > 0.05$ ) differences between the climate data sources (Table 4.6). The difference in simulated mean annual pasture yields between the bias-adjusted downscaled GCMs and the AWAP 0.1 data ranged from -40% to 19%. The mean monthly simulated pasture yield from the AWAP 0.1 data was significantly ( $P < 0.05$ ) higher than GFDL-CM2.1 and MIROC3.2 (medres) data during March and the CSIRO-Mk3.5 data during November. During October the mean monthly simulated pasture yield from the AWAP 0.1 data was significantly ( $P < 0.05$ ) lower than the UKMO-HADCM3 data (Figure 4.5b; Appendix 7.4).

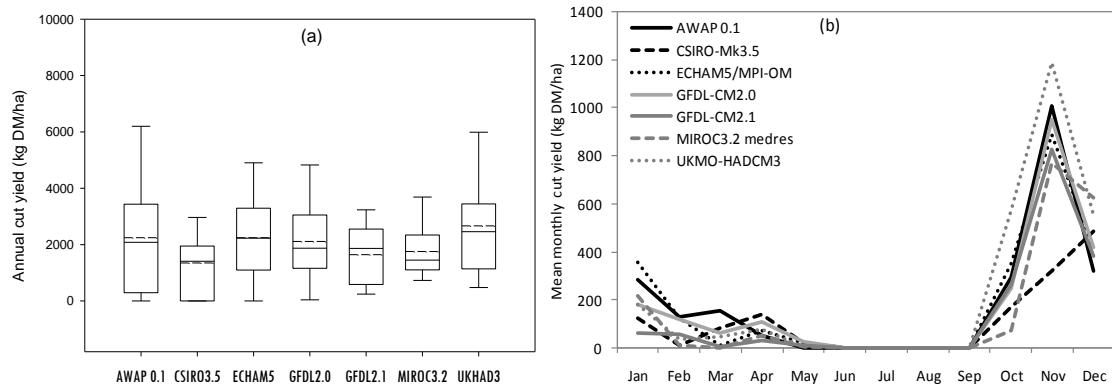


**Figure 4.5** Annual simulated pasture yields (kg DM/ha) for Cressy shown as box plots (10<sup>th</sup>, 25<sup>th</sup>, 50<sup>th</sup>, 75<sup>th</sup>, and 90<sup>th</sup> percentile, with dashed mean line) (a) and mean simulated monthly yield (kg DM/ha) (b) from the climate data sources of AWAP 0.1, CSIRO-Mk3.5, ECHAM5/MPI-OM, GFDL-CM2.0, GFDL-CM2.1, MIROC3.2 (medres) and UKMO-HADCM3 for the period 1990 to 2007.

For the region of Ringarooma, the simulated mean annual pasture yield from each climate data source ranged from 5,457 kg DM/ha (CSIRO-Mk3.5) to 6,134 kg DM/ha (GFDL-CM2.0) (Figure 4.6a) and there was no significant ( $P > 0.05$ ) difference between the climate data sources (Table 4.6). The difference in simulated mean annual pasture yields between the bias-adjusted downscaled GCMs and the AWAP 0.1 data ranged from -10% to 1%. The mean monthly simulated pasture yield from the AWAP 0.1 data was significantly ( $P < 0.05$ ) lower than the CSIRO-Mk3.5 data during April. During September the mean monthly simulated pasture yield from the AWAP 0.1 data was significantly ( $P < 0.05$ ) higher than all downscaled GCMs data except the UKMO-HADCM3 data and during November, the AWAP 0.1 data was significantly ( $P < 0.05$ ) higher than the CSIRO-Mk3.5 data (Figure 4.6b; Appendix 7.5).

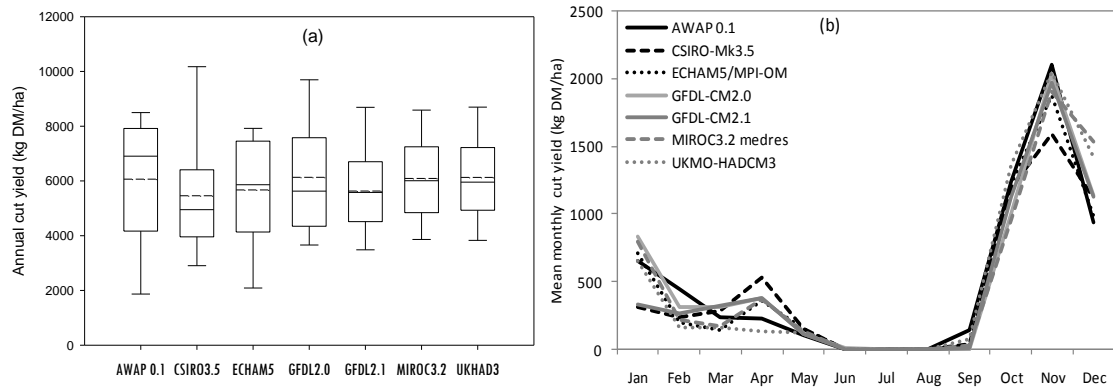


**Figure 4.6** Annual simulated pasture yields (kg DM/ha) for Ringarooma shown as box plots (10<sup>th</sup>, 25<sup>th</sup>, 50<sup>th</sup>, 75<sup>th</sup>, and 90<sup>th</sup> percentile, with dashed mean line) (a) and mean simulated monthly yield (kg DM/ha) (b) from the climate data sources of AWAP 0.1, CSIRO-Mk3.5, ECHAM5/MPI-OM, GFDL-CM2.0, GFDL-CM2.1, MIROC3.2 (medres) and UKMO-HADCM3 for the period 1990 to 2007.

At Ouse, the simulated mean annual pasture yield from each climate data source ranged from 1,682 kg DM/ha (GFDL-CM2.1) to 2,518 kg DM/ha (UKMO-HADCM) (Figure 4.7a) and there was no significant ( $P > 0.05$ ) difference between the climate data sources (Table 4.6). The differences in simulated mean annual pasture yields between the bias-adjusted downscaled GCMs and the AWAP 0.1 data ranged from -20% to 19%. The mean monthly simulated pasture yield from the AWAP 0.1 data was significantly ( $P < 0.05$ ) lower than the CSIRO-Mk3.5 data during April and the ECHAM5/MPI-OM data during May. The mean monthly simulated pasture yield from the AWAP 0.1 data was significantly ( $P < 0.05$ ) higher than the CSIRO-Mk3.5 data during November (Figure 4.7b; Appendix 7.6).

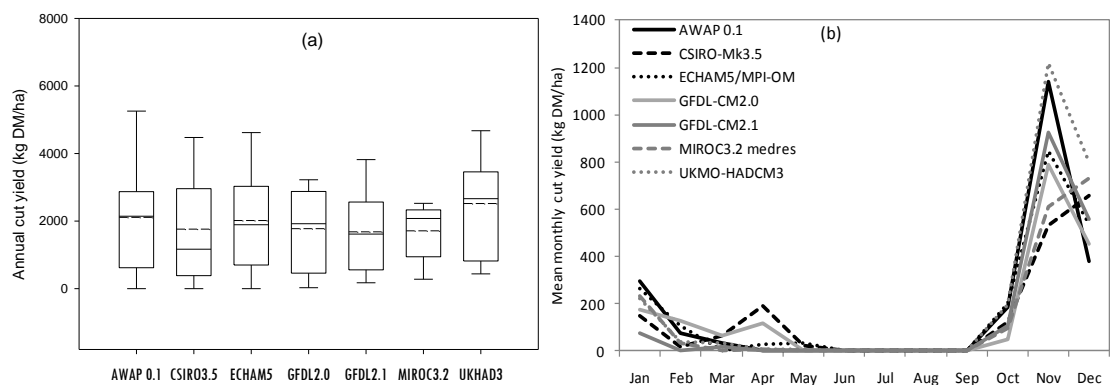


**Figure 4.7** Annual simulated pasture yields (kg DM/ha) for Ouse shown as box plots (10<sup>th</sup>, 25<sup>th</sup>, 50<sup>th</sup>, 75<sup>th</sup>, and 90<sup>th</sup> percentile, with dashed mean line) (a) and mean simulated monthly yield (kg DM/ha) (b) from the climate data sources of AWAP 0.1, CSIRO-Mk3.5, ECHAM5/MPI-OM, GFDL-CM2.0, GFDL-CM2.1, MIROC3.2 (medres) and UKMO-HADCM3 for the period 1990 to 2007.

**Table 4.6** Mean annual simulated pasture yields (kg DM/ha) at Woolnorth, Flowerdale, Merseylea, Cressy, Ringarooma and Ouse from the climate data sources of AWAP 0.1, CSIRO-Mk3.5, ECHAM5/MPI-OM, GFDL-CM2.0, GFDL-CM2.1, MIROC3.2 (medres) and UKMO-HADCM3 for the period 1990 to 2007. Standard deviation is shown in parentheses.

Data source	Woolnorth	Flowerdale	Merseylea	Cressy	Ringarooma	Ouse
AWAP 0.1	8156 (1517)	7834 (2018)	5194 (2386)	2247 (2138)	6063 (2199)	2110 (1789)
CSIRO-Mk3.5	7487 (1966)	7760 (2075)	4607 (2241)	1350 (1400)	5457 (2181)	1760 (1756)
ECHAM5/MPI-OM	7408 (1422)	8298 (2205)	5329 (2208)	2246 (1522)	5673 (2050)	2016 (1528)
GFDL-CM2.0	7722 (1314)	8393 (2378)	5530 (1953)	2112 (1596)	6134 (2119)	1776 (1258)
GFDL-CM2.1	8017 (1539)	8452 (1532)	5411 (1474)	1643 (1107)	5631 (1804)	1682 (1265)
MIROC3.2 medres	8172 (1509)	8682 (1363)	5601 (1371)	1757 (1126)	6090 (1550)	1712 (818)
UKMO-HADCM3	8332 (1861)	8892 (1955)	5891 (1877)	2665 (2114)	6127 (1748)	2518 (1768)
LSD ( $P = 0.05$ )	ns	ns	ns	ns	ns	ns

The variation between the seven climate data sources at each site, ranged from 12% at Woolnorth and Ringarooma to 97% at Cressy. At all sites except Ringarooma, the UKMO-HADCM3 data resulted in the highest mean annual simulated pasture yield. At all sites except Woolnorth and Ouse, the CSIRO-Mk3.5 data had the lowest mean annual simulated pasture yield (Table 4.6). The mean annual simulated pasture yields are reflective of the mean annual rainfall at each site. The UKMO-HADCM3 data had the highest mean annual rainfall whilst the CSIRO-Mk3.5 data had the lowest mean annual rainfall at all sites except Cressy and Ouse (Table 4.4). At all sites except Woolnorth and Flowerdale, the standard deviation of the mean simulated annual pasture yield was highest from the AWAP 0.1 data, reflecting the higher variation in mean annual daily minimum and maximum temperature (Table 4.1; 4.2) and mean annual rainfall (Table 4.4) from this climate data source.

#### 4.4 Conclusion

Systematic evaluations of GCMs provide a foundation for growing confidence in climate model projections (Perkins & Pittman 2009). The evaluation of the bias-adjusted downscaled GCMs against the observed gridded AWAP 0.1 data is an important step in building confidence in the CFT climate models for their use in impact assessment. The ability of GCMs to accurately simulate the historical climate is necessary, but not a completely sufficient condition for an accurate projection of future climate change (Corney *et al.* 2010). This study has found that there were inevitable differences in the climate metrics between the six bias-adjusted downscaled GCMs and the historical gridded AWAP 0.1 data at each of the sites. The differences however, were small enough to give confidence that the six GCMs are acceptable for evaluating agricultural system impacts of future climate scenarios.

A feature of the downscaled CFT model outputs (and almost all climate model simulations) is that climate models are un-phased regarding the real climate system (Perkins *et al.* 2007). That is daily, monthly or annual data does not correlate between individual models and observed climate data (Corney *et al.* 2010). The bias-adjusted CFT model simulations are intended to give an indication of projected climate over decadal time scales (Grose *et al.* 2010). The models are expected to reproduce climate and climate variations that are observed as represented by reproducing the statistics of the mean climate. The mean values and variation of the AWAP 0.1 climate data compared with the bias-adjusted downscaled GCMs were within an acceptable range. The demonstrated ability of the six GCMs to simulate the historical climate gives confidence that the GCMs are able to provide realistic projections of Tasmanian future climate. Furthermore, the variation between the AWAP 0.1 data and the six GCMs data in simulated mean annual and monthly pasture yields for each site were comparable, demonstrating that the variation between the climate data sources at each site is less important than the variation in pasture yields between the six sites. This result implies that the future climate data generated by CFT can be used to study climate change impacts on agricultural production with some degree of confidence.

## **CHAPTER 5: PROJECTED CLIMATE USING THE SIX BIAS-ADJUSTED DYNAMICALLY DOWNSCALED GENERAL CIRCULATION MODELS FOR SIX DAIRY REGIONS**

### **5.1 Introduction**

Climate change is a global occurrence, of which the specific impacts will be felt in changes to dominant local weather conditions. There is a general consensus that the climate will change as a result of increased atmospheric CO<sub>2</sub> concentrations, although there remains variation in the specific projections (Ludwig *et al.* 2009). For example, more warming is likely in polar regions and over land, in contrast to the tropics and oceans (Suppiah *et al.* 2007). The projected global mean temperature change, while beneficial as a measure of the overall strength of greenhouse warming, is not the most relevant measure for regional warming (Smith *et al.* 2005). In order to address this, local or regional climate projections are necessary to quantify the likely effects of climate change on regional areas (Corney *et al.* 2010). This was evident in Tasmania, where high quality, long term climate projections at a local scale to assess climate change impacts on agriculture were previously unavailable.

At a state based scale the CFT climate projections under the A2 emissions scenario show an increase in mean daily temperature of 2.9°C (model range 2.6°C to 3.3°C) throughout the 21<sup>st</sup> century for Tasmania (Grose *et al.* 2010). The projections indicate that temperature increases are lower in the early part of the century, with the rate of change increasing towards the end of the century. The daily maximum temperature rise is projected to be slightly lower (2.8°C) than for daily minimum temperature (2.9°C) (Grose *et al.* 2010). Projected mean annual rainfall shows an average statewide change of less than 100 mm throughout the 21<sup>st</sup> century and decadal variability is projected to remain constant. However, seasonal and regional changes in rainfall are projected to occur throughout the 21<sup>st</sup> century (Grose *et al.* 2010).

The CFT dynamically downscaled climate simulations to a 0.1° grid have captured regional and sub-regional differences across Tasmania, allowing the projected climate change and variability to be quantified at a regional level (Corney *et al.* 2010). Climate change will not only result in regional changes of mean temperature and rainfall distributions but is also expected to affect climate variability (particularly rainfall), as a result of changes in climate processes and feedbacks (Boer 2009).

Both modes of change are relevant for assessing the impacts of climate change (Raisanen 2002). Climate variability has a significant impact on agricultural productivity and is the

strongest driver of inter-annual variability in agricultural production in many environments, particularly rainfed agricultural systems (Ash *et al.* 2007; Crimp *et al.* 2008). Some of the climate variability can be explained by climate forcing, although much remains unexplained and inter-annual and seasonal weather patterns can be notoriously unpredictable (Chapman *et al.* 2008b). Climate variability is the result of an intrinsically non-linear and deterministically chaotic system and there are limitations to what can be predicted about the future climate variability (Anwar *et al.* 2007). Although it is commonly stated that observed climate variability of historical climate data is indicative of future climate variability, it is also probable that there will be increased climate variability in the future (Boer 2009).

Rainfed pasture production systems in Tasmania are highly sensitive to inter-annual climatic variability, particularly rainfall (Anwar *et al.* 2007; Risbey *et al.* 2008). Inter-annual rainfall variability over Tasmania is characterised by a gradient between high rainfall fluctuations in the west and lower variability in the east. Hill *et al.* (2009) summarise that although a gradient exists from west to east as a result of orographic effects in a primarily westerly airstream, inter-annual rainfall variability is island wide.

In this chapter the projected regional climate change and the rate of change across the Tasmanian dairying regions is quantified using the climate metrics of temperature, rainfall and potential evapotranspiration for each of the six dairy regions for the period 1971 to 2100, using daily climate projections data generated from the CFT project.

The objectives of this chapter were to:

1. Quantify regional climate change projections in temperature, rainfall, potential evapotranspiration and solar radiation using the bias-adjusted downscaled GCMs daily climate data, under the A2 scenario at six sites, for the period 1971 to 2100.
2. Quantify regional inter-annual and inter-seasonal variability in temperature, rainfall, potential evapotranspiration and solar radiation using the bias-adjusted downscaled GCMs daily climate data, under the A2 scenario at six sites for the period 1971 to 2100.
3. Quantify regional annual and seasonal rainfall intensity using the bias-adjusted downscaled GCMs daily climate data, under the A2 scenario at six sites, for the period 1971 to 2100.

## 5.2 Materials and methods

The 0.1° gridded bias-adjusted dynamically downscaled CSIRO-Mk3.5, ECHAM5/MPI-OM, GFDL-CM2.0, GFDL-CM2.1, MIROC3.2 (medres) and UKMO-HADCM3 data for each of the six sites (Section 3.2) was obtained from the TPAC portal (<https://dl.tpac.org.au/>). The daily climate data for the period 1<sup>st</sup> January 1961 to 31<sup>st</sup> December 2100, for the climate metrics of maximum and minimum temperature (°C), rainfall (mm) potential evapotranspiration (mm) and solar radiation (MJ/m<sup>2</sup>) were accessed.

An historical baseline climate and three future climate periods were selected to assess the projected climate change and climate variability at each of the six sites. A 30-year climate ‘baseline’ (1971-2000) was selected, although the period 1961 to 1990 is frequently used as a baseline (IPCC 2007), 1971 to 2000 was adopted as the baseline here, as it may better reflect the recent climate (Hennessy 2007; Cullen *et al.* 2009). Three future 30-year climate periods were selected; 2025 (2011-2040), 2055 (2041-2070) and 2085 (2071-2100).

The mean annual and seasonal values of summer (D,J,F), autumn (M,A,M), winter (J, J, A) and spring (S,O,N) for each 30-year period were calculated for the six climate metrics of; maximum and minimum temperature, diurnal temperature range (°C), rainfall (mm), potential evapotranspiration (mm) and solar radiation (MJ/m<sup>2</sup>). Due to the mechanistic, non-stochastic nature of the GCMs climate data, annual and seasonal means are presented as trends. Projected changes in inter-annual and inter-seasonal climate variability were quantified using the coefficient of variation (CV) (standard deviation/average) over a moving 30-year time period.

Rainfall intensity was quantified at each site by using a ‘daily intensity index’ defined as the total annual rainfall (rain days <1 mm were excluded) divided by the total annual number of rain days >1 mm for each year (White *et al.* 2010). Each bias-adjusted downscaled GCM data source was analysed using the above method, and the multi-model mean of the annual and seasonal means are presented.

## 5.3 Results and Discussion

At all sites, both annually and seasonally, across all six climate metrics, there were differences in absolute changes between each of the bias-adjusted downscaled GCMs. Trends in climate variables such as maximum and minimum temperature and potential

evapotranspiration were generally consistent between the models, although there were often differing trends for rainfall.

### 5.3.1 Woolnorth

At Woolnorth, mean annual daily maximum temperature is projected to increase by 2.4°C (model range 2.02°C to 2.79°C) from the baseline to 2085, and mean annual daily minimum temperature is projected to increase by 2.41°C (model range 1.97°C to 2.88°C) from the baseline to 2085 (Table 5.1). There was no discernible change in the projected mean daily diurnal temperature range over the same period. There is no noticeable change in the projected mean annual rainfall (model range - 4 to 8%) from the baseline (model mean, 1031 mm) to 2085 (model mean, 1036 mm) (Table 5.1; Figure 5.1a). Mean annual daily potential evapotranspiration is projected to increase by 4% (model range 3 to 5%) from the baseline (model mean 1034 mm) to 2085 (model mean 1074 mm) (Table 5.1).

**Table 5.1** Multi-model mean of the mean annual daily maximum, minimum and diurnal temperature range (°C), annual rainfall (mm), daily potential evapotranspiration (mm) and daily solar radiation (MJ/m<sup>2</sup>) at Woolnorth, for the baseline, 2025, 2055 and 2085.

Scenario	Daily maxT	Daily minT	Daily diurnalT	Rainfall	Evapotranspiration	Solar radiation
Baseline	16.45 (16.33-16.51)	9.42 (9.31-9.48)	7.03 (7.01-7.05)	1031 (1006-1050)	1034 (1031-1037)	14.42 (14.31-14.51)
2025	17.11 (16.91-17.25)	10.10 (9.86-10.31)	7.01 (6.94-7.07)	1019 (989-1074)	1045 (1041-1046)	14.45 (14.40-14.49)
2055	17.84 (17.55-18.28)	10.80 (10.47-11.31)	7.04 (6.97-7.11)	1017 (977-1093)	1059 (1056-1064)	14.57 (14.52-14.62)
2085	18.85 (18.47-19.23)	11.83 (11.39-12.30)	7.02 (6.92-7.10)	1036 (991-1118)	1074 (1064-1086)	14.55 (14.39-14.69)

Note: model range shown in parenthesis.

The projected increases in daily maximum and minimum temperature at Woolnorth from the baseline to 2085 were similar for each season. Projected seasonal increases in daily maximum temperature ranged from 2.18°C in spring to 2.67°C in summer. Daily minimum temperatures are projected to increase by 2.14°C in spring to 2.65°C in summer. No marked change is projected in the seasonal daily diurnal temperature range over the same period. Mean seasonal rainfall from the baseline to 2085 was projected to decrease by 9% in summer and increase by 5% in winter. No discernible change in rainfall was projected in autumn and spring (Figure 5.1b). Daily potential evapotranspiration was projected to increase by 3% to 4% across all seasons.

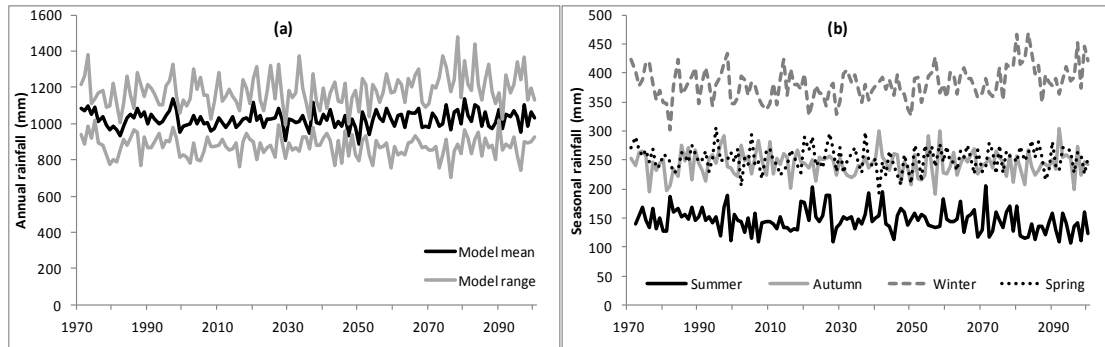


**Figure 5.1** Woolnorth multi-model mean annual rainfall (black line) and model range (grey lines, highest and lowest) (a) and multi-model mean seasonal rainfall (b) for the period 1971 to 2100.

### 5.3.2 Flowerdale

For the region of Flowerdale, mean annual daily maximum temperature is projected to increase by 2.48°C (model range 2.23°C to 2.89°C) from the baseline to 2085, and mean annual daily minimum temperature is projected to increase by 2.58°C (model range 2.21°C to 2.99°C) from the baseline to 2085 (Table 5.2). There was no notable change in the projected mean annual daily diurnal temperature range over the same period. There was no discernible change in the projected mean annual rainfall (model range - 6 to 6%) from the baseline (model mean 1155 mm) to 2085 (model mean 1148 mm) (Table 5.2; Figure 5.2a). Mean annual daily potential evapotranspiration is projected to increase by 4% (model range 3 to 5%) from the baseline (model mean 1028 mm) to 2085 (model mean 1068 mm) (Table 5.2).

**Table 5.2** Multi-model mean of the mean annual daily maximum, minimum and diurnal temperature range (°C), annual rainfall (mm), daily potential evapotranspiration (mm) and daily solar radiation (MJ/m<sup>2</sup>) at Flowerdale, for the baseline, 2025, 2055 and 2085.

Scenario	Daily maxT	Daily minT	Daily diurnalT	rainfall	evapotranspiration	Solar radiation
Baseline	16.21 (16.11-16.26)	8.04 (7.95-8.10)	8.17 (8.15-8.22)	1155 (1132-1181)	1028 (1025-1032)	14.53 (14.41-14.69)
2025	16.89 (16.76-16.99)	8.77 (8.55-8.89)	8.13 (8.05-8.21)	1133 (1084-1184)	1038 (1032-1042)	14.54 (14.42-14.61)
2055	17.66 (17.44-17.94)	9.54 (9.24-9.91)	8.12 (8.02-8.20)	1136 (1091-1224)	1053 (1049-1057)	14.64 (14.59-14.70)
2085	18.69 (18.45-19.10)	10.62 (10.25-11.03)	8.07 (7.92-8.21)	1148 (1091-1226)	1068 (1055-1078)	14.62 (14.40-14.73)

Note: model range shown in parenthesis.

The projected increases in daily maximum and minimum temperature at Flowerdale from the baseline to 2085 were similar for each season. Projected seasonal increases in daily maximum temperature ranged from 2.23°C in winter to 2.74°C in summer. Daily minimum temperatures are projected to increase by 2.28°C in spring to 2.92°C in summer. No notable change is projected in the seasonal daily diurnal temperature range over the same period. No discernible change is projected in seasonal rainfall from the baseline to 2085 (Figure 5.2b). Daily

potential evapotranspiration was projected to increase by a range of 3% (autumn and winter) to 5% (spring).

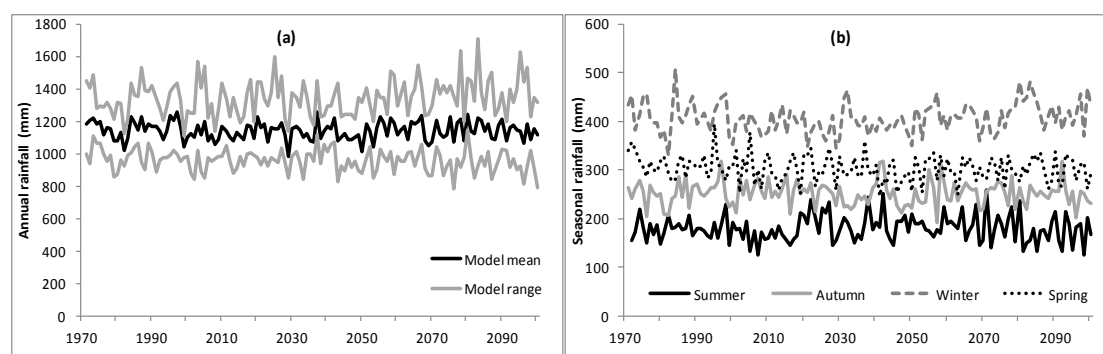


**Figure 5.2** Flowerdale multi-model mean annual rainfall (black line) and model range (grey lines, highest and lowest) (a) and multi-model mean seasonal rainfall (b) for the period 1971 to 2100.

### 5.3.3 Merseylea

At Merseylea, mean annual daily maximum temperature is projected to increase by 2.53°C (model range 2.29°C to 2.96°C) from the baseline to 2085, and mean annual daily minimum temperature is projected to increase by 2.78°C (model range 2.42°C to 3.19°C) from the baseline to 2085 (Table 5.3). Mean annual daily diurnal temperature range is projected to decrease slightly by 0.25°C from the baseline to 2085. Mean annual rainfall is projected to increase by 4% (model range -1 to 10%) from the baseline (model mean 904 mm) to 2085 (model mean 944 mm) (Table 5.3; Figure 5.3a). Mean annual daily potential evapotranspiration is projected to increase by 4% (model range 3 to 5%) from the baseline (model mean 1053 mm) to 2085 (model mean 1092 mm) (Table 5.3).

**Table 5.3** Multi-model mean of the mean annual daily maximum, minimum and diurnal temperature range (°C), annual rainfall (mm), daily potential evapotranspiration (mm) and daily solar radiation (MJ/m<sup>2</sup>) at Merseylea, for the baseline, 2025, 2055 and 2085.

Scenario	Daily maxT	Daily minT	Daily diurnalT	rainfall	evapotranspiration	Solar radiation
Baseline	16.87 (16.78-16.91)	7.24 (7.14-7.28)	9.63 (9.59-9.67)	904 (887-925)	1053 (1050-1056)	15.12 (15.02-15.29)
2025	17.56 (17.38-17.71)	8.03 (7.80-8.13)	9.53 (9.36-9.65)	899 (863-945)	1063 (1054-1068)	15.12 (14.97-15.18)
2055	18.33 (18.14-18.53)	8.86 (8.55-9.24)	9.47 (9.29-9.59)	913 (868-993)	1076 (1071-1083)	15.16 (15.07-15.21)
2085	19.40 (19.16-19.83)	10.02 (9.65-10.43)	9.38 (9.19-9.51)	944 (897-999)	1092 (1080-1104)	15.15 (14.93-15.29)

Note: model range shown in parenthesis.

The projected increases in daily maximum and minimum temperature at Merseylea from the baseline to 2085 were similar for each season. Projected seasonal increases in daily maximum temperature ranged from 2.28°C in winter to 2.75°C in summer. Daily minimum temperatures

are projected to increase by 2.41°C in spring to 3.19°C in summer. No discernible change is projected in the seasonal daily diurnal temperature range over the same period. Mean seasonal rainfall from the baseline to 2085 was projected to increase by a range of 2% in spring to 6% in summer and autumn (Figure 5.3b). Daily potential evapotranspiration was projected to increase by a range of 3% (winter) to 5% (spring).

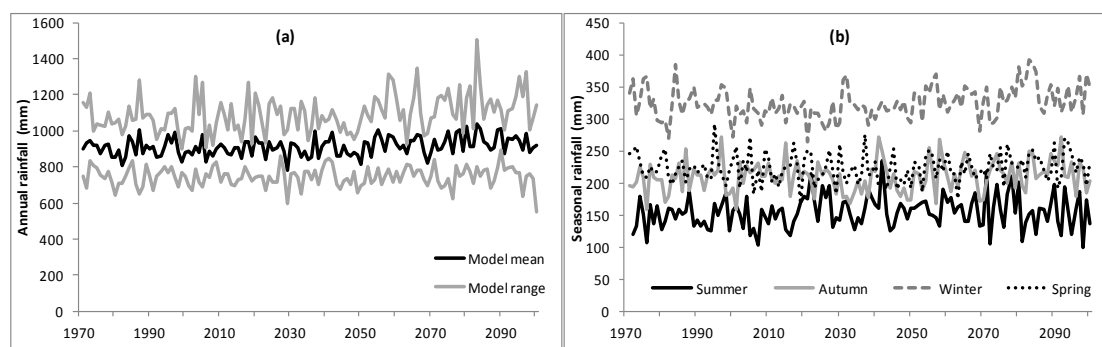


**Figure 5.3** Merseylea multi-model mean annual rainfall (black line) and model range (grey lines, highest and lowest) (a) and multi-model mean seasonal rainfall (b) for the period 1971 to 2100.

### 5.3.4 Cressy

For the region of Cressy, mean annual daily maximum temperature is projected to increase by 2.52°C (model range 2.29°C to 3.02°C) from the baseline to 2085, and mean annual daily minimum temperature is projected to increase by 2.80°C (model range 2.47°C to 3.29°C) from the baseline to 2085 (Table 5.4). Mean annual daily diurnal temperature range is projected to decrease slightly by 0.28°C from the baseline to 2085. Mean annual rainfall is projected to increase by 6% (model range 0 to 15%) from the baseline (model mean 746 mm) to 2085 (model mean 790 mm) (Table 5.4; Figure 5.4a). Mean annual daily potential evapotranspiration is projected to increase by 3% (model range 2 to 5%) from the baseline (model mean 1052 mm) to 2085 (model mean 1088 mm) (Table 5.4).

**Table 5.4** Multi-model mean of the mean annual daily maximum, minimum and diurnal temperature range (°C), annual rainfall (mm), daily potential evapotranspiration (mm) and daily solar radiation (MJ/m<sup>2</sup>) at Cressy, for the baseline, 2025, 2055 and 2085.

Scenario	Daily maxT	Daily minT	Daily diurnalT	rainfall	evapotranspiration	Solar radiation
Baseline	17.35 (17.27-17.40)	5.85 (5.76-5.91)	11.50 (11.45-11.54)	746 (720-767)	1052 (1050-1055)	15.32 (15.23-15.45)
2025	18.03 (17.81-18.21)	6.66 (6.49-6.75)	11.37 (11.19-11.47)	752 (723-799)	1061 (1052-1067)	15.29 (15.15-15.35)
2055	18.81 (18.64-19.01)	7.53 (7.24-7.88)	11.28 (11.04-11.40)	761 (695-837)	1074 (1068-1079)	15.29 (15.20-15.35)
2085	19.87 (19.64-20.37)	8.66 (8.32-9.14)	11.22 (10.99-11.31)	790 (745-859)	1088 (1078-1101)	15.25 (15.05-15.35)

Note: model range shown in parenthesis.

At Cressy, the projected increases in daily maximum and minimum temperature from the baseline to 2085 were similar for each season. Projected seasonal increases in daily maximum temperature ranged from 2.27°C in winter to 2.73°C in summer. Daily minimum temperatures are projected to increase by 2.49°C in spring to 3.13°C in summer. No notable change is projected in the daily diurnal temperature range over the same period. Mean seasonal rainfall from the baseline to 2085 was projected to increase by 3% in spring to 8% in summer and autumn (Figure 5.4b). Daily potential evapotranspiration was projected to increase by 3% (summer, autumn and winter) to 5% (spring).

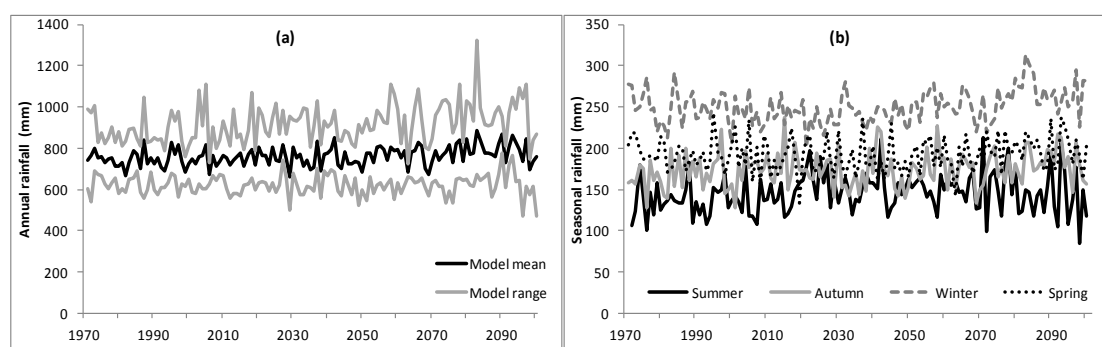


**Figure 5.4** Cressy multi-model mean annual rainfall (black line) and model range (grey lines, highest and lowest) (a) and multi-model mean seasonal rainfall (b) for the period 1971 to 2100.

### 5.3.5 Ringarooma

At Ringarooma, mean annual daily maximum temperature is projected to increase by 2.59°C (model range 2.38°C to 3.01°C) from the baseline to 2085, and mean annual daily minimum temperature is projected to increase by 2.83°C (model range 2.52°C to 3.23°C) from the baseline to 2085 (Table 5.5). Mean annual daily diurnal temperature range from the baseline to 2085 is projected to decrease slightly by 0.24°C. Mean annual rainfall is projected to increase by 6% (model range -2 to 10%) from the baseline (model mean 1128 mm) to 2085 (model mean 1193 mm) (Table 5.5; Figure 5.5a). Mean annual daily potential evapotranspiration is projected to increase by 4% (model range 3 to 5%) from the baseline (model mean 1038 mm) to 2085 (model mean 1076 mm) (Table 5.5).

**Table 5.5** Multi-model mean of the mean annual daily maximum, minimum and diurnal temperature range (°C), annual rainfall (mm), daily potential evapotranspiration (mm) and daily solar radiation (MJ/m<sup>2</sup>) at Ringarooma, for the baseline, 2025, 2055 and 2085.

Scenario	Daily maxT	Daily minT	Daily diurnalT	rainfall	evapotranspiration	Solar radiation
Baseline	16.42 (16.34-16.47)	6.79 (6.70-6.84)	9.63 (9.58-9.66)	1128 (1106-1145)	1038 (1034-1040)	14.22 (14.16-14.38)
2025	17.12 (16.92-17.29)	7.60 (7.37-7.70)	9.52 (9.37-9.64)	1127 (1072-1203)	1046 (1037-1053)	14.18 (14.01-14.25)
2055	17.92 (17.71-18.10)	8.47 (8.16-8.81)	9.45 (9.26-9.55)	1150 (1093-1228)	1061 (1054-1066)	14.22 (14.12-14.28)
2085	19.01 (18.80-19.43)	9.62 (9.32-10.02)	9.39 (9.18-9.48)	1193 (1111-1244)	1076 (1068-1089)	14.18 (14.04-14.29)

Note: model range shown in parenthesis.

The projected increases in daily maximum and minimum temperature at Ringarooma from the baseline to 2085 were similar for each season. Projected seasonal increases in daily maximum temperature ranged from 2.36°C in winter to 2.72°C in summer and autumn. Daily minimum temperatures are projected to increase by 2.51°C in spring to 3.16°C in summer. There was no noticeable change is projected in the seasonal daily diurnal temperature range. Mean seasonal rainfall was projected to increase from the baseline to 2085 by 1% in autumn to 12% in winter (Figure 5.5b). Daily potential evapotranspiration was projected to increase by a range of 3% (summer and autumn) to 5% (spring).

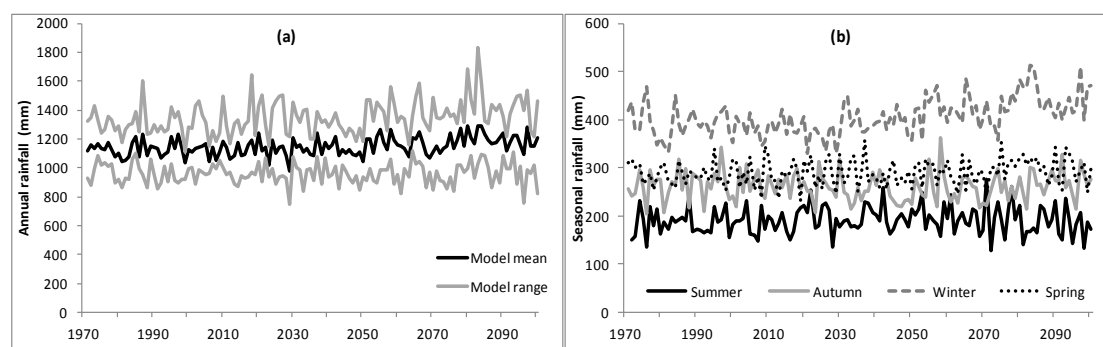


**Figure 5.5** Ringarooma multi-model mean annual rainfall (black line) and model range (grey lines, highest and lowest) (a) and multi-model mean seasonal rainfall (b) for the period 1971 to 2100.

### 5.3.6 Ouse

For the region of Ouse, mean annual daily maximum temperature is project to increase by 2.52°C (model range 2.28°C to 2.98°C) from the baseline to 2085, and mean annual daily minimum temperature is projected to increase by 2.62°C (model range 2.26°C to 3.14°C) from the baseline to 2085 (Table 5.6). No discernible change was projected in mean annual daily diurnal temperature over the same period. Mean annual rainfall is projected to increase by 5% (model range -2 to 17%) from the baseline (model mean 728 mm) to 2085 (model mean 767 mm) (Table 5.6; Figure 5.6a). Mean annual daily potential evapotranspiration is

projected to increase by 3% (model range 3 to 4%) from the baseline (model mean 1012 mm) to 2085 (model mean 1045 mm) (Table 5.6).

**Table 5.6** Multi-model mean of the mean annual daily maximum, minimum and diurnal temperature range (°C), annual rainfall (mm), daily potential evapotranspiration (mm) and daily solar radiation (MJ/m<sup>2</sup>) at Ouse, for the baseline, 2025, 2055 and 2085.

Scenario	Daily maxT	Daily minT	Daily diurnalT	rainfall	evapotranspiration	Solar radiation
Baseline	16.63 (16.57-16.69)	5.19 (5.11-5.23)	11.44 (11.40-11.47)	728 (694-749)	1012 (1008-1014)	14.45 (14.32-14.53)
2025	17.31 (17.14-17.46)	5.93 (5.77-6.11)	11.38 (11.31-11.46)	739 (713-776)	1022 (1019-1025)	14.44 (14.41-14.49)
2055	18.12 (17.93-18.30)	6.72 (6.44-7.05)	11.39 (11.24-11.49)	747 (692-823)	1033 (1029-1035)	14.43 (14.37-14.51)
2085	19.15 (18.91-19.61)	7.80 (7.45-8.33)	11.35 (11.16-11.47)	767 (714-854)	1045 (1041-1054)	14.35 (14.26-14.42)

Note: model range shown in parenthesis.

At Ouse, the projected increases in daily maximum and minimum temperature from the baseline to 2085 were similar for each season. Projected seasonal increases in daily maximum temperature ranged from 2.36°C in winter to 2.72°C in summer. Daily minimum temperatures are projected to increase by a range of 2.55°C in spring to 3.67°C in winter. There was no discernible change projected in the seasonal daily diurnal temperature range over the same period. Mean seasonal rainfall is projected to increase from the baseline to 2085 by 8% in summer, 10% in autumn, and 6% in winter, with no marked change projected for spring (Figure 5.6b). Daily potential evapotranspiration was projected to increase by a range of 3% (summer, autumn and winter) to 4% (spring).

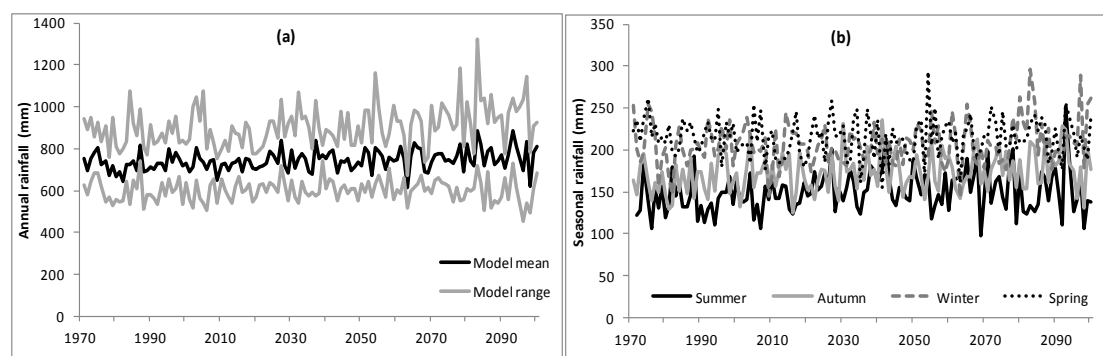


**Figure 5.6** Ouse multi model mean annual rainfall (black line) and model range (grey lines, highest and lowest) (a) and multi-model mean seasonal rainfall (b) for the period 1971 to 2100.

At all sites, there is no discernible change ( $\pm 1\%$ ) projected in both the mean annual daily and mean seasonal solar radiation from the baseline to 2085.

At all sites, a progressive increase is projected in mean annual daily maximum temperatures ranging from 2.40°C at Woolnorth to 2.59°C at Ringarooma from the baseline to the 2085. The

same trend was observed in mean annual daily minimum temperatures at each site, although the range of the projected minimum temperature increase are greater, ranging from 2.41°C at Woolnorth to 2.83°C at Ringarooma. At all sites except Woolnorth, the mean annual daily diurnal temperature range was projected to narrow slightly from the baseline to 2085, due to daily minimum temperatures increasing at a slightly greater rate than daily maximum temperatures. This is in agreement with the observed historical (since 1950) trend in diurnal temperature across Tasmania (Grose *et al.* 2010). Seasonally, the greatest rate of projected increases in both daily maximum and minimum temperatures at each site occur during summer, followed by autumn, spring and winter. The projected changes in mean temperature across Tasmania under the A2 emission scenario are less than projected increases for mainland Australia of 3.4°C (range 2.2°C to 5.0°C) and global projections of 3.4°C (range 2.0°C to 5.4°C) (CSIRO and Bureau of Meteorology 2007). Rises in temperature are generally greater over land than over oceans and as such temperature increases over inland continental Australia are greater than over the coastal regions, Tasmania or New Zealand (Grose *et al.* 2010). As a result, the projected temperature increases for each dairy region across Tasmania are less than the dairy regions on mainland Australia. The projected increases for each of the mainland dairy regions range from 3°C to 4°C by the end of the 21<sup>st</sup> century, except for the coastal dairying regions of Queensland where the projected temperature increase ranges from 2°C to 3°C (CSIRO and Bureau of Meteorology 2007).

There was little regional variation in the rate of the projected increases in daily maximum and minimum temperature. The projected changes to the mean values of daily maximum and minimum temperature exhibit a relatively simplistic response to greenhouse forcing. Grose *et al.* (2010) reported from a statewide analysis of the six bias-adjusted downscaled GCMs, that the rise in the mean annual maximum and minimum temperature is relatively uniform over the state of Tasmania despite the spatially varied mean. Seasonally, the increase in daily maximum and minimum temperatures is less spatially uniform and it is probable that it is a result of the projected changes in the dominant winds across the state within the GCMs simulations. The gradient in the temperature change during summer (greater increase near the west coast) may be related to the projected reduction in the dominant westerly wind, bringing cool air off the ocean (Grose *et al.* 2010).

The inter-model range in the maximum temperature projections showed that the CSIRO-Mk3.5 GCM consistently projected maximum temperature above the multi-model mean value at all sites both annually and seasonally. Conversely the ECHAM5/MPI-OM and GFDL-CM2.0 GCMs consistently projected maximum temperature below the multi-model mean value at each site both annually and seasonally. The inter-model range in the minimum

temperature projections revealed that the CSIRO-Mk3.5 and the UKMO-HADCM3 GCM consistently projected minimum temperature above the multi-model mean value at all sites both annually and seasonally. In contrast the GFDL-CM2.0 GCM consistently projected minimum temperature below the multi-model mean value at each site both annually and seasonally. However, Grose *et al* (2010) state that the inter-model range in temperature is tighter than the GCMs responses for the globe as presented in the IPCC fourth Assessment Report, both for the present climate and into the future. This reduced inter-model range is due to the modelling approach taken by CFT, which included a bias-adjustment of sea surface temperature prior to the downscaling process. Resulting in the sea-surface temperature boundary condition from each parent GCM to correctly reflect the observed climate for the 1961 to 1990 reference period.

Since 1970, Tasmania has observed a reduction in mean annual rainfall across the state of 45 mm per decade (Bureau of Meteorology 2011) along with a reduction in inter-annual rainfall variability (Grose *et al.* 2010). The reduction has been driven by a decrease in autumn rainfall (Alexander *et al.* 2007). At all sites, the projections of the six GCMs in annual and seasonal rainfall throughout the 21<sup>st</sup> century show little change. In contrast, mean annual rainfall projections for the mainland dairy regions show a much greater rate of change, ranging from -30% to +20% in northern and eastern Australia to -30% to +5% across southern Australia (CSIRO and Bureau of Meteorology 2007). At all Tasmanian sites except Woolnorth and Flowerdale, mean annual rainfall is projected to only slightly increase from the baseline to 2085, ranging from 4% at Merseylea to 6% at Cressy and Ringarooma. The absence of significant changes in projected annual and seasonal rainfall trends is not unusual, considering that rainfall is not expected to respond as consistently or strongly to increases in greenhouse gas forcing as temperature (Alexander & Arblaster 2009).

The inter-model range in the rainfall projections showed that the UKMO-HADCM3 GCM consistently projected rainfall above the multi-model mean value at all sites both annually and seasonally. However, the inter-annual rainfall variability of each GCM at each site was generally lower than that from the observed data for the period of 1961 to 2007 (Grose *et al* 2010).

Grose *et al.* (2010), report that GCMs are capable of realistically simulating the general aspects of the Southern Annular Mode (SAM). The local influence of the SAM in the dynamically downscaled GCM simulations was explored using a modified version of the Regional Antarctic Oscillation Index (AOIR) of Meneghini *et al.* (2007). The index is based on the difference in the mean sea level pressure at 40° south and 65° south in the Australian

region. The trend in the AOIR has been positive for all seasons for the period 1955 to 2005 (Meneghini *et al.* 2007) and the CFT GCM projections indicate a continuation of the current trend. The trend means an increasing occurrence of the high phase of the SAM for the region, where mid-latitude westerlies tend to be weaker, resulting in lower moisture transport to western Tasmania. The negative correlation between rainfall anomalies and the AOIR is greatest during summer and the increase in the index is consistent with the projected decrease of summer rainfall at Woolnorth and to a lesser extent Flowerdale. However, the SAM can only partially explain seasonal rainfall trends and variability, and there are other influences on synoptic activity in the region (Meneghini *et al.* 2007).

Autumn rainfall across Tasmania has shown the largest change of any season in the last 30 years (Bureau of Meteorology 2011). The mean GCM simulated rainfall data for this period does not accurately reflect the observed record from the AWAP 0.1 data source. This result indicates that the reduced autumn rainfall that has been observed is not an ongoing climate state throughout the 21<sup>st</sup> century (Grose *et al.* 2010), although it is important to note that the range of rainfall projections between the GCMs is comparable to the observed record. The projected changes in rainfall across Tasmania along with the uncertainty associated with the GCM simulations, indicates that at this point in time it appears that the long term mean annual rainfall over Tasmania is likely to remain relatively stable throughout the 21<sup>st</sup> century (Grose *et al.* 2010).

### **5.3.7 Climate variability**

At all sites, the CV of annual and seasonal maximum and minimum temperatures and CV of annual potential evapotranspiration increased slightly from the baseline to 2085 (data not shown).

At each site, the CV of annual rainfall increased from 1971 to 2100, the increase in the CV of annual rainfall from the baseline to 2085 ranged from 15% at Merseylea to 22% at Ouse (Figure 5.7a-f). The CV of seasonal rainfall at all sites is projected to increase from the baseline to 2085 for each season (Figure 5.7a-f). The projected increase of the CV of summer rainfall from the baseline to 2085, ranges from 3% at Merseylea to 11% at Woolnorth. The projected increase in the CV of autumn rainfall ranges from 12% at Merseylea to 11% at Woolnorth. The projected increase in the CV of winter rainfall ranges from 9% at Ouse to 26% at Flowerdale, while the projected increase in the CV of spring rainfall ranges from 9% at Merseylea to 18% at Ouse. The inter-model range in the projected CV of annual rainfall

showed that the CSIRO-Mk3.5 and GFDL-CM2.1 GCMs consistently projected the CV of rainfall below the multi-model mean value at all sites.

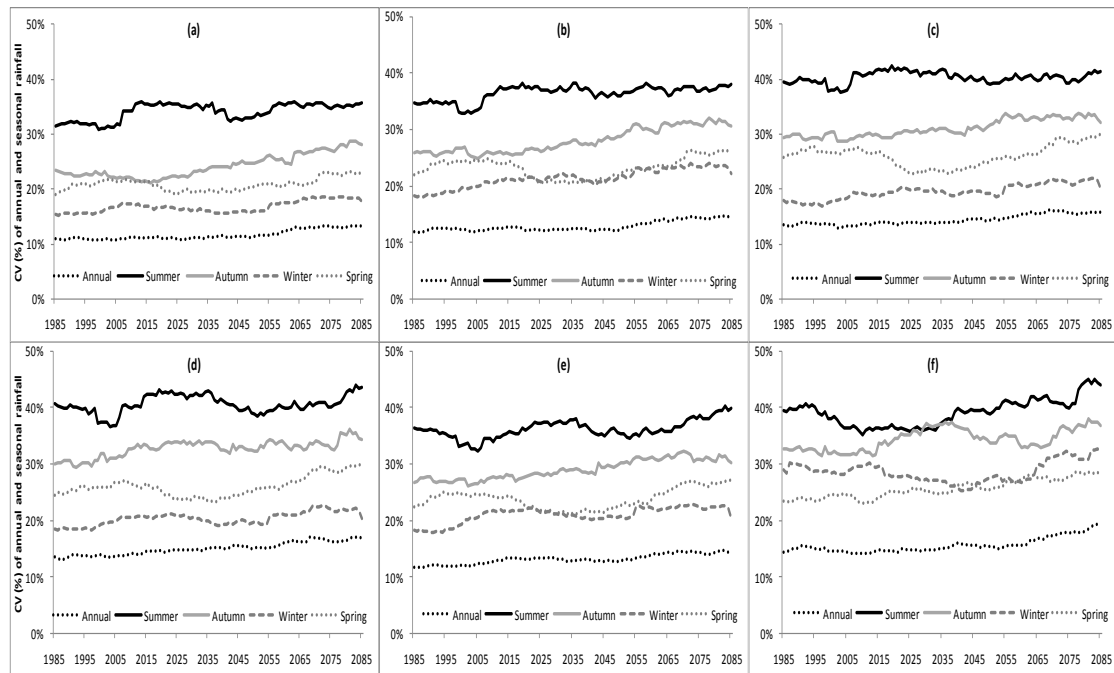


**Figure 5.7** Multi-model rolling 30-year CV (%) of annual and seasonal rainfall at Woolnorth (a), Flowerdale (b), Merseylea (c), Cressy (d), Ringarooma (e) and Ouse (f) for the period 1971 to 2100.

Climate change is commonly expected to result in an increase in annual and seasonal rainfall variability (Salinger 2005; Anwar *et al.* 2007; Boer 2009), this is consistent with the findings presented here. While annual and seasonal rainfall variability has declined since the 1970's at each of the sites, this is attributed to the decrease in the number of exceptionally wet years since the mid 1970's (Grose *et al.* 2010). The recent decline in rainfall variability is projected to reverse throughout the 21<sup>st</sup> century, as a result of increased sea surface temperatures leading to a more energetic atmosphere with increased moisture flux and changes to the mean sea level pressure. Projected changes in sea surface temperatures near Tasmania are likely to affect rainfall and rainfall variability at a local scale (Grose *et al.* 2010). The projected increases in annual and seasonal rainfall variability at each of the six sites are small relative to the mainland dairy regions. Rainfall variability across the mainland dairy regions is projected to increase at a greater rate in response to the projected ranges of -30% to +20% change in mean annual rainfall across each of the mainland dairy regions (CSIRO and Bureau of Meteorology 2007; Quiggin *et al.* 2010).

Inter-annual and inter-seasonal rainfall variability over Tasmania is influenced by the SAM, ENSO, Indian Ocean Dipole (IOD) and atmospheric blocking in the Tasman Sea (Grose *et al.* 2010). The ENSO influence is strongest in the north of the state, whereas the SAM is most prominent over the southwest of the state. Inter-annual and inter-seasonal rainfall variability is driven by direct atmospheric forcing and sea surface temperature variations in the tropical Pacific (Hill *et al.* 2009). Seasonally, the relationships vary between SAM, ENSO and IOD, with different climate drivers having a greater influence on rainfall and rainfall variability in different seasons (Hill *et al.* 2008; Grose *et al.* 2010).

### **5.3.8 Rainfall intensity**

At all sites, mean annual rainfall intensity is projected to increase from the baseline to 2085. The projected increase in rainfall intensity ranged from 7% (Flowerdale) to 13% (Cressy). At all sites, the total annual number of rain days are projected to decrease from the baseline to 2085, ranging from 7% (Woolnorth, Flowerdale) to 3% (Ringarooma) (Figure 5.8a-f). For the region of Woolnorth, the greatest change in seasonal rainfall intensity is projected to occur during winter, increasing 11% by 2085 above the baseline. At the sites of Flowerdale, Merseylea, Cressy and Ringarooma the greatest change in seasonal rainfall intensity is projected to occur during spring, increasing 9%, 17%, 20% and 17% respectively by 2085 above the baseline. At Ouse, the greatest change in seasonal rainfall intensity is projected to occur during summer, increasing 17% by 2085 above the baseline (Appendix 8.0).

The inter-model range in the projected annual rainfall intensity showed that the MIROC3.2(medres) and UKMO-HADCM3 GCMs consistently projected rainfall intensity above the multi-model mean value at all sites. In contrast the CSIRO-Mk3.5, GFDL-CM2.0 and GFDL-CM2.1 GCMs consistently projected annual rainfall intensity below the multi-model mean value at each site. However, these trends tend to be small relative to the mean rainfall intensity.

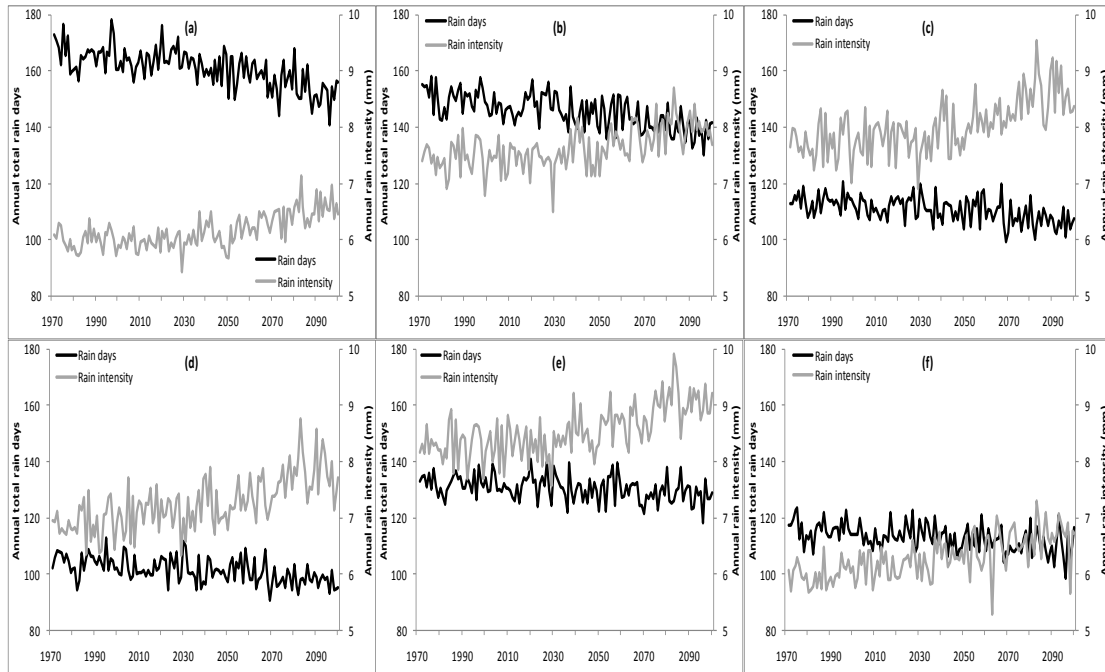


**Figure 5.8** Multi-model mean of the annual total number of rain days (>1 mm) and multi-model mean annual rainfall intensity (mm) at Woolnorth (a), Flowerdale (b), Merseylea (c), Cressy (d), Ringarooma (e) and Ouse (f) for the period 1971 to 2100.

The pattern of change in rainfall intensity in a future warmer climate is related to increases of water vapour and is a consequence of an increase in the capacity of a warmer atmosphere to hold moisture (Meehl *et al.* 2005; Boer 2009). General Circulation Models indicate an increase in rainfall intensity in most regions across the globe, under a warmer climate (Haylock & Nicholls 2000; Hughes 2003; Perkins & Pittman 2009), even in regions where mean rainfall decreases (Christensen & Christensen 2004; Meehl *et al.* 2005; Kharin & Zwiers 2007). Projected rainfall intensity across Tasmania is consistent with these reported findings. Rainfall intensity across Tasmania is projected to increase throughout the 21<sup>st</sup> century (White *et al.* 2010), with projected increases of up to 60% in some seasons, in some coastal regions with an affiliated decrease in the mean number of rain days. Consistent with the analysis by White *et al.* (2010), at all sites in the current study, rainfall intensity is projected to increase, along with a projected decrease in the mean number of annual rain days throughout the 21<sup>st</sup> century.

## 5.4 Conclusion

The bias-adjusted dynamically downscaled GCM simulations undertaken by CFT represented a series of climate change experiments driven by an increase of atmospheric greenhouse gases under the A2 scenario (Corney *et al.* 2010). Increasing greenhouse gases lead to an alteration of the radiative heat balance of the globe, resulting in changes in the entire climate system (Grose *et al.* 2010). At all sites, the bias-adjusted gridded daily climate projections show that the observed temperature trends during the latter half of the 20<sup>th</sup> century are projected to continue into the 21<sup>st</sup> century. Little change is projected in annual and seasonal rainfall, however rainfall variability and rainfall intensity are projected to increase.

In quantifying the scale of future climate projections it is important to recognise the limitations. Climate change projections will inevitably vary as a result of continual improvements in the ability of GCMs to depict global and more importantly, regional climate systems. Uncertainties remain in the parameters of some processes within GCMs, for example cloud formation and dissipation. However, the gap is decreasing as analysis and modelling techniques are constantly evolving (Mitchell 2004; Nicholls 2007). The CFT GCM simulations presented here should not be regarded as forecasts, rather, they are intended to give an indication of projected climate change over decadal time scales (Corney *et al.* 2010).

This study has quantified the projected regional climate change and variability at each of the six dairy regions for the remainder of the 21<sup>st</sup> century. The climatic environment currently experienced at all sites is projected to change, particularly mean temperatures. In order to prepare and adapt pasture based feed systems to a changing climate it is important to ascertain how regional climate change and variability will affect pasture production. Climate and agriculture are inextricably linked and various features of climate change, such as higher atmospheric CO<sub>2</sub> concentrations, increased temperatures and altering rainfall patterns will have varying impacts on pasture production. In the following chapter, the likely impacts of the projected regional climate change on pasture based dairy systems in Tasmania are quantified.

## **CHAPTER 6: MODELLED RESPONSES OF PERENNIAL RYEGRASS TO THE PROJECTED CLIMATE**

### **6.1 Introduction**

Production and consumption of high quality perennial ryegrass pastures underpin the competitiveness of the Tasmanian dairy industry. Any change in climate or climate variability has the potential to alter the feed supply and the management of these pasture based dairy systems. However, the impact of the projected climate change on pasture based dairy systems in the Tasmanian dairy regions remains uncertain. Climate change is projected to vary regionally across Tasmania and as a result the influence of climate change on pasture production is also likely to vary regionally. The rate of change in pasture production will be dependent on the combination of changes to temperature, rainfall and evapotranspiration as well as plant responses to elevated atmospheric CO<sub>2</sub> concentrations (Cullen *et al.* 2009). Regional climate change projections across six differing dairy regions of Tasmania indicate an increase in mean daily temperatures ranging from 2.4°C to 2.7°C by 2085, with the absence of any discernible change in annual and seasonal rainfall. Potential evapotranspiration rates are projected to increase between 3% and 5%.

By providing estimates of pasture growth under a greater range of climate variables than can be feasibly determined through many short term experiments, simulating pasture production under future climate scenarios is a valuable means for management and determining research priorities by extending short-term results to longer term pasture production (Robertson 2006). In Mediterranean and temperate climates, Cullen & Eckard (2011) report that pasture production may increase slightly with both increased warming of 1°C and a reduction in rainfall of 10%, although with further warming of ≈3°C and reduced rainfall of > 10% mean annual pasture production is projected to decline. Pasture production in cool temperate climates, like Tasmania (Bureau of Meteorology 2007), appear to be more resilient to such climatic changes (Cullen & Eckard 2011). However, across Tasmania the projected regional climate change and the rate of change of the climate metrics of temperature, rainfall and potential evapotranspiration have the potential to strongly influence perennial ryegrass production. This may result in changes to total annual pasture growth, changes in the seasonality of the pasture growth and changes in irrigation requirements and water availability. To assess the potential influences of the projected climate change across the Tasmanian dairying regions, pasture production on a daily basis was simulated using the biophysical model DairyMod (Johnson *et al.* 2008) for each of the six dairy regions for the period 1971 to 2100, using daily climate projections data generated from the CFT project.

The objectives of this chapter were to:

1. Quantify projected regional climate change impacts on simulated pasture production using the six dynamically downscaled GCMs daily climate data at six sites for the period 1971 to 2100.
2. Quantify inter-annual and inter-seasonal simulated pasture production variability using the six dynamically downscaled GCMs daily climate data at six sites for the period 1971 to 2100.
3. Quantify the impact of rising atmospheric CO<sub>2</sub> concentrations under the A2 emissions scenario on pasture production at six sites for the period 1971 to 2100.

## 6.2 Materials and methods

The 0.1° gridded bias-adjusted dynamically downscaled CSIRO-Mk3.5, ECHAM5/MPI-OM, GFDL-CM2.0, GFDL-CM2.1, MIROC3.2 (medres) and UKMO-HADCM3 data for each of the six sites (Section 3.2) was obtained from the TPAC portal (<https://dl.tpac.org.au/>). The daily climate data for the period 1<sup>st</sup> January 1961 to 31<sup>st</sup> December 2100, for the climate metrics of maximum and minimum temperature (°C), rainfall (mm) potential evapotranspiration (mm) and solar radiation (MJ/m<sup>2</sup>) were accessed.

Each daily climate data set from the GCMs was run independently within DairyMod. DairyMod version (4.9.2) (Johnson *et al.* 2008) was used to simulate rainfed and irrigated perennial ryegrass growth and the methods and parameters of the model used in this chapter were identical to Section 3.2 with two exceptions. Firstly, the irrigation simulations were parameterised to allow irrigation daily if the Growth Limiting Factor of water (GLF<sub>water</sub>) fell below 0.9 (Table 6.1). Secondly, atmospheric CO<sub>2</sub> concentrations were increased annually within each climate data source consistent with the ISAM A2 emissions scenario (Figure 6.2).

The GLF<sub>temperature</sub> (Section 3.2) and Growth Limiting Factor of Water (GLF<sub>water</sub>) can be used to identify the most limiting factor on simulated pasture growth. The GLF<sub>water</sub> is calculated within DairyMod and is defined from the wilting point, recharge point, field capacity and saturated water content (Figure 6.1). The GLF<sub>water</sub> is on a scale from 0 to 1, if the GLF<sub>water</sub> is 1 then there is no limitation to growth, if it is 0 then there is total limitation. For water contents below the wilting point, the plant cannot extract water from the soil and the GLF<sub>water</sub> is 0. Between the wilting point and recharge point the GLF<sub>water</sub> increases from 0 to 1 and above the recharge point to field capacity, the GLF<sub>water</sub> is 1 (Johnson 2005). For the current study, the recharge point was set at the halfway point (0.5) between wilting point and field capacity for the onset of water stress (0 to 1) and the GLF<sub>water</sub> saturation was set at 0.9.

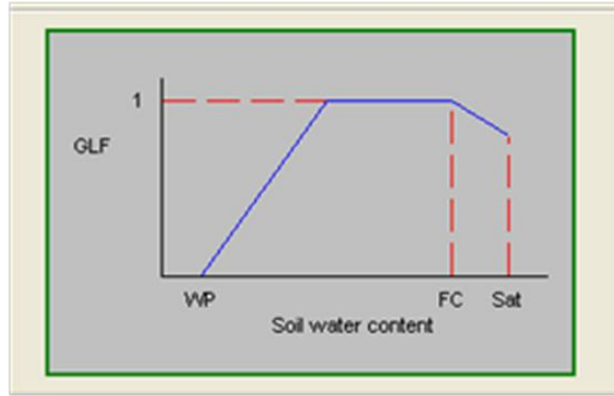


**Figure 6.1** Model parameters used within DairyMod for  $GLF_{water}$  (Johnson *et al* 2005), Growth Limiting Factor Water (GLF), Wilting Point (WP), Field Capacity (FC) and Saturation (Sat).

**Table 6.1** Key irrigation variables and associated parameter values used in DairyMod (Version 4.9.2) to simulate growth of perennial ryegrass pastures on a generic clay loam soil.

Irrigate in response to soil water deficit (SWD)	initiated
Scale factor between WP and FC for the onset of water stress (0-1)	0.50
Irrigate when crop Growth Limiting Factor (%) fall below	90
Minimum days between irrigation applications	1
Target root profile water content as percent of field capacity	100
Depth for SWD calculation (cm)	40
Critical SWD at which to irrigate (cm)	20

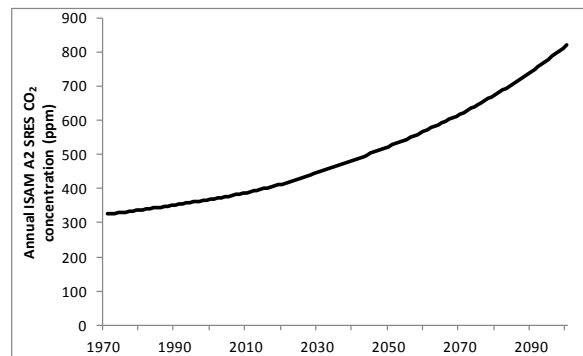


**Figure 6.2** Annual A2 ISAM SRES  $CO_2$  concentration (ppm).

The mean annual and monthly simulated pasture yields, mean annual and monthly irrigation requirements, and the mean annual and monthly growth limiting factors for both water ( $GLF_{water}$ ) and temperature ( $GLF_{temperature}$ ) were calculated for each 30-year period (as defined in Section 5.2). Projected changes in inter-annual and inter-seasonal simulated pasture cut yields were quantified using the CV over a moving 30-year time period. The gross production water-use index (GPWUI) as defined by Purcell and Currey (2003) was used to quantify WUE under the irrigated simulations at all sites. The GPWUI was calculated as the total annual yield divided by the total annual water received (irrigation plus rainfall). Due to the

mechanistic, non-stochastic nature of the GCMs climate data, annual and monthly means are presented as trends and compared for each 30-year period.

The annual pasture yield response of perennial ryegrass to elevated atmospheric CO<sub>2</sub> concentrations were modelled at each site by comparing simulated pasture yields at a baseline CO<sub>2</sub> concentration of 380 ppm (ambient CO<sub>2</sub>) and a yearly incremental increase of atmospheric CO<sub>2</sub>, under the SRES A2 scenario (Figure 6.19), for the period 1971 to 2100.

## **6.3 Results and Discussion**

### **6.3.1 Rainfed and irrigated pasture cut yields**

At all sites, annual rainfed pasture production is projected to increase throughout the 21<sup>st</sup> century (Figure 6.3a-f). At all sites except Woolnorth (Figure 6.3a), the simulated mean annual rainfed pasture yields are projected to progressively increase from the baseline to 2085 at Flowerdale by 46% (model range 39% to 68%), Merseylea by 82% (64% to 114%), Cressy by 150% (131% to 232%), Ringarooma by 81% (64% to 107%) and at Ouse by 137% (109% to 206%). At Woolnorth, the simulated mean annual rainfed pasture yields are projected to peak in 2055 at 30% (20% to 48%) above the baseline, then decline slightly by 2085 (Table 6.2). The inter-model range in the annual rainfed pasture yields showed that the UKMO-HADCM3 GCM consistently projected yields above the multi-model mean value at all sites. In contrast the MIROC3.2 (med res) GCM consistently projected annual yields below the multi-model mean value at each site.

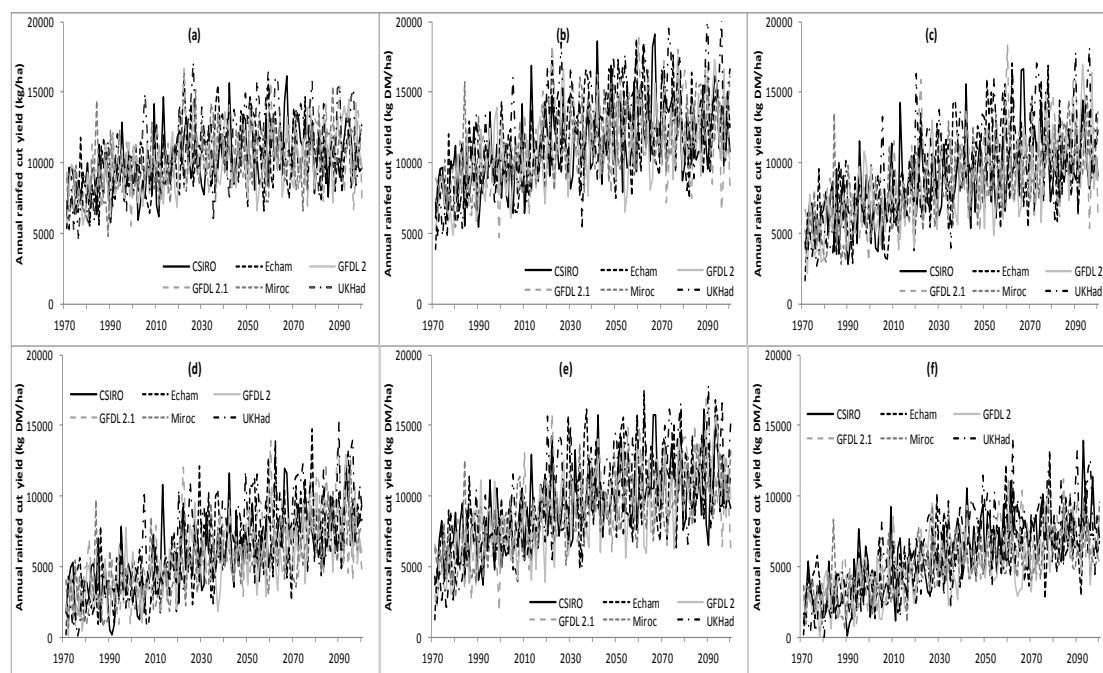


**Figure 6.3** Annual simulated rainfed pasture yields (kg DM/ha), from the six dynamically downscaled GCMs, for Woolnorth (a), Flowerdale (b), Merseylea (c), Cressy (d), Ringarooma (e) and Ouse (f) for the period 1971 to 2100.

**Table 6.2** Multi-model mean of the simulated mean annual rainfed pasture yields (kg DM/ha) at Woolnorth, Flowerdale, Merseylea, Cressy, Ringarooma and Ouse for the baseline, 2025, 2055 and 2085.

Scenario	Woolnorth	Flowerdale	Merseylea	Cressy	Ringarooma	Ouse
Baseline	8618	8837	6059	3292	6246	3088
2025	10628	11674	8792	5616	9220	5285
2055	11169	12680	10078	7000	10550	6700
2085	11094	12892	11021	8233	11299	7319
% change Baseline - 2055	30%	43%	66%	113%	69%	117%
% change Baseline - 2085	29%	46%	82%	150%	81%	137%

At all sites, mean annual irrigated pasture production is projected to increase throughout the 21<sup>st</sup> century (Figure 6.4a-f). The simulated mean annual irrigated pasture yields are projected to increase from the baseline to 2085 by 26% (model range 23% to 29%) at Woolnorth, 34% (31% to 36%) at Flowerdale, 34% (31% to 39%) at Merseylea, 26% (16% to 37%) at Cressy, 41% (36% to 46%) at Ringarooma and by 31% (20% to 44%) at Ouse (Table 6.3). However, at all sites except Flowerdale, the greatest projected increase in mean annual irrigated pasture yields occurs at approximately 2055. At each site excluding Flowerdale, a slight decrease is projected in mean annual irrigated pasture yields from 2055 to 2085, at Woolnorth, the projected decrease is 1%, at Merseylea 2%, at Cressy 9% at Ringarooma 1% and at Ouse 8% (Table 6.3). The inter-model range in the annual irrigated pasture yields showed that the GFDL-CM2.1 GCM consistently projected yields above the multi-model mean value at all

sites, in contrast the MIROC3.2 (med res) GCM consistently projected annual yields below the multi-model mean value at each site. However, the model range of the projected yields under irrigation tended to be much tighter than the model range of the projected yields under dryland conditions where the inter-model range is much larger in comparison. This is a result of the irrigated simulations not being water limited, conversely the rainfed simulations were limited by both water and temperature, creating a greater inter-model range in the projected yields.

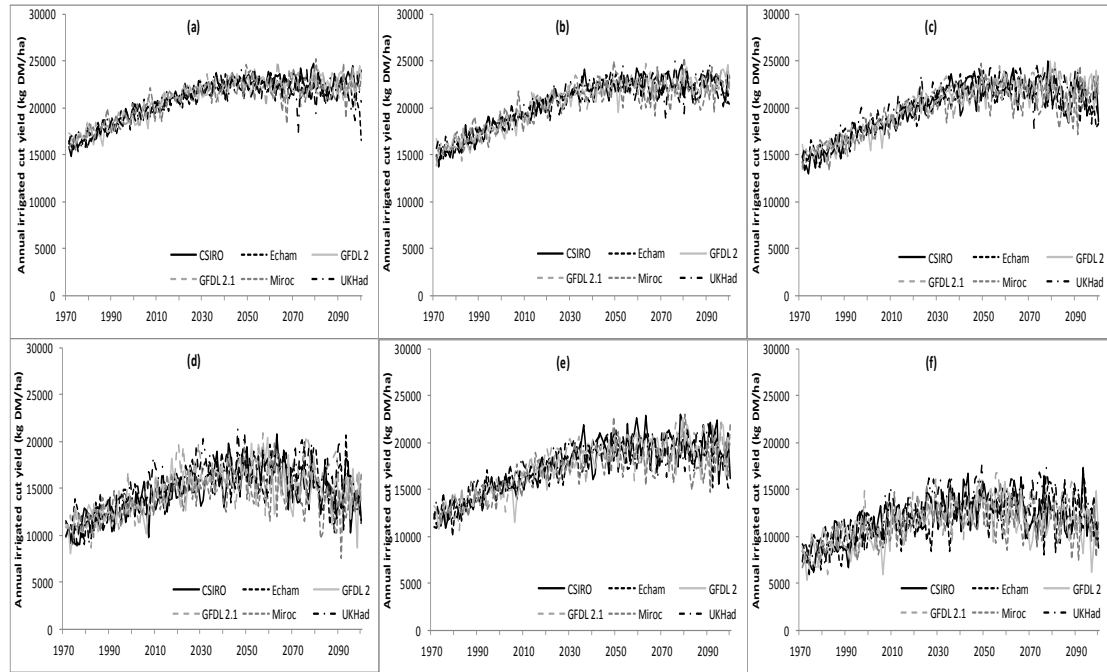


**Figure 6.4** Annual simulated irrigated pasture yields (kg DM/ha), from the six dynamically downscaled GCMs, at Woolnorth (a), Flowerdale (b), Merseylea (c), Cressy (d), Ringarooma (e) and Ouse (f) for the period 1971 to 2100.

**Table 6.3** Multi-model mean of the simulated mean annual irrigated pasture yields (kg DM/ha) at Woolnorth, Flowerdale, Merseylea, Cressy, Ringarooma and Ouse for the baseline, 2025, 2055 and 2085.

Scenario	Woolnorth	Flowerdale	Merseylea	Cressy	Ringarooma	Ouse
Baseline	17715	16705	16092	11992	13644	9298
2025	21568	21014	20612	15727	17861	12452
2055	22570	22423	22140	16541	19310	13210
2085	22238	22439	21631	15094	19254	12208
% change Baseline - 2055	27%	34%	38%	38%	42%	42%
% change Baseline - 2085	26%	34%	34%	26%	41%	31%

The multi-model  $GLF_{\text{temperature}}$  presented in Figure 6.5a-f is representative for both the rainfed and irrigated simulations, while the multi-model  $GLF_{\text{water}}$  is only applicable to the rainfed simulations as water is non-limiting under the irrigation simulations. All sites demonstrated a linear trend in  $GLF_{\text{temperature}}$ , with the values progressively become less limiting for the period

of 1971 to 2100 as a result of the projected increase in temperatures. At Woolnorth, mean annual  $GLF_{\text{temperature}}$  decreases by 9% from the baseline to 2085, at Flowerdale by 12%, at Merseylea by 13% at Cressy by 14% at Ringarooma by 16% and at Ouse by 15%. At all sites, there was little change in the annual  $GLF_{\text{water}}$  from 1971 to 2100 (Figure 6.5a-f).

Under rainfed conditions at Cressy, Ringarooma and Ouse temperature is the most limiting factor for pasture growth throughout the period of 1971 to 2100 (Figure 6.5d-f). At Woolnorth, the most limiting factor for pasture growth changes from temperature to water by approximately 2020, whilst at Flowerdale and Merseylea water becomes most limiting factor for pasture growth at approximately 2070 and 2050 respectively (Figure 6.5a-c).

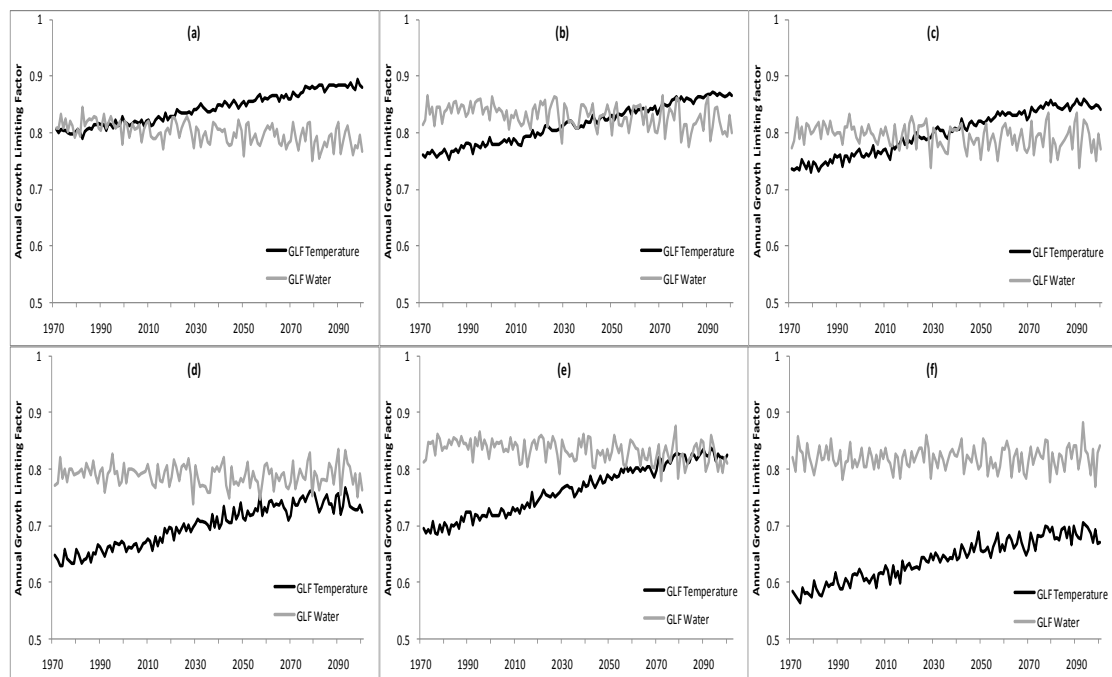


**Figure 6.5** Multi-model mean annual  $GLF_{\text{Temperature}}$  and  $GLF_{\text{Water}}$  at Woolnorth (a), Flowerdale (b), Merseylea (c), Cressy (d), Ringarooma (e) and Ouse (f) for the period 1971 to 2100.

The projected increase in simulated annual rainfed pasture yields above the baseline is driven by a progressively earlier start and increased growth during winter and also an increase in spring growth throughout the 21<sup>st</sup> century (Figure 6.6a-f). This is most noticeable at Merseylea, Cressy, Ringarooma and Ouse which are currently more temperature limited than the other two sites and where lower temperatures are restricting growth during the late winter/early spring period. At Woolnorth and Flowerdale, regions that currently experience relatively mild winter and spring temperatures, winter/spring growth is still projected to increase, though not as substantially in comparison to the inland sites.

At all sites, under simulated rainfed conditions, summer pasture yields are projected to decrease below the baseline value at 2085, but are compensated for by an increase in winter and spring growth (Figure 6.6a-f). The likely explanation for the decrease in summer pasture yields by 2085 is projected higher daily maximum temperatures.

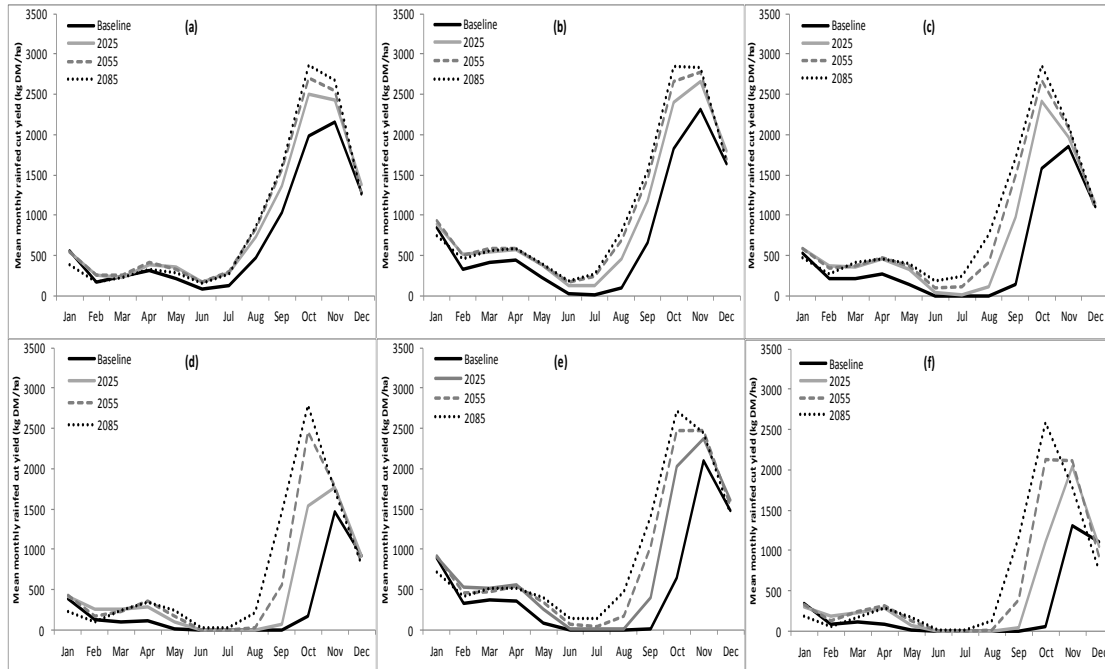


**Figure 6.6** Multi-model mean simulated monthly rainfed pasture yields (kg DM/ha) at Woolnorth (a), Flowerdale (b), Merseylea (c), Cressy (d), Ringarooma (e) and Ouse (f) for the baseline, 2025, 2055 and 2085.

The projected increase in simulated mean annual irrigated pasture yields is also due to a progressively earlier start and increased growth during winter and spring (Figure 6.7a-f). Under irrigated conditions summer pasture yields at Woolnorth and Flowerdale are projected to peak at 2055 then decrease at 2085 (Figure 6.7a,b). At Merseylea, Cressy, Ringarooma and Ouse summer pasture yields are projected to peak at 2025 and begin to decrease at 2055 and continue to decrease at 2085 (Figure 6.7c-f). At all four of these sites, the projected pasture yield during summer in 2085 is below the baseline pasture yield, while at Cressy and Ouse the projected pasture yield at 2055 is below the baseline figure, driven by the projected increase in daily maximum temperatures.

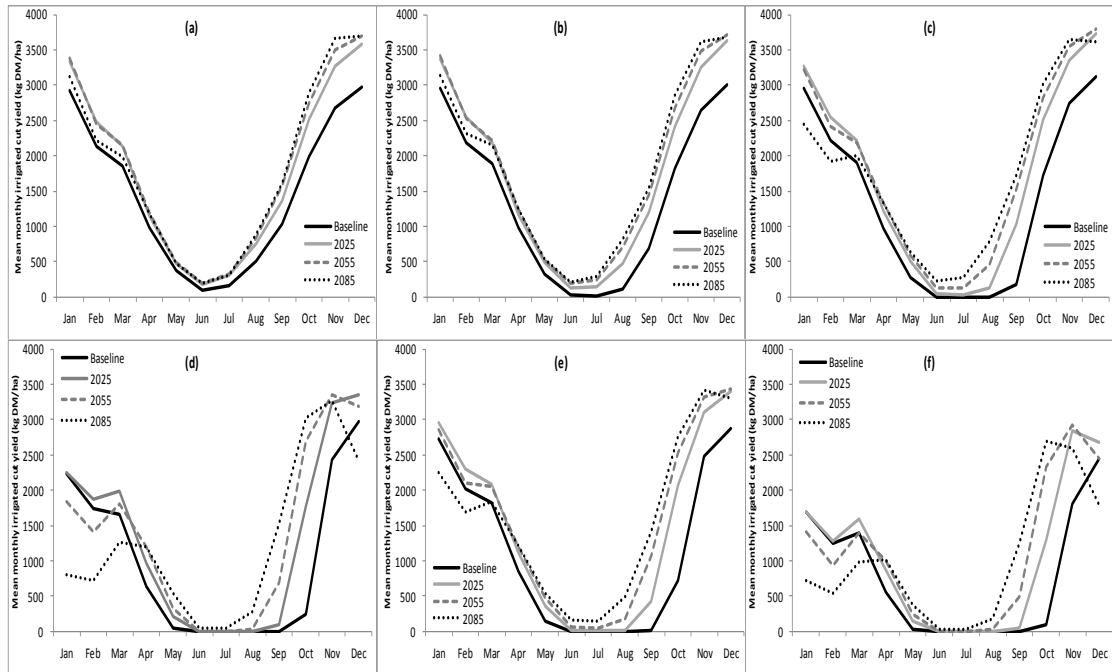


**Figure 6.7** Multi-model mean simulated monthly irrigated pasture yields (kg DM/ha) at Woolnorth (a), Flowerdale (b), Merseylea (c), Cressy (d), Ringarooma (e) and Ouse (f) for the baseline, 2025, 2055 and 2085.

Under the rainfed and irrigated simulations at Woolnorth, Flowerdale, Merseylea and Ringarooma, mean monthly  $GLF_{\text{temperature}}$  is projected to progressively become less limiting from the baseline to 2085 for the months of April to November (Figure 6.8a-c,e). For Cressy and Ouse, mean monthly  $GLF_{\text{temperature}}$  is projected to progressively become less limiting for the months of April to October (Figure 6.8d,f). At Woolnorth and Flowerdale  $GLF_{\text{temperature}}$  is projected to be more limiting for growth during January and February by 2085 in comparison to the baseline. At Merseylea, Cressy, Ringarooma and Ouse  $GLF_{\text{temperature}}$  at 2085 is projected to be increasingly limiting for growth during the months of January, February and December, in comparison to the baseline, particularly at Cressy and Ouse (Figure 6.8d,f). At all sites under rainfed simulations, mean monthly  $GLF_{\text{water}}$  is projected to become a greater limitation for pasture growth during November and December by 2085 in comparison to the baseline period. In addition, at the sites of Woolnorth and Flowerdale mean monthly  $GLF_{\text{water}}$  is also projected to be increasingly limiting for growth during January (Figure 6.8a,b).

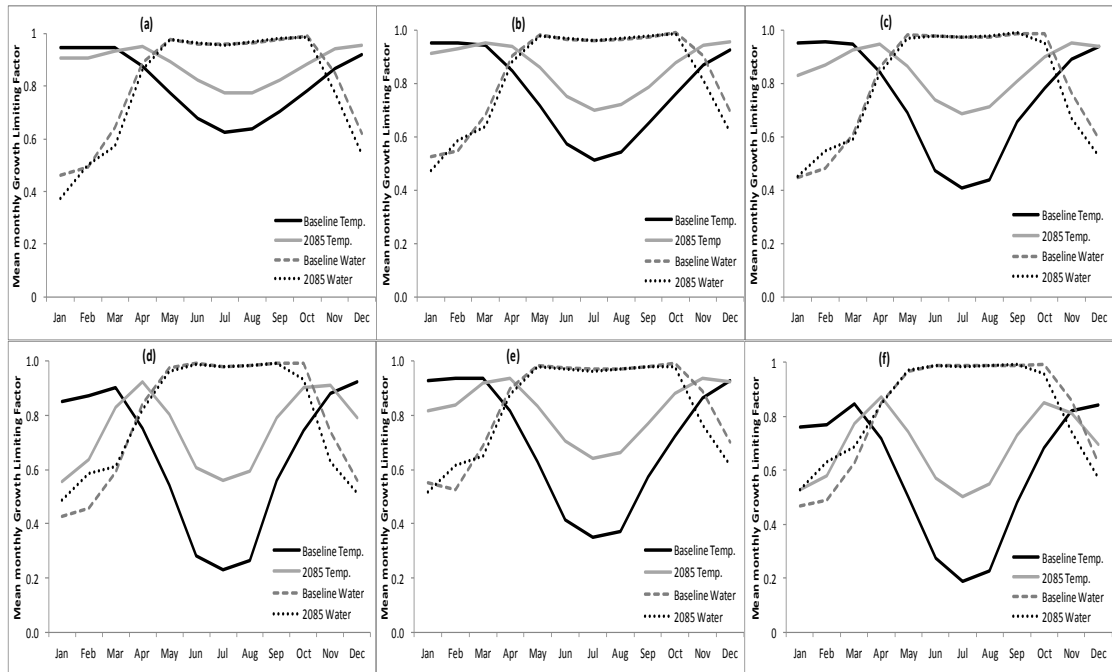


**Figure 6.8** Multi-model mean monthly  $GLF_{\text{temperature}}$  and  $GLF_{\text{water}}$  at Woolnorth (a), Flowerdale (b), Merseylea (c), Cressy (d), Ringarooma (e) and Ouse (f) for the baseline and 2085.

All six sites are temperature limited under the current climatic conditions during winter and spring. Yield increases are projected to be less at sites with currently high potential yields (Woolnorth, Flowerdale) than currently lower yielding sites (Merseylea, Cressy, Ringarooma, Ouse). Primarily due to lower minimum temperatures limiting growth at the inland sites, as opposed to the coastal regions of Woolnorth and Flowerdale, which have relatively milder climates.

Woolnorth and Cressy were selected to demonstrate the regional variation of the projected climate on simulated perennial ryegrass growth. At Woolnorth, simulated mean monthly rainfed pasture yields during August, September and October are projected to increase linearly throughout the 21<sup>st</sup> century (Figure 6.9a). The  $GLF_{\text{temperature}}$  progressively becomes less limiting during the same period, indicating that the projected temperature increases are driving the increase in pasture yields (Figure 6.9b) correspondingly there is a progressive decrease in the number the number of days  $<2^{\circ}\text{C}$  during these months (Figure 6.9c).

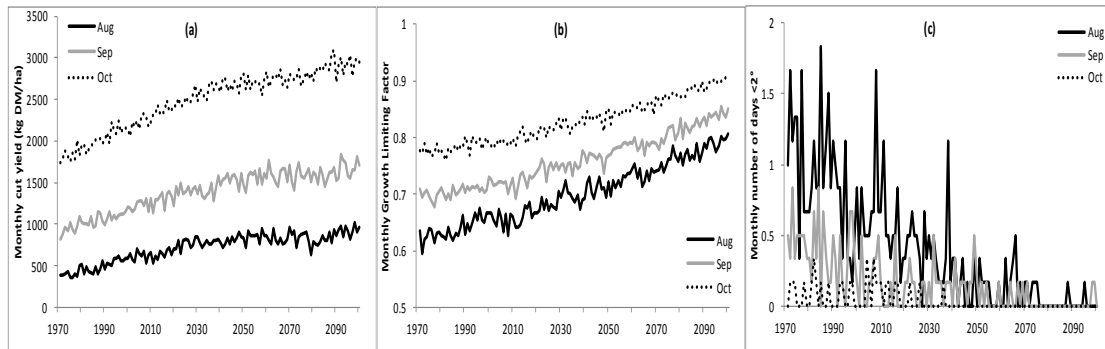


**Figure 6.9** Woolnorth multi-model mean monthly simulated rainfed pasture yield (kg DM/ha) (a) mean monthly  $GLF_{\text{temperature}}$  (b) and total number of days  $< 2^{\circ}\text{C}$  (c) for the months of August, September and October for the period 1971 to 2100.

Rainfed pasture yields at Cressy are also projected to increase linearly throughout the 21<sup>st</sup> century during the months of August, September and October (Figure 6.10a). Similarly,  $GLF_{\text{temperature}}$  progressively becomes less limiting, demonstrating that the projected temperature increases are driving the increase in pasture yields (Figure 6.10b), and there is a progressive decrease in the number of days  $< 2^{\circ}\text{C}$  from 9 days (model range 4 to 16) at the baseline to 3 days (model range 0 to 6) by 2085 (Figure 6.10c). Cressy currently experiences a greater temperature limitation to pasture growth during the winter/spring period than Woolnorth. The temperature limitation for pasture growth is further highlighted by the number of days at Woolnorth that are  $< 2^{\circ}\text{C}$  during the winter/spring period (0 to 1 at the baseline) (Figure 6.9c) in contrast to Cressy where there are 4 to 16 days  $< 2^{\circ}\text{C}$  at the baseline (Figure 6.10c).

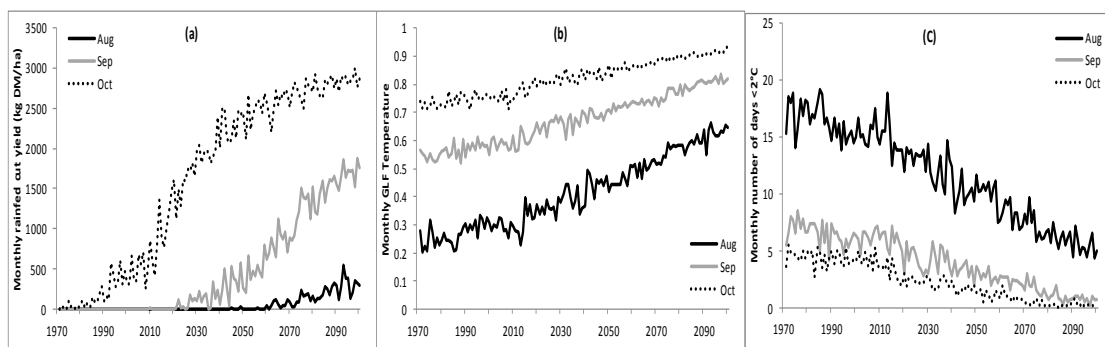


**Figure 6.10** Cressy multi-model mean monthly simulated rainfed pasture yield (kg DM/ha) (a) mean monthly  $GLF_{\text{temperature}}$  (b) and total number of days  $< 2^{\circ}\text{C}$  (c) for the months of August, September and October for the period 1971 to 2100.

Under the irrigated simulations, simulated mean annual pasture yields at Woolnorth are projected to decrease slightly from 2055 to 2085. The slight decrease in mean annual yields is being driven by decreasing summer yields in the months of January, February, March and

December (Figure 6.11a). The  $GLF_{\text{temperature}}$  progressively becomes more limiting for pasture growth from 2055 onwards (Figure 6.11b), as the number of days  $>28^{\circ}\text{C}$  in January, February, March and December increases slightly from  $<1$  day at the baseline to 1 to 2 days at 2085 (Figure 6.11c).

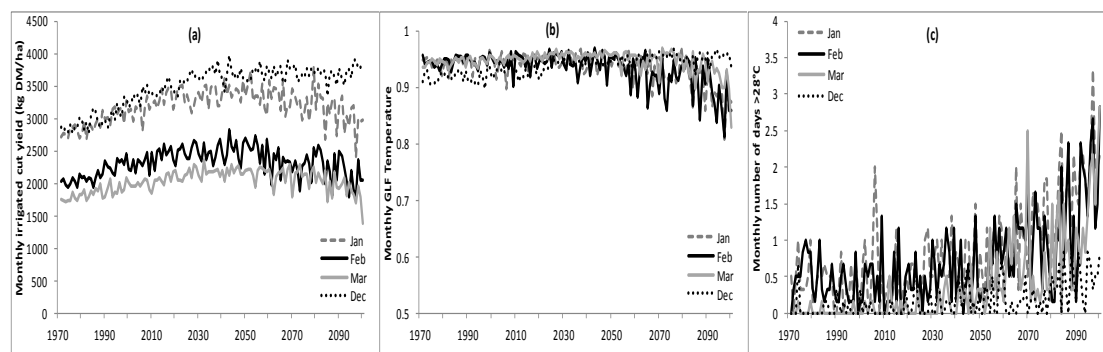


**Figure 6.11** Woolnorth multi-model mean simulated irrigated pasture yield (kg DM/ha) (a) mean monthly  $GLF_{\text{temperature}}$  (b) and total number of days  $>28^{\circ}\text{C}$  (c) for the months of January, February, March and December for the period 1971 to 2100.

Simulated mean annual irrigated pasture yields for the region of Cressy are projected to decrease by 9% from 2055 to 2085, driven by decreasing summer yields in the months of January, February, March and December (Figure 6.12a). The  $GLF_{\text{temperature}}$  becomes increasingly limiting for pasture growth from approximately 2030 onwards during the summer months (Figure 6.12b), with a progressive increase in the number of days  $>28^{\circ}\text{C}$  in December, January, February and March from 2 days (model range 1 to 4) at the baseline to 6 days (model range 4 to 10) at 2085 (Figure 6.12c).

Cressy is projected to experience a greater temperature limitation for pasture growth during summer than Woolnorth through the latter part of the 21<sup>st</sup> century due to a greater number of days exceeding  $28^{\circ}\text{C}$ . In contrast to Woolnorth, the projected rate of increased very warm days at Cressy is limiting growth from approximately 2025 onwards (Figure 6.12a), whereas at Woolnorth pasture growth is not limited during the summer months until approximately 2055 (Figure 6.11a). In addition, the decline of December pasture yields at Cressy is marked in contrast to Woolnorth.

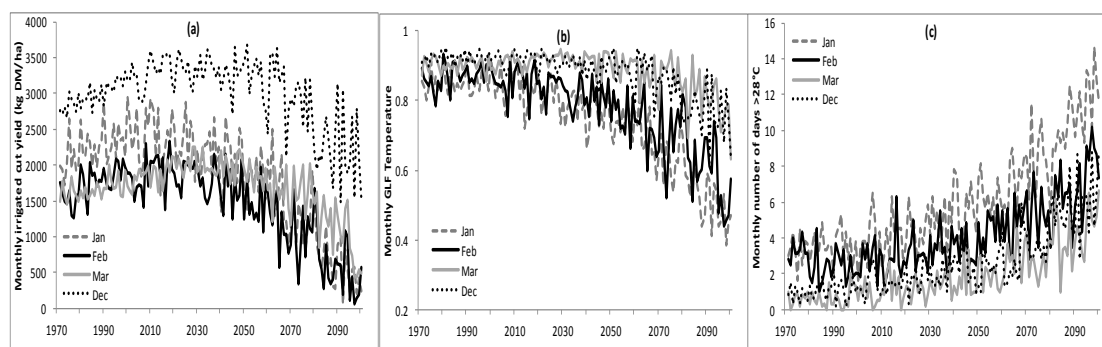


**Figure 6.12** Cressy multi-model mean simulated irrigated pasture yield (kg DM/ha) (a) mean monthly  $GLF_{\text{temperature}}$  (b) and total number of days  $>28^{\circ}\text{C}$  (c) for the months of January, February, March and December for the period 1971 to 2100.

At all sites under rainfed simulations, mean annual pasture yields are projected to increase from the baseline to 2085. Under the irrigated simulations mean annual pasture yields are projected to increase to 2055, then decline slightly through to the end of the 21<sup>st</sup> century. The progressive increase in both minimum and maximum temperatures has driven an increase in pasture growth during winter and spring (Table 6.4) where at all sites, an increasing optimum temperature range for perennial ryegrass growth has occurred. Peacock (1974) states there is a high positive correlation between mean temperature and pasture growth rates and that the growth rates of temperate grasses decreases rapidly below  $10^{\circ}\text{C}$ , with little growth occurring below  $6^{\circ}\text{C}$  (Cooper & Tainton 1968).

Perennial ryegrass growth during winter and early spring in temperate regions is severely restricted by low temperatures (Cressy and Ouse, Table 6.4). This is partly due to frost susceptibility and other factors such as low solar radiation, short days and low daily temperatures (Thomas & Norris 1979; Kemp *et al.* 1989). Plants grown at lower temperatures ( $<10^{\circ}\text{C}$ ) partition less dry weight to leaves and produce thicker shorter leaves (Beevers 1961; Hunt & Halligan 1981). In addition, Cooper (1964) reported a strong negative correlation between the rate of leaf expansion and low temperatures. Leaf expansion is influenced primarily by temperature and to a lesser extent by available soil moisture (Fulkerson & Donaghy 2001). Tillering of perennial ryegrass under optimum temperatures (approximately  $20^{\circ}\text{C}$ ) responds similarly to leaf growth, with new tillers appearing rapidly and producing leaves in quick succession (Langer 1973; Hunt & Thomas 1985).

**Table 6.4** Multi-model mean of the mean spring daily minimum temperature (°C) at Woolnorth, Flowerdale, Merseylea, Cressy, Ringarooma and Ouse, for the baseline, 2025, 2055 and 2085.

Spring	Woolnorth	Flowerdale	Merseylea	Cressy	Ringarooma	Ouse
baseline	8.46	7.19	6.76	5.61	6.05	4.98
2025	9.09	7.85	7.49	6.37	6.78	5.73
2055	9.66	8.48	8.13	7.04	7.49	6.44
2085	10.60	9.47	9.17	8.09	8.56	7.53

The projected decrease of irrigated pasture yields evident from 2055 (from 2025 at Cressy and Ouse) is the result of increased maximum temperatures during summer and early autumn and a progressive increase in the number of days exceeding 28°C, throughout the 21<sup>st</sup> century. The effect of warmer temperatures towards the end of the 21<sup>st</sup> century on summer pasture yields, were greater under the irrigated simulations, primarily due to the simulations not being water limited. In contrast, the rainfed simulations were limited by both water and temperature during the summer months.

Perennial ryegrass being a cool season grass is not adapted to higher temperatures (Waller & Sale 2001). Blaikie & Martin (1987) reported that increasing the temperature from 20°C to 40°C has a significant negative impact on perennial ryegrass growth. As the temperature rose, the rate of net photosynthesis at a given level of irradiance declined, and at 33°C to 38°C was less than half the rate at 21°C to 24°C. The temperature response curve for perennial ryegrass is frequently described as a convex parabola with an optimum of close to 20°C (Hunt & Halligan 1981). Several studies have examined growth responses of perennial ryegrass to temperature in controlled environments. Mitchell (1956) established that the optimum ambient temperature range for perennial ryegrass growth was 17°C to 21°C and that growth can cease above 30°C to 35°C. At Cressy and Ouse, mean daily summer maximum temperatures by 2085 have increased beyond the optimum range for perennial ryegrass growth (Table 6.5), driving a greater decrease in irrigated annual pasture cut yields in comparison to the other four sites.

**Table 6.5** Multi-model mean of the mean summer daily maximum temperature (°C) at Woolnorth, Flowerdale, Merseylea, Cressy, Ringarooma and Ouse, for the baseline, 2025, 2055 and 2085.

Summer	Woolnorth	Flowerdale	Merseylea	Cressy	Ringarooma	Ouse
Baseline	19.94	20.18	21.22	22.86	21.13	22.12
2025	20.67	20.92	21.93	23.54	21.83	22.87
2055	21.49	21.75	22.78	24.41	22.69	23.73
2085	22.61	22.92	23.97	25.59	23.85	24.84

Under the rainfed simulations at all sites, increasing soil moisture deficit by 2085 is projected to become a greater limitation for pasture growth during the months of November and December (Figure 6.8a-f). Perennial ryegrass is sensitive to soil moisture deficit stress, caused by low or intermittent rainfall correlated with high evapotranspiration rates (Guobin & Kemp 1992; Turner & Asseng 2005). Poor persistence of perennial ryegrass is a common problem in high winter rainfall and summer dry regions (Eckard *et al.* 2001; Nie *et al.* 2004) and soil moisture deficits during summer and autumn reduce herbage production and quality and can result in dormancy or death under more severe stress (Waller & Sale 2001). Results from field experiments where moisture stress was imposed for several months, showed that DM production and tiller density can be markedly reduced (Waller & Sale 2001). Perennial ryegrass has a variety of mechanisms that enable it to withstand (to an extent), moisture deficits that occur in dry summers. As soil moisture levels decline, leaf growth decreases, primarily as a result of reduced cell expansion restricting the size of new leaves (Waller & Sale 2001) and smaller leaves reducing water loss through transpiration and via the use of assimilates in respiration (Jones 1988).

It is important to recognise a caveat of DairyMod in that the model is unable to simulate the death of the plant. Therefore when growing conditions improve the plants shift back into growth mode, without any loss of accumulated growth due to plant death e.g. over summer at Cressy and Ouse. Therefore when assessing simulated pasture production from regions that are exposed to either excessive or extended periods of cold or high temperatures, this limitation of the model should be taken into consideration.

### **6.3.2 Annual and monthly irrigation requirements**

At Woolnorth, Flowerdale, Merseylea and Ringarooma the mean annual irrigation requirements progressively increased from the baseline to 2085 (Figure 6.13a-c,e). Mean annual irrigation requirements increased from the baseline to 2085 by 16% at Woolnorth, 14% at Flowerdale, 8% at Merseylea and by 10% at Ringarooma (Table 6.6). At Cressy and Ouse (Figure 6.13d,f) mean annual irrigation requirements increased by 5% and 3% respectively by 2055 above the baseline. However, by 2085 mean annual irrigation requirements decreased slightly below the baseline values by 1% and 2% respectively (Table 6.6).

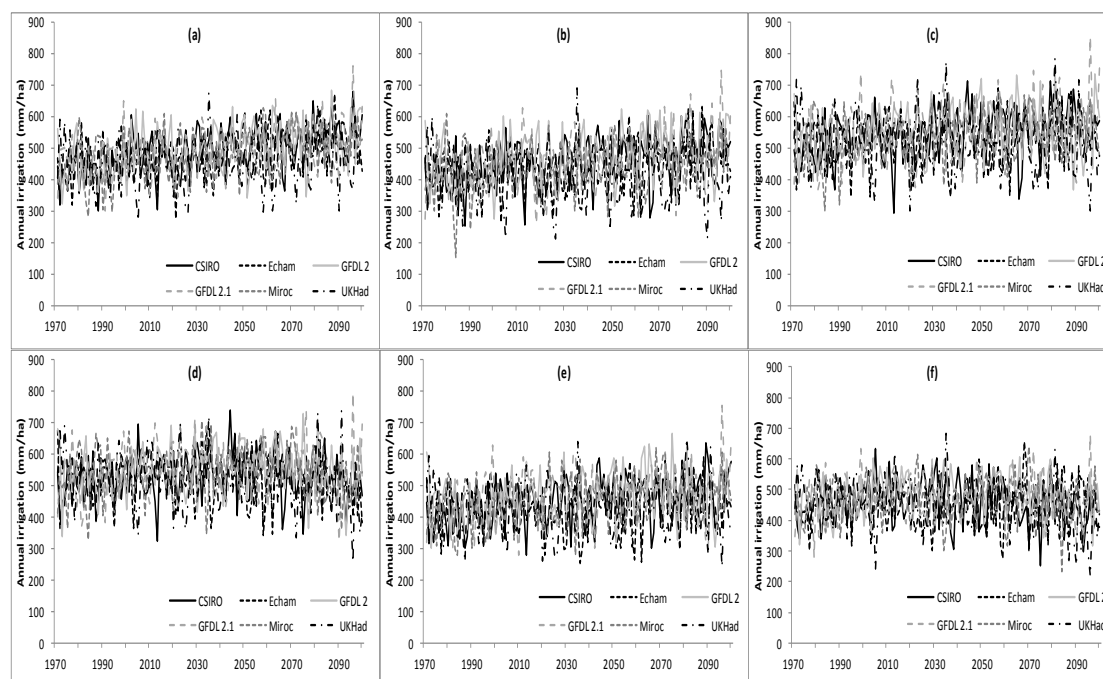


**Figure 6.13** Annual total irrigation (mm/ha) applied, from the six dynamically downscaled GCMs, at Woolnorth (a), Flowerdale (b), Merseylea (c), Cressy (d), Ringarooma (e) and Ouse (f) for the period 1971 to 2100.

**Table 6.6** Multi-model mean of mean annual irrigation (mm/ha) requirements at Woolnorth, Flowerdale, Merseylea, Cressy, Ringarooma and Ouse, for the baseline, 2025, 2055 and 2085.

Scenario	Woolnorth	Flowerdale	Merseylea	Cressy	Ringarooma	Ouse
Baseline	447	416	515	523	422	458
2025	474	439	538	544	444	471
2055	497	457	553	547	459	472
2085	517	474	557	516	467	450
% change Baseline - 2055	11%	10%	7%	5%	9%	3%
% change Baseline - 2085	16%	14%	8%	-1%	10%	-2%

The projected increases in annual irrigation at Woolnorth, Flowerdale, Merseylea and Ringarooma is driven by an increase of both spring and December irrigation requirements from the baseline to 2085 (Figure 6.14a-c,e). At all sites, the decrease of summer irrigation is due to higher daily maximum temperatures that are limiting pasture growth and in turn reducing transpiration rates. Irrigation demand is driven by the potential evapotranspiration rates of the pasture. This is partly a function of plant transpiration rates which are influenced by pasture growth rates. The lower summer pasture yields towards the end of the century mean that there will be a reduction in irrigation requirements. This is particularly evident at Cressy and Ouse, which exhibit the greatest reduction in pasture growth over the summer period due to high temperature stresses.

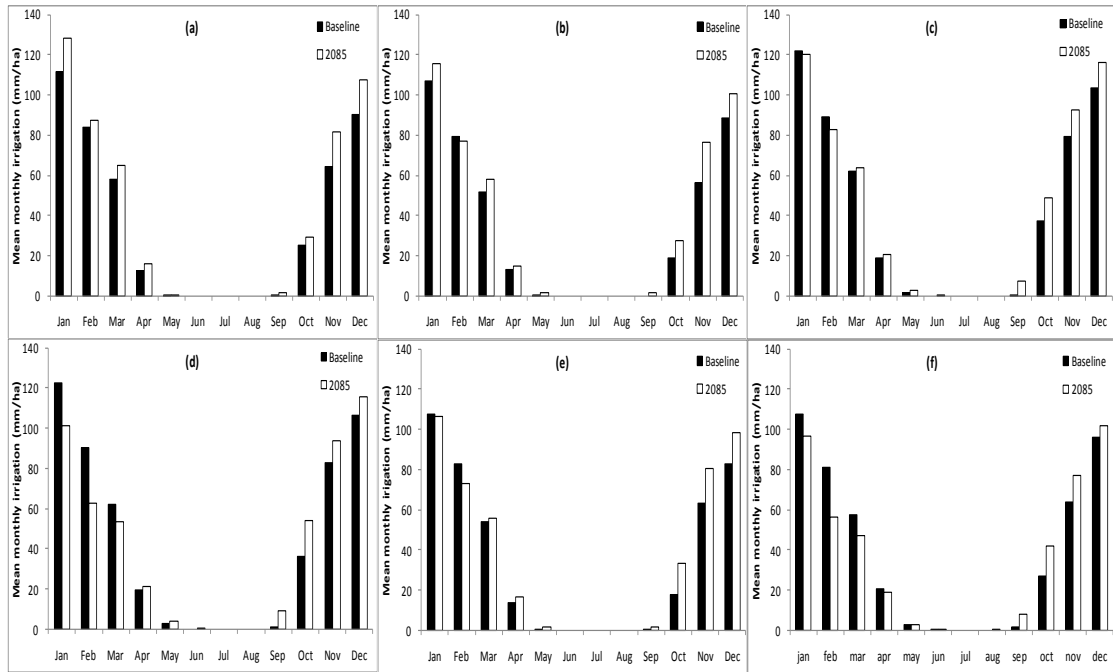


**Figure 6.14** Multi-model mean of mean monthly irrigation (mm/ha) at Woolnorth (a), Flowerdale (b), Merseylea (c), Cressy (d), Ringarooma (e) and Ouse (f) for the baseline and 2085.

Currently the average rate of irrigation water applied per ha across the Tasmanian dairy industry is 4.8 ML/ha (Australian Bureau of Statistics 2010b) (Table 2.4). The simulated baseline irrigation requirements from DairyMod is closely aligned with the current industry figures. The mean simulated rate of irrigation received for the baseline period across each of the six sites is 4.6 ML/ha, giving an acceptable degree of confidence in the projected simulated irrigation requirements for each of the six sites.

### 6.3.3 Gross production water-use index

At all sites, annual GPWUI is projected to increase linearly to approximately 2050, then decline slightly through to 2100 (Figure 6.15a-f).

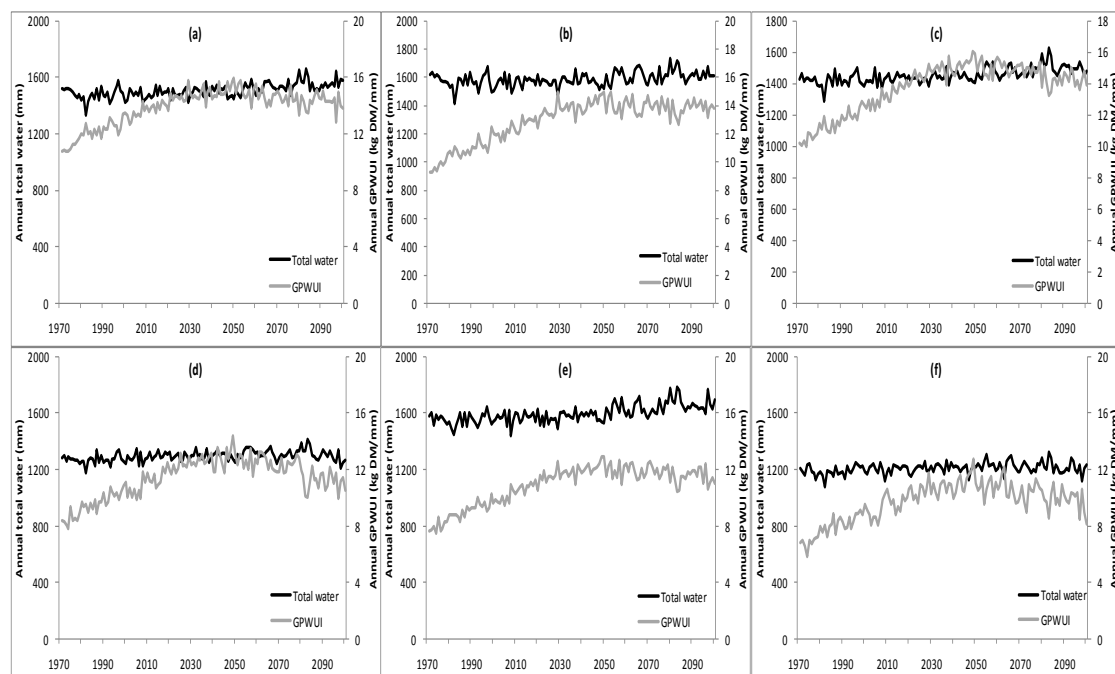


**Figure 6.15** Multi-model mean of annual total water (mm) and annual GPWUI (kg DM/mm) at Woolnorth (a), Flowerdale (b), Merseylea (c), Cressy (d), Ringarooma (e) and Ouse (f) for the period 1971 to 2100.

Under elevated atmospheric CO<sub>2</sub> concentrations, a C<sub>3</sub> plant is expected to have an increase in the net influx of CO<sub>2</sub>, increased stomatal resistance and a decline in transpiration per unit of CO<sub>2</sub> fixed (Clark *et al.* 1995; Long *et al.* 2004). This is likely to result in increased WUE (Casella *et al.* 1996), this response was simulated at each site. The simulated change in WUE was similar to that reported by Schapendonk *et al.* (1997) where under two different levels of CO<sub>2</sub> (350 ppm and 700 ppm) the WUE of perennial ryegrass under the elevated CO<sub>2</sub> level was significantly (up to 50%) higher than at ambient CO<sub>2</sub> levels. This is consistent with the simulated findings in the current study, where the GPWUI from the baseline to 2085 increased at all six sites ranging from 19% at Woolnorth to 32% at Ringarooma (Table 6.7).

From 2055 to 2085 the GPWUI decreased by a range of 2% (Flowerdale) to 9% (Cressy) (Table 6.7). The projected decrease in GPWUI at all sites by 2085 was driven by a decrease in GPWUI during summer, again with notable decreases occurring at Cressy and Ouse as a result of increasing daily maximum temperatures limiting pasture growth (Appendix 9.0).

**Table 6.7** Multi model mean of mean annual total water (mm) and mean annual GPWUI (kg DM/mm) at Woolnorth, Flowerdale, Merseylea, Cressy, Ringarooma and Ouse for the Baseline 2025, 2055 and 2085.

Scenario	Woolnorth		Flowerdale		Merseylea		Cressy		Ringarooma		Ouse	
	Total water	GP-WUI										
Baseline	1478	12.0	1571	10.7	1419	11.4	1269	9.5	1551	8.8	1186	7.8
2025	1493	14.5	1571	13.4	1437	14.4	1296	12.1	1571	11.4	1210	10.3
2055	1514	14.9	1593	14.1	1466	15.1	1308	12.7	1609	12.0	1219	10.9
2085	1553	14.3	1622	13.9	1501	14.4	1306	11.6	1660	11.6	1217	10.0
% change Baseline - 2055	2%	24%	1%	32%	3%	33%	3%	34%	4%	36%	3%	38%
% change Baseline - 2085	5%	19%	3%	30%	6%	27%	3%	22%	7%	32%	3%	28%

### 6.3.4 Annual and seasonal cut yield variability

Regional differences in seasonal pasture growth curves are reflective of both local climatic and soil type conditions (Chapman *et al.* 2008a). Comparing regional means of both annual and seasonal pasture production fails to recognise the inter-annual and inter-seasonal variability. This variability is often a key characteristic of a region and influences many key farm management decisions. To quantify the regional differences in variability and how this is projected to change under future climate scenarios both the CV of the mean annual and seasonal yield over a moving 30-year period were calculated for the time period 1971 to 2100.

At all sites, the CV of the simulated annual rainfed pasture yield is projected to decrease from the baseline to 2085 (Figure 6.16a-f). The projected decrease in CV ranged from 5% at Woolnorth to 41% Ouse. The projected decrease of inter-annual variability under the rainfed simulations is due to increasing temperatures throughout the 21<sup>st</sup> century, particularly at sites that are currently temperature limited such as Cressy and Ouse. The variability of annual rainfall has a significant impact on the inter-annual variability of pasture yields (Ash *et al.* 2007). However at all sites, annual rainfall and inter-annual rainfall variability exhibit little change, indicating that increasing temperatures are driving the simulated decrease in year to year pasture yield variability.

Under the irrigation simulations, at all sites except Cressy, the CV of the simulated annual pasture yield is projected to decrease from the baseline to 2085 (Figure 6.16a-f). The projected decrease in CV ranged from 1% at Ouse to 27% at Flowerdale. At Cressy the CV of the simulated annual pasture yield is projected to increase by 26% from the baseline to 2085 (Figure 6.16d). At all sites, inter-annual variability under the irrigated simulation is

discernibly lower than the variability under the rainfed simulations because under the irrigated simulations the amount and variability of the rainfall and evapotranspiration rates are negated by the use of irrigation.

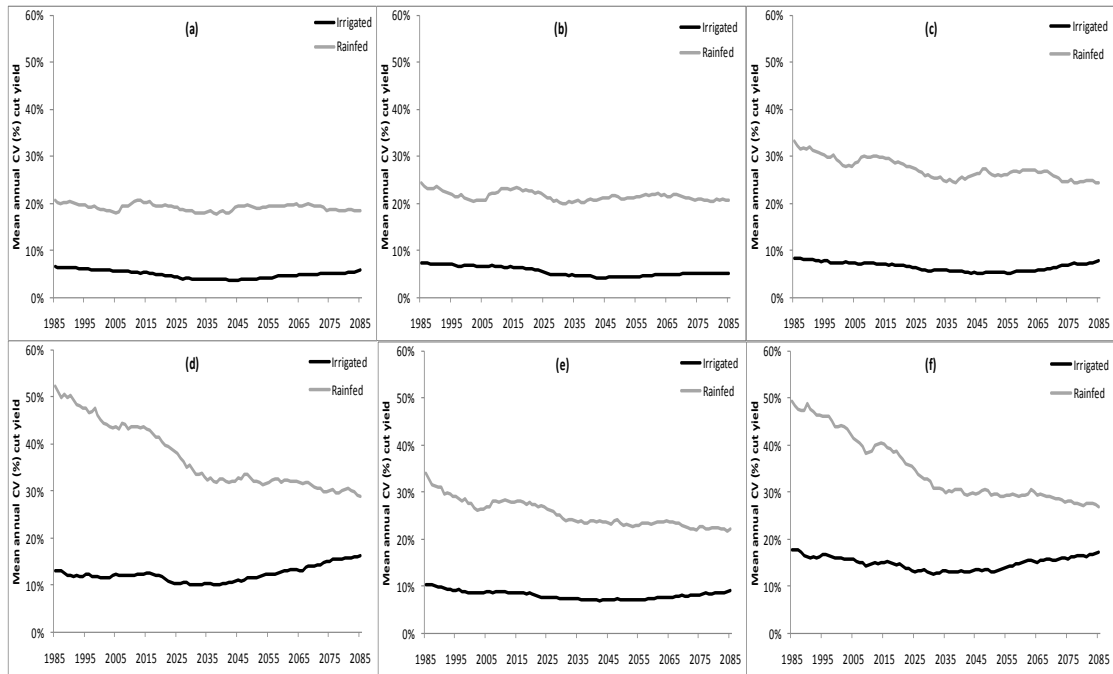


**Figure 6.16** Multi-model mean of rolling 30-year average of CV (%) of rainfed and irrigated annual pasture cut yields for Woolnorth (a), Flowerdale (b), Merseylea (c), Cressy (d), Ringarooma (e) and Ouse (f) for the period 1971 to 2100.

At all sites, the CV of the simulated rainfed summer pasture yields are projected to increase from the baseline to 2085, ranging from 2% at Merseylea to 16% at Ouse (Figure 6.17a-f). At all sites except Woolnorth, the CV of autumn pasture yields are projected to decrease by a range of 9% at Flowerdale to 33% at Ouse. At Woolnorth the CV of autumn yields is projected to increase by 7% (Figure 6.17a). At Woolnorth and Flowerdale, no discernible change is projected of spring CV pasture yields from the baseline to 2085, while at the other four sites the CV of spring yields is projected to decrease by a range of 31% at Merseylea to 59% at Ouse (Figure 6.17a-f). At all sites, the CV of winter yields is projected to decrease notably from the baseline to 2085 (data not shown).

At Cressy and Ouse, the CV of autumn yields decreases rapidly from 1985 to approximately 2030 (Figure 6.17d,f), indicating that the current lower temperature range is limiting pasture growth considering there is no significant change projected in autumn rainfall over the same time period. The CV of spring yields at Merseylea, Cressy, Ringarooma and Ouse progressively decreases from the baseline to 2085 (Figure 6.17c-f), again driven by increasing

temperatures, particularly in early spring. In contrast, at Woolnorth and Flowerdale, sites that currently experience a milder climate, the CV of spring yields is notably lower than the other four sites, and is not projected to change from the baseline to 2085 (Figure 6.17a,b).

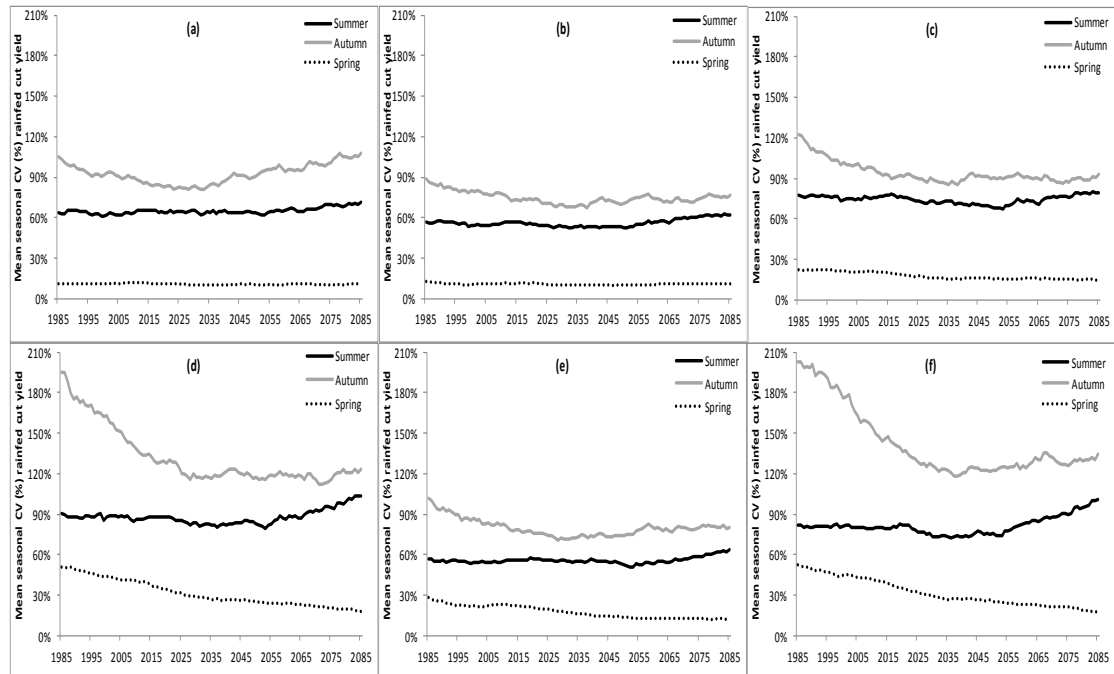


**Figure 6.17** Multi-model mean of rolling 30-year average of CV (%) of rainfed seasonal pasture cut yields for Woolnorth (a), Flowerdale (b), Merseylea (c), Cressy (d), Ringarooma (e) and Ouse (f) for the period 1971 to 2100.

At all sites under the irrigated simulations, the CV of summer pasture yields is projected to increase notably from the baseline to 2085, ranging from 25% at Flowerdale to 193% at Cressy (Figure 6.18a-f). The CV of autumn yields is projected to increase from the baseline to 2085 at all sites, by a range of 19% at Merseylea to 49% at Cressy. The CV of spring yields is projected to decrease at all sites ranging from 24% at Woolnorth to 61% at Ouse (Figure 6.18a-f) At all sites, the CV of winter yields is projected to markedly decrease from the baseline to 2085 (data not shown).

Similar to the trends under the rainfed simulations, inter-annual variability of spring and winter irrigated pasture yields are projected to decrease throughout the 21<sup>st</sup> century. Again this is most notable at those sites that are currently the most temperature limited (Merseylea, Cressy, Ringarooma and Ouse) (Figure 6.18a-f). At all sites, a marked increase in the inter-annual variability during summer and autumn is projected from the baseline to 2085. The projected increases of pasture yield variability during summer and autumn is driven by increasing temperatures, where higher daily maximum temperatures are beginning to restrict

growth and increase year to year seasonal variability. This is most notable during summer at the sites of Cressy and Ouse from approximately 2030 (Figure 6.8d,f) and to lesser extent at Merseylea and Ringarooma from 2050. At all sites, the increasing daily maximum temperatures during March is driving the increase in autumn cut yield variability, which is further reflected in the  $GLF_{\text{temperature}}$  values (Figure 6.8a-f).

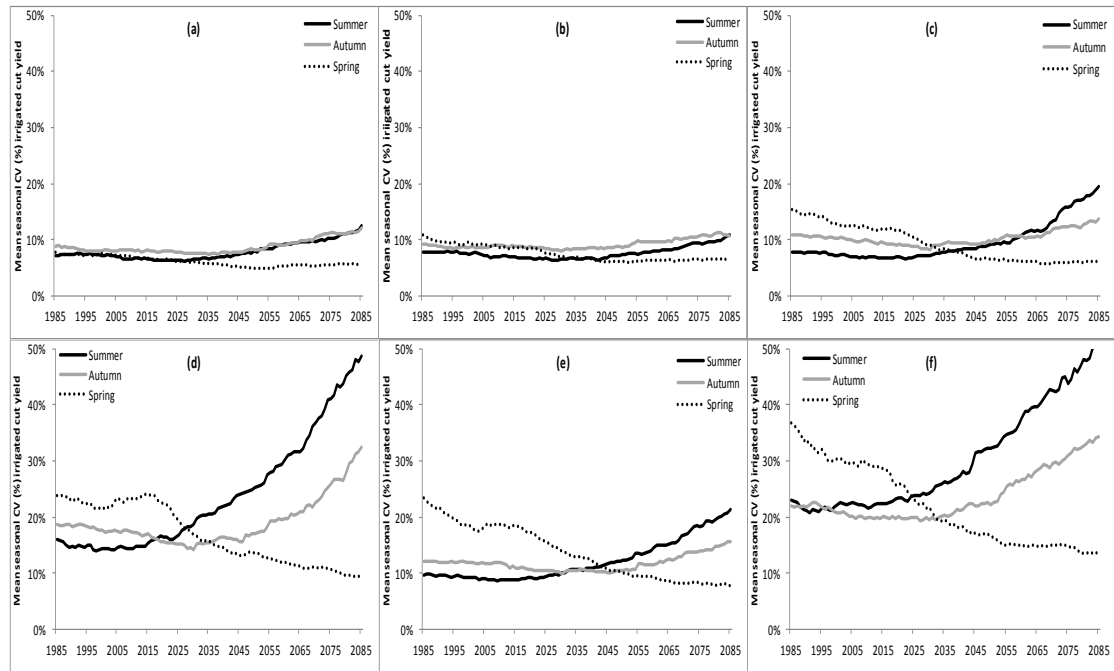


**Figure 6.18** Multi-model mean of rolling 30 year average of CV (%) of irrigated seasonal pasture cut yields for Woolnorth (a), Flowerdale (b), Merseylea (c), Cressy (d), Ringarooma (e) and Ouse (f) for the period 1971 to 2100.

The projected changes in climatic conditions at all sites, has shown that not only will the changes affect the mean state of the climate, but also affect the variability of the climate. Changes in climate variability are more relevant to agricultural production than changes in the mean climate (Luo *et al.* 2005). Climate variability has a significant impact on pasture productivity (Ash *et al.* 2007), and stems from variation between years of primarily rainfall as well as other climatic factors, such as temperature, that influence plant growth (Chapman *et al.* 2009). The projected increases in minimum and maximum temperatures during winter and spring throughout the 21<sup>st</sup> century, along with minimal change in rainfall and/or rainfall variability has increased the optimum climatic conditions for perennial ryegrass growth under the rainfed simulations and resulted in a decrease in the inter-annual variability of pasture production at all sites. However, under irrigated conditions inter-annual seasonal pasture yield variability during summer and autumn is projected to increase at all sites from the baseline to 2085 driven by increasing mean daily maximum temperatures. At all sites, the variability of

daily maximum temperatures during summer and autumn does not increase notably, however, the pasture yield variability increases due to daily maximum temperatures exceeding 28°C with increased frequency, impacting on pasture yields via a reduction in the optimum temperature range for pasture growth (Mitchell 1956; Waller & Sale 2001).

### 6.3.5 Perennial ryegrass growth comparisons under two CO<sub>2</sub> scenarios

The annual pasture yields response to elevated CO<sub>2</sub> concentration was modelled at each site by comparing production at 380 ppm CO<sub>2</sub> (ambient) with the ISAM SRES A2 CO<sub>2</sub> concentration (Figure 6.19).

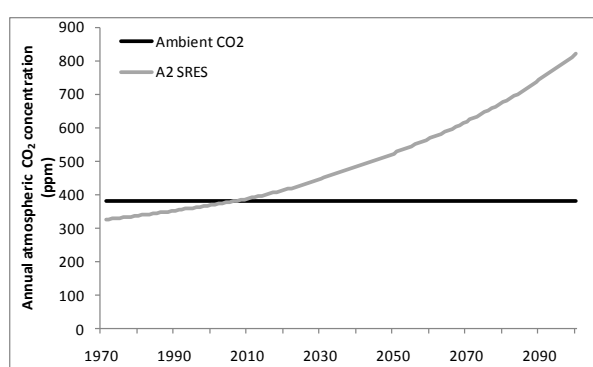


**Figure 6.19** Annual ambient CO<sub>2</sub> (380 ppm) and SRES A2 CO<sub>2</sub> concentration.

At all sites, mean annual pasture yields are projected to progressively increase under both rainfed and irrigated simulations at a greater rate under the A2 CO<sub>2</sub> scenario in comparison to the ambient CO<sub>2</sub> (Table 6.8). By 2085 under the A2 CO<sub>2</sub> levels, the increase in rainfed pasture yields ranged from 19% (Woolnorth, Flowerdale) to 24% (Ouse) above the yields achieved under the ambient CO<sub>2</sub> (Table 6.8). Similarly, mean annual irrigated pasture yields increased under the A2 CO<sub>2</sub> levels in comparison to the ambient CO<sub>2</sub> ranging from 17% (Woolnorth, Flowerdale) to 23% (Ouse) (Table 6.8). In addition at all sites, the pasture yield responses under the A2 CO<sub>2</sub> levels were greater under the rainfed simulations than under the irrigated simulations (Figure 6.20a-f).

**Table 6.8** Simulated mean annual rainfed and irrigated pasture cut yield percentage difference between the ambient CO<sub>2</sub> and A2 CO<sub>2</sub> levels at Woolnorth, Flowerdale, Merseylea, Cressy, Ringarooma and Ouse for the baseline 2025, 2055 and 2085.

	Woolnorth		Flowerdale		Merseylea		Cressy		Ringarooma		Ouse	
	Rainfed	Irrigation	Rainfed	Irrigation	Rainfed	Irrigation	Rainfed	Irrigation	Rainfed	Irrigation	Rainfed	Irrigation
Baseline	-9%	-8%	-10%	-9%	-11%	-9%	-14%	-10%	-11%	-9%	-14%	-11%
2025	11%	10%	11%	10%	12%	10%	15%	12%	12%	10%	16%	13%
2055	17%	14%	17%	15%	18%	15%	21%	18%	18%	16%	22%	19%
2085	19%	17%	19%	17%	20%	18%	22%	21%	20%	18%	24%	23%

Mitscherlich's law of physiological relations states that the yield response of plants to an increase of a limiting nutrient is proportional to the decrement from the maximum yield attainable (A): The integral form of differential equation of Mitscherlich law takes the form,

$$dY/dX = (A-Y) K \text{ (equation 1)}$$

Which relates the rate of response of  $dY/dX$  of the yield with respect to the factor to the difference between the maximum obtainable yield A and the actual yield Y. The incremental increase in yield is proportional (with coefficient K) to the decrement from the maximum.

Upon integration the exponential form of this equation is;

$$Y = A(1 - e^{-kx}) \text{ (equation 2) or}$$

$$Y = A(1 - e^{-(\ln 2/h)x}) \text{ (equation 3)}$$

Where h is the quantity of nutrient required to give a half maximum yield also known as the 'Baule unit' and x is the amount of the 'growth factor' (independent variable), in this instance CO<sub>2</sub>. Table 6.9 shows the yield increase with increasing amounts of CO<sub>2</sub> (A2 SRES) in comparison to the ambient CO<sub>2</sub>, using equation 3.

The Mitscherlich equation is based on Liebig's law of the minimum and describes the response of a crop to an increase in the factor that is limiting growth, other factors being constant (Von Liebig 1855; Mitscherlich 1909; 1913). Although Mitscherlich's equation was assumed to apply to all factors that could limit growth such as light, temperature, water and nutrients, it is most commonly applied to nutrients.

At all sites, under the rainfed simulations the maximum pasture yield difference between the A2 CO<sub>2</sub> and ambient CO<sub>2</sub> levels range from 19.8% at both Woolnorth and Flowerdale to

24.9% at Ouse. The increase in atmospheric CO<sub>2</sub> above the baseline that achieved half the maximum yield ranged from 49.4 ppm at Ouse, to 57.1 ppm at Woolnorth. Under the irrigated simulation the maximum yield difference ranged from 17.5% at Woolnorth to 24% at Ouse. The increase in atmospheric CO<sub>2</sub> above the 380 ppm baseline that achieved the half maximum yield ranged from 56.2 ppm at Ringarooma to 60.1 ppm at Cressy (Table 6.9).

The projected increase in mean maximum annual pasture yield at Woolnorth is 30%, with 66% of this yield increase being attributed to increasing CO<sub>2</sub> levels under the A2 scenario (Table 6.9). In contrast at Cressy, mean annual rainfed pasture yields are projected to increase by 150% above the baseline at 2085, whilst only 16% of the projected yield increase can be attributed to elevated CO<sub>2</sub> levels.

Under the irrigated simulations at all sites, mean annual pasture yields are projected to increase the highest above the baseline at 2055, ranging from 27% at Woolnorth to 42% at both Ringarooma and Ouse (Table 6.3). At Woolnorth 65% of the projected maximum increase in mean annual pasture yields of 27% at 2055 can be explained by the increase of CO<sub>2</sub> levels under the A2 scenario. Similarly at Ouse, the increasing CO<sub>2</sub> levels under the A2 scenario can explain 57% of the projected 42% increase in mean annual cut yields at 2055.

**Table 6.9** The maximum yield difference expressed as percentage between A2 and ambient CO<sub>2</sub> scenario at each site under rainfed and irrigation conditions and the corresponding increase in atmospheric CO<sub>2</sub> concentration above the 380 ppm ambient level that attains half this yield increase using equation 3.

Site	Rainfed			Irrigated		
	Yield max %	<i>x</i> half	R <sup>2</sup>	Yield max %	<i>x</i> half	R <sup>2</sup>
Woolnorth	19.8%	57.1 ppm	98.1	17.5%	58.1 ppm	98.2
Flowerdale	19.8%	55.2 ppm	98.3	17.7%	56.5 ppm	98.3
Merseylea	20.9%	52.8 ppm	98.2	18.4%	57.3 ppm	98.3
Cressy	23.7%	48.6 ppm	97.6	22.0%	60.1 ppm	98
Ringarooma	20.7%	52.3 ppm	98.2	18.7%	56.2 ppm	98.3
Ouse	24.9%	49.4 ppm	97.5	24.0%	58.7 ppm	97.9

The impact of increasing levels of CO<sub>2</sub> on pasture growth under rainfed conditions is more pronounced at those sites that are currently not as temperature limited, such as Woolnorth and Flowerdale (Figure 6.20a,b). Proportionally, the sites of Cressy and Ouse and to a lesser extent Merseylea and Ringarooma, gain a much larger increase in mean annual pasture yields in response to the projected temperature increases (Figure 6.20c-f). Temperature is a dominant variant on plant growth, accordingly, it is evident that temperature influences the response of perennial ryegrass to increased atmospheric CO<sub>2</sub>. Leaf emergence and leaf extension rates in perennial ryegrass is temperature dependant and the potential for increased

shoot growth under elevated CO<sub>2</sub> concentrations is also reliant on temperature. Therefore under optimal soil nutrient supply, increased DM production under elevated CO<sub>2</sub> levels would be restricted at below optimal temperatures (Idso *et al.* 1987; Soussana *et al.* 1996). In addition, Nijs & Impens (1996) reported significant stimulation by elevated CO<sub>2</sub> (700 ppm) was observed in perennial ryegrass growth at a constant temperature of 19°C but not at 15°C. Greer *et al.* (2000) conclude this photosynthetic activity is stimulated more by elevated CO<sub>2</sub> at higher temperatures, than at lower temperatures.

At all sites, under irrigated conditions the response to the increasing levels of CO<sub>2</sub> contributing to increased pasture yields is comparable between each site ranging from 45% at Ringarooma to 65% at Woolnorth. At all sites except Woolnorth, pasture growth responses to increasing levels of CO<sub>2</sub> were proportionally higher under the irrigated simulations, due to the absence of soil moisture deficits during summer and autumn. Under the rainfed simulations, where summer and early autumn pasture growth is restricted by soil moisture deficits, the greatest yield increases occur in late winter and spring and the projected increase in temperatures are the primary driver of increased growth, most noticeable at those sites that are currently temperature limited.

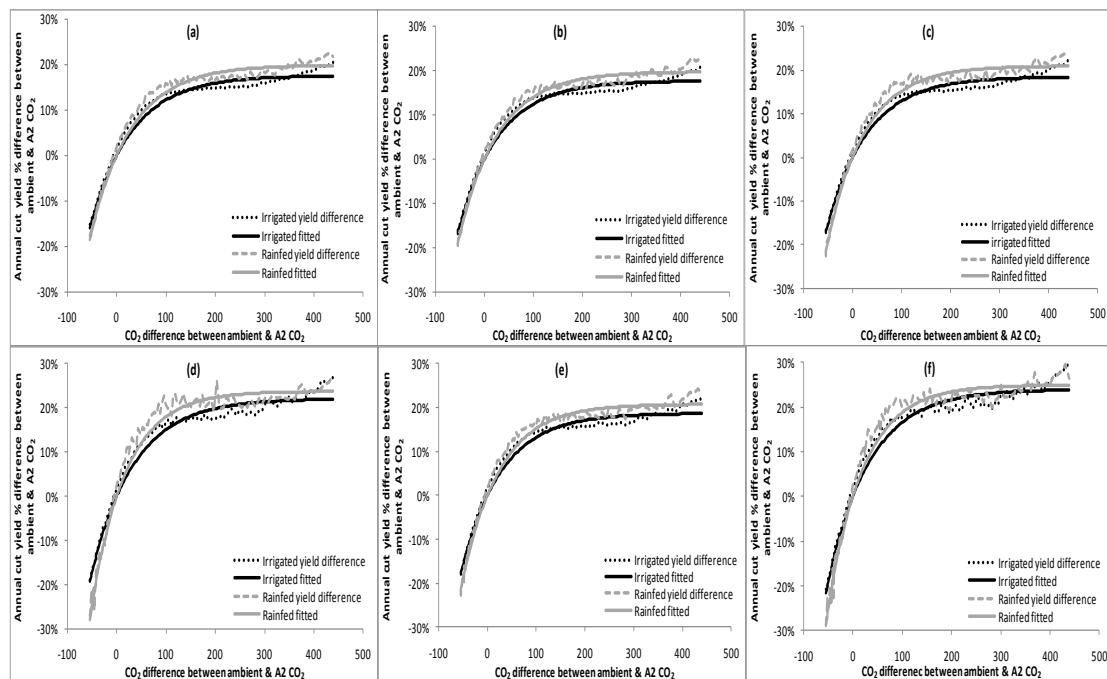


**Figure 6.20** Rainfed and irrigated annual pasture cut yield percentage difference of maximum yield between the ambient CO<sub>2</sub> and A2 CO<sub>2</sub> concentrations, with fitted Mitscherlich equation at Woolnorth (a), Flowerdale (b), Merseylea (c), Cressy (d), Ringarooma (e) and Ouse (f) for the period 1971 to 2100.

Exposed to elevated CO<sub>2</sub> concentrations, plants exhibit three physiological responses: an increase in photosynthetic potential, a decrease in stomatal conductance, (and therefore canopy conductance) and a decrease in plant N content (Long *et al.* 2004). Increased photosynthetic rates under elevated CO<sub>2</sub> generally persist and lead to enhanced growth provided there is an adequate supply of nutrients and water under favorable environmental conditions (Fischer *et al.* 1997). At all sites under both rainfed and irrigated simulations, the increase in DM production associated with elevated CO<sub>2</sub> levels ranged from 17 to 24%. The simulated DM production increases are consistent with those reported in literature, where soil nutrients were non-limiting. For example, under optimum environmental conditions the additional DM production of perennial ryegrass due to elevated CO<sub>2</sub> levels has shown to be between 7 to 25% at 600 ppm (Daepf *et al.* 2000) but up to a 30% increase (Daepf *et al.* 2001), a 19% increase at 630 ppm (Nijs *et al.* 1989) and between a 14 to 20% increase at 700 ppm (Casella *et al.* 1996).

## 6.4 Conclusion

Annual pasture production in the dairy regions of Tasmania is projected to increase throughout the 21<sup>st</sup> century with the majority of the additional growth occurring during winter and spring. Increased temperatures and elevated atmospheric CO<sub>2</sub> concentrations are projected to positively increase regional pasture production in the absence of any significant changes in rainfall patterns or rainfall variability. Pasture production in each of the Tasmanian dairy regions was shown to be relatively resilient to the projected climate change until later in the century where higher daily maximum temperatures are projected to begin to limit pasture growth during summer and early autumn, most notably under irrigated conditions. Year to year variability of pasture production was shown to decrease throughout the century with a slight increase in the projected irrigation requirements, correlated with increased WUE of the pasture as a result of increasing atmospheric CO<sub>2</sub> levels. Regional responses to the projected climate change were relatively similar between sites although greater increases in pasture production were projected at sites that are currently temperature limited, such as Cressy and Ouse, in contrast to the coastal sites of Woolnorth and Flowerdale. The projected results suggest that pasture based dairy production systems can continue to be viable as the basis of the dairy industry in Tasmania.

The projected increase in irrigation demand throughout the 21<sup>st</sup> century will be reliant on available water, most notably projected runoff and River flows. Projected changes in seasonal rainfall and evapotranspiration can manifest in altered runoff and River flows, thereby possibly reducing seasonal water security for irrigation demand. In the following chapter the projected surface runoff at all sites and River flow at the site of Ringarooma are quantified to ascertain whether the projected surface runoff will meet the projected irrigation demand throughout the 21<sup>st</sup> century.

## **CHAPTER 7: MODELLED SURFACE RUNOFF IN RESPONSE TO PROJECTED CLIMATE CHANGE AT EACH SITE AND PROJECTED RIVER FLOW AT RINGAROOMA**

### **7.1 Introduction**

The climate drives the hydrological cycle (Crosbie *et al.* 2010) and projected changes in spatial and temporal patterns of the climate variables will impact on regional hydrological processes, in particular changes in rainfall will be amplified as an impact on surface runoff (Chiew 2006; Wang *et al.* 2010). Rainfall is the largest factor in the water balance of catchment runoff and flows into rivers and farm dams (Mpelasoka & Chiew 2008). Higher temperatures increase potential evapotranspiration which may further lead to a reduction in surface runoff and also soil moisture levels (Chiew & McMahon 2002; Crosbie *et al.* 2010).

Surface runoff is an important but variable component of the hydrological balance of a grazed pasture system (Murphy *et al.* 2004). Runoff is influenced by a range of rainfall characteristics such as amount of rainfall, seasonal distribution and rainfall intensity. Surface runoff is also influenced by soil type and pasture conditions. Ground cover, which is defined as any non-soil material influences both the frequency and the magnitude of runoff events. During a rainfall event, both the soil water content and the available storage capacity of the soil profile influence the water infiltration rate and as a direct result the generation of surface runoff (Murphy *et al.* 2004). The relationship between the volume of water that reaches water catchments and rainfall is non-linear since it is reliant on soil moisture levels and the implication regarding water balances is that a given reduction in rainfall leads to greater reduction in the water flowing into catchments (Murphy & Timbal 2008; Chiew *et al.* 2010; Wang *et al.* 2010).

Large multi-decadal changes in rainfall have been observed across Australia since the 1950's (Gallant *et al.* 2007). A significant impact of rainfall decline, correlated with increases in temperature in south eastern Australia has been a reduction in runoff in water catchments (Hennessy 2007; Chiew *et al.* 2010). Since the mid 1970's in Tasmania, a decline has been observed in mean annual statewide rainfall. This decline has been particularly noticeable since the mid 1990s (Bennett *et al.* 2010; Bureau of Meteorology 2011). The decline in rainfall has resulted in an estimated 7% decline in surface runoff for the period 1997 to 2007, compared to the long term average (1924 to 2007) (Viney *et al.* 2009). However, Bennett *et al.* (2010) as part of the CFT project, projected runoff and river flows to the end of the 21<sup>st</sup> century and reported that the observed recent decline of statewide runoff is not projected to

continue throughout the 21<sup>st</sup> century, consistent with the absence of any significant trend in the projected statewide rainfall (Bennett *et al.* 2010; Grose *et al.* 2010).

Regional variation in the amount of surface runoff is projected under future climate scenarios. In the central highlands of Tasmania, mean annual surface runoff is projected to significantly decrease by up to 30%, while in the eastern regions mean annual surface runoff is projected to increase. In addition to annual runoff changes, modelling of 78 river flows across Tasmania has indicated that on average 28 of the 78 rivers modelled are projected to have decreased mean annual flows by 2100 (Bennett *et al.* 2010).

In Tasmania, approximately 67% of dairy farms utilise some form of irrigation, with approximately 30% of dairy land irrigated (Australian Bureau of Statistics 2010b). Irrigation provides the opportunity for more intensive pasture production resulting in higher and more reliable yields. The Tasmanian dairy industry is the major consumer of irrigation water using approximately 38% of the total water, on approximately 23% of the total area of irrigated land (Australian Bureau of Statistics 2010b). Irrigation water for the dairy industry is primarily sourced from surface water, which includes rivers and streams (33%) and on-farm storage dams (49%). A small percentage of irrigation water in the southern region of the state is sourced from government irrigation schemes (e.g. Coal river Valley irrigation scheme) as well as limited access to groundwater supplies (Australian Bureau of Statistics 2010b). Profitability of the Tasmanian dairy industry is in part dependant on water availability and water security. Climatic conditions affect both the availability of water for irrigation and the need to irrigate in order to supplement rainfall. The availability and security of irrigation water for the Tasmania dairy industry is a major issue, with the increasing demand from the dairy industry occurring at a time when irrigation water availability in many river catchments is in a state of decline, along with increasing conflicts between competing agricultural, urban and environmental demands for water.

To assess the potential influences of the projected climate change on surface runoff across the Tasmanian dairying regions, Bennett *et al.* (2010) simulated surface runoff using the hydrological model SIMHYD (Chiew *et al.* 2002) for each of the six dairy regions for the period 1971 to 2100 using daily climate data projections generated from the CFT project.

The objectives of this chapter were to:

1. Quantify the projected regional climate change impact on surface runoff from the six bias-adjusted dynamically downscaled GCMs for the six sites over the period 1971 to 2100.
2. Undertake an on-farm case study analysis at Ringarooma, quantifying surface runoff and river flow projections on irrigation requirements using the six bias-adjusted dynamically downscaled GCMs for the period 1971 to 2100.

## 7.2 Materials and methods

The daily SIMHYD (Chiew *et al.* 2002) surface runoff data generated by Bennett *et al.* (2010) as part of the CFT project was generated on a 0.05° grid, calibrated to interpolated observations from the SILO Data Drill 0.05° gridded data source (Jeffrey *et al.* 2001). Previously in this report, rainfall data from the AWAP 0.05° data source (Jones *et al.* 2009), interpolated to a 0.1° grid (AWAP 0.1) had been used as the basis for rainfall calibrations. However, the hydrological model SIMHYD is calibrated to interpolated observations from the SILO Data Drill 0.05° gridded data source (Jeffrey *et al.* 2001). SIMHYD is configured to accept 0.05° gridded data, accordingly, the CFT GCM climate simulations were re-gridded from a 0.1° grid down to a 0.05° grid using a cubic spline interpolation. Further details of the SIMHYD daily runoff data modelling methods are described in Bennett *et al.* (2010).

Bennett *et al.* (2010) generated 0.05° gridded bias adjusted daily runoff projections using the ensemble of the dynamically downscaled GCMs of CSIRO-Mk3.5, ECHAM5/MPI-OM, GFDL-CM2.0, GFDL-CM2.1, MIROC3.2 (medres) and UKMO-HADCM3 data for each of the six sites (Section 3.2). The SIMHYD daily runoff data for the period 1<sup>st</sup> January 1961 to 31<sup>st</sup> December 2100 was obtained from the TPAC portal (<https://dl.tpac.org.au/>).

An irrigated dairy farm at Ringarooma was selected as a case study farm to highlight the influences of projected climate change impacts on on-farm water availability. Bennett *et al.* (2010) generated Ringarooma river flow projections from the TasSY (Ling *et al.* 2009), River models using the ensemble of the dynamically downscaled GCMs of CSIRO-Mk3.5, ECHAM5/MPI-OM, GFDL-CM2.0, GFDL-CM2.1, MIROC3.2 (medres) and UKMO-HADCM3 data for the Ringarooma site (Section 3.2). The daily Ringarooma river flow data for the period 1<sup>st</sup> January 1961 to 31<sup>st</sup> December 2100 was obtained from the TPAC portal (<https://dl.tpac.org.au/>). Using the runoff and river flow projections a water budget of the current and projected irrigation requirements for the case study dairy farm was created for the period 1971 to 2100.

The Ringarooma dairy farm is 166 ha in size, with 75 ha (45%) of the farm supported by irrigation infrastructure. Irrigation water is accessed from both an on-farm catchment (dam) and access to river flows (Ringarooma river) (Plate 7.1). The area under irrigation from the on-farm storage dam is 38 ha (51% of the irrigated area) while the area under irrigation from water accessed from the Ringarooma river is 37 ha (49% of the irrigated area).

The on-farm storage dam has a holding capacity of 89 ML and is supported by a surrounding catchment area of 104 ha (Plate 7.1). The farm has a water allocation license to harvest annual surface runoff, however, the water allocation license and amount of harvestable water is determined by two catchment 'seasons' a 'winter season' and 'summer season'. The 'winter season' catchment period runs from May 1<sup>st</sup> to November 30<sup>th</sup>. The farm has a water allocation license to harvest 20% of total surface runoff during the 'winter season', the remaining 80% is released for downstream users and environmental flows (Van Brecht pers. comm. 2011). The 'summer season' catchment period runs from December 1<sup>st</sup> to April 30<sup>th</sup>. The farm has a water allocation license to harvest 0.34 ML of surface runoff per day for 100 days, resulting in a total allocation of 34 ML during the 'summer season'.

To irrigate the remaining 37 ha water is sourced from the Ringarooma river during the 'summer season' of December to April. The farm has a water allocation license of 1.125 ML per day for 100 days, in total 112.5 ML of irrigation water is available for the 'summer season' for this area.

The projected River flows for the Ringarooma river are the flows remaining after all water extractions, diversions and other losses have been accounted for (Bennett *et al.* 2010). The extractions, diversions and other losses were calculated according to operating guidelines and water licenses that were current as of December 31, 2007. No account has been taken concerning future changes to land use or water management practices that could affect the river flow. The projected river flow under the future climate scenarios presented in this chapter are the changes caused only by climate.

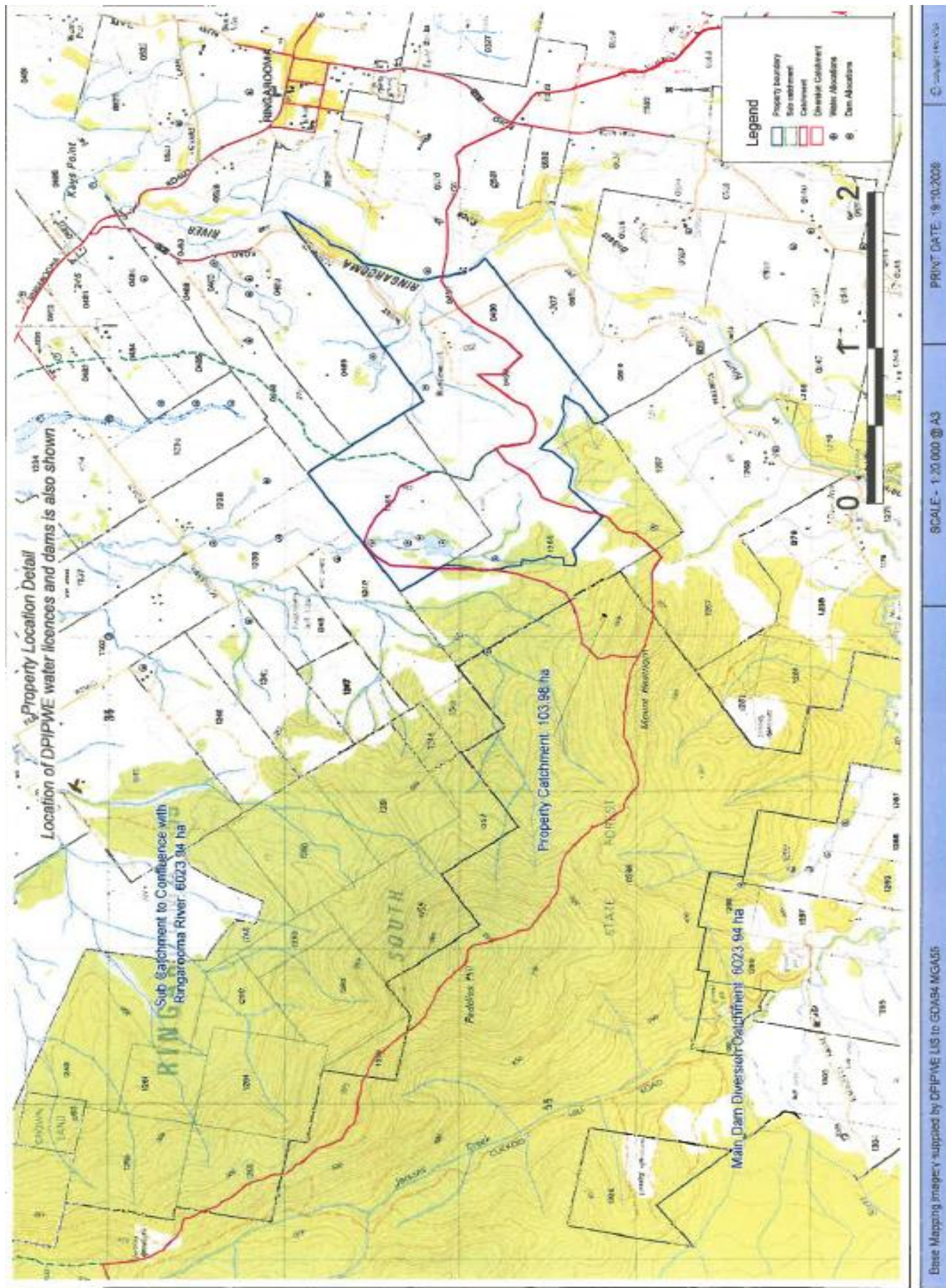


Plate 7.1 Ringarooma case study farm site.

Simulated mean annual and monthly surface runoff values for each region and simulated mean annual and monthly river flow for the Ringarooma river for each 30-year period were calculated. Due to the mechanistic, non-stochastic nature of the GCMs, annual and monthly surface runoff and Ringarooma river flow means are presented and compared for each 30-year period. In addition (Appendix 10), simulated monthly surface runoff for each region was analysed as one-way ANOVA with replication (year) using SPSS. Least significant difference (LSD), as defined by Steel and Torrie (1960) was used to compare differences between means of the four climate periods.

Averaging projections from the ensemble of the six GCMs is a useful method in summarising projected changes and the method is commonly used in climate studies. The runoff simulations at all sites include natural inter-decadal variations that are present in the GCMs. Natural variations may present as a wet decade or a dry decade at any particular time for a given GCM (as is observed in historical records). Averaging GCMs has the effect of reducing inter-decadal variations within individual GCMs, meaning that the projected changes shown are more likely to be the result of climate change as opposed to the natural variability of an individual GCM (Bennett *et al.* 2010).

## **7.3 Results and Discussion**

### **7.3.1 Surface runoff at each of the six dairy regions**

For the region of Woolnorth, simulated mean annual runoff is projected to increase by 7% (model range -8% to 42%) above the baseline (model mean 156 mm) by 2085 (model mean 167 mm) (Figure 7.1a). Mean monthly runoff is projected to increase significantly ( $P < 0.05$ ) by 2085 above the baseline from June through to November (Figure 7.1b) (Appendix 10.1).

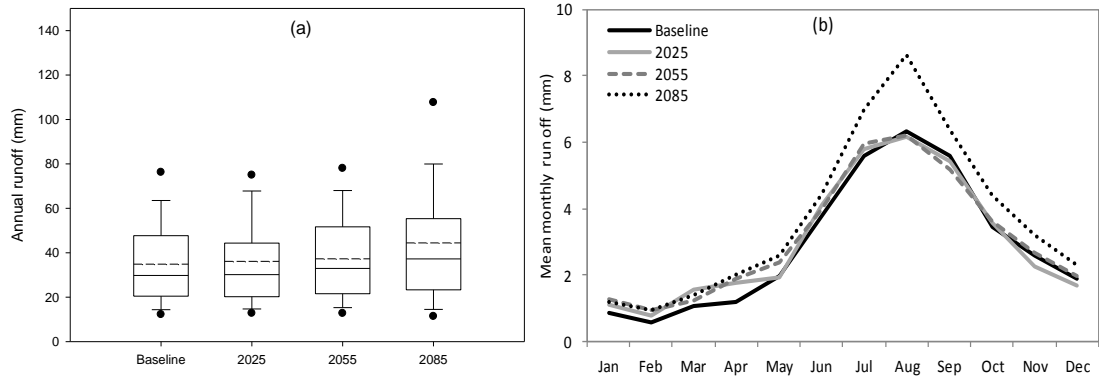


**Figure 7.1** Annual simulated runoff (mm/ha) for Woolnorth shown as box plots (5<sup>th</sup>, 10<sup>th</sup>, 25<sup>th</sup>, 50<sup>th</sup>, 75<sup>th</sup>, 90<sup>th</sup> and 95<sup>th</sup> percentile, with dashed mean line) (a) and mean simulated monthly runoff (mm/ha) (b) from the six bias-adjusted dynamically downscaled GCMs for the baseline, 2025, 2055 and 2085.

At Flowerdale, simulated mean annual runoff is projected to increase slightly by 2% (model range -6 to 13%) above the baseline (model mean 498 mm) by 2085 (model mean 508 mm) (Figure 7.2a). Mean monthly runoff is projected to increase significantly ( $P < 0.05$ ) by 2085 above the baseline from June through to August (Figure 7.2b) (Appendix 10.2).

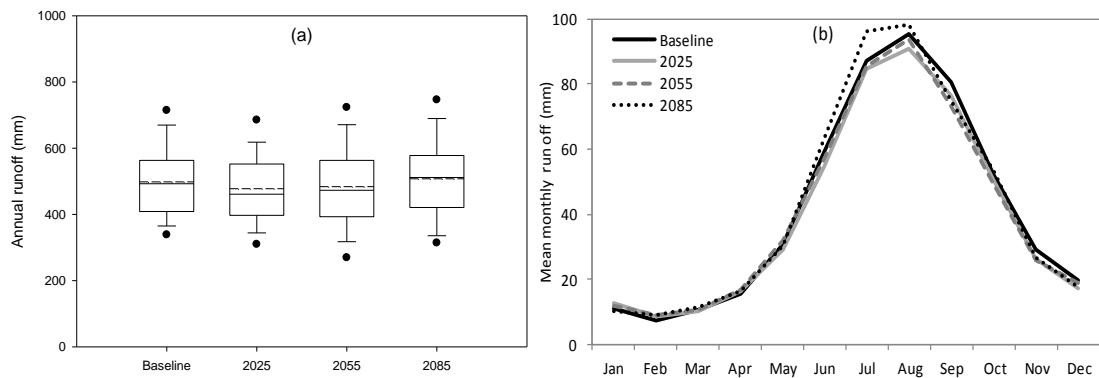


**Figure 7.2** Annual simulated runoff (mm/ha) for Flowerdale shown as box plots (5<sup>th</sup>, 10<sup>th</sup>, 25<sup>th</sup>, 50<sup>th</sup>, 75<sup>th</sup>, 90<sup>th</sup> and 95<sup>th</sup> percentile, with dashed mean line) (a) and mean simulated monthly runoff (mm/ha) (b) from the six bias-adjusted dynamically downscaled GCMs for the baseline, 2025, 2055 and 2085.

For the region of Merseylea, simulated mean annual runoff is projected to increase 15% (model range -3 to 50%) above the baseline (model mean 237 mm) by 2085 (model mean 268 mm) (Figure 7.3a). Mean monthly runoff is projected to increase significantly ( $P < 0.05$ ) by 2085 above the baseline from May to August (Figure 7.3b) (Appendix 10.3).

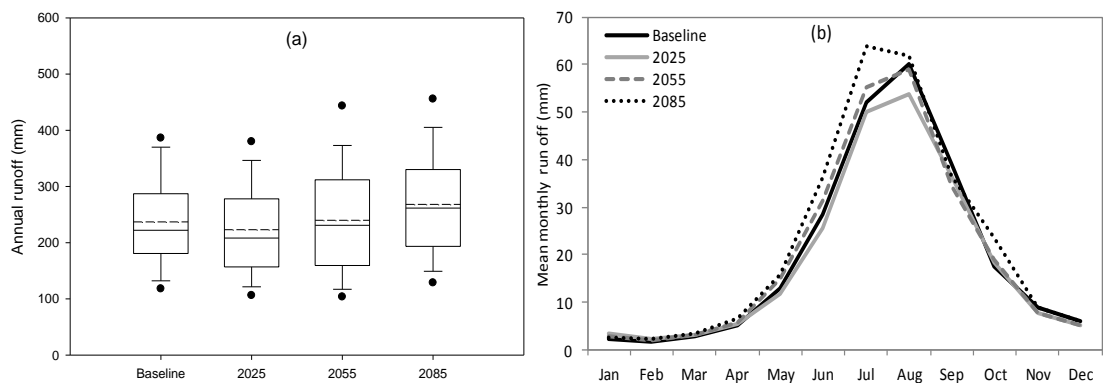


**Figure 7.3** Annual simulated runoff (mm/ha) for Merseylea shown as box plots (5<sup>th</sup>, 10<sup>th</sup>, 25<sup>th</sup>, 50<sup>th</sup>, 75<sup>th</sup>, 90<sup>th</sup> and 95<sup>th</sup> percentile, with dashed mean line) (a) and mean simulated monthly runoff (mm/ha) (b) from the six bias-adjusted dynamically downscaled GCMs for the baseline, 2025, 2055 and 2085.

At Cressy, simulated mean annual runoff is projected to increase 17% (model range -1 to 47%) above the baseline (model mean 119 mm) by 2085 (model mean 140 mm) (Figure 7.4a). Mean monthly runoff is projected to increase significantly ( $P < 0.05$ ) by 2085 above the baseline from June to August, along with increases during October and November (Figure 7.4b) (Appendix 10.4).

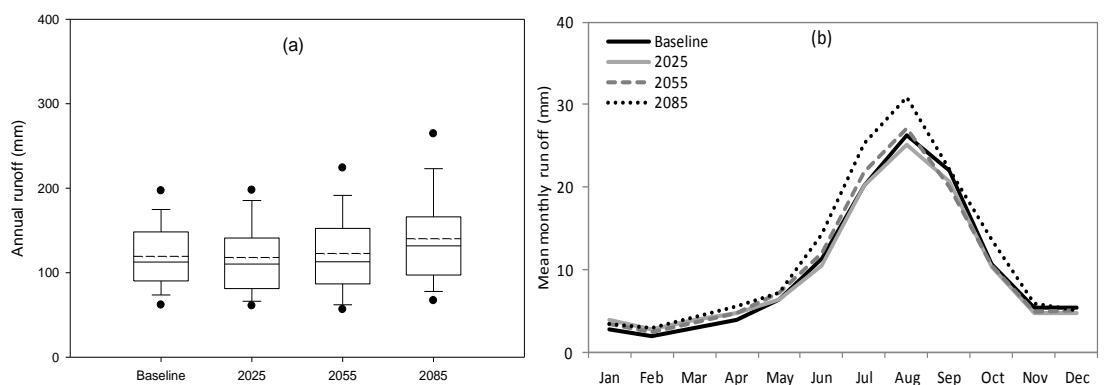


**Figure 7.4** Annual simulated runoff (mm/ha) for Cressy shown as box plots (5<sup>th</sup>, 10<sup>th</sup>, 25<sup>th</sup>, 50<sup>th</sup>, 75<sup>th</sup>, 90<sup>th</sup> and 95<sup>th</sup> percentile, with dashed mean line) (a) and mean simulated monthly runoff (mm/ha) (b) from the six bias-adjusted dynamically downscaled GCMs for the baseline, 2025, 2055 and 2085.

For the region of Ringarooma, simulated mean annual runoff is projected to increase by 12% (model range -4 to 28%) above the baseline (model mean 484 mm) by 2085 (model mean 541 mm) (Figure 7.5a). Mean monthly runoff is projected to increase significantly ( $P < 0.05$ ) by 2085 above the baseline from June through to November (Figure 7.5b) (Appendix 10.5).

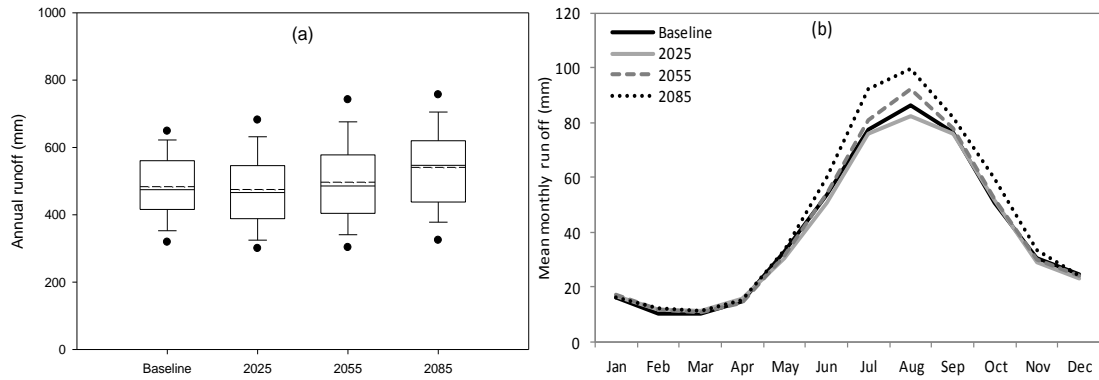


**Figure 7.5** Annual simulated runoff (mm/ha) for Ringarooma shown as box plots (5<sup>th</sup>, 10<sup>th</sup>, 25<sup>th</sup>, 50<sup>th</sup>, 75<sup>th</sup>, 90<sup>th</sup> and 95<sup>th</sup> percentile, with dashed mean line) (a) and mean simulated monthly runoff (mm/ha) (b) from the six bias-adjusted dynamically downscaled GCMs for the baseline, 2025, 2055 and 2085.

At Ouse, simulated mean annual runoff is projected to increase by 27% (model range -2 to 88%) above the baseline (model mean 35 mm) by 2085 (model mean 44 mm) (Figure 7.5a). Mean monthly runoff is projected to increase significantly ( $P < 0.05$ ) by 2085 above the baseline during May, and from July through to December (Figure 7.5b) (Appendix 10.6).

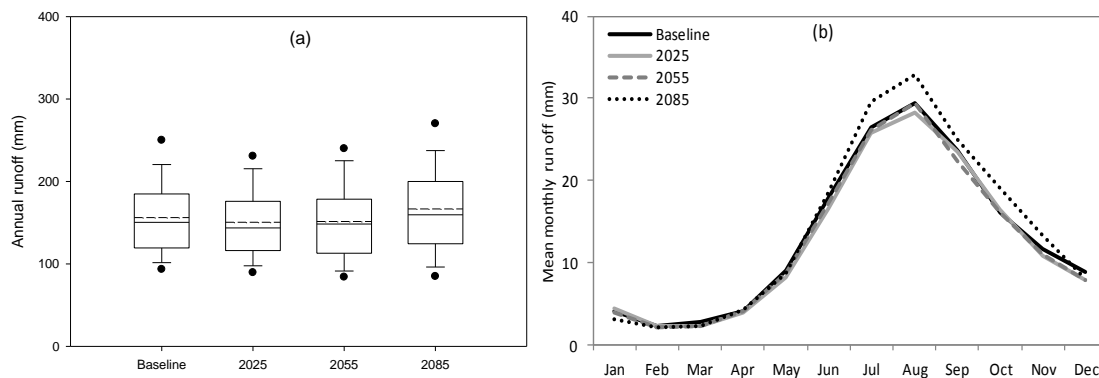


**Figure 7.6** Annual simulated runoff (mm/ha) for Ouse shown as box plots (5<sup>th</sup>, 10<sup>th</sup>, 25<sup>th</sup>, 50<sup>th</sup>, 75<sup>th</sup>, 90<sup>th</sup> and 95<sup>th</sup> percentile, with dashed mean line) (a) and mean simulated monthly runoff (mm/ha) (b) from the six bias-adjusted dynamically downscaled GCMs for the baseline, 2025, 2055 and 2085.

At all sites, there is considerable variation between the GCMs of projected mean annual surface runoff. However, all the GCMs project a general increasing trend in future surface runoff and the modelled mean annual surface runoff projections show increases at each site above the baseline levels.

At all sites except Ouse, the simulated mean annual surface runoff is projected to decrease slightly by 2025 ranging from 1% at Cressy to 6% at Merseylea (Table 7.1). The slight decrease in projected runoff is the result of decreased winter rainfall over the same time period. As rainfall is the main driver of surface runoff (Chiew *et al.* 2010; Vaze & Tang 2011) it is not surprising that at all sites except Ouse, winter rainfall is projected to decrease, although this decrease is only in the range of 2% to 4%. Each site has winter dominant rainfall and even a slight contraction in projected winter rainfall has manifested as a reduction in runoff. These results are consistent with similar studies with Chiew *et al.* (2010) reporting that across the winter dominant rainfall region of south eastern Australia, a projected decrease in winter rainfall will lead to a decrease in winter runoff. By 2085 the simulated mean annual surface runoff is projected to increase at all sites by a range of 2% to 27% above the baseline levels (Table 7.1). The increase is the result of the increased runoff during the winter and spring months. Winter rainfall by 2085 is projected to increase at all sites by 2% at Flowerdale to 12% at Ringarooma, while spring rainfall is projected to increase at the sites of Merseylea, Cressy and Ringarooma.

**Table 7.1** Mean annual simulated surface runoff (mm/ha) at Woolnorth, Flowerdale, Merseylea, Cressy, Ringarooma and Ouse for the baseline, 2025, 2050 and 2085.

Scenario	Woolnorth	Flowerdale	Merseylea	Cressy	Ringarooma	Ouse
Baseline	156	498	237	119	484	35
2025	151	478	223	118	475	36
2055	151	484	240	123	497	37
2085	167	508	268	140	541	44
% change Baseline - 2025	-4%	-4%	-6%	-1%	-2%	4%
% change Baseline - 2055	-3%	-3%	1%	3%	3%	7%
% change Baseline - 2085	7%	2%	13%	17%	12%	27%

Changes in the projected surface runoff rates are not necessarily caused by average changes in precipitation alone. Increases in average daily rainfall intensities are just as likely to increase mean annual and monthly runoff as much as increases in mean annual and monthly rainfall (Bennett *et al.* 2010; White *et al.* 2010). Rainfall intensity at any location varies, and is reliant on the duration of rainfall (Freebairn & Boughton 1981), short duration high intensity rainfall events are associated with a high magnitude of surface runoff (Preston & Jones 2008; Post *et al.* 2009). As noted previously (Section 5.3.8), at all sites, by 2085 mean annual rainfall intensity is projected to increase above the baseline ranging from 7% at Flowerdale to 13% at Cressy (Figure 5.8). At Woolnorth, the greatest change in seasonal rainfall intensity is projected to occur during winter, increasing 11% above the baseline by 2085. At the sites of Flowerdale, Merseylea, Cressy and Ringarooma the greatest change in seasonal rainfall intensity is projected to occur during spring, increasing 9%, 17%, 20% and 17% respectively above the baseline by 2085. At Ouse, the greatest change in seasonal rainfall intensity is

projected to occur during summer, increasing 17% above the baseline by 2085 (Appendix 8.0).

Rainfall intensity is a relatively robust feature of climate projections and is a consequence of an increase in the capacity of a warmer atmosphere to hold moisture (Meehl *et al.* 2005; Boer 2009). It has been widely reported that in a projected warmer climate, GCM simulations exhibit a general increase in rainfall intensity, even in regions where mean rainfall decreases (Christensen & Christensen 2004; Meehl *et al.* 2005; Kharin & Zwiers 2007; Post *et al.* 2009). White *et al.* (2010) reported that rainfall intensity across the whole of Tasmania is projected to increase throughout the 21<sup>st</sup> century, with an increase of up to 60% in some seasons, in some coastal regions. Paradoxically, the number of rain days across Tasmania are likely to decrease. This is consistent with the findings presented here, where at each site rainfall intensity is projected to increase throughout the 21<sup>st</sup> century. These changes are also accompanied by a decrease in the mean number of annual rain days at all sites (Figure 5.13).

### **7.3.2 Ringarooma on-farm catchment and irrigation supply**

For the region of Ringarooma, mean annual simulated irrigated pasture yields are projected to increase by 41% above the baseline by 2085 (Table 6.3). This is driving a progressive increase in irrigation requirements throughout the 21<sup>st</sup> century and by 2085 irrigation requirements for the region are projected to be 10% above the baseline level (Table 6.6). Mean annual rainfall is projected to increase by 6% above the baseline by 2085 (Table 5.5), while mean annual runoff is projected to increase by 12% above the baseline by 2085 (Table 7.1).

At Ringarooma, the total rainfall during the ‘winter season’ (May to November) is projected to decline slightly by 2025 (model mean 782 mm) from the baseline level (model mean 796 mm). However, by 2055 and 2085 the ‘winter season’ rainfall is projected to increase above the baseline mean value (Figure 7.7a). Using the case study farm with a catchment area of 104 ha, the total surface runoff/ha during the ‘winter season’ is projected to decrease slightly by 2025. From 2055 onwards the total surface runoff/ha during the ‘winter season’ is projected to increase above the baseline and 2025 levels (Figure 7.7b).

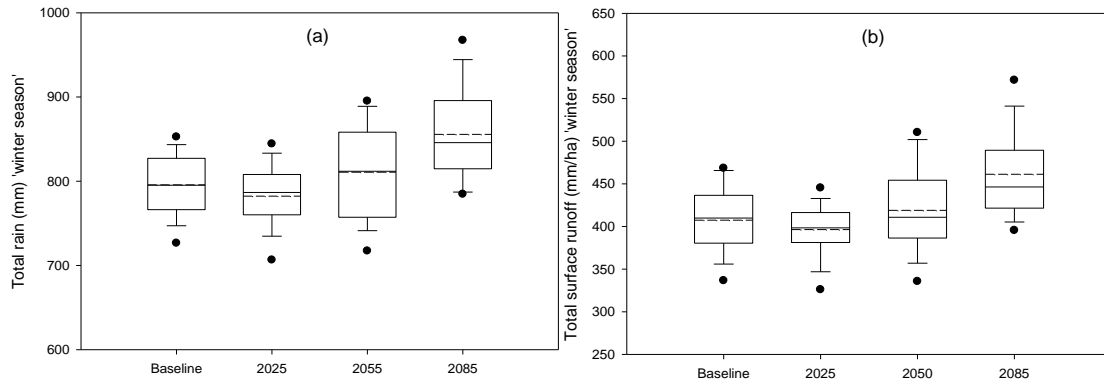


**Figure 7.7** Total rainfall (mm) during the ‘winter season’ (a), and total surface runoff (mm/ha) during the ‘winter season’ (b) for Ringarooma shown as box plots (5<sup>th</sup>, 10<sup>th</sup>, 25<sup>th</sup>, 50<sup>th</sup>, 75<sup>th</sup>, 90<sup>th</sup> and 95<sup>th</sup> percentile, with dashed mean line) from the six bias-adjusted dynamically downscaled GCMs for the baseline, 2025, 2055 and 2085.

At Ringarooma, the total rainfall during the ‘summer season’ (December to April) is projected to increase by 2025 (model mean 345 mm) from the baseline level (model mean 333 mm), then decrease slightly through to 2085 (model mean 337 mm) below the 2025 value (Figure 7.8a). The pasture irrigation requirements as simulated by DairyMod during the ‘summer season’ are projected to progressively increase from the baseline level of 3.41 ML/ha to 3.50 ML/ha by 2085 (Figure 7.8b). In addition, the total pasture evapotranspiration during the ‘summer season’ is projected to slightly increase above the baseline level of 554 mm to >565 mm for the future climate scenarios (Figure 7.8c).

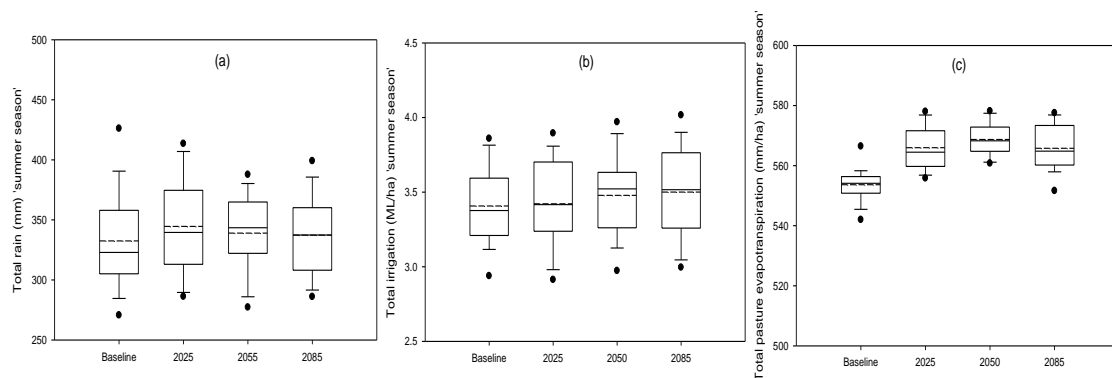


**Figure 7.8** Total rainfall (mm) received (a), total irrigation required (ML/ha) (b) and total pasture evapotranspiration (mm/ha) (c) during the ‘summer season’ shown as box plots (5<sup>th</sup>, 10<sup>th</sup>, 25<sup>th</sup>, 50<sup>th</sup>, 75<sup>th</sup>, 90<sup>th</sup> and 95<sup>th</sup> percentile, with dashed mean line) from the six bias-adjusted dynamically downscaled GCMs for the baseline, 2025, 2055 and 2085.

The total harvestable surface runoff during the ‘winter season’ and maximum storage capacity of the on-farm dam (89 ML) is shown in Figure 7.9a. Maximum on-farm storage capacity is

reached irregularly prior to 2050, however, post 2050, maximum on-farm storage capacity is reached with greater frequency. Maximum on-farm storage capacity for the baseline period is reached 37% of the time (3.7 years in 10). By 2025 the number of years maximum on-farm storage capacity is reached declines to 13% (1.3 years in 10). By 2055 maximum on-farm storage capacity is reached 47% of the time (4.7 years in 10) and by 2085 maximum on-farm storage capacity is reached 73% of the time (7.3 years in 10) (Table 7.2). The harvestable surface runoff of 34 ML that is available for the Ringarooma farm during the ‘summer season’ is currently reliant on the amount and security of the ‘summer season’ surface runoff. Total surface runoff for the ‘summer season’ period is not projected to markedly change from the baseline level to the end of the 21<sup>st</sup> century (data not shown) indicating that the current 34 ML harvested during the ‘summer season’ is projected to be relatively reliable into the future.

Figure 7.8b shows the annual total harvestable ‘winter and summer season’ surface runoff from the 104 ha catchment and total irrigation requirements of the 38 ha during the ‘summer season’. Figure 7.8c shows the total difference between the irrigation pasture requirements of the 38 ha during the ‘summer season’ and allocated surface runoff from the 104 ha catchment area during the ‘winter and summer season’. The current baseline irrigation requirements for the 38 ha of the Ringarooma case study farm are rarely achieved (Figure 7.8c). The baseline irrigation requirements are met just 23% of the time. By 2025 the irrigation requirements are projected to be met only 13% of the time. By 2055 however, the irrigation requirements are projected to be met 20% of the time and by 2085 the irrigation requirements are projected to be met 50% of the time (Table 7.2).

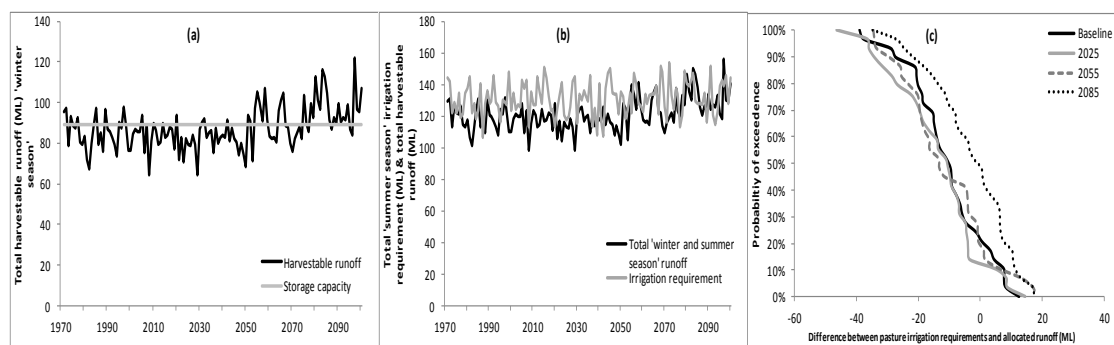


**Figure 7.9** Multi-model mean total harvestable surface runoff (20% of total surface runoff from the 104 ha catchment) (ML) (black line) and maximum on-farm storage capacity of 89 ML (grey line) during the ‘winter season’ (a). Total harvestable ‘winter and summer season’ surface runoff from the 104 ha catchment (ML) and total irrigation requirements (ML) during the ‘summer season’ (b) for the period 1971 to 2100. Cumulative distribution functions of the total difference between irrigation pasture requirements during the ‘summer season’ and allocated ‘winter and summer season’ surface runoff (c) for the baseline, 2025, 2055 and 2085.

**Table 7.2** Percentage on-farm maximum storage capacity reached during the ‘winter season’ and percentage irrigation demand during the ‘summer season’ is met from the ‘winter and summer season’ harvestable runoff at Ringarooma for the baseline, 2025, 2055 and 2085.

Scenario	% on-farm storage capacity reached	% irrigation demand met
Baseline	37%	23%
2025	13%	13%
2055	47%	20%
2085	73%	50%

### 7.3.3 Ringarooma River flows and irrigation supply

Mean annual simulated flows for the Ringarooma river are projected to slightly increase by 3% above the baseline (model mean 85 GL) by 2085 (model mean 88 GL) (Figure 7.10a). The projected mean annual increase in the Ringarooma river flow by 2085 is being driven by increases in monthly flows during July and August (Figure 7.10b) (Appendix 11.1).

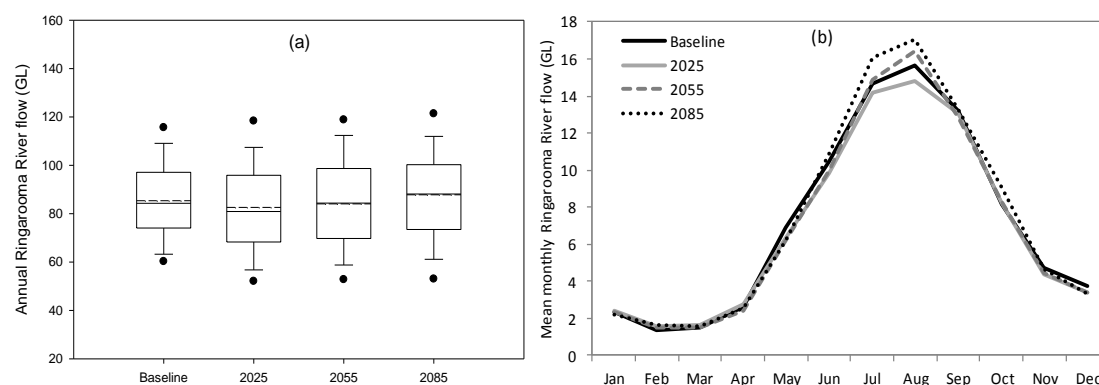


**Figure 7.10** Annual simulated Ringarooma river flow (GL) shown as box plots (5<sup>th</sup>, 10<sup>th</sup>, 25<sup>th</sup>, 50<sup>th</sup>, 75<sup>th</sup>, 90<sup>th</sup> and 95<sup>th</sup> percentile, with dashed mean line) (a) and mean simulated monthly Ringarooma river flow (GL) (b) from the six bias-adjusted dynamically downscaled GCMs for the baseline, 2025, 2055 and 2085.

At Ringarooma, mean annual river flows during the ‘summer season’ are projected to peak above the baseline at 2025 (11.8 GL), then slightly decline for the remainder of the century below the baseline level (Figure 7.11a). The Ringarooma case study farm is currently allowed to harvest 112.5 ML (1.125 ML per day for 100 days) during the ‘summer season’. The projected slight decline in the Ringarooma river flow during the ‘summer season’ from 2055 onwards will not have an adverse effect on the supply and security of irrigation water for this farm. However, the current irrigation allocation frequently fails to meet the total irrigation requirements for the available 37 ha (Figure 7.11b). The irrigation requirements during the ‘summer season’ are met only 6% of the time from the available allocated water supply. This highlights the need for the adoption of practices that achieve higher WUE. This could include

the growing of fodder crops such as forage brassica and forage maize which intrinsically have higher WUE than perennial pastures (Eckard *et al.* 2001; Jacobs *et al.* 2006; Neal *et al.* 2011) or the adoption of deficit irrigation approaches which have been shown to increase the WUE of perennial pastures (Rawnsley *et al.* 2009).

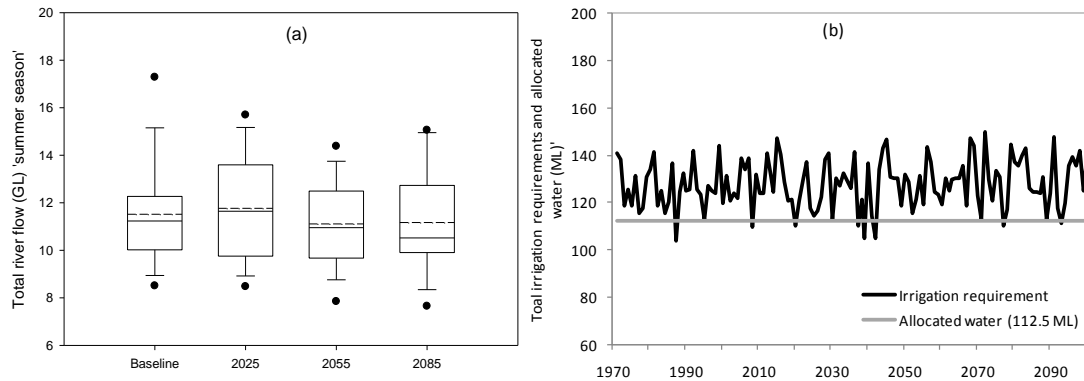


**Figure 7.11** Total Ringarooma river flow (GL) for the ‘summer season’ shown as box plots (5<sup>th</sup>, 10<sup>th</sup>, 25<sup>th</sup>, 50<sup>th</sup>, 75<sup>th</sup>, 90<sup>th</sup> and 95<sup>th</sup> percentile, with dashed mean line) for the baseline, 2025, 2055 and 2085 (a) and pasture irrigation requirements and allocated water entitlement (ML) (b) for the ‘summer season’ at Ringarooma for the period 1971 to 2100 from the six bias-adjusted dynamically downscaled GCMs.

A total water budget for the Ringarooma case study farm has shown that the current reliance on ‘summer season’ rainfall to meet pasture water requirements is projected to continue. Existing allocations of irrigation water from both harvested surface runoff and river flow fails to meet the irrigation requirements of the farms 75 ha of irrigated land. In the absence of other changes, such as land use change, increased water allocation or larger on-farm storage dams, this reliance is projected to continue into the future, most notably in the near future.

## 7.4 Conclusion

This chapter has examined the potential impacts of climate change on surface runoff at the six dairy sites using the data generated by Bennett *et al.* (2010) from the hydrological model SIMHYD. The modelled mean surface runoff using the climate change projections from the six GCMs at each site is projected to increase by a range of 2% to 27% throughout the 21<sup>st</sup> century, driven by increased seasonal runoff during winter and spring. At all sites however, a slight contraction in surface runoff is projected in the near future (2025) relative to the baseline levels, before increasing above the baseline levels by the end of the century (2085). Regional responses and the rate of change in surface runoff to the projected climate were relatively similar in both the amounts and seasonal distribution.

Precipitation runoff and flows into rivers and farm dams are a vital component of irrigated agricultural production and large reductions in water storage as a result of decreased runoff could potentially affect the viability of some currently irrigated farming systems within Tasmania. A total farm water budget out to 2100 for the Ringarooma case study dairy farm showed that a reduction in catchment runoff is projected in the near future, increasing the dependence on summer rain events to meet pasture water requirements. The analysis has highlighted the need for the Ringarooma case study farm to adopt approaches to improve its current WUE to meet both the current and future irrigation demands

This chapter has quantified the influences of climate projections on water availability and water requirements for a given farm enterprise. A similar approach could be extended to quantify the likely changes in water availability at a regional level and examine the adoption of key adaptation strategies. These adaptation strategies could be at a farm level up to a whole of catchment/regional level. This would be highly valuable for adaptation research regarding the management of catchment/regions water storages under a changing future climate.

## CHAPTER 8: CONCLUSION AND RECOMMENDATIONS

The primary aim of this thesis was to provide the Tasmania dairy industry with sound knowledge regarding the projected regional climate change influences on the current forage base of Tasmania's dairying production systems. A vast amount of information now exists regarding the nature and extent to which regional changes in climate have already occurred in Australia, combined with information of the projected climate change across Australia from coarse resolution climate models (Crimp *et al.* 2008). This study has added to the knowledge base of projected climate change by providing an assessment of climate change at a regional level using fine scale model projections.

In Tasmania, dairy is the largest agriculture industry and the production and consumption of high quality temperate pastures along with the availability of irrigation water underpin the competitiveness of the industry. Regional impacts of the projected climate change on pasture production, irrigation demand and surface runoff were quantified using simulation modeling for six dairy regions across Tasmania. The research was undertaken to quantify and provide information for the Tasmanian dairy industry to prepare for the uncertainty and develop adaptation strategies to the projected future climate.

Previous studies of climate change impacts on Tasmanian pasture based dairy systems have used perturbed historical climate data with anomalies calculated from GCMs, such as those associated with the OzClim database (Ricketts & Page 2007). This method guarantees the baseline climate period is the same scale as observations. The climate projections using this method are generated by adjusting the baseline observations by the anomaly. Variables such as temperature are adjusted additively and rainfall is adjusted proportionally. The CFT generated climate data used in this study was unique in capturing changes in climate at any particular location that are the result of changes in synoptic meteorology and local climate processes. Changes in the seasonality, frequency and intensity of synoptic patterns such as, high and low pressure systems which change the frequency distributions of the climate variables have been captured and accounted for.

General Circulation Models have variable skill and inherent biases (Corney *et al.* 2010). To address this, the CFT project bias-adjusted the dynamically downscaled GCMs using the historical AWAP 0.1° gridded climate data source. Optimal use of the CFT generated projections requires an understanding of the features of the GCM outputs and also of observed data (Holz *et al.* 2010). There are three frequently used sources of historic continuous daily climate data available; SILO Patched Point data (observed), SILO Data Drill

(0.05°) and Australian Water Availability Project (AWAP 0.05°). Climate Futures for Tasmania generated a fourth, AWAP 0.1°, interpolated from the AWAP 0.05° gridded data source. The AWAP 0.1° data source was created to compare directly to the regional climate models and is not commercially available as a formal gridded data source.

A meteorological and biophysical comparison between the four sources of observed and interpolated daily climate data for the period 1971 to 2007 was undertaken for each dairying region. No previous analysis has been undertaken regarding comparisons between the four sources of observed and interpolated climate data sources, and this study was unique in that these differences were quantified. Differences were observed between the four daily climate data sources for each site for the climate variables; mean daily minimum temperature, rainfall and potential evaporation. In addition, outputs from the biophysical model DairyMod (version 4.9.2) compared simulated monthly and annual pasture production. There were few significant differences in annual pasture production. The mean annual simulated pasture yields from the four sets of observed and interpolated data sources were generally comparable, giving confidence that the use of CFT generated AWAP 0.1° data source for the bias-adjustment of the dynamically downscaled GCMs simulations was suitable.

To establish confidence in the CFT bias-adjusted dynamically downscaled GCMs climate projections, the GCMs outputs were compared against the interpolated historical climate data of AWAP 0.1°. The suitability of the downscaled bias-adjusted GCM outputs for use in a biophysical model was evaluated by comparing the climate metrics of mean daily maximum, minimum and diurnal temperature range, rainfall and solar radiation against the AWAP 0.1° data source for the period 1990 to 2007. Differences were observed between the AWAP 0.1° data source and the bias-adjusted downscaled GCMs at each of the six sites, most notably between mean daily minimum temperature. Simulated mean monthly and annual pasture production outputs from the biophysical model DairyMod (version 4.9.2) were compared between the AWAP 0.1 data source and the six GCMs. The mean monthly and annual simulated pasture yields from the AWAP 0.1° data source and the downscaled bias-adjusted GCMs were comparable, giving an acceptable degree of confidence that the bias-adjusted GCM simulations were suitable for projections of pasture production.

The projected climate under the A2 emissions scenario at each site was described over the period of 1971 to 2100. The mean daily maximum and daily minimum temperatures at each site are projected to increase from the baseline period to 2085 ranging from 2.4°C at Woolnorth to 2.7°C at Ringarooma. At each site except Flowerdale, mean annual rainfall is projected to slightly increase from the baseline period to 2085. Seasonal rainfall is projected

to increase slightly at each site except Woolnorth (summer) and Flowerdale (summer and spring). At all sites from the baseline to 2085, inter-annual rainfall variability is projected to increase and mean annual potential evapotranspiration rates are projected to increase by 3% to 4%. No changes in solar radiation are projected for any of the regions.

In assessing the impacts of the projected future climate on pasture based systems for each dairying region the biophysical model DairyMod (version 4.9.2) was used to simulate the growth of perennial ryegrass under rainfed and irrigated conditions. Throughout the 21<sup>st</sup> century mean annual pasture yields under rainfed conditions at each site are projected to increase above the baseline varying from 29% at Woolnorth to 150% at Cressy by 2085. Mean annual irrigated pasture yields are projected to increase until approximately 2050, then decrease to 2085. The reduction of irrigated pasture yields in the latter half of this century is the result of an increase in the number of warmer days, characterised by maximum temperatures exceeding 28°C. The impacts of higher daily maximum temperatures are more evident under the irrigated simulations, because the irrigated simulations were not limited by soil moisture. In contrast, the major limitation to pasture growth in the rainfed simulations during the summer months is available moisture. Pasture yield increases, under both rainfed and irrigated simulations are projected to occur during late winter and spring. This increase is a result of increased daily temperatures and the associated increases in the atmospheric concentration of CO<sub>2</sub>.

At each site, under both the rainfed and irrigated simulations, inter-annual pasture yield variability is projected to decrease from the baseline to 2085 except at Cressy under irrigation. The decrease in inter-annual yield variability is being driven by a notable reduction in seasonal pasture yield variability during autumn and spring. Inter-annual variability was consistently greater in regions where the baseline pasture yields were lower (Cressy and Ouse).

At all sites, except Cressy and Ouse, irrigation demand progressively increases throughout the 21<sup>st</sup> century. Whilst irrigation requirements are projected to increase, there is a corresponding increase in the WUE of the pasture. The increase in WUE is driven by increasing atmospheric CO<sub>2</sub> concentrations as a result of increased net influx of CO<sub>2</sub>, increased stomatal resistance and a decline in transpiration per unit of CO<sub>2</sub> fixed (Long *et al.* 2004).

Surface runoff for each of the six sites, was quantified from the downscaled bias-adjusted GCMs outputs using the hydrological model SIMHYD for the period 1971 to 2100 (Bennett *et al.* 2010). At all sites, except Flowerdale, mean annual surface runoff by 2085 is projected

to increase as a result of increased surface runoff during the winter months. An on-farm case study at Ringarooma was undertaken to quantify the projected surface runoff and River flow impacts on an irrigated pasture based dairy system. Irrigation water is accessed from both on-farm catchment (dam) and access to River flows (Ringarooma River). By 2085, irrigation demand met by the on-farm storage dam is projected to be met 50% of the time, increasing above the current baseline of 23%. In contrast, the current water entitlement from the Ringarooma River during summer is projected to increasingly fail to meet irrigation demand from the baseline to 2085, the result of both a limited water allocation, and an increasing irrigation demand from the pasture bases.

This thesis has evaluated the projected regional climate change and quantified the likely impacts the projected change will have on the forage base for the Tasmanian dairy industry. Biophysical modelling indicates a progressive increase in pasture growth within Tasmania throughout the 21<sup>st</sup> century. Currently the low cost of milk production associated with pasture based dairy systems underpins the national and international competitive advantage of the Tasmania dairy industry. This study has indicated that the most likely changes in pasture production for Tasmanian dairy regions is that annual pasture production will increase in the short to medium term with higher levels of pasture growth occurring during the winter and early spring period. The probable implication of this is that adaptations are likely to be within system options that are learned and not sudden. These are likely to include adjustments to stocking rates and calving dates to better match feed supply and feed demand, along with increased forage conservation opportunities during spring. A greater demand for nitrogen fertiliser (and other nutrients) is also probable, if the potential increases in pasture growth are to be captured. Pasture production during summer is projected to increase in the short to medium term across each region, however the current summer feed deficits will remain, requiring supplementary feed to meet the summer feed gap, while the demand for irrigation water will also remain high during the summer months.

This study has found the current forage base of Tasmanian dairy regions is relatively resilient to future climate scenarios and whilst no adaptation management options were considered in this study. In reality dairy farmers will gradually adapt to the projected climate change with the industry continuing to focus on milk production per hectare and pasture consumption per hectare as key determinants of business success.

This study has implications for future research directions for the Tasmanian dairy industry. Further climatic research can be undertaken concerning the impacts of a changing climate on regional pasture production, particularly drought frequency, heat waves and extreme rainfall

events. Further research is needed in the area of on-farm adaptation options and management to minimise the risk of climate change and variability, with particular focus on alternative pasture species such as deeper rooted C<sub>3</sub> perennials and or the inclusion of C<sub>4</sub> pasture species. The projected pasture yield increases reported in this study are partly reliant on the realisation of beneficial CO<sub>2</sub> effects on pasture growth and WUE as currently measured in experimental trials (Parry *et al.* 2004). The potential long term effects of CO<sub>2</sub> in the field remain uncertain. Understanding the long term impacts of elevated CO<sub>2</sub> on pasture based systems especially on WUE and carbon uptake of the pasture remains a priority for quantifying the impacts of climate change. In addition, availability and security of irrigation water for the Tasmanian dairy industry is an important and ongoing issue. This study has gone some way to quantifying the changes in irrigation demand and associated water availability for the main dairy regions under a changing future climate. Further research quantifying the projected regional surface runoff to meet the projected regional irrigation demands of the Tasmanian agricultural industries is also required.

## References

- Ainsworth, E.A. & Long, S.P. 2004. 'What have we learned from 15 years of free-air CO<sub>2</sub> enrichment (FACE)? A meta-analytic review of the responses of photosynthesis, canopy properties and plant production to rising CO<sub>2</sub>', *New Phytologist*, vol. 165, pp. 351-372.
- Alexander, L.V., Hope, P., Collins, D., Trewin, B., Lynch, A. & Nicholls, N. 2007. 'Trends in Australia's climate means and extremes: a global context', *Australian Meteorological Magazine*, vol. 56, pp. 1-18.
- Alexander, L.V & Arblaster, J.M. 2009. 'Assessing trends in observed and modelled climate extremes over Australia in relation to future projections', *International Journal of Climatology*, vol. 29, pp. 417-435.
- Anonymous 2009, Into Dairy. <http://www.intodairy.com.au/index>.
- Anwar, M.R., O'Leary, G., McNeil, D., Hossain, H. & Nelson, R. 2007. 'Climate change impact on rainfed wheat in south-eastern Australia', *Field Crops Research*, vol. 104, pp. 139-147
- Armstrong, D., Knee, J., Prichard, K., & Gyles, O. 2000. 'Water use efficiency on irrigated dairy farms in northern Victoria and southern New South Wales', *Australian Journal of Experimental Research*, vol. 40, pp. 643-653.
- Ash, A., McIntosh, P., Cullen, B., Carberry, P. & Smith, M.S. 2007. 'Constraints and opportunities in applying seasonal climate forecasts in agriculture'. *Australian Journal of Agricultural Research*, vol. 58, pp. 952-965.
- Australian Bureau of Statistics. 2010a. *Value of Agricultural Commodities*, Cat. No. 7503.0
- Australian Bureau of Statistics. 2010b. *Water use on Australian farms 2008-09*, Cat. No. 4618.0
- Bailey, D., Ashton, D. & Gordon, W. 2004, Livestock outlook for 2004-05 and farm performance in Tasmania. Tasmanian Regional Outlook Conference, Launceston, Tasmania, ABARE Conference Paper 04.22.
- Barlow, R. 2008. *National feedbase stocktake report*, Draft for Dairy Australia.
- Bazzaz, F.A. & McConnaughay, K.D.M. 1992. 'Plant-plant interactions in elevated CO<sub>2</sub> environments'. *Australian Journal of Botany*, vol. 40, pp. 547-563.
- Beesley, C.A., Frost, A.J. & Zajaczkowski, J. 2009. 'A comparison of the BAWAP and SILO spatially interpolated daily rainfall datasets', 18<sup>th</sup> World IMACS/MODSIM Congress, Cairns, Australia 13-17 July 2009.

- Beevers, L. 1961. *Genotypic differences in herbage grasses in respect of biochemical characters*, Ph.D. Thesis, University College of Wales, Aberystwyth.
- Bennett, J.C., Ling, F.L.N., Graham, B., Grose, M.R., Cornet, S.P., White, C.J., Holz, G.K., Post, D.A., Gaynor, S.M. & Bindoff, N.L. 2010. *Climate Futures for Tasmania: water and catchments report technical report*, Antarctic Climate and Ecosystems cooperative Research Centre, Hobart, Tasmania.
- Beukes, P.C., Thorrold, B.S., Wastney, M.E., Palliser, C.C., MacDonald, K.A., Bright, K.P., Lancaster, J.A.S., Palmer, C.A.J. & Auld, M.J. 2005. 'Modelling the bi-peak lactation curves of summer calvers in New Zealand dairy farm systems', *Australian Journal of Experimental Agriculture*, vol. 45, pp. 643-649.
- Blaikie, S.J. & Martin, F.M. 1987. 'Limit to the productivity of irrigated pastures in southeast Australia', in *Temperature Pastures*, ed. Wheeler, J.L., Pearson, C.J. & Robards, G.E., Australian Wool Corporation Technical Publication, CSIRO Australia.
- Boer, G.J. 2009. 'Changes in interannual variability and decadal potential predictability under global warming', *Journal of Climate*, vol. 22, pp. 3098-3109.
- Boschma, S.P., Hill, M.J., Scott, J.M. & Rapp, G.G. 1996. 'Effect of different intensities of drought and defoliation upon the mortality of perennial grasses', In 'Proceedings of the 8<sup>th</sup> Australian agronomy conference'. Australian Society of Agronomy, Carlton, Victoria.
- Brankovic, C., Srncic, L. & Pataric, M. 2010. 'An assessment of global and regional climate change based on the EH5OM climate model ensemble', *Climatic Change*, vol. 98, pp. 21-49.
- Bryant, J.R. & Snow, V.O. 2008. 'Modelling pastoral farm agro-ecosystems: a review', *New Zealand Journal of Agricultural Research*, vol. 51, pp 349-363.
- Bureau of Meteorology, 1993. *Climate of Tasmania*, Bureau of Meteorology, Victorian Printing, Pty Ltd.
- Bureau of Meteorology, 2011. <http://www.bom.gov.au/>
- Cai, W. & Cowan, T. 2008. 'Dynamics of late autumn rainfall reduction over southeastern Australia', *Geophysical Research Letters*, vol. 35, L09708.
- Casella, E., Soussana, J.F. & Loiseau, P. 1996. 'Long-term effects of CO<sub>2</sub> enrichment and temperature increase on a temperate grass sward', *Plant and Soil*, vol. 182, pp. 83-99.
- Chapman, D.F., Kenny, S.N., Beca, D. & Johnson, I.R. 2008a, 'Pasture and forage crop systems for non-irrigated dairy farms in southern Australia. 1. Physical production and economic performance', *Agricultural systems*, vol. 97, pp. 108-125.

- Chapman, D.F., Kenny, S.N., Beca, D. & Johnson, I.R. 2008b, 'Pasture and forage crop systems for non-irrigated dairy farms in southern Australia. 2. Inter-annual variation in forage supply, and business risk', *Agricultural systems*, vol. 97, pp. 126-138.
- Chapman, D.F., Cullen, B.R., Johnson, I.R. & Beca, D. 2009. 'Interannual variation in pasture growth rate in Australian and New Zealand dairy regions and its consequences for system management', *Animal Production Science*, vol. 49, pp. 1071-1079.
- Chiew, F.H.S. & McMahon, T.A. 2002. 'Modelling the impacts of climate change on Australian streamflow', *Hydrological Processes*, vol. 16, pp. 1235-1245.
- Chiew, F.H.S., Peel, M.C. & Western, A.W. 2002. 'Application and testing of the simple rainfall-runoff model SIMHYD', *Mathematical models of small watershed hydrology applications*, Singh, V.P. & Frevert, D.K. (eds), Water Resources Publications, Littleton, USA, pp. 335-367.
- Chiew, F.H.S. 2006. 'Estimation of rainfall elasticity of streamflow in Australia', *Hydrological Sciences Journal*, vol. 51, pp. 613-625.
- Chiew, F.H.S., Young, W.J., Cai, W. & Teng, J. 2010. 'Current drought and future hydroclimate projections in southeast Australia and implications for water resources management', *Stochastic Environmental Research Risk Assessment*, vol. 25, pp. 601-612.
- Christie, K. 2006, 'A comparison of the growth and utilization of three temperate grasses under irrigated conditions in the field and predicted with DairyMod', Honours Thesis, University of Tasmania, Hobart.
- Clark, H., Newton, P.C.D., Bell, C.C. & Glasgow, E.M. 1995. 'The influence of elevated CO<sub>2</sub> and simulated seasonal changes in temperature on tissue turnover in pasture turves dominated by perennial ryegrass (*Lolium perenne*) and white clover (*Trifolium repens*)', *Journal of Applied Ecology*, vol. 32, pp. 128-136.
- Collins, D.A., Della-Marta, P.M., Plummer, N. & Trewin, B.C. 2000, 'Trends in annual frequencies of extreme temperature events in Australia', *Australian Meteorological Magazine*, vol. 49, pp. 277-292.
- Cooper, J.P. 1964. 'Climatic variation in forage grasses 1. Leaf development in climatic race of *Lolium* and *Dactylis*', *Journal of Applied Ecology*, vol. 1, pp. 45-61.
- Cooper, J.P. & Tainton, N.M. 1968. 'Light and temperature requirements for the growth of tropical and temperate grasses', *Herbage Abstracts*, vol. 38, pp. 167-176.
- Corney, S.P., Katzefey, J.J., McGregor, J.L., Grose, M.R., Bennett, J.B White, C.J., Holz, G.K., Gaynor, S.M. & Bindoff N.L. 2010. '*Climate Futures for Tasmania: climate modelling technical report*', Antarctica Climate & Ecosystems Cooperative Research Center, Hobart, Tasmania.

- Covey, C. 2003. 'An overview of results from the coupled model Intercomparison project' *Global and Planetary Change*, vol. 37, pp. 103-133.
- Crimp, S., Gartman, A., DeVoil, P., Gaydon, D., Howden, M. & Odgers J. 2008. 'Adapting Australian farming systems to climate change: a participatory approach', Final Report for the Department of Climate Change, Canberra, ACT.
- Christensen, O.B. & Christensen, J.H. 2004. 'Intensification of extreme European summer precipitation in a warmer climate', *Global Planet Change*, vol. 44, pp. 107-117.
- Crosbie, R.S., McCallum, J.L., Walker, G.R. & Chiew, F.H.S. 2010. 'Modelling climate change impacts on groundwater recharge in the Murray-Darling Basin, Australia', *Hydrogeology Journal*, vol. 18, pp. 1639-1656.
- Crush, J.R., Waller, J.E. & Care, D.A. 2005, 'Root distribution and nitrate interception in eleven temperate forage grass', *Grass and Forage Science*, vol.60, 385-392.
- CSIRO and BoM 2007. '*Climate Change in Australia. Technical Report 2007*'. Pearce, K.B. Hopler, P.N., Hopkins, M., Bouma, W.J., Whetton, P.H., Hennessy, K.J. & Power, S. B. (eds), CSIRO and Australian Bureau of Meteorology, <http://climatechangeinaustralia.gov.au/>
- Cullen, B.R., Chapman, D.F. & Quigley, P.E. 2006. 'Comparative defoliation tolerance of temperate perennial grasses', *Grass and Forage Science*, vol. 61, pp. 405-412.
- Cullen, B.R., Eckard, R.J., Callow, M.N., Johnson, I.R., Chapman, D.F., Rawnsley, R.P., Garcia, S.C., White, T. & Snow, V.O. 2008. 'Simulating pasture growth rates in Australia and New Zealand grazing systems', *Australian Journal of Agricultural Research*, vol. 59, pp. 761-768.
- Cullen, B.R., Johnson, I.R., Eckard, R.J., Lodge, G.M., Walker, R.G., Rawnsley, R.P. & McCaskill, M.R. 2009. 'Climate change effects on pasture systems in south-eastern Australia', *Crop and Pasture Science*, vol. 60, pp. 933-942.
- Cullen, B.R. & Eckard, R.J. 2011. 'Impacts of future climate scenarios on the balance between productivity and total greenhouse gas emissions from pasture based dairy systems in south eastern Australia', vol. 166-167, pp. 721-735.
- Daepf, M., Suter, D., Almeida, J.P.F., Isopp, H., Hartwig, U.A., Frehner, M., Blum, H., Nosberger, J. & Luscher, A. 2000. 'Yield response of *Lolium perenne* swards to free air CO<sub>2</sub> enrichment increased over six years in a high N input system on fertile soil', *Global Change Biology*, vol. 6, pp. 805-816.
- Daepf, M., Nosberger, J. & Luscher, A. 2001. 'Nitrogen fertilization and developmental stage alter the response of *Lolium perenne* to elevated CO<sub>2</sub>', *New Phytologist*, vol. 150, pp. 347-358.

- Dairy Australia 2011. 'Dairy in Tasmania regional profile' <http://dairyaustralia.com.au/Industry-overview/Dairy-regions/Tasmania>
- Daly, C. 2006. 'Guidelines for assessing the suitability of spatial climate data sets', *International Journal of Climatology*, vol. 26, pp. 707-721.
- Daly, C., Gibson, W. P., Taylor, G. H., Johnson, G. L. & Pasteris, P. 2002. 'A knowledge Based approach to the statistical mapping of climate', *Climate Research*, vol. 22, pp. 99-113.
- Deuter, P. 2006. *Scoping study into climate change and climate variability*. Project No. VG05051, Queensland Department of Primary Industries and Fisheries, Horticulture Australia.
- Dodson, R. & Marks, D. 1997. 'Daily air temperature interpolated at high spatial resolution Over a large mountainous region', *Climate Research*, vol.8, pp. 1-20.
- Donaghy, D.J., Scott, J.M. & Fulkerson, W.J. 1997. 'Effect of defoliation frequency and Summer irrigation on survival of (*Lolium perenne*) and biennial (*Lolium multiflorum*) ryegrass in the subtropics', *Australian Journal of Experimental Agriculture*, vol. 37, pp. 537-545.
- Doyle, P.T., Stockdale, C.R., Lawson, A.R. & Cohen, D.C. 2000. 'Pastures for dairy production in Victoria', Department of Natural Resources and Environment, Kyabram, Victoria.
- Dunbabin, J.S., Hume, I.H. & Ireson, M.E. 1997. 'Effects of irrigation frequency and transient waterlogging on the production of a perennial ryegrass – white clover pasture', *Australian Journal of Experimental Agriculture*, vol. 37, pp. 165-171.
- Eckard, R.J., Salardini, A.A., Hannah, M. & Franks, D.R. 2001. 'The yield, quality and irrigation response of summer forage crops suitable for a dairy pasture renovation program in north-western Tasmania', *Australian Journal of Experimental Agriculture* vol. 41, pp. 37-44.
- England, M.H., Ummenhofer, C.C. & Santoso, A. 2005. 'Interannual rainfall extremes over southwestern Australia linked to Indian Ocean climate variability'. *Journal of Climate*, vol. 19, pp. 1948-1969.
- Fereres, E. & Auxiliadora Soriano, M. 2007. 'Deficit irrigation for reducing agriculture water use'. *Journal of Experimental Botany*, vol. 58, pp. 147-159.
- Fischer, B.U., Frehner, M., Hebeissen, T., Zanetti, S., Stadelmann, F., Luscher, A., Hartwig, U.A., Hendry, G.R., Blum, H. & Noseberger, J. 1997. 'Source-sink relations in *Lolium perenne* L. as reflected by carbohydrate concentrations in leaves and pseudo-stems during regrowth in a free air carbon dioxide enrichment (FACE) experiment', *Plant Cell Environment*, vol. 20, pp. 945-952.

- Forde, B. 1966. 'Effects of various environments on the autonomy and growth of perennial ryegrass and cocks foot', *New Zealand Journal of Botany*, vol. 4, pp. 455-468.
- Freebairn, D.M & Boughton, W.C. 1981. 'Surface runoff experiments on the eastern Darling Downs', *Australian Journal of Soil Research*, vol. 19, pp. 133-146.
- Fulkerson, W.J. & Donaghy, D.J. 2001. 'Plant soluble carbohydrate reserves and senescence key criteria for developing an effective grazing management system for ryegrass-based pastures: a review', *Australian Journal of Experimental Agriculture*, vol. 41, pp. 261-275.
- Gallant, A.J.E., Hennessy, K.J. & Risbey, J. 2007. 'Trends in rainfall indices for six Australian regions: 1910 – 2005', *Australian Meteorological Magazine*, vol. 56, pp. 223-239.
- Garcia, S.C. & Fulkerson, W.J. 2005. 'Opportunities for future Australian dairy systems: A review', *Australian Journal of Experimental Agriculture*, vol. 45, pp. 1041-1055.
- Gifford, R.M., Farquhar, G.D., Nicholls, N. & Roderick, M.L. 2005. Workshop summary in: Gifford, R.M (ed). *Pan evaporation: an example of the detection and attribution of trends in climate variables*. Australian Academy of Science National Committee for Earth System Science. [www.science.org.au/natcoms/pan-evap.pdf](http://www.science.org.au/natcoms/pan-evap.pdf)
- Gobin, A. 2010. 'Modelling climate impacts on crop yields in Belgium', *Climate Research*, vol. 44, pp. 55-68.
- Greer, D.H., Laing, W.A., Campbell, B.D. & Halligan, E.A. 2000. 'The effect of perturbations in temperature and photon flux density on the growth and photosynthetic responses of five pasture species to elevated CO<sub>2</sub>', *Australian Journal of Plant Physiology*, vol. 27, pp. 301-310.
- Grose, M.R., Barnes-Keoghan I., Corney, S.P., White, C.J., Holz, G.K., Bennett, J.B., Gaynor, S.M. & Bindoff, N.L. 2010. *Climate Futures for Tasmania general climate Impacts technical report*, Antarctic Climate & Ecosystems Cooperative Research Centre, Hobart, Tasmania.
- Guobin, L. & Kemp, D.R. 1992. 'Water stress affects the productivity, growth components, competitiveness and water relations phalaris and white clover growing in a mixed pasture', *Australian Journal of Agricultural Research*, vol. 43, pp. 659-672.
- Harle, K.J., Howden, S.M., Hunt, L.P. & Dunlop, M. 2006. 'The potential impact of climate change on the Australian wool industry by 2030', *Agricultural Systems*, vol. 93, pp. 61-89.
- Harrison, J., Tonkinson, C., Eagles, C. & Foyer, C. 1997. 'Acclimation to freezing Temperatures in perennial ryegrass (*Lolium perenne*)', *Physiologiae Plantarum*, vol. 19, pp. 505-515.

- Haylock, M. & Nicholls, N. 2000. 'Trends in extreme rainfall indices for an updated high quality data set for Australia, 1910-1998', *International Journal of Climatology*, vol. 20, pp. 1533-1541.
- Hennessy K.J. 2007. 'Climate change in Australian dairy regions', CSIRO Atmospheric Research: Aspendale, Vic.
- Hijmans, R. J., Cameron, S. E., Parra, J. L., Jones, P. G. & Jarvis, A. 2005. 'Very high Resolution interpolated climate surfaces for global land areas', *International Journal of Climatology*, vol. 25, pp. 1965-1978.
- Hill, K.J., Santoso, A. & England, M.H. 2008. *Interannual Tasmanian rainfall variability associated with the Southern Annular Mode and ENSO*. University of New South Wales, Climate Change Research Centre, School of Mathematics and Statistics.
- Hill, K.J., Santoso, A. & England, M.H. 2009. 'Interannual Tasmanian rainfall variability associated with large-scale climate modes', *Journal of Climate*, vol. 22, pp. 4383-4397.
- Holz, G.K., Grose, M.K., Bennett, J.C., Corney, S.P., White, C.J., Phelan, D., Potter, K., Kriticos, D., Rawnsley, R., Parsons, D., Lisson, S., Gaynor, S.M. & Bindoff, N.L. 2010. *Climate Futures for Tasmania: Impacts on agriculture technical report*, Antarctic Climate and Ecosystems Cooperative Research Centre, Hobart, Tasmania.
- Hughes, L. 2003. 'Climate change and Australia: trends, projections and impacts', *Austral Ecology*, vol. 28, pp. 423-443.
- Hunt, W.F. & Halligan, G. 1981. 'Growth and development responses of perennial ryegrass grown at constant temperature. I. Influence of light and temperature on growth and net assimilation'. *Australian Journal of Plant Physiology*, vol. 8, pp. 181-190.
- Hunt, W.F. & Thomas, V.J. 1985 'Growth and developmental responses of perennial ryegrass grown at a constant temperature II. Influence of light and temperature on leaf, tiller root appearance', *Australian Journal of Plant Physiology*, vol. 12, pp. 69-76.
- Hunt, B.G. 2008. 'Multi-annual dry episodes in Australian climatic variability', *International Journal of Climatology*, Published online (<http://www.interscience.wiley.com>).
- Idso, S.B., Kimball, B.A. Mauney, J.R. 1987. 'Atmospheric carbon dioxide enrichment effects on cotton midday foliage temperature: implications for plant water use and crop yield', *Agronomy Journal*, vol. 79, pp. 667-672.
- IPCC 2007. *Climate Change 2007: The physical Science Basis. Contribution of working Group I to the Fourth Assessment Report of the Intergovernmental Panel on Climate Change*. Cambridge University Press, Cambridge, United Kingdom and New York, NY, USA.

- Jacobs, J.L., Ward, G.N., McKenzie, F.R. & Kearney, G. 2006. 'Irrigation and nitrogen fertiliser effects on dry matter yield, water use efficiency and nutritive characteristics of summer forage crops in south-west Victoria', *Australian Journal of Experimental Agriculture*, vol. 46, pp. 1139-1149.
- Jeffrey, S.J., Carter, J.O., Moodie, K.M. & Beswick, A.R. 2001. 'Using spatial software to construct a comprehensive archive of Australian climate data', *Environmental Modelling and Software*, vol. 16, pp. 309-330.
- Johnson, I.R., Lodge, G.M. & White, R.E. 2003. 'The sustainable grazing systems pasture model: description, philosophy and application to the SGS national experiment', *Australian Journal of Experimental Agriculture*, vol. 43, pp. 711-728.
- Johnson, I.R. 2005. *Biophysical Modeling*, IMJ Consultants, Pty Ltd. <http://www.imj.com.au/dm>
- Johnson, I.R., Chapman, D.F., Snow, V.O., Eckard, R.J., Parsons, A.J., Lambert, M.G. & Cullen, B.R. 2008. 'DairyMod and EcoMod: biophysical pasture-simulation models for Australia and New Zealand', *Australian Journal of Experimental Agriculture* vol. 48, pp. 621-631.
- Jones, M.B. 1988. 'Water relations' in *The grass crop: the physiological basis of production*, Ed Jones M.B. & Lazenby, A., Chapman and Hall Ltd, London, England.
- Jones, D.A., Wang, W. & Fawcett, R. 2007. 'Climate data for the Australian Water Availability Project', Australian Water Availability Project Final Milestone Report, National Climate Centre, Australian Bureau of Meteorology.
- Jones, D.A., Wang, W. & Fawcett, R. 2009. 'High-quality spatial climate data-sets for Australia', *Australian Meteorological and Oceanographic Journal*, vol. 58, pp. 233-248.
- Jovanovic, B., Jones, D.A. & Collins, D. 2008. 'A high-quality monthly pan evaporation dataset for Australia', *Climatic Change*, vol. 87, pp. 517-535.
- Karoly, D., Risbey, J., Reynolds, A. & Braganza, K. 2003. 'Global warming contributes to Australia's worst drought', *Australasian Science*, vol. 24, pp. 14-17.
- Karoly, D.J. & Braganza, K. 2005. 'Attribution of recent temperature changes in the Australian region', *Journal of Climate*, vol. 18, pp. 457-464.
- Keating, B.A., Carberry, P.S., Hammer, G.L., Probert, M.E., Robertson, M.J., Holzworth, D., Huth, N.I., Hargreaves, J.N.G., Meinke, H., Hochman, Z., McLean, G., Verbug, K., Snow, V., Dimes, J.P., Silburn, M., Wang, E., Brown, S., Bristow, K.L., Asseng, S., Chapman, S., McCown, R.L., Freebairn, D.M. & Smith, C.J. 2003. 'An overview of APSIM, a model designed for farming systems simulation', *European Journal of Agronomy*, vol. 18, pp. 267-288.

- Kemp, D.R., Eagles, C.F. & Humphreys, M.O. 1989. 'Leaf growth and apex development of perennial ryegrass during winter and spring', *Annals of Botany*, vol. 63, pp. 349-355.
- Kharin, V.W. & Zwiers, F.W. 2000. 'Changes in extremes in an ensemble of transient climate simulations with a coupled atmospheric ocean GCM', *Journal of Climate*, vol. 13, pp. 3760-3788.
- Kirono, D.G.C., Jones, R.N. & Cleugh, H.A. 2009. 'Pan-evaporation measurements and Morton-point potential evaporation in Australia: are their trends the same?', *International Journal of Climatology*, vol. 29, pp. 711-718.
- Laing, W.A., Greg, D.H. & Campbell, B.D. 2002. 'Strong responses of growth and photosynthesis of five C<sub>3</sub> pasture species to elevated CO<sub>2</sub> at low temperatures', *Functional Plant Biology*, vol.29, pp. 1089-1096.
- Langer, R.H.M. 1973. *Pastures and Pasture Plants*, Dai Nippon Printing Co. Ltd, Hong Kong, China.
- Langford, J. 1965. *Weather and Climate, Atlas of Tasmania*, J.L. Davies, Hobart, Lands and Survey Department.
- Lawson, A.R., Kelly, K.B. & Sale, P.W.G. 1997. 'Effect of defoliation frequency on an irrigated perennial pasture in northern Victoria 2. Individual plant morphology', *Australian Journal of Agricultural Research*, vol. 48, pp. 819-829.
- Lazenby, A. & Swain, F.G. 1972, *Intensive Pasture Production*, Angus and Robertson, Sydney, Australia.
- Leakey, A.D.B., Ainsworth, E.A., Bernacchi, C.J., Rogers, A., Long, S.P. & Ort, D.R. 2009. 'Elevated CO<sub>2</sub> effects on plant carbon, nitrogen and water relations: six important lessons from FACE', *Journal of Experimental Botany*, vol. 60, pp. 2859-2876.
- Le Quere, C., Raupach, M.R., Canadell, J.G., Marland, G., Bopp, L., Ciais, P., Conway, T.J., Doney, S.C., Feely, R.A., Foster, P., Friedlingstein, P., Gurney, K., Houghton, R.A., House, J.I., Huntingford, C., Levy, P.E., Lomas, M.R., Majkut, J., Metz, N., Ometto, J.P., Peters, G.P., Prentice, I.C., Randerson, J.T., Running, S.W., Sarmiento, J.L., Schuster, U., Sitch, S., Takahashi, T., Viovy, N., van der Werf, G.R. & Woodward, F.I. 2009. 'Trends in the sources and sinks of carbon dioxide', *Nature Geoscience*, vol. 2, pp. 831-836.
- Ling, F.L.N., Gupta, V., Willis, M., Bennett, J.C., Robinson, K.A., Paudel, K., Post, D.A. & Marvanek, S. 2009. CSIRO Water for a Healthy Country Flagship, Australia <http://www.csiro.au/partnerships/TasSY.html>
- Long, S.P., Ainsworth, E.A., Rogers, A. & Ort, D.R. 2004. 'Global atmospheric carbon dioxide: Plants FACE the future', *Annual Review Plant Biology*, vol. 55, pp. 591-628.

- Long, S.P., Ainsworth, E.A., Leakey, A.D.B. & Morgan, P.B. 2005. 'Global food insecurity. Treatment of major food crops with elevated carbon dioxide or ozone under large-scale fully open-air conditions suggests recent models may have overestimated future yields', *Philosophical Transactions of the Royal Society*, vol. 360, pp. 2011-2020.
- Lovett, J.V. & Scott, J.M. 1997. *Pasture production and management*, Inkata Press, Melbourne, Victoria.
- Ludwig, F. & Asseng, S. 2006. 'Climate change impacts on wheat production in a Mediterranean environment in Western Australia', *Agricultural Systems*, vol. 90, pp. 159-179.
- Ludwig, F., Milroy, S.P. & Asseng, S. 2009. 'Impacts of recent climate change on wheat production systems in Western Australia', *Climatic Change*, vol. 92, pp. 495-517.
- Luo, Q., Bellotti, W., Williams, M. & Bryan, B. 2005. 'Potential impact of climate change on wheat yield in South Australia', *Agricultural and Forest Meteorology*, vol. 132, pp. 273-285.
- MacDonald, K.A., Penno, J.W., Lancaster, J.A.S. & Roche, J.R. 2008. 'Effect of stocking rate on pasture production, milk production and reproduction of dairy cows in pasture based systems', *Journal of Dairy Science*, vol. 91, pp. 2151-2163.
- MacDonald, K.A., Glassey, C.B. & Rawnsley, R.P. 2010. 'The emergence, development and effectiveness of decision rules for pasture based dairy systems', *Proceedings of the 4<sup>th</sup> Australasian Dairy Science Symposium*, pp. 199-209.
- McInnes, K.L., Bathols, J., Page, C., Suppiah, R. & Whetton, P.H. 2004. *Climate change in Tasmania*, Draft Report, Climate Impact Group, CSIRO Atmospheric Research.
- McIntosh, P., Pook, M. & McGregor, J. 2005. *Study of future and current climate: A scenario for the Tasmanian region*, CSIRO Marine and Atmospheric Research.
- Meehl, G.A., Arblaster, J.M. & Tebaldi, C. 2005. 'Understanding future patterns of increased precipitation intensity in climate model simulations', *Geophysical Research Letters*, vol 32, L18719.
- Meneghini, B., Simmonds, I. & Smith I. N. 2007. 'Association between Australian rainfall and the Southern Annular Mode', *International Journal of Climatology*, vol. 27, pp. 109-121.
- Mitchell, J.F.B. 2004. 'Can we believe predictions of climate change?', *Quarterly Journal of the Meteorological Society*, vol, 130, pp. 2341-2360.
- Mitchell, K.J. 1956. 'Growth of pasture species under controlled environment. 1. Growth at various levels of constant temperature', *New Zealand Journal of Scientific Technology*, vol. 38A, pp. 203-216.

- Mitscherlich, E.A. 1909. 'The law of the minimum and the law of diminishing soil productivity', *landwirtschaftliche Jahrbuecher*, vol. 43, pp. 49-216.
- Mitscherlich, E.A. 1913. Soil science for agriculture and forestry, 2<sup>nd</sup> edition, Verlag Paul Barry, Berlin.
- Monteith, J.L. 1965. 'Evaporation and the environment, the state and movement of living organisms', XIXth Symposium, Cambridge University Press, Swansea.
- Moore, A.D., Donnelly, J.R. & Freer, M. 1997. 'GRAZPLAN: Decision support model for Australian grazing enterprises. III. Pasture growth and soil submodels, and the GrassGro DSS', *Agricultural Systems* 55:535.
- Mpelasoka, F.S. & Chiew, F.H.S. 2008. 'Runoff projections sensitivity to rainfall scenario methodology', *International congress on Environmental Modelling and Software* 4<sup>th</sup> Biennial Meeting of iEMSSs, <http://www.iemss.org/iemss2008/index.php>
- Murphy, S.R., Lodge, G.M. & Harden S. 2004. 'Surface soil water dynamics in pastures in northern New South Wales. 2. Surface runoff'. *Australian Journal of Experimental Agriculture*, vol. 44, pp. 283-298.
- Murphy, B.F. & Timbal, B. 2008. 'A review of recent climate variability and climate change in southeastern Australia', *International Journal of Climatology*, vol. 28, pp. 859-879
- Nakicenovic, N & Swart, R. (eds) 2000. *Special Report on Emissions Scenarios. A special Report of Working Group III of the Intergovernmental Panel on Climate Change*. Cambridge University Press, Cambridge, United Kingdom and New York, NY, USA.
- Neal, J.S., Fulkerson, W.J. & Sutton, B.G. 2011. 'Differences in water-use efficiency among perennial forages used by the dairy industry under optimum and deficit irrigation', *Irrigation Science*, vol. 29, pp. 213-229.
- Nicholls, N. 2007. 'Detecting, understanding and attributing climate change', Department of the Environment and Water Resources: Australian Greenhouse Office, Canberra.
- Nie, Z.N., Chapman, D.F., Tharamaraj, J. & Clements, R. 2004. 'Effects of pasture species mixture, management and environment on the productivity and persistence of dairy pastures in south-west Victoria. 1. Herbage accumulation and seasonal growth pattern pattern', *Australian Journal of Agricultural Research*, vol. 55, pp. 625-636.
- Nijs, I., Impens, I. & Behaeghe, T. 1989. 'Leaf and Canopy responses of *Lolium perenne* to long-term elevated atmospheric carbon-dioxide concentration', *Planta*, vol. 177, pp. 312-320.
- Nijs, I. & Impens, I. 1996. 'Effects of elevated CO<sub>2</sub> concentration and climate-warming on photosynthesis during winter in *Lolium perenne*'. *Journal of Experimental Botany*, vol. 47, pp. 915-924.

- Nunez, M. 2004. 'Tasmanian water environments in the middle of the 21<sup>st</sup> century: results using the CCAM regional climate model' Department of Primary Industries, Water and Environment, Tasmania.
- Oke, A. M. C., Frost, A. J. & Beesley, C. A. 2009. 'The use of TRMM satellite data as a predictor in the spatial interpolation of daily precipitation over Australia', 18<sup>th</sup> World IMACS/MODSIM Congress, Cairns, Australia 13-17 July 2009.
- Panofsky, H.A. & Brier, G.W. 1968. '*Some applications of statistics to Meteorology*', University Park, Pennsylvania. Pennsylvania State University Press.
- Parry, M.L., Rosenzweig, A., Iglesias, A., Livermore, M. & Fischer, G. 2004. 'Effects of climate change on global food production under SRES emissions and socio-economic scenarios', *Global Environmental Change*, vol. 14, pp. 53-67.
- Peacock, J.M. 1974. 'Temperature and leaf growth in *Lolium perenne* 1. The thermal microclimate: its measurement and relation to crop growth', *Journal of Applied Ecology*, vol. 12, pp. 99-114.
- Perkins, S.E, Pitman, A.J., Holbrook, N.J. & McAneney, J. 2007. 'Evaluation of the AR4 Climate Models' Simulated Daily Maximum Temperature, Minimum Temperature and Precipitation over Australia using Probability Density functions', *Journal of Climate*, vol.20, pp. 4356-4376.
- Perkins, S.E. & Pitman, A.J. 2009. 'Do weak AR4 models bias projections of future climate changes over Australia?', *Climatic Change* vol. 93, pp. 527-558.
- Pessarakli, M. 1999, *Handbook of Plant and Crop Stress*, 2<sup>nd</sup> ed, Marcel Dekker inc. New York, USA.
- Petit,J.R., Jouzel, J., Raynaud, D., Barkov, N.I., Barnola, J.M, Basile, I. Benders, M., Chappellaz, J., Davis, M., Delaygue, G., Delmotte, M., Kotlyakov, V.M., Legrand, M., Lipenkov, V.Y., Lorius, C., Pepin, L., Ritz, C., Saltzman, E. & Stievenard, M. 1999. 'Climate and atmospheric history of the past 420,000 years from the Vostok ice core, Antarctica', *Nature*, vol. 339, pp. 429-436.
- Pittock, B. 2003. *Climate change: an Australian guide to the science and potential impacts*, Australian Greenhouse Office, Commonwealth of Australia, Canberra, ACT.
- Post, D.A., Chiew, F.H.S., Yang, A., Viney, N.R., Vaze, J. & Teng, J. 2009. 'The hydrological impact of daily versus seasonal scaling of rainfall in climate change studies', 18<sup>th</sup> World IMACS/MODSIM Congress Cairns, Australia 13-17 July 2009, <http://mssanz.org.au/modsim09>
- Preston, B.L. & Jones, R. 2008. 'A national assessment of the sensitivity of Australian runoff to climate change', *Atmospheric Science Letters*, vol. 9, pp. 202-208.

- Priestly, C.H.B. & Taylor, R.J. 1972. 'On the assessment of surface heat fluxes and evaporation using large-scale parameters', *Monthly Weather Review*, vol. 100, pp. 81-92.
- Purcell, J. & Currey, A. 2003. 'National program for sustainable irrigation. Gaining acceptance of water use efficiency framework, terms and definitions', Final report – Stage 2, AQC 1. National Program for Sustainable Irrigation, Canberra, ACT.
- Quiggin, J., Adamson, D., Chambers, S. & Schrobback, P. 2010. 'Climate change, uncertainty and adaptation: The case of irrigated agriculture in the Murray-Darling Basin in Australia', *Canadian Journal of Agricultural Economics*, vol. 58, pp. 531-554.
- Raisanen, J. 2002. 'CO<sub>2</sub> induced changes in interannual temperature and precipitation variability in 19 CMIP2 experiments', *Journal of Climate*, vol.15. pp. 2395-2411.
- Randall, D.A., Wood, R.A., Bony, S., Colman, R., Fichefet, T., Fyfe, J., Kattsov, V., Pitman, A., Shukla, J., Srinivasan, J., Stoffer, R.J., Sumi, A. & Taylor, K.E. 2007. *Climate models and their evaluation*, In *Climate Change 2007: The Physical Science Basis. Contribution of Working group 1 to the Fourth Assessment Report of the Intergovernmental Panel on Climate Change*, Cambridge University Press, Cambridge, United Kingdom and New York, NY, USA.
- Rawnsley, R.P., Donahy, D.J. & Stevens, D.R. 2008, 'What is limiting production and consumption of perennial ryegrass in temperate dairy regions of Australia and New Zealand?', Invited Review Paper. Tasmanian Institute of Agricultural Research, University of Tasmania, Burnie.
- Rawnsley, R.P., Cullen, B.R., Turner, L.R., Donahy, D.J., Freeman, M. & Christie, K.M. 2009. 'Potential deficit irrigation to increase marginal irrigation response of perennial Ryegrass (*Lolium perenne* L) on Tasmanian dairy farms', *Crop and Pasture Science*, Vol. 60, pp. 1156-1164.
- Rayner, D. P., Moodie, K. B., Beswick, A. R., Clarkson, N. M. & Hutchinson, R. L. 2004. 'New Australian daily historical climate surfaces using CLIMARC', Queensland Department of Natural Resources, Mines and Energy.
- Rayner, D.P. 2006. 'Wind run changes: the dominant factor affecting pan evaporation trends in Australia', *Journal of Climate*, vol. 20, pp. 3379-3394.
- Ricketts, J.H. & Page, C.M. 2007. 'A web based version of OzClim for exploring climate change impacts and risks in the Australian region', <http://www.csiro.au/ozclim/home>
- Risbey, J.S., Pook, M.J., McIntosh, P.C., Ummenhofer, C.C. & Meyers, G. 2008, 'Characteristics and variability of synoptic features associated with cool season rainfall in southeastern Australia', *International Journal of Climatology*, Published online, [www.interscience.wiley.com](http://www.interscience.wiley.com)

- Robertson, S.M. 2006. 'Predicting pasture and sheep production in the Victorian Mallee with the decision support tool, GrassGro', *Australian Journal of Experimental Agriculture*, vol. 46, pp. 1005-1014.
- Roderick, M.L. & Farquhar, G.D. 2004. 'Changes in Australian pan evaporation from 1970 – 2002'. *International Journal of Climatology*, vol. 24, pp. 1077-1090.
- Rogers, A., Fischer, B.U., Bryant, J., Frehner, M., Blum, H., Raines, C.A. & Long, S.P. 1998. 'Acclimation of photosynthesis to elevated CO<sub>2</sub> under low-nitrogen nutrition is affected by the capacity for assimilate utilization. Perennial ryegrass under Free-Air CO<sub>2</sub> enrichment', vol. 118, pp. 683-689.
- Romanova, A.K. 2005. 'Physiological and biochemical aspects and molecular mechanisms of plant adaptation to the elevated concentration of atmospheric CO<sub>2</sub>', *Russian Journal of Plant Physiology*, Vol. 52, pp. 112-126.
- Ryle, G.J.A., Powell, C.E. & Tewson, V. 1992. 'Effect of elevated CO<sub>2</sub> on the photosynthesis, respiration and growth of perennial ryegrass', *Journal of Experimental Botany*, vol.43, pp. 811-818.
- Salinger, M.J. 2005. 'Climate variability and change: past, present and future an overview', *Climatic Change*, vol. 70, pp. 9-29.
- Schapendonk, A.H.C.M., Dijkstra, P., Groenwold, J., Pot, C.S. & Van De Geijn, S.C. 1997. 'Carbon balance and water use efficiency of frequently cut *Lolium perenne* L. swards at elevated carbon dioxide', *Global Change Biology*, vol. 3, pp. 207-216.
- Schenk, U., Jager, H.J. & Weigel, H.J. 1997. 'The response of perennial ryegrass/white clover swards to elevated atmospheric CO<sub>2</sub> concentrations', *New Phytology*, vol.135, pp. 67-69.
- Shepherd, D.J. 1995, 'Some characteristics of Tasmanian rainfall', *Australian Meteorology Magazine*, vol. 44. pp. 261-274.
- Shuttleworth, W.J., Serrat-Capdevila, A., Roderick, M.L. & Scott, R.L. 2009. 'On the theory relating changes in area-average and pan evaporation'. *Quarterly Journal of the Royal Meteorological Society*. Vo. 135, pp. 1230 -1247.
- Smith, S.J, Thomson, A.M., Rosenberg, N.J., Izaurralde, R.C., Brown, R.A. & Wigley, T.M. 2005. 'Climate change impacts for the conterminous USA: an integrated assessment, Part 1. Scenarios and context', *Climatic change*, vol. 69, pp. 7-25.
- Soussana, J.F., Casella, E. & Loiseau, P. 1996. 'Long-term effects of CO<sub>2</sub> enrichment and temperature increase on a temperate grass sward. II. Plant nitrogen budgets and root fraction', *Plant and Soil*, vol. 182, pp. 101-114.

- Soussana, J.F., Graux, A.I. & Tubiello, F.N. 2010. 'Improving the use of modelling for projections of climate change impacts on crops and pastures', *Journal of Experimental Botany*, vol. 61, pp. 2217-2228.
- Steel, R.D.G. & Torrie, J.H. 1960, Principles and Procedures in Statistics, New York: McGraw-Hill Book Co.
- Suppiah, R. 2004. 'Trends in the Southern Oscillation phenomenon and Australian rainfall and changes in their relationship', *International Journal of Climatology*, vol. 24, pp. 269-290.
- Suppiah, R., Hennessey, K.J., Whetton, P.H., McInnes, K., Macadam, I., Bathols, J., Ricketts, J. & Page, C.M. 2007. 'Australian climate change projections derived from simulations performed for the IPCC 4<sup>th</sup> Assessment Report', *Australian Meteorological Magazine*, vol. 56, pp. 131-152.
- Suter, D., Nosberger, J. & Luscher, A. 2001. 'Response of perennial ryegrass to free-air CO<sub>2</sub> enrichment (FACE) is related to the dynamics of sward structure during regrowth', *Crop Science*, vol.41, pp. 810-817.
- Taschetto, A.S. & England, M.H. 2009. 'An analysis of late twentieth century trends in Australian rainfall'. *International Journal of Climatology*, vol. 29, pp.791-807.
- Thomas, H. & Norris, I.B. 1979. 'Winter growth of contrasting ryegrass varieties at two altitudes in mid-Wales', *Journal of Applied Ecology*, vol. 16, pp. 553-565.
- Thomson, A.M., Brown, R.A., Ghan, S.J., Izaurralde, R.C., Rosenberg, N.J. & Leung, L.R. 2002. 'Elevation dependence of winter wheat production in eastern Washington state with climate change: a methodological study', *Climatic change*, vol. 54, pp. 141-164.
- Thomson, A.M., Brown, R.A., Rosenberg, N.J., Izaurralde, R.C. & Benson, V. 2005. 'Climate change impacts for the conterminous USA: an integrated assessment, Part 3. Dryland production of grain and forage crops', *Climatic change*, vol. 69, pp. 43-65.
- Trenberth, k. & Hoar, T.J. 1997. 'El Nino and climate change', *Geophysical Research Letters*, vol. 24, pp. 3057-3060.
- Turner, N.C. & Asseng, S. 2005. 'Productivity, sustainability and rainfall-use efficiency in Australian rainfed Mediterranean agricultural systems', *Australian journal of Experimental Research*, vol. 56, pp. 1123-1136.
- Ummerhofer, C.C., England, M.H., McIntosh, P.C., Meyers, G.A., Pook, M.J., Risbey, J.S., Sen Gupta, A. & Taschetto, A.S. 2009. 'What causes Australia's worst droughts?', *Geophysical Research letters*, vol. 36, L04706.
- Van Brecht, T. 2011. Personal Communication.

- Vaze, J. & Tang, J. 2011. 'Future climate and runoff projections across New South Wales, Australia: results and practical applications', *Hydrological Processes*, vol. 25, pp.18 – 35.
- Viney, N.R., Perraud, J., Vaze, J., Chiew, F.H.S., Post, D.A. & Yang, A. 2009. 'The usefulness of bias constraints in model calibration for regionalization to ungauged catchments', 18<sup>th</sup> World IMACS/MODSIM Congress, Cairns, Australia 13-17 July 2009. <http://mssanz.org.au/modsim09>
- Von Liebig, J. 1855. *The basics of agricultural chemistry with reference to the experiments conducted in England*. Vieweg and Sohn, Braunschweig, Germany.
- Wang, J., Wang, E. & Liu, D.L. 2010. 'Modelling the impacts of climate change on wheat yield and field water balance over the Murray-Darling Basin in Australia', *Theoretically Applied Climatology*, vol. 104, pp. 285-300.
- Wastney, M.E., Palliser, C.C., Lile, J.A., MacDonald, K.A., Penno, J.W. & Bright, K.P. 2002. 'A whole-farm model applied to a dairy system', *Proceedings of the New Zealand Society of Animal Production*, vol. 62, pp. 120-123.
- Waller, R.A. & Sale, P.W.G. 2001. 'Persistence and productivity of perennial ryegrass in sheep pastures in south-western Victoria: a review', *Australian Journal of Experimental Agriculture*, vol. 41, pp. 117-144.
- White, J. & Hodgson, J. 1999. *New Zealand Pasture and Crop Science*, Oxford University Press, Auckland, New Zealand.
- White, T.A., Johnson, I.R. & Snow, V.O. 2008. 'Comparison of outputs of a biophysical simulation model for pasture growth and composition with measured data under dryland and irrigated conditions in New Zealand', *Grass and Forage Science*, vol. 63, pp. 339-349.
- White, C.J., Sanabria, L.A., Grose, M.R., Corney, S.P., Bennett, J.C., Holz, G.K., McInnes, K.L., Cechet, R.P., Gaynor, S.M. & Bindoff, N.F. 2010. *Climate Futures for Tasmania: extreme events technical report*, Antarctic Climate and Ecosystems Cooperative Research Centre, Hobart, Tasmania.
- Willmott, C. J. & Johnson, M. L. 2005. 'Resolution errors associated with gridded precipitation fields', *International Journal of Climatology*, vol. 25, pp. 1957-1963.
- Zhang, B., Valentine, I. & Kemp, P.D. 2007. 'Spatially explicit modeling of the impact of climate changes on pasture production in the North Island, New Zealand', *Climatic Change*, vol.84. pp. 203-216.
- Ziska, L.H. & Bunce, J.A. 2007. 'Predicting the impact of changing CO<sub>2</sub> on crop yields: some thoughts on food', *New Phytologist*, vol. 175, pp. 607-618.

## Appendix 1.0

Mean monthly maximum temperature from the data sources of AWAP 0.1, AWAP 0.05, PP and DD for the period 1971 to 2007, for the sites of Woolnorth, Flowerdale, Merseylea, Cressy, Ringarooma and Ouse.

**Appendix 1.1** Mean monthly maximum temperature (°C) at Woolnorth from the data sources of AWAP 0.1, AWAP 0.05, PP and DD for the period 1971 to 2007.

	Jan	Feb	Mar	Apr	May	Jun	Jul	Aug	Sep	Oct	Nov	Dec
AWAP 0.1	20.35 <sup>ab</sup>	20.98 <sup>ab</sup>	19.73 <sup>ab</sup>	17.46	15.24 <sup>ab</sup>	13.36 <sup>ab</sup>	12.71 <sup>b</sup>	13.19 <sup>ab</sup>	14.22 <sup>a</sup>	15.63 <sup>a</sup>	17.11 <sup>a</sup>	18.68 <sup>ab</sup>
AWAP 0.05	20.45 <sup>a</sup>	21.07 <sup>ab</sup>	19.83 <sup>ab</sup>	17.56	15.34 <sup>ab</sup>	13.46 <sup>ab</sup>	12.82 <sup>ab</sup>	13.29 <sup>a</sup>	14.33 <sup>a</sup>	15.73 <sup>a</sup>	17.21 <sup>a</sup>	18.78 <sup>a</sup>
PP	19.93 <sup>b</sup>	20.69 <sup>b</sup>	19.39 <sup>b</sup>	17.14	15.12 <sup>b</sup>	13.20 <sup>b</sup>	12.68 <sup>b</sup>	13.03 <sup>b</sup>	13.92 <sup>b</sup>	15.12 <sup>b</sup>	16.66 <sup>b</sup>	18.26 <sup>b</sup>
DD	20.53 <sup>a</sup>	21.24 <sup>a</sup>	19.87 <sup>a</sup>	17.53	15.46 <sup>a</sup>	13.49 <sup>a</sup>	13.00 <sup>a</sup>	13.42 <sup>a</sup>	14.38 <sup>a</sup>	15.65 <sup>a</sup>	17.25 <sup>a</sup>	18.86 <sup>a</sup>
LSD ( $P = 0.05$ )	0.52	0.44	0.46	ns	0.31	0.28	0.24	0.26	0.29	0.24	0.41	0.45

Means with differing subscripts next to values indicate a significant difference at  $P < 0.05$ .

**Appendix 1.2** Mean monthly maximum temperature (°C) at Flowerdale from the data sources of AWAP 0.1, AWAP 0.05, PP and DD for the period 1971 to 2007.

	Jan	Feb	Mar	Apr	May	Jun	Jul	Aug	Sep	Oct	Nov	Dec
AWAP 0.1	20.61	21.12	19.62	17.10	14.66	12.49 <sup>b</sup>	11.88 <sup>b</sup>	12.38 <sup>b</sup>	13.80	15.60 <sup>b</sup>	17.58	19.11
AWAP 0.05	20.85	21.36	19.89	17.38	14.93	12.79 <sup>a</sup>	12.19 <sup>a</sup>	12.67 <sup>a</sup>	14.09	15.86 <sup>a</sup>	17.85	19.36
PP	20.90	21.32	19.81	17.29	14.88	12.80 <sup>a</sup>	12.22 <sup>a</sup>	12.77 <sup>a</sup>	14.04	15.77 <sup>ab</sup>	17.72	19.34
DD	20.90	21.32	19.81	17.29	14.88	12.80 <sup>a</sup>	12.22 <sup>a</sup>	12.77 <sup>a</sup>	14.04	15.77 <sup>ab</sup>	17.72	19.34
LSD ( $P = 0.05$ )	ns	ns	ns	ns	ns	0.18	0.24	0.28	ns	0.26	ns	ns

Means with differing subscripts next to values indicate a significant difference at  $P < 0.05$ .

**Appendix 1.3** Mean monthly maximum temperature (°C) at Merseylea from the data sources of AWAP 0.1, AWAP 0.05, PP and DD for the period 1971 to 2007.

	Jan	Feb	Mar	Apr	May	Jun	Jul	Aug	Sep	Oct	Nov	Dec
AWAP 0.1	21.72	22.27	20.58	17.93 <sup>a</sup>	15.09 <sup>a</sup>	12.63 <sup>a</sup>	11.98 <sup>a</sup>	12.81 <sup>a</sup>	14.41 <sup>a</sup>	16.22 <sup>a</sup>	18.36 <sup>a</sup>	19.99
AWAP 0.05	21.65	22.19	20.48	17.81 <sup>ab</sup>	14.97 <sup>a</sup>	12.50 <sup>ab</sup>	11.86	12.67 <sup>a</sup>	14.29 <sup>a</sup>	16.12 <sup>a</sup>	18.27 <sup>ab</sup>	19.90
PP	21.75	22.15	20.50	17.70 <sup>ab</sup>	14.93 <sup>a</sup>	12.64 <sup>a</sup>	12.02 <sup>a</sup>	12.76 <sup>a</sup>	14.22 <sup>a</sup>	16.10 <sup>a</sup>	18.24 <sup>ab</sup>	20.09
DD	21.44	21.92	20.27	17.42 <sup>b</sup>	14.61 <sup>b</sup>	12.27 <sup>b</sup>	11.64 <sup>b</sup>	12.37 <sup>b</sup>	13.83 <sup>b</sup>	15.75 <sup>b</sup>	17.90 <sup>b</sup>	19.76
LSD ( $P = 0.05$ )	ns	ns	ns	0.45	0.28	0.30	0.24	0.27	0.34	0.29	0.46	ns

Means with differing subscripts next to values indicate a significant difference at  $P < 0.05$ .

**Appendix 1.4** Mean monthly maximum temperature (°C) at Cressy from the data sources of AWAP 0.1, AWAP 0.05, PP and DD for the period 1971 to 2007.

	Jan	Feb	Mar	Apr	May	Jun	Jul	Aug	Sep	Oct	Nov	Dec
AWAP 0.1	23.55	23.89	21.46	18.04	14.71	11.73	11.31	12.56	14.69	16.92	19.49	21.45
AWAP 0.05	23.58	23.90	21.47	18.05	14.71	11.73	11.31	12.55	14.69	16.91	19.50	21.46
PP	23.68	24.03	21.68	17.97	14.58	11.73	11.36	12.50	14.50	16.85	19.41	21.82
DD	23.33	23.74	21.46	17.81	14.48	11.72	11.27	12.37	14.31	16.64	19.17	21.49
LSD ( $P = 0.05$ )	ns											

Means with differing subscripts next to values indicate a significant difference at  $P < 0.05$ .

**Appendix 1.5** Mean monthly maximum temperature (°C) at Ringarooma from the data sources of AWAP 0.1, AWAP 0.05, PP and DD for the period 1971 to 2007.

	Jan	Feb	Mar	Apr	May	Jun	Jul	Aug	Sep	Oct	Nov	Dec
AWAP 0.1	21.76	22.11	20.39 <sup>ab</sup>	17.28 <sup>ab</sup>	14.38 <sup>a</sup>	11.99 <sup>a</sup>	11.35 <sup>a</sup>	12.08 <sup>a</sup>	13.70 <sup>ab</sup>	15.84 <sup>ab</sup>	17.90 <sup>ab</sup>	19.91
AWAP 0.05	21.96	22.30	20.59 <sup>a</sup>	17.49 <sup>a</sup>	14.59 <sup>a</sup>	12.21 <sup>a</sup>	11.57 <sup>a</sup>	12.32 <sup>a</sup>	13.94 <sup>a</sup>	16.06 <sup>a</sup>	18.10 <sup>ab</sup>	20.12
PP	21.97	22.34	20.55 <sup>a</sup>	17.43 <sup>a</sup>	14.59 <sup>a</sup>	12.09 <sup>a</sup>	11.49 <sup>a</sup>	12.30 <sup>a</sup>	14.00 <sup>a</sup>	16.11 <sup>a</sup>	18.28 <sup>a</sup>	20.30
DD	21.51	21.93	20.09 <sup>b</sup>	16.88 <sup>b</sup>	14.02 <sup>b</sup>	11.52 <sup>b</sup>	10.90 <sup>b</sup>	11.66 <sup>b</sup>	13.38 <sup>b</sup>	15.54 <sup>b</sup>	17.77 <sup>b</sup>	19.81
LSD ( $P = 0.05$ )	ns	ns	0.45	0.44	0.29	0.31	0.27	0.32	0.38	0.37	0.47	ns

Means with differing subscripts next to values indicate a significant difference at  $P < 0.05$ .

**Appendix 1.6** Mean monthly maximum temperature (°C) at Ouse from the data sources of AWAP 0.1, AWAP 0.05, PP and DD for the period 1971 to 2007.

	Jan	Feb	Mar	Apr	May	Jun	Jul	Aug	Sep	Oct	Nov	Dec
AWAP 0.1	22.64	23.23	20.55	17.02	13.78 <sup>b</sup>	10.75 <sup>b</sup>	10.57 <sup>b</sup>	12.13 <sup>b</sup>	14.14 <sup>b</sup>	16.47 <sup>b</sup>	18.99	20.86
AWAP 0.05	23.08	23.64	20.99	17.48	14.24 <sup>a</sup>	11.14 <sup>a</sup>	11.01 <sup>a</sup>	12.63 <sup>a</sup>	14.63 <sup>ab</sup>	16.94 <sup>a</sup>	19.41	21.30
PP	23.40	23.76	21.07	17.52	14.24 <sup>a</sup>	11.39 <sup>a</sup>	11.18 <sup>a</sup>	12.73 <sup>a</sup>	14.72 <sup>a</sup>	16.95 <sup>a</sup>	19.46	21.50
DD	23.40	23.76	21.07	17.52	14.24 <sup>a</sup>	11.39 <sup>a</sup>	11.18 <sup>a</sup>	12.73 <sup>a</sup>	14.72 <sup>a</sup>	16.95 <sup>a</sup>	19.46	21.50
LSD ( $P = 0.05$ )	ns	ns	ns	ns	0.38	0.39	0.33	0.43	0.52	0.43	ns	ns

Means with differing subscripts next to values indicate a significant difference at  $P < 0.05$ .

## Appendix 2.0

Mean monthly minimum temperature from the data sources of AWAP 0.1, AWAP 0.05, PP and DD for the period 1971 to 2007, for the sites of Woolnorth, Flowerdale, Merseylea, Cressy, Ringarooma and Ouse.

**Appendix 2.1** Mean monthly minimum temperature (°C) at Woolnorth from the data sources of AWAP 0.1, AWAP 0.05, PP and DD for the period 1971 to 2007.

	Jan	Feb	Mar	Apr	May	Jun	Jul	Aug	Sep	Oct	Nov	Dec
AWAP 0.1	12.47	12.87	12.03	10.53	9.10	7.29	6.53 <sup>b</sup>	7.05	7.61	8.42	9.74	11.17
AWAP 0.05	12.47	12.87	12.01	10.51	9.08	7.30	6.57 <sup>b</sup>	7.08	7.62	8.45	9.74	11.17
PP	12.42	12.93	12.09	10.60	9.41	7.64	6.97 <sup>a</sup>	7.28	7.76	8.48	9.71	11.09
DD	12.38	12.87	11.92	10.35	9.13	7.30	6.62 <sup>ab</sup>	7.01	7.60	8.38	9.62	11.05
LSD ( $P = 0.05$ )	ns	ns	ns	ns	ns	ns	0.40	ns	ns	ns	ns	ns

Means with differing subscripts next to values indicate a significant difference at  $P < 0.05$ .

**Appendix 2.2** Mean monthly minimum temperature (°C) at Flowerdale from the data sources of AWAP 0.1, AWAP 0.05, PP and DD for the period 1971 to 2007.

	Jan	Feb	Mar	Apr	May	Jun	Jul	Aug	Sep	Oct	Nov	Dec
AWAP 0.1	11.56	12.00	10.90	9.04	7.34	5.35	4.73	5.15	6.00	7.12	8.93	10.31
AWAP 0.05	11.72	12.13	11.01	9.12	7.35	5.37	4.75	5.24	6.12	7.26	9.09	10.47
PP	11.65	12.04	10.61	8.65	7.09	5.17	4.58	5.00	5.89	6.98	8.70	10.10
DD	11.65	12.04	10.61	8.64	7.09	5.10	4.47	4.95	5.88	6.97	8.70	10.10
LSD ( $P = 0.05$ )	ns	ns	ns	ns	ns	ns	ns	ns	ns	ns	ns	ns

Means with differing subscripts next to values indicate a significant difference at  $P < 0.05$ .

**Appendix 2.3** Mean monthly minimum temperature (°C) at Merseylea from the data sources of AWAP 0.1, AWAP 0.05, PP and DD for the period 1971 to 2007.

	Jan	Feb	Mar	Apr	May	Jun	Jul	Aug	Sep	Oct	Nov	Dec
AWAP 0.1	11.38	11.61	10.03	7.97	5.88	3.75 <sup>ab</sup>	3.13 <sup>b</sup>	4.03	5.37	6.74	8.64	10.13
AWAP 0.05	11.26	11.49	9.89	7.84	5.77	3.65 <sup>b</sup>	3.05 <sup>b</sup>	3.92	5.25	6.62	8.51	10.01
PP	11.45	11.65	10.10	7.94	6.11	4.15 <sup>a</sup>	3.73 <sup>a</sup>	4.24	5.39	6.66	8.47	10.01
DD	11.29	11.51	9.97	7.84	6.00	3.83 <sup>ab</sup>	3.38 <sup>ab</sup>	4.04	5.24	6.52	8.31	9.83
LSD ( $P = 0.05$ )	ns	ns	ns	ns	ns	0.46	0.42	ns	ns	ns	ns	ns

Means with differing subscripts next to values indicate a significant difference at  $P < 0.05$ .

**Appendix 2.4** Mean monthly minimum temperature (°C) at Cressy from the data sources of AWAP 0.1, AWAP 0.05, PP and DD for the period 1971 to 2007.

	Jan	Feb	Mar	Apr	May	Jun	Jul	Aug	Sep	Oct	Nov	Dec
AWAP 0.1	10.25	10.34	8.60	6.24	3.91 <sup>b</sup>	1.89 <sup>b</sup>	1.34 <sup>c</sup>	2.49 <sup>b</sup>	4.11	5.48	7.52	9.04
AWAP 0.05	10.21	10.30	8.56	6.18	3.86 <sup>b</sup>	1.85 <sup>b</sup>	1.31 <sup>c</sup>	2.45 <sup>b</sup>	4.06	5.44	7.47	8.98
PP	10.14	10.18	8.39	6.20	4.58 <sup>a</sup>	3.40 <sup>a</sup>	3.11 <sup>a</sup>	3.37 <sup>a</sup>	4.27	5.39	7.17	8.73
DD	10.41	10.51	8.73	6.44	4.35 <sup>ab</sup>	2.15 <sup>b</sup>	1.78 <sup>b</sup>	2.69 <sup>b</sup>	4.19	5.58	7.40	9.00
LSD ( $P = 0.05$ )	ns	ns	ns	ns	0.58	0.44	0.42	0.30	ns	ns	ns	ns

Means with differing subscripts next to values indicate a significant difference at  $P < 0.05$ .

**Appendix 2.5** Mean monthly minimum temperature (°C) at Merseylea from the data sources of AWAP 0.1, AWAP 0.05, PP and DD for the period 1971 to 2007.

	Jan	Feb	Mar	Apr	May	Jun	Jul	Aug	Sep	Oct	Nov	Dec
AWAP 0.1	10.92 <sup>ab</sup>	11.34 <sup>ab</sup>	9.67	7.60	5.45	3.52 <sup>b</sup>	2.77 <sup>b</sup>	3.49 <sup>b</sup>	4.63	5.92 <sup>ab</sup>	7.84	9.49 <sup>a</sup>
AWAP 0.05	11.03 <sup>a</sup>	11.43 <sup>a</sup>	9.78	7.71	5.56	3.61 <sup>ab</sup>	2.87 <sup>b</sup>	3.59 <sup>ab</sup>	4.74	6.04 <sup>ab</sup>	7.95	9.60 <sup>a</sup>
PP	10.85 <sup>ab</sup>	11.17 <sup>ab</sup>	9.72	7.67	5.80	3.92 <sup>a</sup>	3.40 <sup>a</sup>	3.81 <sup>a</sup>	4.91	6.08 <sup>a</sup>	7.94	9.43 <sup>ab</sup>
DD	10.49 <sup>b</sup>	10.83 <sup>b</sup>	9.42	7.41	5.57	3.61 <sup>ab</sup>	2.97 <sup>ab</sup>	3.46 <sup>b</sup>	4.58	5.75 <sup>b</sup>	7.57	9.05 <sup>b</sup>
LSD ( $P = 0.05$ )	0.47	0.52	ns	ns	ns	0.40	0.45	0.30	ns	0.32	ns	0.39

Means with differing subscripts next to values indicate a significant difference at  $P < 0.05$ .

**Appendix 2.6** Mean monthly minimum temperature (°C) at Ouse from the data sources of AWAP 0.1, AWAP 0.05, PP and DD for the period 1971 to 2007.

	Jan	Feb	Mar	Apr	May	Jun	Jul	Aug	Sep	Oct	Nov	Dec
AWAP 0.1	9.20 <sup>b</sup>	9.05 <sup>b</sup>	7.49 <sup>b</sup>	5.68	3.59 <sup>c</sup>	1.61 <sup>b</sup>	1.07 <sup>c</sup>	1.95 <sup>b</sup>	3.43 <sup>b</sup>	5.07 <sup>b</sup>	6.73	8.28
AWAP 0.05	9.51 <sup>ab</sup>	9.34 <sup>ab</sup>	7.77 <sup>ab</sup>	5.88	3.75 <sup>bc</sup>	1.77 <sup>b</sup>	1.22 <sup>bc</sup>	2.16 <sup>b</sup>	3.69 <sup>ab</sup>	5.36 <sup>ab</sup>	7.03	8.60
PP	9.77 <sup>a</sup>	9.63 <sup>a</sup>	8.01 <sup>a</sup>	6.05	4.38 <sup>a</sup>	2.97 <sup>a</sup>	2.59 <sup>a</sup>	2.91 <sup>a</sup>	4.04 <sup>a</sup>	5.45 <sup>a</sup>	7.07	8.60
DD	9.77 <sup>a</sup>	9.63 <sup>a</sup>	8.01 <sup>a</sup>	5.96	4.13 <sup>ab</sup>	1.90 <sup>b</sup>	1.47 <sup>b</sup>	2.25 <sup>b</sup>	3.84 <sup>a</sup>	5.40 <sup>a</sup>	7.05	8.59
LSD ( $P = 0.05$ )	0.40	0.54	0.40	ns	0.49	0.46	0.34	0.36	0.41	0.30	ns	ns

Means with differing subscripts next to values indicate a significant difference at  $P < 0.05$ .

### Appendix 3.0

Mean monthly rainfall from the data sources of AWAP 0.1, AWAP 0.05, PP and DD for the period 1971 to 2007, for the sites of Woolnorth, Flowerdale, Merseylea, Cressy, Ringarooma and Ouse.

#### Appendix 3.1 Mean monthly rainfall (mm) at Woolnorth from the data sources of AWAP 0.1, AWAP 0.05, PP and DD for the period 1971 to 2007.

	Jan	Feb	Mar	Apr	May	Jun	Jul	Aug	Sep	Oct	Nov	Dec
AWAP 0.1	48	40	60	85	99	124	128	119	104	86	65	66
AWAP 0.05	46	40	59	83	101	113	130	115	103	85	64	61
PP	43	37	55	74	91	106	121	113	95	79	62	57
DD	48	41	61	84	102	118	134	125	106	89	68	63
LSD ( $P = 0.05$ )	ns											

Means with differing subscripts next to values indicate a significant difference at  $P < 0.05$ .

#### Appendix 3.2 Mean monthly rainfall (mm) at Flowerdale from the data sources of AWAP 0.1, AWAP 0.05, PP and DD for the period 1971 to 2007.

	Jan	Feb	Mar	Apr	May	Jun	Jul	Aug	Sep	Oct	Nov	Dec
AWAP 0.1	59	42	56	92	111	124	142	141	133	103	77	79
AWAP 0.05	59	42	58	96	123	129	151	138	128	106	78	80
PP	60	43	58	95	122	131	151	138	126	102	78	79
DD	59	42	58	92	119	128	149	136	125	105	77	78
LSD ( $P = 0.05$ )	ns											

Means with differing subscripts next to values indicate a significant difference at  $P < 0.05$ .

#### Appendix 3.3 Mean monthly rainfall (mm) at Merseylea from the data sources of AWAP 0.1, AWAP 0.05, PP and DD for the period 1971 to 2007.

	Jan	Feb	Mar	Apr	May	Jun	Jul	Aug	Sep	Oct	Nov	Dec
AWAP 0.1	53	35	50	71	88	99	111	106	90	75	62	60
AWAP 0.05	55	37	53	75	96	107	119	118	94	80	67	65
PP	60	39	56	73	101	115	134	127	108	87	73	65
DD	54	36	50	72	90	109	126	113	95	80	64	59
LSD ( $P = 0.05$ )	ns											

Means with differing subscripts next to values indicate a significant difference at  $P < 0.05$ .

#### Appendix 3.4 Mean monthly rainfall (mm) at Cressy from the data sources of AWAP 0.1, AWAP 0.05, PP and DD for the period 1971 to 2007.

	Jan	Feb	Mar	Apr	May	Jun	Jul	Aug	Sep	Oct	Nov	Dec
AWAP 0.1	51	31	43	58	70	74 <sup>a</sup>	84 <sup>a</sup>	89 <sup>a</sup>	76	63	56	55
AWAP 0.05	53	32	44	60	71	73 <sup>a</sup>	84 <sup>a</sup>	88 <sup>a</sup>	78	63	57	56
PP	46	28	41	48	54	54 <sup>b</sup>	63 <sup>b</sup>	69 <sup>b</sup>	66	53	49	49
DD	52	30	43	56	68	67 <sup>ab</sup>	81 <sup>a</sup>	86 <sup>ab</sup>	75	61	55	52
LSD ( $P = 0.05$ )	ns	ns	ns	ns	ns	13	18	19	ns	ns	ns	ns

Means with differing subscripts next to values indicate a significant difference at  $P < 0.05$ .

**Appendix 3.5** Mean monthly rainfall (mm) at Ringarooma from the data sources of AWAP 0.1, AWAP 0.05, PP and DD for the period 1971 to 2007.

	Jan	Feb	Mar	Apr	May	Jun	Jul	Aug	Sep	Oct	Nov	Dec
AWAP 0.1	66	44	61	91	114	112	132	136	111	95	82	75
AWAP 0.05	72	47	61	96	128	126	146	152	120	110	87	84
PP	72	45	59	93	121	120	143	144	123	106	84	79
DD	70	45	61	96	120	120	146	144	116	109	86	79
LSD ( $P = 0.05$ )	ns											

Means with differing subscripts next to values indicate a significant difference at  $P < 0.05$ .

**Appendix 3.6** Mean monthly rainfall (mm) at Ouse from the data sources of AWAP 0.1, AWAP 0.05, PP and DD for the period 1971 to 2007.

	Jan	Feb	Mar	Apr	May	Jun	Jul	Aug	Sep	Oct	Nov	Dec
AWAP 0.1	46 <sup>ab</sup>	33	46 <sup>a</sup>	59 <sup>a</sup>	58 <sup>a</sup>	62 <sup>a</sup>	76 <sup>a</sup>	70 <sup>a</sup>	79 <sup>a</sup>	83 <sup>a</sup>	61 <sup>ab</sup>	64 <sup>a</sup>
AWAP 0.05	51 <sup>a</sup>	36	43 <sup>ab</sup>	59 <sup>a</sup>	53 <sup>ab</sup>	63 <sup>a</sup>	72 <sup>a</sup>	77 <sup>a</sup>	73 <sup>ab</sup>	84 <sup>a</sup>	65 <sup>a</sup>	61 <sup>a</sup>
PP	38 <sup>b</sup>	27	34 <sup>b</sup>	42 <sup>b</sup>	42 <sup>b</sup>	42 <sup>b</sup>	53 <sup>b</sup>	58 <sup>b</sup>	58 <sup>b</sup>	62 <sup>b</sup>	50 <sup>b</sup>	44 <sup>b</sup>
DD	39 <sup>b</sup>	28	34 <sup>b</sup>	43 <sup>b</sup>	44 <sup>ab</sup>	44 <sup>b</sup>	54 <sup>b</sup>	59 <sup>b</sup>	60 <sup>b</sup>	63 <sup>b</sup>	50 <sup>b</sup>	46 <sup>b</sup>
LSD ( $P = 0.05$ )	11	ns	11	11	15	14	17	16	17	19	15	14

Means with differing subscripts next to values indicate a significant difference at  $P < 0.05$ .

**Appendix 4.0**

Mean monthly potential evaporation from the data sources of AWAP 0.1, AWAP 0.05, PP and DD for the period 1971 to 2007, for the sites of Woolnorth, Flowerdale, Merseylea, Cressy, Ringarooma and Ouse.

**Appendix 4.1** Mean monthly potential evaporation (mm) at Woolnorth from the data sources of AWAP 0.1, AWAP 0.05, PP and DD for the period 1971 to 2007.

	Jan	Feb	Mar	Apr	May	Jun	Jul	Aug	Sep	Oct	Nov	Dec
AWAP 0.1	153 <sup>ab</sup>	123 <sup>b</sup>	92 <sup>b</sup>	47 <sup>b</sup>	23 <sup>b</sup>	12 <sup>b</sup>	17 <sup>b</sup>	35 <sup>b</sup>	62 <sup>b</sup>	101 <sup>a</sup>	127 <sup>a</sup>	154 <sup>a</sup>
AWAP 0.05	154 <sup>b</sup>	123 <sup>b</sup>	92 <sup>b</sup>	47 <sup>b</sup>	23 <sup>b</sup>	12 <sup>b</sup>	17 <sup>b</sup>	35 <sup>b</sup>	62 <sup>b</sup>	101 <sup>a</sup>	127 <sup>a</sup>	154 <sup>a</sup>
PP	158 <sup>ab</sup>	134 <sup>a</sup>	108 <sup>a</sup>	68 <sup>a</sup>	47 <sup>a</sup>	36 <sup>a</sup>	41 <sup>a</sup>	53 <sup>a</sup>	69 <sup>a</sup>	97 <sup>b</sup>	119 <sup>b</sup>	147 <sup>b</sup>
DD	160 <sup>a</sup>	135 <sup>a</sup>	109 <sup>a</sup>	69 <sup>a</sup>	48 <sup>a</sup>	37 <sup>a</sup>	42 <sup>a</sup>	54 <sup>a</sup>	70 <sup>a</sup>	98 <sup>b</sup>	121 <sup>b</sup>	148
LSD ( $P = 0.05$ )	6	6	4	3	2	2	2	2	3	3	4	7

Means with differing subscripts next to values indicate a significant difference at  $P < 0.05$ .

**Appendix 4.2** Mean monthly potential evaporation (mm) at Flowerdale from the data sources of AWAP 0.1, AWAP 0.05, PP and DD for the period 1971 to 2007.

	Jan	Feb	Mar	Apr	May	Jun	Jul	Aug	Sep	Oct	Nov	Dec
AWAP 0.1	158	124 <sup>b</sup>	97 <sup>b</sup>	49 <sup>b</sup>	24 <sup>b</sup>	12 <sup>b</sup>	16 <sup>b</sup>	34 <sup>b</sup>	61 <sup>b</sup>	104 <sup>a</sup>	131 <sup>a</sup>	160 <sup>a</sup>
AWAP 0.05	160	125 <sup>b</sup>	99 <sup>b</sup>	50 <sup>b</sup>	24 <sup>b</sup>	13 <sup>b</sup>	16 <sup>b</sup>	35 <sup>b</sup>	62 <sup>b</sup>	105 <sup>a</sup>	133 <sup>a</sup>	162 <sup>a</sup>
PP	159	132 <sup>a</sup>	107 <sup>a</sup>	67 <sup>a</sup>	45 <sup>a</sup>	35 <sup>a</sup>	39 <sup>a</sup>	51 <sup>a</sup>	68 <sup>a</sup>	98 <sup>b</sup>	122 <sup>b</sup>	150 <sup>b</sup>
DD	159	132 <sup>a</sup>	107 <sup>a</sup>	67 <sup>a</sup>	45 <sup>a</sup>	35 <sup>a</sup>	39 <sup>a</sup>	51 <sup>a</sup>	68 <sup>a</sup>	98 <sup>b</sup>	122 <sup>b</sup>	150 <sup>b</sup>
LSD ( $P = 0.05$ )	ns	6	4	2	2	2	2	2	3	3	4	6

Means with differing subscripts next to values indicate a significant difference at  $P < 0.05$ .

**Appendix 4.3** Mean monthly potential evaporation (mm) at Merseylea from the data sources of AWAP 0.1, AWAP 0.05, PP and DD for the period 1971 to 2007.

	Jan	Feb	Mar	Apr	May	Jun	Jul	Aug	Sep	Oct	Nov	Dec
AWAP 0.1	166	131 <sup>b</sup>	103 <sup>b</sup>	52 <sup>b</sup>	26 <sup>b</sup>	13 <sup>b</sup>	16 <sup>b</sup>	36 <sup>b</sup>	63 <sup>b</sup>	109 <sup>a</sup>	138 <sup>a</sup>	168 <sup>a</sup>
AWAP 0.05	164	130 <sup>b</sup>	103 <sup>b</sup>	51 <sup>b</sup>	25 <sup>b</sup>	13 <sup>b</sup>	16 <sup>b</sup>	36 <sup>b</sup>	62 <sup>b</sup>	108 <sup>a</sup>	137 <sup>a</sup>	167 <sup>a</sup>
PP	168	139 <sup>a</sup>	112 <sup>a</sup>	68 <sup>a</sup>	43 <sup>a</sup>	33 <sup>a</sup>	36 <sup>a</sup>	49 <sup>a</sup>	69 <sup>a</sup>	103 <sup>b</sup>	129 <sup>b</sup>	159 <sup>b</sup>
DD	168	139 <sup>a</sup>	112 <sup>a</sup>	67 <sup>a</sup>	42 <sup>a</sup>	31 <sup>a</sup>	35 <sup>a</sup>	48 <sup>a</sup>	68 <sup>a</sup>	102 <sup>b</sup>	128 <sup>b</sup>	159 <sup>b</sup>
LSD ( $P = 0.05$ )	ns	6	4	2	2	2	3	2	3	3	5	7

Means with differing subscripts next to values indicate a significant difference at  $P < 0.05$ .

**Appendix 4.4** Mean monthly potential evaporation (mm) at Cressy from the data sources of AWAP 0.1, AWAP 0.05, PP and DD for the period 1971 to 2007.

	Jan	Feb	Mar	Apr	May	Jun	Jul	Aug	Sep	Oct	Nov	Dec
AWAP 0.1	168 <sup>b</sup>	131 <sup>b</sup>	102 <sup>b</sup>	49 <sup>b</sup>	24 <sup>b</sup>	11 <sup>b</sup>	14 <sup>b</sup>	33 <sup>b</sup>	61 <sup>b</sup>	104	137	170
AWAP 0.05	168 <sup>b</sup>	131 <sup>b</sup>	102 <sup>b</sup>	49 <sup>b</sup>	24 <sup>b</sup>	11 <sup>b</sup>	14 <sup>b</sup>	33 <sup>b</sup>	62 <sup>b</sup>	105	138	170
PP	182 <sup>a</sup>	152 <sup>a</sup>	119 <sup>a</sup>	68 <sup>a</sup>	40 <sup>a</sup>	28 <sup>a</sup>	32 <sup>a</sup>	46 <sup>a</sup>	71 <sup>a</sup>	106	137	171
DD	179 <sup>a</sup>	148 <sup>a</sup>	118 <sup>a</sup>	68 <sup>a</sup>	41 <sup>a</sup>	29 <sup>a</sup>	32 <sup>a</sup>	46 <sup>a</sup>	69 <sup>a</sup>	105	135	169
LSD ( $P = 0.05$ )	7	7	5	3	2	2	2	2	3	ns	ns	ns

Means with differing subscripts next to values indicate a significant difference at  $P < 0.05$ .

**Appendix 4.5** Mean monthly potential evaporation (mm) at Ringarooma from the data sources of AWAP 0.1, AWAP 0.05, PP and DD for the period 1971 to 2007.

	Jan	Feb	Mar	Apr	May	Jun	Jul	Aug	Sep	Oct	Nov	Dec
AWAP 0.1	153 <sup>b</sup>	119 <sup>b</sup>	97 <sup>b</sup>	46 <sup>b</sup>	24 <sup>b</sup>	11 <sup>b</sup>	15 <sup>b</sup>	33 <sup>b</sup>	56 <sup>c</sup>	96 <sup>b</sup>	127 <sup>a</sup>	155
AWAP 0.05	152 <sup>b</sup>	119 <sup>b</sup>	97 <sup>b</sup>	46 <sup>b</sup>	24 <sup>b</sup>	11 <sup>b</sup>	15 <sup>b</sup>	32 <sup>b</sup>	56 <sup>c</sup>	96 <sup>b</sup>	127 <sup>a</sup>	155
PP	161 <sup>a</sup>	130 <sup>a</sup>	104 <sup>a</sup>	61 <sup>a</sup>	38 <sup>a</sup>	28 <sup>a</sup>	33 <sup>a</sup>	48 <sup>a</sup>	70 <sup>a</sup>	102 <sup>a</sup>	125 <sup>ab</sup>	154
DD	160 <sup>a</sup>	131 <sup>a</sup>	105 <sup>a</sup>	61 <sup>a</sup>	37 <sup>a</sup>	26 <sup>a</sup>	30 <sup>a</sup>	44 <sup>a</sup>	65 <sup>b</sup>	97 <sup>b</sup>	120 <sup>b</sup>	150
LSD ( $P = 0.05$ )	7	8	5	3	2	2	2	3	4	4	6	ns

Means with differing subscripts next to values indicate a significant difference at  $P < 0.05$ .

**Appendix 4.6** Mean monthly potential evaporation (mm) at Ouse from the data sources of AWAP 0.1, AWAP 0.05, PP and DD for the period 1971 to 2007.

	Jan	Feb	Mar	Apr	May	Jun	Jul	Aug	Sep	Oct	Nov	Dec
AWAP 0.1	166 <sup>a</sup>	128	94 <sup>b</sup>	45 <sup>b</sup>	21 <sup>b</sup>	10 <sup>b</sup>	14 <sup>b</sup>	34 <sup>b</sup>	63	104 <sup>a</sup>	137 <sup>a</sup>	164 <sup>a</sup>
AWAP 0.05	169 <sup>a</sup>	131	95 <sup>ab</sup>	46 <sup>b</sup>	21 <sup>b</sup>	10 <sup>b</sup>	15 <sup>b</sup>	35 <sup>b</sup>	64	106 <sup>a</sup>	139 <sup>a</sup>	168 <sup>a</sup>
PP	154 <sup>b</sup>	126	98 <sup>a</sup>	59 <sup>a</sup>	38 <sup>a</sup>	26 <sup>a</sup>	30 <sup>a</sup>	44 <sup>a</sup>	64	94 <sup>b</sup>	118 <sup>b</sup>	146 <sup>b</sup>
DD	154 <sup>b</sup>	126	98 <sup>a</sup>	59 <sup>a</sup>	38 <sup>a</sup>	26 <sup>a</sup>	30 <sup>a</sup>	44 <sup>a</sup>	64	94 <sup>b</sup>	118 <sup>b</sup>	146 <sup>b</sup>
LSD ( $P = 0.05$ )	7	ns	4	3	3	2	2	3	ns	4	6	8

Means with differing subscripts next to values indicate a significant difference at  $P < 0.05$ .

## Appendix 5.0

Mean simulated monthly pasture cut yield (kg DM/ha) from the data sources of AWAP 0.1, AWAP 0.05, PP and DD for the period 1971 to 2007, for the sites of Woolnorth, Flowerdale, Merseylea, Cressy, Ringarooma and Ouse.

**Appendix 5.1** Woolnorth mean simulated monthly pasture cut yield (kg DM/ha) from the data sources of AWAP 0.1, AWAP 0.05, PP and DD for the period 1971 to 2007.

	Jan	Feb	Mar	Apr	May	Jun	Jul	Aug	Sep	Oct	Nov	Dec
AWAP 0.1	656	270	335	674 <sup>a</sup>	648 <sup>a</sup>	384	428 <sup>b</sup>	891	1552	2423 <sup>a</sup>	2390	1374
AWAP 0.05	588	240	313	623 <sup>ab</sup>	636 <sup>a</sup>	386	435 <sup>ab</sup>	901	1574	2441 <sup>a</sup>	2362	1268
PP	611	132	251	425 <sup>b</sup>	463 <sup>b</sup>	379	478 <sup>a</sup>	928	1562	2344 <sup>b</sup>	2287	1431
DD	701	227	283	543 <sup>ab</sup>	569 <sup>ab</sup>	406	471 <sup>ab</sup>	930	1582	2432 <sup>a</sup>	2540	1641
LSD ( $P = 0.05$ )	ns	ns	ns	233	131	ns	44	ns	ns	60	ns	ns

Means with differing subscripts next to values indicate a significant difference at  $P < 0.05$ .

**Appendix 5.2** Flowerdale mean simulated monthly pasture cut yield (kg DM/ha) from the data sources of AWAP 0.1, AWAP 0.05, PP and DD for the period 1971 to 2007.

	Jan	Feb	Mar	Apr	May	Jun	Jul	Aug	Sep	Oct	Nov	Dec
AWAP 0.1	909	503	358	574	541	222	170	529 <sup>ab</sup>	1254 <sup>ab</sup>	2275 <sup>ab</sup>	2450	1666
AWAP 0.05	899	498	335	591	541	233	185	592 <sup>a</sup>	1320 <sup>a</sup>	2337 <sup>a</sup>	2455	1641
PP	1036	481	318	432	425	179	142	459 <sup>b</sup>	1180 <sup>b</sup>	2224 <sup>b</sup>	2524	1782
DD	1023	468	309	430	419	174	136	417 <sup>b</sup>	1148 <sup>b</sup>	2223 <sup>b</sup>	2546	1788
LSD ( $P = 0.05$ )	ns	ns	ns	ns	ns	ns	ns	116	130	102	ns	ns

Means with differing subscripts next to values indicate a significant difference at  $P < 0.05$ .

**Appendix 5.3** Merseylea mean simulated monthly pasture cut yield (kg DM/ha) from the data sources of AWAP 0.1, AWAP 0.05, PP and DD for the period 1971 to 2007.

	Jan	Feb	Mar	Apr	May	Jun	Jul	Aug	Sep	Oct	Nov	Dec
AWAP 0.1	561	363	261	294	339	43	16	97 <sup>ab</sup>	890 <sup>ab</sup>	2258 <sup>a</sup>	1878	1003
AWAP 0.05	655	411	283	334	346	37	13	75 <sup>b</sup>	789 <sup>ab</sup>	2235 <sup>a</sup>	1989	1154
PP	843	435	305	322	327	54	45	183 <sup>a</sup>	988 <sup>a</sup>	2199 <sup>ab</sup>	2158	1412
DD	748	367	246	241	236	46	23	91 <sup>b</sup>	740 <sup>b</sup>	2084 <sup>b</sup>	2105	1299
LSD ( $P = 0.05$ )	ns	92	200	139	ns	ns						

Means with differing subscripts next to values indicate a significant difference at  $P < 0.05$ .

**Appendix 5.4** Cressy mean simulated monthly pasture cut yield (kg DM/ha) from the data sources of AWAP 0.1, AWAP 0.05, PP and DD for the period 1971 to 2007.

	Jan	Feb	Mar	Apr	May	Jun	Jul	Aug	Sep	Oct	Nov	Dec
AWAP 0.1	517	194	216	121	55	0	0	0	23 <sup>b</sup>	1007	1884 <sup>a</sup>	866
AWAP 0.05	523	198	225	130	51	0	0	0	18 <sup>b</sup>	977	1864 <sup>a</sup>	885
PP	486	104	126	54	14	7	0	2	125 <sup>a</sup>	1058	1392 <sup>b</sup>	776
DD	600	145	150	74	42	0	0	0	25 <sup>b</sup>	860	1704 <sup>ab</sup>	949
LSD ( $P = 0.05$ )	ns	72	ns	431	ns							

Means with differing subscripts next to values indicate a significant difference at  $P < 0.05$ .

**Appendix 5.5** Ringarooma mean simulated monthly pasture cut yield (kg DM/ha) from the data sources of AWAP 0.1, AWAP 0.05, PP and DD for the period 1971 to 2007.

	Jan	Feb	Mar	Apr	May	Jun	Jul	Aug	Sep	Oct	Nov	Dec
AWAP 0.1	1162	609	537	607	340	30	9	23 <sup>b</sup>	412 <sup>b</sup>	1786 <sup>ab</sup>	2540	1766
AWAP 0.05	1313	687	599	629	359	37	12	33 <sup>ab</sup>	517	1890 <sup>a</sup>	2641	1924
PP	1164	537	486	484	376	53	19	75 <sup>a</sup>	697 <sup>a</sup>	1942 <sup>a</sup>	2482	1858
DD	1224	559	492	465	323	35	12	31 <sup>ab</sup>	397 <sup>b</sup>	1616 <sup>b</sup>	2508	1965
LSD ( $P = 0.05$ )	ns	ns	ns	ns	ns	ns	ns	49	205	261	ns	ns

Means with differing subscripts next to values indicate a significant difference at  $P < 0.05$ .

**Appendix 5.6** Ouse mean simulated monthly pasture cut yield (kg DM/ha) from the data sources of AWAP 0.1, AWAP 0.05, PP and DD for the period 1971 to 2007.

	Jan	Feb	Mar	Apr	May	Jun	Jul	Aug	Sep	Oct	Nov	Dec
AWAP 0.1	531	173	154	188 <sup>a</sup>	61	0	0	0	12 <sup>b</sup>	570 <sup>c</sup>	1910	998
AWAP 0.05	481	161	141	176 <sup>ab</sup>	56	0	0	0	31 <sup>b</sup>	934 <sup>ab</sup>	1989	949
PP	474	77	64	58 <sup>c</sup>	36	4	0	0	110 <sup>a</sup>	1194 <sup>a</sup>	1751	849
DD	490	90	61	66 <sup>bc</sup>	26	0	0	0	46 <sup>ab</sup>	840 <sup>bc</sup>	1753	903
LSD ( $P = 0.05$ )	ns	ns	ns	114	ns	ns	ns	ns	72	313	ns	ns

Means with differing subscripts next to values indicate a significant difference at  $P < 0.05$ .

## Appendix 6.0

Mean monthly rainfall (mm) from the data sources of AWAP 0.1, CSIRO-Mk3.5, ECHAM5/MPI-OM, GFDL-CM2.0, GFDL-CM2.1, MIROC3.2 (medres) and UKMO-HADCM3 for the period 1990 to 2007, at the sites of Woolnorth, Flowerdale, Merseylea, Cressy, Ringarooma and Ouse.

**Appendix 6.1** Woolnorth mean monthly rainfall (mm) from the data sources of AWAP 0.1, CSIRO-Mk3.5, ECHAM5/MPI-OM, GFDL-CM2.0, GFDL-CM2.1, MIROC3.2 (medres) and UKMO-HADCM3 for the period 1990 to 2007.

Data source	Jan	Feb	Mar	Apr	May	Jun	Jul	Aug	Sep	Oct	Nov	Dec
AWAP 0.1	50	47	52	80	84 <sup>b</sup>	126	127	123	103	84	61 <sup>b</sup>	60
CSIRO-Mk3.5	39	38	67	79	97 <sup>ab</sup>	134	125	119	94	72	67 <sup>ab</sup>	64
ECHAM5/MPI-OM	44	42	58	89	101 <sup>ab</sup>	127	130	116	109	76	75 <sup>ab</sup>	57
GFDL-CM2.0	48	40	64	70	109 <sup>a</sup>	127	122	116	105	78	68 <sup>ab</sup>	54
GFDL-CM2.1	42	44	65	84	114 <sup>a</sup>	125	127	129	100	87	69 <sup>ab</sup>	50
MIROC3.2 (medres)	38	53	59	91	101 <sup>ab</sup>	128	120	127	97	74	82 <sup>a</sup>	65
UKMO-HADCM3	43	35	62	81	100 <sup>ab</sup>	134	132	130	105	79	82 <sup>a</sup>	70
LSD ( $P = 0.05$ )	ns	ns	ns	ns	21	ns	ns	ns	ns	ns	20	ns

Means with differing subscripts next to values indicate a significant difference at  $P < 0.05$ .

**Appendix 6.2** Flowerdale mean monthly rainfall (mm) from the data sources of AWAP 0.1, CSIRO-Mk3.5, ECHAM5/MPI-OM, GFDL-CM2.0, GFDL-CM2.1, MIROC3.2 (medres) and UKMO-HADCM3 for the period 1990 to 2007.

Data source	Jan	Feb	Mar	Apr	May	Jun	Jul	Aug	Sep	Oct	Nov	Dec
AWAP 0.1	60	47	45 <sup>b</sup>	76	95	129	139	151	137	100	80	72
CSIRO-Mk3.5	45	50	74 <sup>a</sup>	78	94	140	131	133	112	87	78	74
ECHAM5/MPI-OM	53	48	68 <sup>ab</sup>	92	95	122	140	126	138	92	89	69
GFDL-CM2.0	57	51	71 <sup>a</sup>	83	107	130	136	128	129	96	84	69
GFDL-CM2.1	52	48	72 <sup>a</sup>	92	117	126	147	146	124	97	87	59
MIROC3.2 (medres)	49	60	69 <sup>ab</sup>	92	100	119	131	141	121	85	104	76
UKMO-HADCM3	51	43	65 <sup>ab</sup>	83	99	137	140	150	136	101	101	83
LSD ( $P = 0.05$ )	ns	ns	26	ns								

Means with differing subscripts next to values indicate a significant difference at  $P < 0.05$ .

**Appendix 6.3** Merseylea mean monthly rainfall (mm) from the data sources of AWAP 0.1, CSIRO-Mk3.5, ECHAM5/MPI-OM, GFDL-CM2.0, GFDL-CM2.1, MIROC3.2 (medres) and UKMO-HADCM3 for the period 1990 to 2007.

Data source	Jan	Feb	Mar	Apr	May	Jun	Jul	Aug	Sep	Oct	Nov	Dec
AWAP 0.1	60 <sup>a</sup>	41	36 <sup>b</sup>	62	75	101	105	110	94	70	65	54
CSIRO-Mk3.5	37 <sup>b</sup>	41	67 <sup>a</sup>	64	75	107	101	104	79	62	63	65
ECHAM5/MPI-OM	47 <sup>ab</sup>	39	60 <sup>ab</sup>	72	79	91	114	104	99	65	69	61
GFDL-CM2.0	48 <sup>ab</sup>	47	61 <sup>a</sup>	66	87	106	108	102	92	72	62	55
GFDL-CM2.1	43 <sup>ab</sup>	39	58 <sup>ab</sup>	70	94	99	121	111	92	65	64	52
MIROC3.2 (medres)	40 <sup>ab</sup>	47	59 <sup>ab</sup>	75	80	96	105	108	86	60	78	65
UKMO-HADCM3	43 <sup>ab</sup>	32	53 <sup>ab</sup>	67	78	107	104	122	100	71	70	68
LSD ( $P = 0.05$ )	21	ns	24	ns								

Means with differing subscripts next to values indicate a significant difference at  $P < 0.05$ .

**Appendix 6.4** Cressy mean monthly rainfall (mm) from the data sources of AWAP 0.1, CSIRO-Mk3.5, ECHAM5/MPI-OM, GFDL-CM2.0, GFDL-CM2.1, MIROC3.2 (medres) and UKMO-HADCM3 for the period 1990 to 2007.

Data source	Jan	Feb	Mar	Apr	May	Jun	Jul	Aug	Sep	Oct	Nov	Dec
AWAP 0.1	60 <sup>a</sup>	37	30 <sup>b</sup>	52	59	75	82	90	76	59	56	49
CSIRO-Mk3.5	38 <sup>b</sup>	40	59 <sup>a</sup>	53	56	78	80	85	64	53	61	64
ECHAM5/MPI-OM	45 <sup>ab</sup>	34	54 <sup>a</sup>	66	58	71	89	82	80	56	62	56
GFDL-CM2.0	41 <sup>ab</sup>	45	56 <sup>a</sup>	54	64	76	81	84	77	62	59	50
GFDL-CM2.1	41 <sup>ab</sup>	33	53 <sup>a</sup>	53	72	70	93	91	76	56	53	50
MIROC3.2 (medres)	40 <sup>b</sup>	39	53 <sup>a</sup>	58	60	68	81	88	68	52	73	60
UKMO-HADCM3	43 <sup>ab</sup>	30	48 <sup>ab</sup>	54	56	75	84	98	86	60	63	64
LSD ( $P = 0.05$ )	19	ns	21	ns								

Means with differing subscripts next to values indicate a significant difference at  $P < 0.05$ .

**Appendix 6.5** Ringarooma mean monthly rainfall (mm) from the data sources of AWAP 0.1, CSIRO-Mk3.5, ECHAM5/MPI-OM, GFDL-CM2.0, GFDL-CM2.1, MIROC3.2 (medres) and UKMO-HADCM3 for the period 1990 to 2007.

Data source	Jan	Feb	Mar	Apr	May	Jun	Jul	Aug	Sep	Oct	Nov	Dec
AWAP 0.1	73 <sup>a</sup>	46	45 <sup>b</sup>	77	101 <sup>b</sup>	115	123	150	110 <sup>b</sup>	92	81	63
CSIRO-Mk3.5	46 <sup>b</sup>	50	77 <sup>a</sup>	77	105 <sup>ab</sup>	132	120	142	115 <sup>ab</sup>	75	67	85
ECHAM5/MPI-OM	56 <sup>ab</sup>	44	65 <sup>ab</sup>	96	103 <sup>ab</sup>	118	136	132	138 <sup>a</sup>	88	76	71
GFDL-CM2.0	61 <sup>ab</sup>	58	66 <sup>ab</sup>	77	123 <sup>ab</sup>	122	126	129	127 <sup>ab</sup>	86	72	78
GFDL-CM2.1	52 <sup>ab</sup>	52	65 <sup>ab</sup>	86	136 <sup>a</sup>	111	141	146	127 <sup>ab</sup>	86	66	70
MIROC3.2 (medres)	55 <sup>ab</sup>	60	66 <sup>ab</sup>	97	116 <sup>ab</sup>	122	126	134	116 <sup>ab</sup>	76	90	84
UKMO-HADCM3	59 <sup>ab</sup>	38	60 <sup>ab</sup>	86	112 <sup>ab</sup>	135	129	142	139 <sup>a</sup>	89	80	82
LSD ( $P = 0.05$ )	22	ns	24	ns	32	ns	ns	ns	27	ns	ns	ns

Means with differing subscripts next to values indicate a significant difference at  $P < 0.05$ .

**Appendix 6.6** Ouse mean monthly rainfall (mm) from the data sources of AWAP 0.1, CSIRO-Mk3.5, ECHAM5/MPI-OM, GFDL-CM2.0, GFDL-CM2.1, MIROC3.2 (medres) and UKMO-HADCM3 for the period 1990 to 2007.

Data source	Jan	Feb	Mar	Apr	May	Jun	Jul	Aug	Sep	Oct	Nov	Dec
AWAP 0.1	49	34	40 <sup>b</sup>	56	48 <sup>b</sup>	67	75	81	79	81 <sup>a</sup>	57 <sup>b</sup>	60
CSIRO-Mk3.5	38	36	69 <sup>a</sup>	52	47 <sup>ab</sup>	75	61	85	74	57 <sup>ab</sup>	77 <sup>ab</sup>	67
ECHAM5/MPI-OM	46	35	61 <sup>ab</sup>	64	47 <sup>ab</sup>	74	64	63	71	66 <sup>ab</sup>	79 <sup>ab</sup>	51
GFDL-CM2.0	49	44	53 <sup>ab</sup>	54	56 <sup>ab</sup>	66	72	67	80	65 <sup>ab</sup>	70 <sup>ab</sup>	52
GFDL-CM2.1	35	34	63 <sup>ab</sup>	53	68 <sup>a</sup>	66	67	85	69	75 <sup>ab</sup>	67 <sup>ab</sup>	52
MIROC3.2 (medres)	41	38	57 <sup>ab</sup>	53	60 <sup>ab</sup>	68	57	72	67	61 <sup>b</sup>	85 <sup>a</sup>	70
UKMO-HADCM3	45	36	56 <sup>ab</sup>	52	54 <sup>ab</sup>	67	83	70	80	71 <sup>ab</sup>	86 <sup>a</sup>	60
LSD ( $P = 0.05$ )	ns	ns	25	ns	19	ns	ns	ns	ns	20	25	ns

Means with differing subscripts next to values indicate a significant difference at  $P < 0.05$ .

## Appendix 7.0

Mean simulated monthly pasture cut yield (kg DM/ha) from the data sources of AWAP 0.1, CSIRO-Mk3.5, ECHAM5/MPI-OM, GFDL-CM2.0, GFDL-CM2.1, MIROC3.2 (medres) and UKMO-HADCM3 for the period 1990 to 2007, at the sites of Woolnorth, Flowerdale, Merseylea, Cressy, Ringarooma and Ouse.

**Appendix 7.1** Woolnorth mean simulated monthly pasture cut yield (kg DM/ha) from the data sources of AWAP 0.1, CSIRO-Mk3.5, ECHAM5/MPI-OM, GFDL-CM2.0, GFDL-CM2.1, MIROC3.2 (medres) and UKMO-HADCM3 for the period 1990 to 2007.

Data source	Jan	Feb	Mar	Apr	May	Jun	Jul	Aug	Sep	Oct	Nov	Dec
AWAP 0.1	307	144	230	263	278	109	202	654 <sup>a</sup>	1342 <sup>a</sup>	2193	1817	618 <sup>b</sup>
CSIRO-Mk3.5	282	97	82	278	235	86	176	574 <sup>ab</sup>	1201 <sup>b</sup>	2172	1453	851 <sup>ab</sup>
ECHAM5/MPI-OM	391	89	106	157	245	118	192	583 <sup>ab</sup>	1190 <sup>b</sup>	2172	1560	606 <sup>ab</sup>
GFDL-CM2.0	352	126	156	235	219	115	158	554 <sup>b</sup>	1123 <sup>b</sup>	2166	1835	684 <sup>ab</sup>
GFDL-CM2.1	259	68	149	284	238	98	179	615 <sup>ab</sup>	1192 <sup>b</sup>	2158	1928	849 <sup>ab</sup>
MIROC3.2 (medres)	319	64	164	316	220	72	161	574 <sup>ab</sup>	1237 <sup>ab</sup>	2151	1743	1150 <sup>a</sup>
UKMO-HADCM3	243	8	130	224	261	97	194	620 <sup>ab</sup>	1162 <sup>b</sup>	2208	1949	1236 <sup>a</sup>
LSD ( $P = 0.05$ )	ns	99	113	ns	ns	474						

Means with differing subscripts next to values indicate a significant difference at  $P < 0.05$ .

**Appendix 7.2** Flowerdale mean simulated monthly pasture cut yield (kg DM/ha) from the data sources of AWAP 0.1, CSIRO-Mk3.5, ECHAM5/MPI-OM, GFDL-CM2.0, GFDL-CM2.1, MIROC3.2 (medres) and UKMO-HADCM3 for the period 1990 to 2007.

Data source	Jan	Feb	Mar	Apr	May	Jun	Jul	Aug	Sep	Oct	Nov	Dec
AWAP 0.1	456	307	233	191 <sup>b</sup>	190	39 <sup>b</sup>	39	182	948 <sup>a</sup>	2051	2086	1111 <sup>b</sup>
CSIRO-Mk3.5	369	167	388	480 <sup>ab</sup>	295	38 <sup>ab</sup>	30	215	904 <sup>ab</sup>	2083	1714	1076 <sup>ab</sup>
ECHAM5/MPI-OM	664	194	243	442 <sup>ab</sup>	319	87 <sup>a</sup>	55	288	894 <sup>ab</sup>	2047	1984	1080 <sup>ab</sup>
GFDL-CM2.0	640	266	367	410 <sup>ab</sup>	274	64 <sup>ab</sup>	19	174	788 <sup>b</sup>	2064	2210	1116 <sup>ab</sup>
GFDL-CM2.1	426	197	256	539 <sup>a</sup>	277	45 <sup>ab</sup>	24	252	939 <sup>ab</sup>	2033	2258	1207 <sup>ab</sup>
MIROC3.2 (medres)	548	117	352	389 <sup>ab</sup>	272	30 <sup>ab</sup>	38	174	905 <sup>ab</sup>	2059	2150	1649 <sup>ab</sup>
UKMO-HADCM3	515	106	406	362 <sup>ab</sup>	240	46 <sup>ab</sup>	36	259	923 <sup>ab</sup>	2077	2205	1717 <sup>a</sup>
LSD ( $P = 0.05$ )	ns	ns	ns	299	ns	43	ns	ns	156	ns	ns	588

Means with differing subscripts next to values indicate a significant difference at  $P < 0.05$ .

**Appendix 7.3** Merseylea mean simulated monthly pasture cut yield (kg DM/ha) from the data sources of AWAP 0.1, CSIRO-Mk3.5, ECHAM5/MPI-OM, GFDL-CM2.0, GFDL-CM2.1, MIROC3.2 (medres) and UKMO-HADCM3 for the period 1990 to 2007.

Data source	Jan	Feb	Mar	Apr	May	Jun	Jul	Aug	Sep	Oct	Nov	Dec
AWAP 0.1	225	270	242	137	62 <sup>b</sup>	6	14	15	355	1860	1447 <sup>a</sup>	562
CSIRO-Mk3.5	191	51	183	306	216 <sup>a</sup>	3	0	3	295	1835	874 <sup>b</sup>	650
ECHAM5/MPI-OM	477	148	112	187	177 <sup>ab</sup>	1	0	0	458	1824	1258 <sup>ab</sup>	687
GFDL-CM2.0	408	208	120	284	160 <sup>ab</sup>	7	0	0	194	1896	1623 <sup>ab</sup>	629
GFDL-CM2.1	168	165	55	311	202 <sup>a</sup>	6	0	4	394	1961	1447 <sup>ab</sup>	699
MIROC3.2 (medres)	377	42	65	288	217 <sup>a</sup>	1	0	0	261	1824	1446 <sup>ab</sup>	1080
UKMO-HADCM3	280	45	128	171	136 <sup>ab</sup>	3	0	4	511	2014	1624 <sup>ab</sup>	975
LSD ( $P = 0.05$ )	ns	ns	ns	ns	128	ns	ns	ns	ns	ns	518	ns

Means with differing subscripts next to values indicate a significant difference at  $P < 0.05$ .

**Appendix 7.4** Cressy mean simulated monthly pasture cut yield (kg DM/ha) from the data sources of AWAP 0.1, CSIRO-Mk3.5, ECHAM5/MPI-OM, GFDL-CM2.0, GFDL-CM2.1, MIROC3.2 (medres) and UKMO-HADCM3 for the period 1990 to 2007.

Data source	Jan	Feb	Mar	Apr	May	Jun	Jul	Aug	Sep	Oct	Nov	Dec
AWAP 0.1	286	128	156 <sup>a</sup>	54	1	0	0	0	0	294 <sup>b</sup>	1009 <sup>a</sup>	319
CSIRO-Mk3.5	123	10	82 <sup>ab</sup>	141	20	0	0	0	0	169 <sup>ab</sup>	320 <sup>b</sup>	486
ECHAM5/MPI-OM	359	125	11 <sup>ab</sup>	74	23	0	0	0	0	352 <sup>ab</sup>	887 <sup>ab</sup>	415
GFDL-CM2.0	180	117	65 <sup>ab</sup>	111	28	0	0	0	0	248 <sup>ab</sup>	948 <sup>ab</sup>	416
GFDL-CM2.1	61	58	7 <sup>b</sup>	29	13	0	0	0	0	266 <sup>ab</sup>	824 <sup>ab</sup>	385
MIROC3.2 (medres)	218	9	0 <sup>b</sup>	55	7	0	0	0	0	75 <sup>ab</sup>	770 <sup>ab</sup>	624
UKMO-HADCM3	182	39	50 <sup>ab</sup>	78	7	0	0	0	0	572 <sup>a</sup>	1187 <sup>ab</sup>	551
LSD ( $P = 0.05$ )	ns	ns	147	ns	ns	ns	ns	ns	ns	224	529	ns

Means with differing subscripts next to values indicate a significant difference at  $P < 0.05$ .

**Appendix 7.5** Ringarooma mean simulated monthly pasture cut yield (kg DM/ha) from the data sources of AWAP 0.1, CSIRO-Mk3.5, ECHAM5/MPI-OM, GFDL-CM2.0, GFDL-CM2.1, MIROC3.2 (medres) and UKMO-HADCM3 for the period 1990 to 2007.

Data source	Jan	Feb	Mar	Apr	May	Jun	Jul	Aug	Sep	Oct	Nov	Dec
AWAP 0.1	654	441	236	222 <sup>b</sup>	100	0	0	0	137 <sup>a</sup>	1240	2101 <sup>a</sup>	933
CSIRO-Mk3.5	308	233	279	534 <sup>a</sup>	154	0	0	0	39 <sup>b</sup>	1196	1595 <sup>b</sup>	1118
ECHAM5/MPI-OM	714	198	136	361 <sup>ab</sup>	148	0	0	0	30 <sup>b</sup>	1222	1876 <sup>ab</sup>	988
GFDL-CM2.0	831	315	312	375 <sup>ab</sup>	110	6	0	0	3 <sup>b</sup>	1007	2041 <sup>ab</sup>	1133
GFDL-CM2.1	333	261	322	380 <sup>ab</sup>	108	0	0	0	5 <sup>b</sup>	1126	1970 <sup>ab</sup>	1126
MIROC3.2 (medres)	795	219	166	365 <sup>ab</sup>	127	0	0	0	31 <sup>b</sup>	956	1901 <sup>ab</sup>	1531
UKMO-HADCM3	648	163	157	135 <sup>ab</sup>	118	0	0	0	70 <sup>ab</sup>	1367	2044 <sup>ab</sup>	1425
LSD ( $P = 0.05$ )	ns	ns	ns	261	ns	ns	ns	ns	85	ns	407	ns

Means with differing subscripts next to values indicate a significant difference at  $P < 0.05$ .

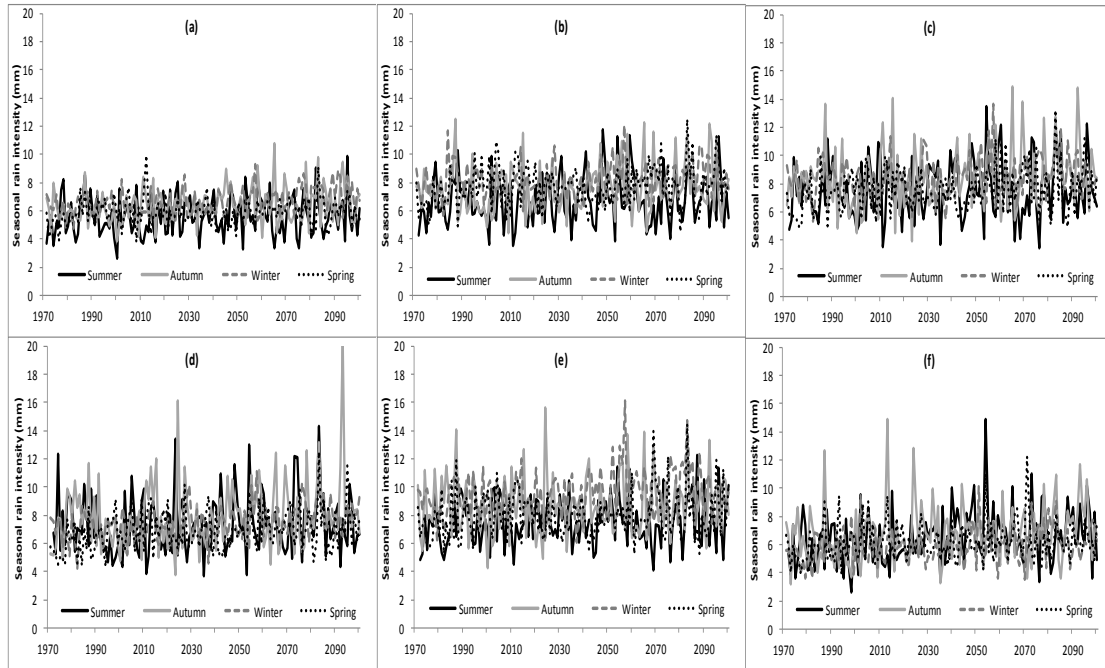
**Appendix 7.6** Ouse mean simulated monthly pasture cut yield (kg DM/ha) from the data sources of AWAP 0.1, CSIRO-Mk3.5, ECHAM5/MPI-OM, GFDL-CM2.0, GFDL-CM2.1, MIROC3.2 (medres) and UKMO-HADCM3 for the period 1990 to 2007.

Data source	Jan	Feb	Mar	Apr	May	Jun	Jul	Aug	Sep	Oct	Nov	Dec
AWAP 0.1	294	77	31	3 <sup>b</sup>	0 <sup>b</sup>	0	0	0	0	187	1138 <sup>a</sup>	379
CSIRO-Mk3.5	150	17	64	190 <sup>a</sup>	25 <sup>ab</sup>	0	0	0	0	125	532 <sup>b</sup>	658
ECHAM5/MPI-OM	264	109	0	25 <sup>b</sup>	32 <sup>a</sup>	0	0	0	0	203	847 <sup>ab</sup>	536
GFDL-CM2.0	177	129	66	115 <sup>ab</sup>	1 <sup>b</sup>	0	0	0	0	49	786 <sup>ab</sup>	453
GFDL-CM2.1	73	0	18	0 <sup>b</sup>	2 <sup>b</sup>	0	0	0	0	108	925 <sup>ab</sup>	557
MIROC3.2 (medres)	234	35	0	5 <sup>b</sup>	1 <sup>b</sup>	0	0	0	0	95	609 <sup>b</sup>	733
UKMO-HADCM3	220	39	33	6 <sup>b</sup>	5 <sup>ab</sup>	0	0	0	0	197	1221 <sup>a</sup>	797
LSD ( $P = 0.05$ )	ns	ns	ns	115	28	ns	ns	ns	ns	ns	501	ns

Means with differing subscripts next to values indicate a significant difference at  $P < 0.05$ .

## Appendix 8.0

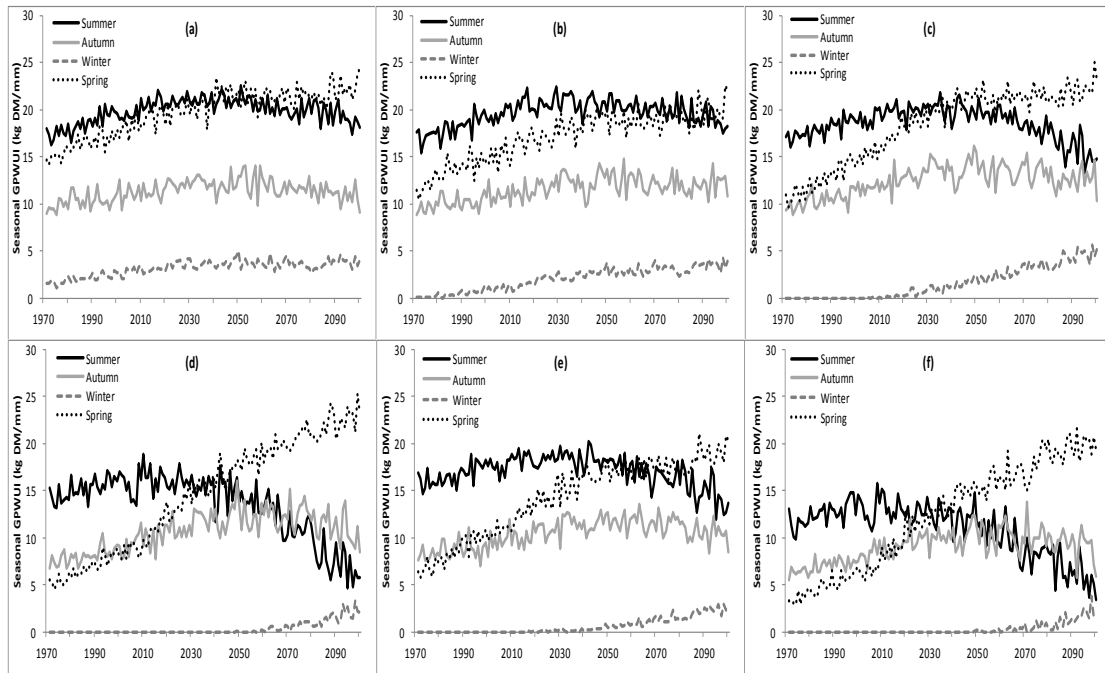
Multi-model mean seasonal rainfall intensity (mm) from the data sources of CSIRO-Mk3.5, ECHAM5/MPI-OM, GFDL-CM2.0, GFDL-CM2.1, MIROC3.2 (medres) and UKMO-HADCM3 for the period 1971 to 2100, at the sites of Woolnorth, Flowerdale, Merseylea, Cressy, Ringarooma and Ouse.



**Appendix 8.0** Multi-model mean seasonal rainfall intensity (mm) at Woolnorth (a), Flowerdale (b), Merseylea (c), Cressy (d), Ringarooma (e) and Ouse (f) for the period 1971 to 2100.

## Appendix 9.0

Multi-model mean seasonal GPWUI (kg DM/mm) from the data sources of CSIRO-Mk3.5, ECHAM5/MPI-OM, GFDL-CM2.0, GFDL-CM2.1, MIROC3.2 (medres) and UKMO-HADCM3 for the period 1971 to 2100, at the sites of Woolnorth, Flowerdale, Merseylea, Cressy, Ringarooma and Ouse.



**Appendix 9.0** Multi-model mean of seasonal GPWUI (kg DM/mm) at Woolnorth (a), Flowerdale (b), Merseylea (c), Cressy (d), Ringarooma (e) and Ouse (f) for the period 1971 to 2100.

## Appendix 10.0

Mean simulated monthly runoff (mm) from the data sets of AWAP 0.1, CSIRO-Mk3.5, ECHAM5/MPI-OM, GFDL-CM2.0, GFDL-CM2.1, MIROC3.2 (medres) and UKMO-HADCM3 at the sites of Woolnorth, Flowerdale, Merseylea, Cressy, Ringarooma and Ouse, for the baseline, 2025, 2055 and 2085.

**Appendix 10.1** Woolnorth multi-model mean simulated monthly runoff (mm) for the baseline, 2025, 2055 and 2085.

	Jan	Feb	Mar	Apr	May	Jun	Jul	Aug	Sep	Oct	Nov	Dec
Baseline	4.09 <sup>a</sup>	2.30	2.79 <sup>a</sup>	4.02	8.98	17.91 <sup>ab</sup>	26.47 <sup>b</sup>	29.40 <sup>b</sup>	23.61 <sup>ab</sup>	16.16 <sup>b</sup>	11.69 <sup>ab</sup>	8.80
2025	4.34 <sup>a</sup>	2.27	2.27 <sup>ab</sup>	3.88	8.26	16.59 <sup>b</sup>	25.87 <sup>b</sup>	28.29 <sup>b</sup>	23.48 <sup>ab</sup>	16.48 <sup>b</sup>	10.86 <sup>b</sup>	7.91
2055	3.96 <sup>ab</sup>	2.16	2.31 <sup>ab</sup>	4.15	8.70	17.17 <sup>ab</sup>	26.14 <sup>b</sup>	29.39 <sup>b</sup>	22.41 <sup>b</sup>	16.05 <sup>b</sup>	11.07 <sup>b</sup>	7.90
2085	3.09 <sup>b</sup>	2.05	2.22 <sup>b</sup>	4.20	8.73	18.61 <sup>a</sup>	29.55 <sup>a</sup>	32.87 <sup>a</sup>	24.94 <sup>a</sup>	19.05 <sup>a</sup>	13.28 <sup>a</sup>	8.11
LSD ( $P = 0.05$ )	0.90	ns	0.55	ns	ns	1.79	2.33	2.73	2.12	1.84	1.64	ns

Means with differing subscripts next to values indicate a significant difference at  $P < 0.05$ .

**Appendix 10.2** Flowerdale multi-model mean simulated monthly runoff (mm) for the baseline, 2025, 2055 and 2085.

	Jan	Feb	Mar	Apr	May	Jun	Jul	Aug	Sep	Oct	Nov	Dec
baseline	11.03 <sup>ab</sup>	7.45	10.50	15.66	30.81	59.02 <sup>ab</sup>	87.22 <sup>b</sup>	95.24 <sup>ab</sup>	80.63 <sup>a</sup>	51.97	29.00 <sup>a</sup>	19.68
2025	12.57 <sup>a</sup>	8.67	10.12	16.52	29.20	54.49 <sup>b</sup>	84.84 <sup>b</sup>	90.62 <sup>b</sup>	76.45 <sup>ab</sup>	50.42	26.42 <sup>ab</sup>	17.24
2055	11.68 <sup>ab</sup>	8.88	10.72	16.67	32.20	57.27 <sup>ab</sup>	85.39 <sup>b</sup>	93.75 <sup>ab</sup>	73.27 <sup>b</sup>	49.48	25.83 <sup>b</sup>	18.68
2085	10.10 <sup>b</sup>	8.83	11.53	16.54	30.57	63.41 <sup>a</sup>	96.31 <sup>a</sup>	98.09 <sup>a</sup>	74.58 <sup>b</sup>	53.40	26.84 <sup>ab</sup>	17.52
LSD ( $P = 0.05$ )	2.19	ns	ns	ns	ns	6.89	7.85	6.88	5.76	ns	2.71	ns

Means with differing subscripts next to values indicate a significant difference at  $P < 0.05$ .

**Appendix 10.3** Merseylea multi-model mean simulated monthly runoff (mm) for the baseline, 2025, 2055 and 2085.

	Jan	Feb	Mar	Apr	May	Jun	Jul	Aug	Sep	Oct	Nov	Dec
baseline	2.27 <sup>b</sup>	1.61 <sup>b</sup>	2.96	5.21	12.91 <sup>ab</sup>	28.49 <sup>b</sup>	51.93 <sup>b</sup>	60.00 <sup>a</sup>	39.20 <sup>a</sup>	17.64 <sup>b</sup>	8.94	5.86
2025	3.36 <sup>a</sup>	2.35 <sup>a</sup>	3.12	5.40	11.80 <sup>b</sup>	25.61 <sup>b</sup>	50.16 <sup>b</sup>	53.81 <sup>b</sup>	36.53 <sup>ab</sup>	18.24 <sup>b</sup>	7.66	5.10
2055	2.74 <sup>ab</sup>	2.03 <sup>ab</sup>	3.02	5.82	14.84 <sup>ab</sup>	31.22 <sup>b</sup>	55.25 <sup>b</sup>	58.95 <sup>ab</sup>	34.38 <sup>b</sup>	18.81 <sup>b</sup>	7.80	5.06
2085	2.63 <sup>ab</sup>	2.33 <sup>a</sup>	3.48	6.55	15.77 <sup>a</sup>	36.31 <sup>a</sup>	63.98 <sup>a</sup>	61.97 <sup>a</sup>	36.49 <sup>ab</sup>	23.66 <sup>a</sup>	8.95	5.94
LSD ( $P = 0.05$ )	0.91	0.66	ns	ns	3.17	5.06	6.92	6.05	4.46	3.04	ns	ns

Means with differing subscripts next to values indicate a significant difference at  $P < 0.05$ .

**Appendix 10.4** Cressy multi-model mean simulated monthly runoff (mm) for the baseline, 2025, 2055 and 2085.

	Jan	Feb	Mar	Apr	May	Jun	Jul	Aug	Sep	Oct	Nov	Dec
Baseline	2.78 <sup>b</sup>	1.93 <sup>b</sup>	3.02	3.99 <sup>b</sup>	6.36	11.28 <sup>b</sup>	20.28 <sup>b</sup>	26.33 <sup>a</sup>	22.09	10.71 <sup>b</sup>	5.32 <sup>ab</sup>	5.33
2025	3.99 <sup>a</sup>	2.85 <sup>a</sup>	4.00	4.73 <sup>ab</sup>	6.36	10.43 <sup>b</sup>	20.19 <sup>b</sup>	25.09 <sup>a</sup>	20.67	10.31 <sup>b</sup>	4.67 <sup>b</sup>	4.70
2055	3.41 <sup>ab</sup>	2.52 <sup>ab</sup>	3.60	4.72 <sup>ab</sup>	7.17	12.04 <sup>b</sup>	21.79 <sup>b</sup>	27.05 <sup>a</sup>	20.10	10.48 <sup>b</sup>	4.83 <sup>b</sup>	5.01
2085	3.41 <sup>ab</sup>	2.91 <sup>a</sup>	4.20	5.53 <sup>a</sup>	7.17	14.26 <sup>a</sup>	25.24 <sup>a</sup>	30.88 <sup>b</sup>	22.10	13.68 <sup>a</sup>	5.84 <sup>a</sup>	5.05
LSD ( $P = 0.05$ )	0.86	0.62	ns	1.31	ns	1.98	2.88	2.92	ns	1.6	0.87	ns

Means with differing subscripts next to values indicate a significant difference at  $P < 0.05$ .

**Appendix 10.5** Ringarooma multi-model mean simulated monthly runoff (mm) for the baseline, 2025, 2055 and 2085.

	Jan	Feb	Mar	Apr	May	Jun	Jul	Aug	Sep	Oct	Nov	Dec
baseline	16.20	10.31 <sup>b</sup>	10.25	14.66	33.12	53.50 <sup>b</sup>	77.17 <sup>b</sup>	86.12 <sup>bc</sup>	76.43 <sup>b</sup>	50.75 <sup>b</sup>	30.35 <sup>b</sup>	24.69
2025	16.88	11.89 <sup>ab</sup>	11.20	15.67	30.67	50.95 <sup>b</sup>	75.69 <sup>b</sup>	82.20 <sup>c</sup>	76.09 <sup>b</sup>	51.65 <sup>b</sup>	29.07 <sup>b</sup>	23.31
2055	17.02	11.63 <sup>ab</sup>	10.81	14.48	31.53	54.04 <sup>b</sup>	81.00 <sup>b</sup>	92.08 <sup>b</sup>	77.68 <sup>ab</sup>	52.31 <sup>b</sup>	30.27 <sup>b</sup>	24.08
2085	16.34	12.49 <sup>a</sup>	11.27	15.29	33.70	60.06 <sup>a</sup>	92.34 <sup>a</sup>	99.71 <sup>a</sup>	82.04 <sup>a</sup>	59.82 <sup>a</sup>	33.61 <sup>a</sup>	24.35
LSD ( $P = 0.05$ )	ns	1.79	ns	ns	ns	5.95	6.79	6.31	5.52	4.02	2.60	ns

Means with differing subscripts next to values indicate a significant difference at  $P < 0.05$ .

**Appendix 10.6** Ouse multi-model mean simulated monthly runoff (mm) for the baseline, 2025, 2055 and 2085.

Scenario	Jan	Feb	Mar	Apr	May	Jun	Jul	Aug	Sep	Oct	Nov	Dec
Baseline	0.85 <sup>b</sup>	0.55 <sup>b</sup>	1.08	1.20 <sup>b</sup>	1.95 <sup>b</sup>	3.80	5.59 <sup>b</sup>	6.34 <sup>b</sup>	5.59 <sup>ab</sup>	3.44 <sup>b</sup>	2.57 <sup>ab</sup>	1.90 <sup>ab</sup>
2025	1.09 <sup>ab</sup>	0.77 <sup>ab</sup>	1.56	1.76 <sup>ab</sup>	1.95 <sup>b</sup>	4.09	5.80 <sup>ab</sup>	6.18 <sup>b</sup>	5.44 <sup>ab</sup>	3.57 <sup>b</sup>	2.27 <sup>b</sup>	1.68 <sup>b</sup>
2055	1.27 <sup>a</sup>	0.92 <sup>a</sup>	1.24	1.88 <sup>a</sup>	2.39 <sup>ab</sup>	3.97	5.97 <sup>ab</sup>	6.19 <sup>b</sup>	5.16 <sup>b</sup>	3.61 <sup>ab</sup>	2.68 <sup>ab</sup>	1.98 <sup>ab</sup>
2085	1.20 <sup>ab</sup>	0.96 <sup>a</sup>	1.38	2.01 <sup>a</sup>	2.57 <sup>a</sup>	4.44	6.99 <sup>a</sup>	8.63 <sup>a</sup>	6.36 <sup>a</sup>	4.38 <sup>a</sup>	3.20 <sup>a</sup>	2.31 <sup>a</sup>
LSD ( $P = 0.05$ )	0.39	0.29	ns	0.64	0.56	ns	1.27	1.76	1.06	0.79	0.65	0.53

Means with differing subscripts next to values indicate a significant difference at  $P < 0.05$ .

**Appendix 11.0**

Mean simulated monthly River flow (GL) from the data sets of AWAP 0.1, CSIRO-Mk3.5, ECHAM5/MPI-OM, GFDL-CM2.0, GFDL-CM2.1, MIROC3.2 (medres) and UKMO-HADCM3 at Ringarooma, for the baseline, 2025, 2055 and 2085.

**Appendix 11.0** Ringarooma multi-model mean simulated monthly River flow (GL) for the baseline, 2025, 2055 and 2085.

Scenario	Jan	Feb	Mar	Apr	May	Jun	Jul	Aug	Sep	Oct	Nov	Dec
Baseline	2315	1385	1481	2587	6902	10488	14690 <sup>b</sup>	15624 <sup>bc</sup>	13219	8189 <sup>b</sup>	4731	3748
2025	2420	1594	1623	2729	6331	9852	14175 <sup>b</sup>	14792 <sup>c</sup>	13044	8252 <sup>b</sup>	4385	3403
2055	2305	1487	1504	2412	6162	9957	14855 <sup>b</sup>	16441 <sup>ab</sup>	12848	8280 <sup>b</sup>	4416	3405
2085	2171	1612	1579	2521	6180	10887	16091 <sup>a</sup>	17084 <sup>a</sup>	13258	9044 <sup>a</sup>	4624	3286
LSD ( $P = 0.05$ )	ns	ns	ns	ns	ns	ns	1185	1164	ns	681	ns	ns

Means with differing subscripts next to values indicate a significant difference at  $P < 0.05$ .

*“For the gardens end, is where the wilderness begins”*